

Development of BIM-based Automated Methods for Building Management and Structural Safety Assessment

Mojtaba Valinejadshoubi

A Thesis in

The Department

of

Building, Civil, and Environmental Engineering

Presented in Partial Fulfillment of the Requirements for the Degree of

Doctor of Philosophy (Civil Engineering) at

Concordia University

Montreal, Quebec, Canada

November, 2021

© Mojtaba Valinejadshoubi, 2021

CONCORDIA UNIVERSITY

School of Graduate Studies

This is to certify that the thesis prepared

By: Mojtaba Valinejadshoubi

Entitled: **Development of BIM-based Automated Methods for Building Management and Structural Safety Assessment**

and submitted in partial fulfillment of the requirements for the degree of

DOCTOR OF PHILOSOPHY (Civil Engineering)

complies with the regulations of the University and meets the accepted standards with respect to originality and quality.

Signed by the final Examining Committee:

_____ Chair
Dr. Anjali Awasthi

_____ External Examiner
Dr. Sheryl Staub-French

_____ External to Program
Dr. Amin Hammad

_____ Examiner
Dr. Khaled E. Galal

_____ Examiner
Dr. Sang Hyeok Han

_____ Thesis Co-Supervisor
Dr. Osama Moselhi

_____ Thesis Co-Supervisor
Dr. Ashutosh Bagchi

Approved by _____
Dr. Mazdak Nik-Bakht, Graduate Program Director

November 25, 2021 _____
Mourad Debbabi, Dean, Faculty of Engineering and Computer Science

Abstract

Development of BIM-based Automated Methods for Building Management and Structural Safety Assessment

Mojtaba Valinejadshoubi, Ph.D.

Concordia University, 2021

Despite the progress made in modern project management methods, there is still a lack of appropriate automated tools that support digital integration over the project life cycle. There is considerable demand for fully embracing the latest technological opportunities such as Building Information Modeling (BIM), Internet of Things (IoT), Structural Health Monitoring (SHM), and prefabrication to support that digital transformation in construction. The aim of this study is to develop a set of automated management solutions and related tools to address the issues highlighted above. The thesis is presented as a collection of manuscripts of five peer-reviewed journal articles authored based on the present research. The first development is of a BIM-based method for 3D model visualization of buildings and their non-structural elements and their corresponding seismic risk levels and locations. It supports automated assessment of seismic risk of these elements. The second focuses on the development of a novel data-driven SHM technique to monitor the structural behavior of individual building modules to detect possible damages during their transportation. It consists of two main components, a sensor-based data acquisition (DAQ) and storage module, and an automated data analysis module that uses unsupervised machine learning techniques to identify damages during transportation using onboard captured acceleration data. It can be used to ascertain the safety of delivered modules before their assembly on site. The third accounts for the development of an automated BIM-based framework to facilitate effective

data management and representation of sensory components of the SHM tool used in buildings. It allows for visualization of damages in building components based on the interpretation of the captured sensor data. It is designed to facilitate effective visualization capabilities for a rapid and efficient structural condition assessment. The fourth development is designed to dynamically update the thermal comfort data in monitored buildings by integrating their BIM models with captured sensor data. The default range utilized in this development is based on the American Society of Heating, Refrigerating, and Air-Conditioning Engineers (ASHRAE) Standard. It is expected to provide a robust and practical tool for data collection, analysis, and visualization to facilitate intelligent monitoring of the thermal condition in buildings and help decision-makers take needed timely data-driven decisions. The fifth and last development is designed to alert IoT companies of malfunctioning of deployed sensors utilizing a BIM platform and a cloud database to process and transfer related actionable information.

Acknowledgments

I would like to express my sincere appreciation to my supervisors, Dr. Osama Moselhi, and Dr. Ashutosh Bagchi for their guidance, encouragement, and critical supervision. This thesis could not have been accomplished without their academic and personal advice.

I am grateful to my examining committee members — Dr. Amin Hammad, Dr. Khaled Galal, Dr. Anjali Awasthi, Dr Sang Hyeok Han, and Dr. Sheryl Staub-French for their comments and feedback which encouraged me to bring my work to its highest level.

The financial support of the Natural Sciences and Engineering Research Council of Canada (NSERC), the India-Canada Centre for Innovative Multidisciplinary Partnerships to Accelerate Community Transformation and Sustainability (IC-IMPACTS) Network, and Canadian National Railway is also gratefully acknowledged. I would like to acknowledge the collaboration of the industrial partner, RCM Solutions Modulaires, in conducting the field test.

Finally, I would like to express appreciation to my beloved family members, my wife, sons, and parents.

Table of Contents

List of Figures	xi
List of Tables.....	xiv
List of Nomenclature.....	xv
Chapter 1: Introduction and Organization of the Thesis	1
1.0. Introduction	1
1.1. Thesis Organization.....	4
Chapter 2: Identifying At-Risk Non-Structural Elements in Buildings using BIM: A Case Study Application	8
General.....	8
Abstract.....	8
2.1. Introduction	9
2.2. Proposed Methodology.....	10
2.3. Example Application	15
2.3.1. Building Characteristics.....	15
2.3.2. Seismic Risk Assessment of Non-Structural Elements	16
2.3.3. Non-Structural Elements with Higher Seismic Risk	18
2.3.4. Automatic Color-Coding of NSEs Based on Their Seismic Risk Score (CSA-S832)	22
2.4. Conclusion.....	24
References	25
Updated Literature Review and Related Materials.....	26
Chapter 3: Automated Damage Detection System for Prefabricated Building Modules during Transportation	29
General.....	29
Abstract.....	29

3.1. Introduction	31
3.2. Literature Review	33
3.3. Research Mission.....	37
3.4. Research Methodology	41
3.5. The System Framework.....	44
3.5.1. Hardware configuration of the system.....	44
3.5.2. Data Collection and Pre-processing.....	47
3.5.3. Damage sensitive feature extraction	48
3.5.4. Noise Elimination	48
3.5.5. Data Dimensionality Reduction.....	49
3.5.6. Pattern Recognition.....	50
3.6. Case Study	53
3.7. System Implementation	57
3.8. Validation	63
3.8.1. Damage Simulation on the Test Data	63
3.8.2. Evaluation of Clustering Methods Based on Proposed Scenarios	64
3.9. Evaluating the Accuracy of Different Clustering Algorithms.....	73
3.10. Sensor Failure Analysis Module.....	77
3.11. Discussion.....	79
3.12. Conclusion	85
References	87
Chapter 4: Development of a BIM-Based Data Management System for Structural Health Monitoring with application to Modular Buildings: A Case Study.....	95
General.....	95
Abstract.....	95

4.1. Introduction	97
4.2. BIM and its Role in the Modular Building Construction	101
4.3. SHM in Modular Buildings	102
4.4. Determining the Locations of Strain Sensors	104
4.5. Data Management Challenges in SHM Process	107
4.6. Research Methodology	108
4.7. The System Framework.....	111
4.7.1. The Conceptual Framework of Wireless Strain Monitoring System.....	111
4.7.2. SHM System Modeling in the BIM Model.....	114
4.7.3. Defining the Sensor Database Model	115
4.7.4. Connecting to the Database	118
4.7.5. Extracting Parameters from the BIM Model	118
4.7.6. BIM Model to the Database Linkage.....	118
4.7.7. Automatic Reading of Sensor Values from MySQL Database Server	119
4.7.8. Updating the Virtual Sensor Parameter in the BIM Model	119
4.7.9. Defining the Threshold Strain Value	120
4.7.10. Mapping a Virtual Sensor in the BIM Model to the intersecting Structural Framing Members	121
4.7.11. Color-Coding of Damage Structural BIM Element.....	121
4.8. Model Implementation	122
4.9. Discussion.....	131
4.10. Conclusions	133
References	135
Updated Literature Review and Related Materials.....	140
Chapter 5: Development of an IoT and BIM-Based Automated Alert System for Thermal Comfort Monitoring in Buildings	142

General.....	142
Abstract.....	142
5.1. Introduction	144
5.2. Literature Review	148
5.3. Thermal Comfort Assessment and Monitoring	154
5.4. Research Methodology	157
5.5. The System Framework.....	162
5.5.1. Hardware configuration of the system.....	162
5.5.2. Development of the BIM model	164
5.5.3. MySQL database.....	165
5.5.4. Extracting parameters from the BIM model	170
5.5.5. Connecting the BIM model to the database.....	171
5.5.6. Automatic reading of sensor values from MySQL database server	171
5.5.7. Updating the virtual sensors parameters in the BIM model	172
5.5.8. Defining the conditional statements and updating room parameters.....	172
5.6. System Implementation	174
5.7. Policy implication.....	183
5.8. Discussion.....	185
5.9. Conclusion	188
References	191
Updated Literature Review and Related Materials.....	200
Chapter 6: Integrating BIM into Sensor-based Facilities Management Operations.....	202
General.....	202
Abstract.....	202
6.1. Introduction	205

6.2. Building Information Modeling.....	207
6.3. Utilizing Building Information Modeling in Sensor-Based Facilities Management.....	208
6.4. Research Methodology	209
6.5. Integrating Sensor-Based Facilities Management with Building Information Modeling .	212
6.5.1. Placing sensors in the Building Information Modeling model	212
6.5.2. Creating a schedule of sensors used in the BIM model	213
6.6. Results	216
6.6.1. Discussion	222
6.7. Conclusion	224
References	225
Chapter 7: Summary and Conclusions	228
7.1. Summary.....	228
7.2. Conclusions	232
7.3. Limitations and future research	233
References	234

List of Figures

Figure 1-1: The scope of presented papers and their connection to each other	7
Figure 2-1: Hierarchy of the study	14
Figure 2-2: The BIM model of the case-study building with its non-structural elements	16
Figure 2-3: Color-coding of different ranges of seismic risk scores in the BIM model	22
Figure 2-4: Automatic updating the seismic risk score and the color of elements based on their location	23
Figure 2-3r: Color-coding of different ranges of seismic risk scores in the BIM model	28
Figure 3-1: Damages observed in the prefabricated building after transportation (Smith et al., 2007).....	39
Figure 3-2: The overall architecture of the developed monitoring system framework.....	41
Figure 3-3: The detailed architecture of the developed monitoring system framework	45
Figure 3-4: The PCA process	49
Figure 3-5: Sample of actual damages (cracks) on prefabricated individual modules caused by the transportation-induced forces	54
Figure 3-6: The transportation route of the instrumented prefabricated module	55
Figure 3-7: The instrumented prefabricated module’s floor plan and the monitoring systems’ position	55
Figure 3-8: The pictures of the instrumented prefabricated modules in the factory and installation site	56
Figure 3-9: Acceleration data plot for two monitoring system units	57
Figure 3-10: The RMS dataset	59
Figure 3-11: The number of RMS data points after noise elimination	59
Figure 3-12: The pair plot of the RMS dataset before and after noise elimination step	60
Figure 3-13: The PCs of the RMS dataset for each direction	61
Figure 3-14: The scatter plot of PCA data	62
Figure 3-15: The cluster resulting from <i>k-means</i> clustering	63
Figure 3-16: PCA plots based on different damage classifications	65
Figure 3-17: The optimum number of clusters for the first and third scenarios calculated by the Elbow method	66

Figure 3-18: The optimum number of clusters for the first and third scenarios calculated by the *silhouette* analysis67

Figure 3-19: *K-means* clustering classification result on the scenario 1 data68

Figure 3-20: *K-means* clustering classification result on the scenario two and scenario three data68

Figure 3-21: *Mean shift* clustering classification result on (a) scenario two and (b) scenario three data (b)..... 70

Figure 3-22: The *agglomerative* clustering classification result on the scenario two (a, c) and scenario three data (b, d)71

Figure 3-23: The *DBSCAN* clustering classification result on the scenario one, two and three (a, b, and c respectively).....73

Figure 3-24: The heat map plot used to show the correlation between the sensors78

Figure 3-25: The data points plot before and after PCA81

Figure 3-26: The high accuracy of *DBSCAN* clustering83

Figure 4-1: Random Vibration Profiles of Trucks (ASTM D4169 Truck Assurance Levels 1 to 3) 105

Figure 4-2: A sample of random vibration simulation of a pipe chassis module..... 106

Figure 4-3: Hierarchy of the steps in this study 112

Figure 4-4: The conceptual framework of a wireless strain monitoring system..... 113

Figure 4-5: Developing the BIM model and the virtual strain sensor..... 115

Figure 4-6: Automated generation of a schema and table for the strain gauge in database..... 116

Figure 4-7: ERD of the SHM System Database..... 117

Figure 4-8: The physical strain sensor reading introduced to the database 123

Figure 4-9: Automatic reading of strain sensor data and updating BIM model..... 124

Figure 4-10: Updating BIM parameter based on maximum strain value in $\mu\epsilon$ 125

Figure 4-11: Checking the intersection between the virtual sensor and the BIM structural element 126

Figure 4-12: Threshold strain value definition and color-coding of damaged structural BIM elements..... 128

Figure 4-13: 3D damage visualization of damaged structural BIM element 129

Figure 4-14: The workflow for integrating BIM into SHM process..... 130

Figure 5-1: Different levels of BIM (BIMtaskgroup, 2011) 149

Figure 5-2: Hierarchy of the study 160

Figure 5-3: Developed dataflow schema..... 161

Figure 5-4: DAQ system hardware used in this research..... 163

Figure 5-5: The instrumented office room, virtual sensors, and their parameters in the BIM model
..... 165

Figure 5-6: ERD of the Monitoring System Database 168

Figure 5-7: The overall workflow for integrating BIM into thermal comfort monitoring..... 169

Figure 5-8: Transferring sensors reading remotely to the database (18th-time interval)..... 175

Figure 5-9: Reading and sorting the second time-interval temperature data from the database.. 176

Figure 5-10: Setting the developed workflow to automatically update the system every 5 minutes
..... 177

Figure 5-11: Automatic updating of temperature sensor parameters in the BIM model 178

Figure 5-12: Picture of thermal comfort monitoring test setup in the second-time interval 179

Figure 5-13: Screenshots of BIM user interface: (a) first time interval (b) 18th time interval 180

Figure 5-14: Temperature_measurement_history table data at the end of the test 181

Figure 5-15: room table data at the end of the test..... 182

Figure 5-16: Temperature recording map in the instrumented office 182

Figure 5-17: The data representation of the instrumented room in the cloud (a) with a smartphone
(b) 184

Figure 6-1: 3D view of the case-study building..... 211

Figure 6-2: Developed dataflow schema..... 211

Figure 6-3: Visualization of sensors in 2D and 3D views in the BIM model 214

Figure 6-4: Sensor schedule table created in the BIM model and location of sensors in 2D view
..... 215

Figure 6-5: Extracting, combining, and sorting room information from the BIM model..... 218

Figure 6-6: Extracting, combining, and sorting sensor information from the BIM model 219

Figure 6-7: Integrating BIM model into a cloud-based database..... 220

Figure 6-8: Updating some of the parameters of sensor and room elements in the BIM model . 221

Figure 6-9: Real-time notification and updating of rooms and sensors status in a cloud database
..... 221

List of Tables

Table 2-1: The indices for determining vulnerability index, (R), for NSEs (CSA-S832, 2014)....	12
Table 2-2: The indices for determining consequence index, (C), for NSEs (CSA-S832, 2014) ...	13
Table 2-3: Parameters for seismic risk assessment of non-structural elements according to FEMA-E-74 Standard (2011).....	14
Table 2-4: List of all types of NSEs used for this study	15
Table 2-5: Samples of seismic risk index tables created in Revit for ceiling and diffusers.....	17
Table 2-6: Seismic risk assessment of non-structural elements with high seismic risk (RS)	21
Table 3-1: The proposed scenarios description.....	64
Table 3-2: The structure of <i>confusion matrix</i>	74
Table 3-3: The accuracy performance of different clustering algorithms for different sizes of the event in case of existing one level of damage.....	75
Table 3-4: The accuracy performance of different clustering algorithms for different sizes of the event in case of existing two levels of damage	76
Table 3-5: The correlation between different sensors	79
Table 5-1: Previous studies on a BIM-based sensor-integrated solution.....	152
Table 5-2: Acceptable operative temperature ranges (ASHRAE Standard 55, 2017)	155
Table 5-3: Acceptable operative temperature ranges in the wintertime used in this study.....	158
Table 5-4: Specifications of Sensors (Waspmote datasheets, 2012).....	163
Table 5-5: MySQL database model specifications used in this study.....	166
Table 5-6: Classification of office rooms based on their thermal comfort level and color.....	179
Table 6-1: Types of sensors used in this study.....	213

List of Nomenclature

AEC	Architecture, Engineering and Construction
API	Application Programming Interface
BIM	Building Information Modeling
SHM	Structural Health Monitoring
IoT	Internet of Things
DAQ	Data Acquisition
NSEs	Non-Structural Elements
TVA	Threshold Value Analysis
BMS	Building Management System
3D	Three Dimensions: x, y, z
ASHRAE	American Society of Heating, Refrigerating, and Air-Conditioning Engineers
FM	Facility Management
HVAC	Heating, ventilation, and air conditioning
FEMA	The Federal Emergency Management Agency
ASCE	The American Society of Civil Engineers
CSA	Canadian Standards Association
IFC	Industry Foundation Classes

OFC	Operational and Functional Component
NBCC	National Building Code of Canada
LS	Life safety
PL	Property Loss
FL	Functional Loss
NE	Non-engineered
PR	Prescriptive
ER	Engineering Required
MEP	Mechanical, Electrical and Plumbing
RS	Risk Score
RMS	Root Mean Square
DBSCAN	Density-Based Spatial Clustering of Applications with Noise
FEM	Finite Element Modeling
K-NN	K-Nearest Neighbors
2D	Two Dimensions: x, y
MSC	Mean Shift Clustering
PPV	Particle Peak Velocities
PCA	Principal Component Analysis

SI	Silhouette Index
MEMs	Micro-Electro-Mechanical System
KDE	Kernel Density Estimation
SSE	Sum of Squared Errors
TP	True Positive
TN	True Negative
FP	False Positive
FN	False Negative
LCF	Local connection failure
LVDT	Linear Variable Displacement Transducer
PSD	Power Spectral Density
SDMS	SHM Data Management System
ERD	Entity Relationship Diagram
IAQ	Indoor Air Quality
CCOHS	Canadian Centre for Occupational Health and Safety
EPBD	European Energy Performance of Buildings Directive
IECC	International Energy Conservation Code
IAI	International Alliance for Interoperability

HSE	Health and Safety Executive
PMV	Predictive Mean Vote
PLC	Programmable Logic Controller
HMI	Human-Machine Interface
SCADA	Supervisory Control and Data Acquisition
NIST	National Institute of Standards and Technology

Chapter 1: Introduction and Organization of the Thesis

1.0. Introduction

Most industries have experienced noticeable changes in recent decades, focusing on utilizing digital transformation to achieve higher levels of efficiency. There is also an increasing implementation of digital technologies in the construction industry. From the overview of academic research, research analysis reveals increasing implementation and adoption of digital technologies for construction operations (Morgan, 2019; Pan et al., 2020). The McKinsey Global Institute (2017) research indicates that digital transformation can lead to 14 to 15 percent productivity gains and 4 to 6 percent cost reductions. However, the transformation effects encompassing digital technology implementation are yet to be fully utilized within the architectural, engineering, and construction (AEC) industry. There has been some hesitation about fully embracing the latest technological opportunities. It has been recently recognized that the construction industry is close to a “major” digital technology implementation (Murray, 2018; Autodesk, 2020) despite anticipated difficulties. Although the implementation of digital technologies such as BIM, IoT, SHM, laser scanning, prefabrication, and machine learning solutions throughout the built asset lifecycle are expected to boost productivity and enhance project performance and safety (Agarwal et al., 2016), they may lead to new challenges, such as, poor digital skills amongst the workforce, which was cited as a significant limiting factor to the adoption of processes such as BIM by the fifth annual Construction Manager BIM survey (2020), resistance to change etc. On the other hand, there is still a lack of automated tools to support digital transformation over the project life cycle.

The aim of this research is to develop a set of automated management solutions to address the issues highlighted above by supporting digital transformation over the building project life cycle. And accordingly help facility managers to increase the efficiency of buildings’

operations in terms of occupants' safety and indoor air quality, and help management teams in reliable delivery of modular and off-site construction. To achieve the aim of this thesis, the following main objectives and tasks were undertaken, which are briefly listed below:

1. Developing a standardized framework for visualizing and prioritizing the seismic risk level of Non-Structural Elements (NSEs) in buildings using BIM.
 - Creating a BIM model with all NSEs and developing a framework to link between NSEs BIM elements and their seismic risk score to be able to prioritize and identify the most hazardous elements and automatically update their seismic risk score based on their position and type.
2. Developing a Multi-functional data-driven SHM system for monitoring prefabricated building modules during transportation
 - Developing a cost-effective sensor-based DAQ and storage module to be easily attached to the prefabricated modules to monitor them during transportation.
 - Developing a novel and effective visualization-based method to identify the failed sensors before starting the data analysis.
 - Developing a data analysis method to identify and classify different levels of damage that might occur on prefabricated modules during transportation.
 - Comparing and evaluating the performance of different clustering algorithms using *accuracy score* and *confusion matrix* to identify the algorithm with the highest damage identification and classification accuracy in the case of transportation monitoring through a real case study.
 - Validating the developed monitoring system through a real case study (two prefabricated modules).

3. Developing a workflow to integrate BIM into the SHM process to represent and access sensor data, run a data interpretation or damage assessment process, and map it on the corresponding virtual building components.
 - Creating sensory system components in the BIM model with all essential monitoring parameters.
 - Designing a specific relational database model to embody the SHM sensor measurement.
 - Proposing a conceptual framework of the wireless strain monitoring system.
 - Developing a workflow including eight modules to have a near real-time BIM-based monitoring system visualization using Threshold Value Analysis (TVA) method.
4. Developing an IoT and BIM-based automated alert system for thermal comfort monitoring in buildings
 - Developing a cost-effective wireless monitoring system to measure temperature and humidity level of indoor spaces.
 - Designing a specific relational database model to embody the thermal monitoring measurements.
 - Developing an integrated workflow, including nine major modules, to compile, standardize, integrate, and visualize monitoring data in a BIM environment to have a self-updating BIM model to provide real-time thermal condition monitoring
5. Developing an integrated BIM-based framework for alert generation in the events of malfunctioning Facility Management (FM) sensors in smart IoT environments.
 - Creating a BIM model with FM-related sensors with all associated parameters.
 - Developing a workflow to integrate the associated sensors and maintenance-related information into a cloud-based tool.

1.1. Thesis Organization

The present thesis is organized as a manuscript-based thesis that has a collection of five journal manuscripts produced as a result of the research conducted. The primary purposes of this research are to develop primarily BIM-based and sensor driven automated methods for efficient monitoring and management of occupants' thermal comfort in built facilities in a cost-efficient manner, and assist facility managers in tracking and transferring the status of the monitoring sensors needed for the methods referred to above. This chapter provides a brief introduction and background, problem statement, research motivation, objectives, brief description of developed methods, and thesis organization.

This thesis is organized into seven Chapters. The methodologies and research findings are elaborated in the five journal manuscripts provided in Chapters 2 to 6, respectively. The current chapter also discusses how the manuscripts in Chapters 2 to 6 are connected to achieve the proposed objectives. In keeping with common practice in preparation of manuscript-based theses, published papers are presented as is, along with an added section on updated literature review.

The first manuscript, Valinejadshoubi et al. (2018), is provided in Chapter 2 and was published in the Journal of Earthquake Engineering. The paper describes a newly developed framework for automated seismic risk assessment of NSEs in buildings using BIM. The end-users of the developed method presented in this manuscript are facility managers and their staff by enabling them to identify, visualize, quantify, and prioritize the most vulnerable NSEs in built facilities to apply suitable risk mitigation measures. The outputs of this paper can also be potentially expanded to the case of prefabricated building modules to identify the most vulnerable NSEs against transportation vibration forces.

The third Chapter presents the second manuscript, Valinejadshoubi et al. (2021), submitted to the Journal of Automation in Construction. It focuses on the development of SHM tools to assess transportation-induced damage in prefabricated building modules for offsite construction to improve the reliability of the modules' delivery. This paper developed a novel data-driven SHM tool to monitor the structural behavior of individual prefabricated building modules during transportation to ascertain their safe delivery. This multi-functional tool can be used for different purposes, such as structural damage detection and sensor failure analysis, leading to a safer delivery of construction projects, primarily in modular construction projects. The developed tool provides reliable delivery for modular construction projects, supports manufacturers' claim on repair and modification costs from the insurance company, and improves the customer perceptions of the quality of prefab construction. After building modules were delivered and installed, management of the operational phase of the building begins with a focus on the structural safety of constructed facilities and occupants' satisfaction as described in the third, fourth and fifth papers.

The fourth Chapter presents the third manuscript, Valinejadshoubi et al. (2019), on developing an integrated BIM-based monitoring system for rapid detection of damaged critical elements during building operations with updated info about the current state of structural elements. This paper was accepted and published in the ASCE Journal of Computing in Civil Engineering. Such integration is essential for increasing the efficiency of SHM of buildings in the operational phase. The end-users of the developed tool are engineers and facility managers to interpret and assess the ongoing condition of critical structural elements during the building operation and identify hidden damaged elements for their timely replacement. It also supports them in providing all the maintenance and repair-related information about the damaged components.

Besides the structural health of a building during its operation, a building needs to provide healthy environment for its occupants in terms of thermal comfort and indoor environmental quality, which is the primary purpose of the fourth manuscript, presented in Chapter 5 of this thesis. The fourth paper, Valinejadshoubi et al. (2021), presents a developed IoT-BIM-based system that works as an alert tool for thermal comfort monitoring purposes in an indoor building space. This paper was accepted and published in the Journal of Sustainable Cities and Society. The developed tool is expected to provide a robust and practical tool for reliable data collection, analysis, and visualization to facilitate intelligent monitoring of the thermal condition in buildings and help decision-makers make faster and better decisions, which may help in maintaining the level of occupants' thermal comfort to a satisfactory level. The developed tool is expected to support facility managers and related decision-makers in remotely tracking the thermal condition status of building spaces and taking needed timely actions accordingly. These actions can be taken considering different reasons such as possible damages to the building envelop, overheating issues in prefabricated timber buildings, and HVAC system failure or malfunction.

Chapter 6 presents the fifth manuscript on developing a method for BIM-based integration of sensor data and their maintenance-related information into a cloud-based tool to provide a fast and efficient communication platform between the building facility manager and IoT companies for intelligent sensor management. This paper was published in the Journal of Facilities Management in 2021. The developed method is expected to improve the sensors' operation and maintenance plan during the building operational phase. The end-users of the developed workflow are facility managers to improve their communication and information sharing with involved IoT companies in management events of sensors' failure or malfunction.

The seventh and concluding chapter summarizes the overall primary findings of the performed research and its contributions. This chapter highlights how BIM is used in each chapter of this thesis. It also summarizes research limitations provides recommendations for future research. Figure 1-1 shows an overview of the scope of the five papers presented in this thesis and how they are interconnected to each other.

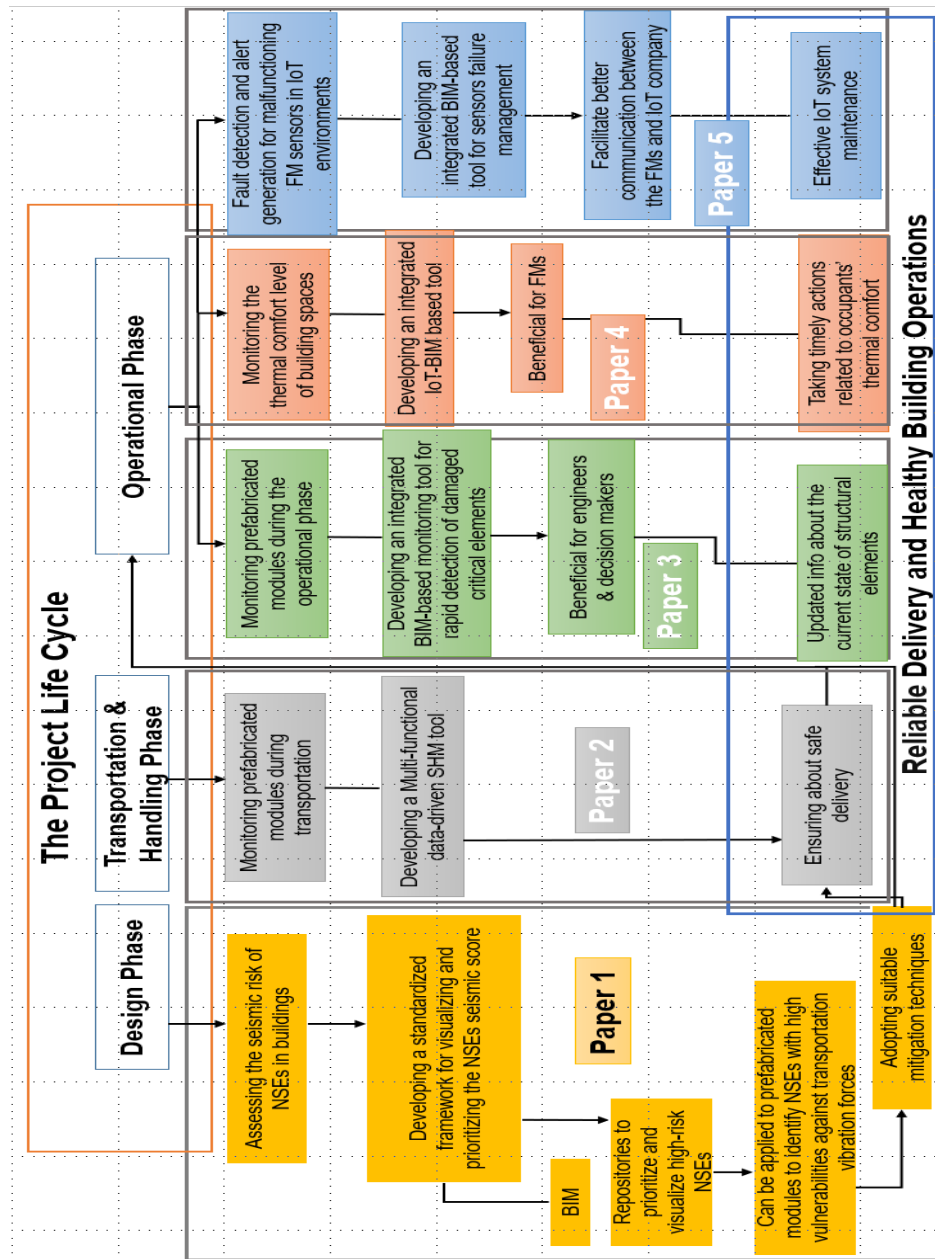


Figure 1-1: The scope of presented papers and their connection to each other

Chapter 2: Identifying At-Risk Non-Structural Elements in Buildings using BIM: A Case Study Application

General

In this chapter, the published paper is presented as is, followed by an updated literature review section. This paper was accepted and published in the journal of Earthquake Engineering in 2018*. The main objective of this paper is to integrate seismic risk evaluation with BIM to enable visualization and prioritization related to seismic risk levels of NSEs in built facilities.

Abstract

The non-structural elements (NSE) of a building could be hazardous in the event of an earthquake. Hence, a seismic risk assessment is critical for identifying hazardous elements. This paper proposes a method for visualizing a building's NSEs to assess their seismic risks using Building Information Modeling (BIM) to visualize and automatically mapping risk factors. The relevant Canadian and American standards were used to calculate the level of risk associated with each NSE for a typical six-story residential building.

Keywords: Non-Structural Elements, Seismic Risk Assessment; Building Information Modeling; Operational and Functional Component; Visualization

* Valinejadshoubi. M, Bagchi. A, and Moselhi. O, (2018), Journal of Earthquake Engineering, Vol 24. Issue 5, Pages 869-880

2.1. Introduction

Previous earthquakes have demonstrated that when buildings' non-structural components are not properly fastened, they can pose significant risk to the occupants' safety (FEMA 74, 2005; International Risk Management Institute, 2017). Observations from many earthquakes have shown that even though the structural elements are undamaged, extensive damage to Non-Structural Elements (NSE) can lead to injury or loss of life, and disruption of services (International Association for the Seismic Performance of Non-Structural Elements, 2015). Therefore, knowing the seismic risk level of NSEs in new and existing buildings could help to decide whether measures to mitigate risk are necessary. A three-dimensional (3D) visualization tool can improve communication between engineers and owners. Foo and Cheung (2004) demonstrated how to reduce the seismic risk of NSEs using the method provided in the relevant Canadian Standard (CSA-S832). Wang (2008) presented the CSA S832 seismic risk assessment procedures as a valuable tool in seismic risk assessment of both new and existing buildings. Seismic risk assessment methodologies provided in FEMA and ASCE (FEMA-E-74, 2011; ASCE/SEI, 2010) also provide necessary tools for mitigating the seismic risk of NSEs.

This study uses Building Information Modeling (BIM) to develop a seismic risk assessment framework for visualizing and mapping the seismic risk levels for NSEs in buildings based on existing Canadian (CSA-S832-14) and American (FEMA-E-74) standards. BIM provides a useful visualization tool for 3D digital representation of a building's physical characteristics. Recently, researchers used BIM to assess seismic risk of both structural and non-structural systems effectively. Welch et al. (2014) investigated BIM capabilities in the assessment and mitigation of seismic risks in buildings. BIM centralizes building data and its components, and then adds the

capability to create a 3D model and to exchange data with other software systems using the standard data format, Industrial Foundation Classes (IFC).

2.2. Proposed Methodology

First, an architectural model with all non-structural components and building contents is modeled in a BIM software, such as the Revit 2016 architectural template. Then, the model is linked to its mechanical components and plumbing system, such as water heaters, heating, ventilation, and air conditioning (HVAC) system (ducts and diffusers), and cold and hot water piping. After modeling the building's NSEs, their risk index (R) values are determined, using CSA-S832 and FEMA-E-74 standards, and assigned in the generated BIM model. The components with high-risk value (R) are identified and prioritized in the developed 3D and 2D visual models of the building's NSEs. Consequently, the level of seismic damage of the NSEs and related downtime and property losses (PLs) are brought to the attention of stakeholders for devising cost-effective seismic mitigation strategies. CSA-S832 (2014) is the standard for seismic risk reduction of NSEs in buildings in Canada. In this standard, NSEs are referred to as Operational and Functional Components (OFCs) of buildings and provides a procedure for determining the risk level corresponding to the significant seismic hazards as defined in the National Building Code of Canada (NBCC 2010) (International Risk Management Institute, 2017; Foo and Cheung, 2004). The CSA-S832 determines the seismic risk index of NSEs, R, in the following equation:

$$R = V \times C \quad (1)$$

Where V is the seismic vulnerability index, and C is the consequence index.

$$V = VG \times VB \times VE/10 \quad (2)$$

$$C = \sum (RS) \quad (3)$$

In Eq. (2), VG , VB , and VE indicate the ground motion characteristic index, the building characteristic index, and the OFC characteristic index, respectively. C is determined from the sum of the Rating Score (RS) related to the performance objectives. Table 2-1 and Table 2-2 show the indices used in determining the vulnerability (V) and consequence (C) indices.

The American standard of “FEMA-E-74 (2011)” is also used in the model to reduce the seismic risks of non-structural components in buildings. It provides a framework for the seismic risk rating of NSEs in buildings using indices, such as shaking intensity, life safety (LS) risk, PL risk, and functional loss (FL) risk. Shaking intensity is related to the location of the building and its prevailing low, moderate, or high ground motion. LS is the risk of being injured by non-structural components, while PL is the risk of incurring a repair or replacement cost to an item because of damage. FL represents the risk attributed to the malfunction of impacted components. Also, the standard includes the type of component detail and whether it is non-engineered (NE), prescriptive (PR), or engineering required (ER) (FEMA-E-74, 2011).

Table 2-3 describes the parameters needed for assessing the seismic risk of NSEs by the FEMA-E-74 standard. Figure 2-1 illustrates this study’s hierarchy.

Table 2-1: The indices for determining vulnerability index, (R), for NSEs (CSA-S832, 2014)

Vulnerability Index (V)	$V=VG \times VB \times VE/10$	VG (the ground motion characteristics index) = $F_a \times S_a(0.2)/1.25$	F_a = acceleration-based site coefficient as defined in NBCC $S_a(0.2)$ = spectral response acceleration value for a period of 0.2 s		
		VB: The building characteristics index	Based on predominant type of seismic force resisting system of the building structure. (e.g., for 6 stories reinforced concrete moment resistant frame built on site class D stiff soil 1.4) Table 4, CSA		
		VE: The NSE characteristics index	Obtained by the weighted sum of four rating scores ($\sum_{i=1}^4 (RS_i \times WFi)$) shown below:		
			Range	RS	WF
	NSE restraint (RS1)	Full restraint		1	4
		Partial restraint/questionable		5	4
		No restraint		10	4
	Impact/pounding (RS2)	Gap adequate		1	3
		Gap inadequate/questionable		10	3
	NSE overturning (RS3) h: distance from support or restraint to center of gravity or top of OFC d: horizontal distance between NSE supports	NSE fully restrained against overturning or $h/d \leq 1/(1.2F_a \times S_a(0.2))$		1	2
		$h/d > 1/(1.2F_a \times S_a(0.2))$		10	2
	NSE flexibility and location in building (RS4)	Stiff or flexible NSE on or below ground floor		1	1
		Stiff NSE above ground floor		5	1
		Flexible NSE above ground floor		10	1

Table 2-2: The indices for determining consequence index, (C), for NSEs (CSA-S832, 2014)

Consequence Index (C)	C=Σ(RS)	Parameter range	Rating Score (RS)
			Life safety (LS) [Mandatory]
		Threat to few ($1 < N < 10$)	5
		Threat to many ($N \geq 10$)	10
Limited Functionality (LF) [Higher than mandatory]		Not applicable or NSE breakdown greater than one week is tolerable	0
		NSE breakdown up to one week is tolerable	1
		NSE in high importance category building, not required to be fully functional	3
		NSE in post-disaster facility, not required to be fully functional	5
Full Functionality (FF) [Highest]		N/A	0
		NSE, required to be fully functional	10
Property Protection (PP) [Optional]		NSE damage can lead to financial losses related to asset damage, replacement, and in interruption business due to non-operational components Score may vary from 0 to 10 as determined by the owner/operator	0-10

Table 2-3: Parameters for seismic risk assessment of non-structural elements according to FEMA-E-74 Standard (2011)

<i>FEMA-E-74 Standard</i>	Shaking intensity: Low (L), Medium (M), High (H) Life safety (LS) Property Loss (PL) Functional Loss (FL) Type of detail: Non-engineered (NE), Prescriptive (PR), or Engineering Required (ER)
----------------------------------	--

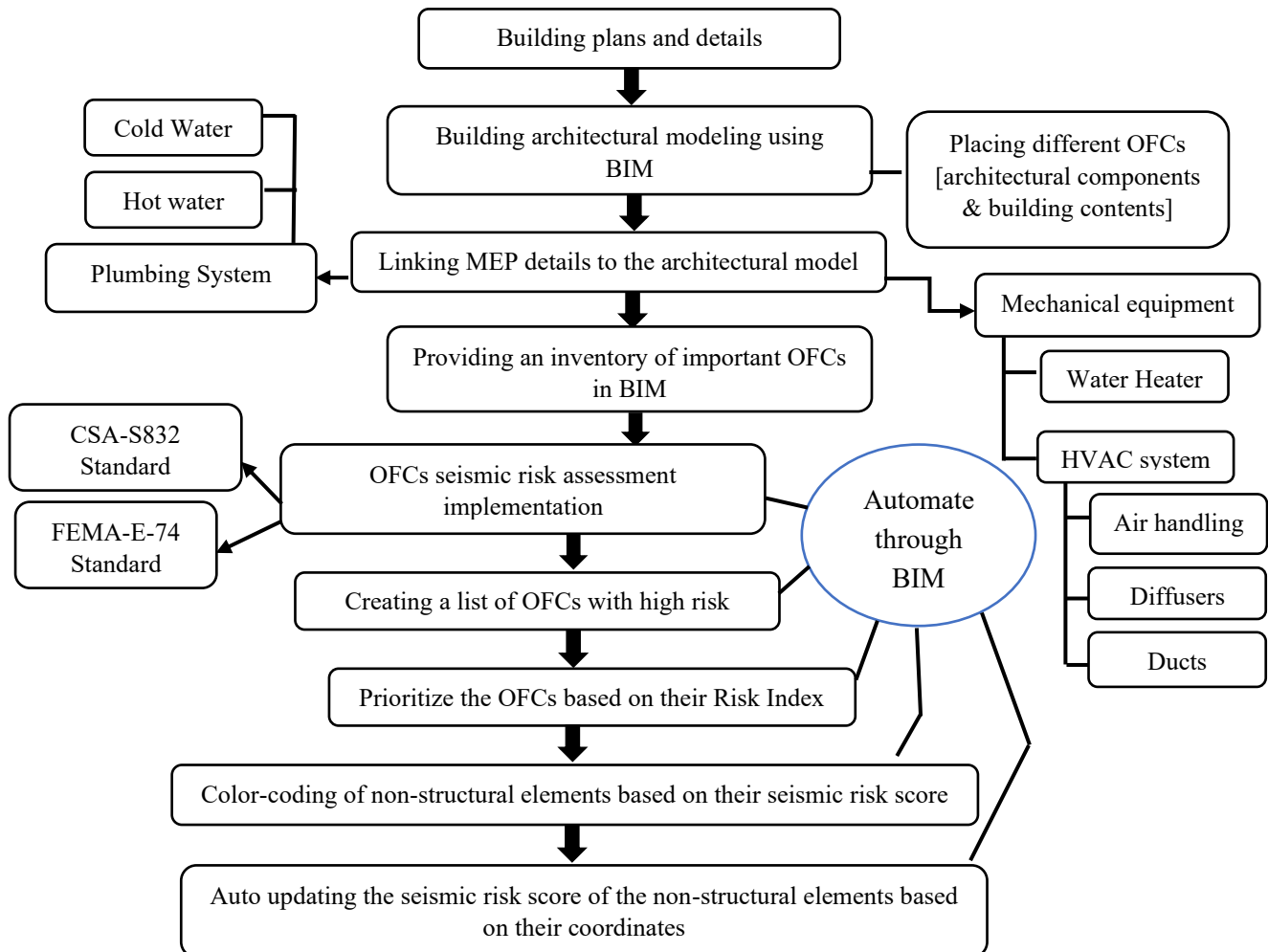


Figure 2-1: Hierarchy of the study

2.3. Example Application

2.3.1. Building Characteristics

For this study, we use a six-story reinforced concrete apartment building with moment resisting frames in the longitudinal and transversal directions founded on stiff soil. Moreover, the apartment building is assumed to be subjected to a seismic hazard level corresponding to that of Montreal, Canada. The building was modeled in Revit 2016, where different types of architectural components, building contents, mechanical equipment, and plumbing systems were considered. Pertinent assumptions relating to the type of attachment, flexibility, functionality, and so forth, for NSEs were based on standard practices in building construction. Table 2- 4 shows the kinds of NSEs used in this study.

Table 2-4: List of all types of NSEs used for this study

Category	Type	Assumptions
Building Contents	M-Entertainment center(shelving), (2743×762×2134mm)	Against the partition wall, free standing with no connection
Architectural Components	Suspended compound ceiling: 600×1200mm grid, outer layer: ceiling tile	Has no sway braces, tiles are tight to the walls, heavy duty suspended ceiling system
	Glazed curtain system panel	Not anchored, tight to the exterior walls
	Interior partition wall	attached to the suspended ceiling
	Parapet	Over public sidewalk, not anchored
	Windows	Tight to the exterior walls
Mechanical Equipment & Plumbing	Supply diffuser 600×600 face and 300×300 connection (HVAC)	Partially anchored to the ceiling, must be fully functional except for toilet
	Round HVAC duct	Partially seismic restraint
	Water heater	Full restraint, must be fully functional
	Pipes (hot and cold-water plumbing)	Partially seismic restraint, against the partition wall and ceiling, must be fully functional

2.3.2. Seismic Risk Assessment of Non-Structural Elements

Figure 2-2 shows the architectural plan and 3D model of the building, including the NSEs and the mechanical, electrical, and plumbing (MEP) details. After modeling the building and its NSEs, all indices needed for seismic risk assessment of the NSEs, including those required for determining the vulnerability index (V) and consequence index (C), were assigned to each corresponding element in the model to generate their seismic risk assessment tables in the architectural and the MEP model. CSA-S832 (2014) accords a risk index of 16 or below to a low level of seismic risk where no mitigation measures are required. For each NSE with a risk index higher than 16, an appropriate mitigation measure is needed, and its priority depends on its ranking relative to the other elements.

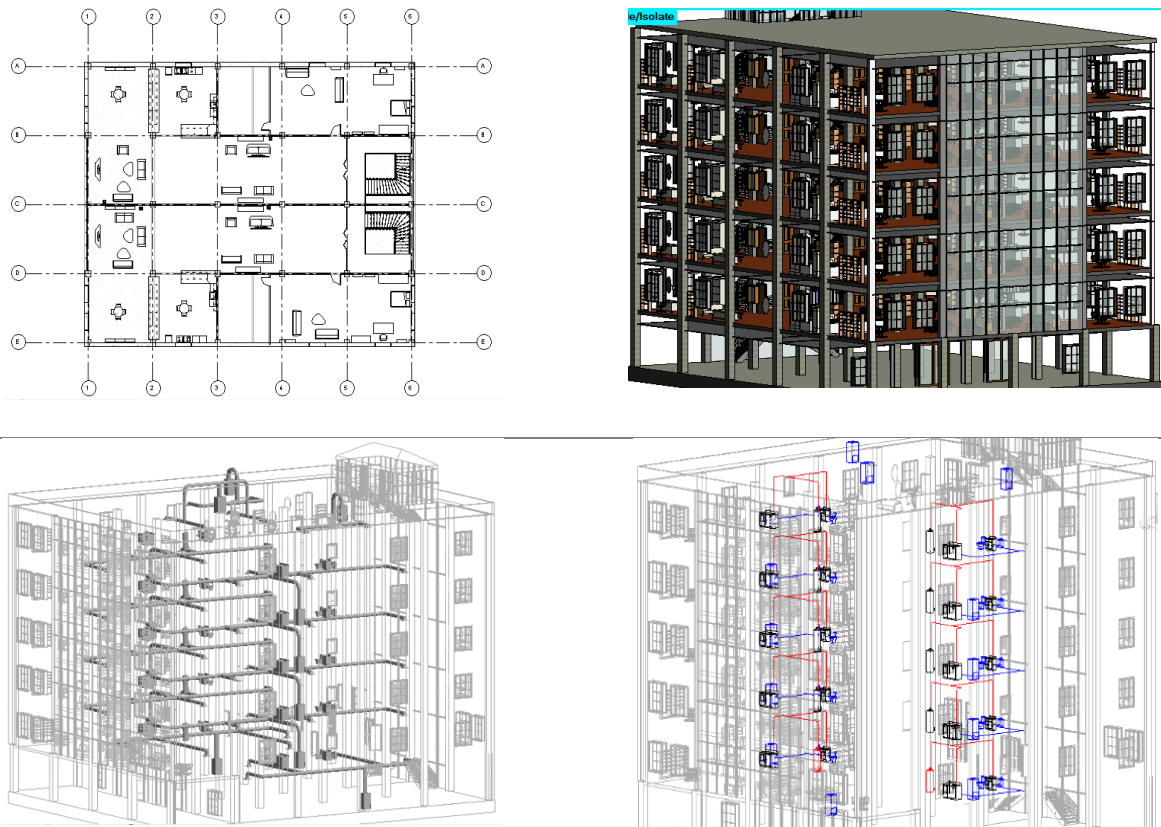


Figure 2-2: The BIM model of the case-study building with its non-structural elements

Table 2-5: Samples of seismic risk index tables created in Revit for ceiling and diffusers

A	B	C	D	E	F	G	H	I	J	K	L	M	N
Family	Level	Vulnerability Index	Consequence Index	Seismic Risk Index	F_a (D_i)	S_a (0.2)	VG (D_i)	VB	RS (R)	WF (R)	Weighted RS1	RS (I)	WF (I)
M_Supply Diffuser	Level 1	5.066342	15	75.995136	1.14	0.64	0.58	1.4	5	4	20	10	3
M_Supply Diffuser	Level 1	5.066342	15	75.995136	1.14	0.64	0.58	1.4	5	4	20	10	3
M_Supply Diffuser	Level 1	5.066342	15	75.995136	1.14	0.64	0.58	1.4	5	4	20	10	3
M_Supply Diffuser	Level 1	5.066342	15	75.995136	1.14	0.64	0.58	1.4	5	4	20	10	3
M_Supply Diffuser	Level 1	5.066342	15	75.995136	1.14	0.64	0.58	1.4	5	4	20	10	3
M_Supply Diffuser	Level 1	5.066342	11	55.729766	1.14	0.64	0.58	1.4	5	4	20	10	3
M_Supply Diffuser	Level 1	5.066342	11	55.729766	1.14	0.64	0.58	1.4	5	4	20	10	3
M_Supply Diffuser	Level 1	5.066342	11	55.729766	1.14	0.64	0.58	1.4	5	4	20	10	3
M_Supply Diffuser	Level 1	5.066342	2	10.132685	1.14	0.64	0.58	1.4	5	4	20	10	3
M_Supply Diffuser	Level 1	5.066342	2	10.132685	1.14	0.64	0.58	1.4	5	4	20	10	3
Family	Level	Vulnerability Index	Consequence Index	Seismic Risk Index	F_o	S_a (0.2)	VG	VB	RS (R)	WF (R)	Weighted RS1	RS (I)	WF (I)
Compound Ceiling	GF	6.700646	11	73.70711	1.14	0.64	0.58	1.4	10	4	40	10	3
Compound Ceiling	GF	6.700646	11	73.70711	1.14	0.64	0.58	1.4	10	4	40	10	3
Compound Ceiling	GF	6.700646	11	73.70711	1.14	0.64	0.58	1.4	10	4	40	10	3
Compound Ceiling	GF	6.700646	6	40.203878	1.14	0.64	0.58	1.4	10	4	40	10	3
Compound Ceiling	GF	6.700646	6	40.203878	1.14	0.64	0.58	1.4	10	4	40	10	3
Compound Ceiling	GF	6.700646	6	40.203878	1.14	0.64	0.58	1.4	10	4	40	10	3
Compound Ceiling	GF	6.700646	6	40.203878	1.14	0.64	0.58	1.4	10	4	40	10	3
Compound Ceiling	Level 1	6.700646	6	40.203878	1.14	0.64	0.58	1.4	10	4	40	10	3
Compound Ceiling	Level 1	6.700646	6	40.203878	1.14	0.64	0.58	1.4	10	4	40	10	3
Compound Ceiling	Level 1	6.700646	6	40.203878	1.14	0.64	0.58	1.4	10	4	40	10	3
Compound Ceiling	Level 1	6.700646	6	40.203878	1.14	0.64	0.58	1.4	10	4	40	10	3
Compound Ceiling	Level 1	6.700646	2	13.401293	1.14	0.64	0.58	1.4	10	4	40	10	3
Compound Ceiling	Level 1	6.700646	2	13.401293	1.14	0.64	0.58	1.4	10	4	40	10	3

Table 2-5 shows two samples of seismic risk assessment tables of building's NSEs created in the BIM model to assign the seismic risk rating to each NSE in the model. They were prioritized based on their risk index and those elements with seismic scores more than 16 were highlighted automatically in red using the conditional formatting defined in the model. In Montreal, the acceleration-based site coefficient, F_a is 1.14, and the spectral response acceleration (S_a) corresponding to the building period of 0.2s, is 0.64. The values of V_B for a six-story reinforced concrete moment resistant frame in site class D stiff soil is 1.4 according to CSA-S832 (2014). With these values, V_G is $F_a \times S_a (0.2)/1.25$ or 0.58, which is constant for all NSEs.

2.3.3. Non-Structural Elements with Higher Seismic Risk

Table 2-6 shows the seismic risks of the NSEs to the building rated using CSA-S832 and FEMA-E-74 standards. The seismic risk score (RS) can be used to assess the vulnerability of NSEs during an earthquake. The seismic risks of an NSE can be injury or loss of life, loss of function of the NSE, and direct and indirect financial setback. According to CSAS832, a seismic RS of less than 16 represents a low seismic risk, whereas a rating of 16–49 represents a moderate risk, and a rating larger than 49 represents a high risk. Therefore, the components with seismic RS exceeding 16 are shown in the table and were prioritized based on their respective score as the risk for those elements needs to be mitigated. The seismic RSs of the NSEs of the building, as shown in shown in Table 2-6, were calculated using Eqs. (1–3) corresponding to the CSA standard, the assumptions made in Table 2-4, and the indices determined from Tables 2-1 and 2-2. For example, the seismic RS of a curtain panel (east) was calculated as follows. Table 2-4 assumes that the glazed curtain panels are not anchored and are tight to the exterior walls. To determine R, the first vulnerability

index (V) and consequence index (C) need to be calculated. To calculate V, as shown in Table 2-1, three indices, VG, VB and VE must be determined. VG is dependent on the location of the building (Montreal) and VB is dependent on the type of building (e.g., six-story reinforced concrete moments resistant frame built on site class D stiff soil). VE is obtained from the weighted sum of four rating scores, RS1 (NSE restraint), RS2 (impact/pounding), RS3 (overturning), and RS4 (NSE flexibility and location in building). As assumed in Table 2-4, no restraint was used for the curtain panels. Therefore, the RS and weight factor, WF, are determined 10.0 and 4.0, respectively; RS1 was calculated at 40.0. Regarding RS2, it was also assumed that there is no gap between the curtain panels and the walls. Therefore, their RS and WF are taken as 10.0 and 3.0, respectively; RS2 is calculated at 30.0. Accordingly, RS and WF for RS3 and RS4 are 1.0, 2.0, and 10.0, 1.0, respectively. Therefore, VE (the NSE characteristic index) is calculated as 82.0. And consequently, V is calculated as 6.70 using Eq. (2). To calculate C, the LS and functionality indices are used, as shown in Table 3. Since the main entrance of the building faces east, and the curtain panels are used for the living rooms of the building, the damaged curtain walls may cause injury to people. Therefore, their RS for LS is determined as 10.0. The curtain panels are required to be fully functional because if they are damaged or broken due to an earthquake, the building may not be suitable for occupancy. Therefore, RS for functionality the index is assumed at 10.0 for the curtain panels, and C is calculated as 20.0 using Eq. (3). In this case, the total seismic RS is 134.0 using Eq. (1)

The last column of Table 2-6 shows the four indices required for seismic risk assessment of the NSEs of the building based on the FEMA-E-74 standard. In this column, the FEMA E-74 RSs of H, M, and L refer to high, medium, and low, respectively, as described in Table 2-3. For example, for the curtain panel in the east H, M, H, ER mean that its risks

associated with LS, PL, and FL are high, moderate, and high respectively; and ER implies that engineering parameters are required for its installation. Table 2-4 shows the assumptions made for risk assessment using both the Canadian and American standards. As seen in Table 2-6, the results provided by both methods are similar except for a few elements such as the diffuser. According to FEMA-E-74 (2011), in zones of moderate seismic hazard like Montreal, the risks associated with LS and PL resulting from diffusers are high. In the present case study, the risk of such diffusers is deemed medium since they are assumed to be partially anchored to the ceiling (Table 2-4). This also applies to shelving where the LS risk is usually high in a location with moderate seismic hazard but based on its position in the building and anchorage system, the LS risk is evaluated as low.

By developing a list of possible damage and mitigation techniques for high-risk NSEs, one can investigate what mitigation measures will be useful in reducing seismic risk. For instance, as shown in Table 2-6, according to the current assumptions, the glazed curtain wall panel in the east view has the highest seismic risk. Therefore, if vibration isolation is provided for the building's glazed curtain panels to control vibration due to earthquake, and if a type of glass that will shatter safely is used, its vulnerability index will be reduced to 4.5 and its seismic RS will be considerably decreased from 134 (High Risk) to 49.4 (almost Moderate Risk) (around a 63% reduction). Such changes in an element's seismic RS can be automatically updated and saved in the BIM after its consequence and vulnerability RSs have been modified.

Table 2-6: Seismic risk assessment of non-structural elements with high seismic risk (RS)

*(R – Restrained; I – Impact; O – Overturn; FX – Flexibility; LS – Life Safe; FO – Fully Operational, HR – High Risk, MR – Moderate Risk)

OFC	RS (R)*	WF (R)	W RS1	RS (I)*	WF (I)	W RS 2	RS (O)*	WF (O)	W RS 3	RS (FX)*	WF (FX)	W RS 4	VE	V	RS (LS)*	RS (FO)*	C	Seismic Risk Score	
																		CSA	FEMA
Curtain Panel (East)	10	4	40	10	3	30	1	2	2	10	1	10	82	6.7	10	10	20	134.0 HR	H, M, H, ER
Curtain Panel (West)	10	4	40	10	3	30	1	2	2	10	1	10	82	6.7	5	10	15	100.5 HR	M, M, H, ER
Interior Partition	10	4	40	10	3	30	1	2	2	10	1	10	82	6.7	5	10	15	100.5 HR	M, M, H, ER
Diffuser	5	4	20	10	3	30	1	2	2	10	1	10	62	5.1	5	10	15	76.0 HR	H, H,L,ER
Windows (except for toilet)	1	4	4	10	3	30	1	2	2	10	1	10	46	3.7	5	10	15	56.4 HR	M, M, H, NE
Hot water pipe (bath)	5	4	20	10	3	30	1	2	2	10	1	10	62	5.1	1	10	11	55.7 HR	L, M, H, ER
Parapet	10	4	40	1	3	3	10	2	20	5	1	5	68	5.5	10	0	10	55.6 HR	H, L, L, ER
Cold water pipe (bath)	5	4	20	10	3	30	1	2	2	10	1	10	62	5.1	0	10	10	50.7 HR	L, M, M, ER
HVAC duct (dining room)	5	4	20	1	3	3	1	2	2	10	1	10	35	2.9	5	10	15	42.9 MR	L, M, L, ER
Shelving (dining room)	10	4	40	10	3	30	10	2	20	10	1	10	100	8.2	5	0	5	40.8 MR	L, M, L, NE
Ceiling	10	4	40	10	3	30	1	2	2	10	1	10	82	6.7	5	1	6	40.2 MR	M, M, M, PR
Water heater	1	4	4	1	3	3	10	2	20	10	1	10	37	3.0	1	10	11	33.2 MR	M, H, L, PR
HVAC duct (Toilet)	5	4	20	1	3	3	1	2	2	10	1	10	35	2.9	1	10	11	31.5 MR	L, L, L, ER

2.3.4. Automatic Color-Coding of NSEs Based on Their Seismic Risk Score (CSA-S832)

The NSEs of the building are now represented by different colors based on their seismic RS. By color-coding the NSEs of the building, engineers and owners can visually assess the seismic risk condition of the building NSEs. For automatic color-coding of the NSEs based on their RSs, we used a visual programming tool called Dynamo BIM (2017). The seismic RSs for the NSEs were categorized and color coded into six ranges: white was used for seismic RS between 0 and 16, yellow was used for the seismic RSs between 30.0 and 60.0, and red was used for seismic RSs between 120.0 and 140.0. Figure 2-3 shows the color-based representation of the NSEs of the building's first level in the Revit model. As shown, the curtain panels represented in red have the highest seismic RS.

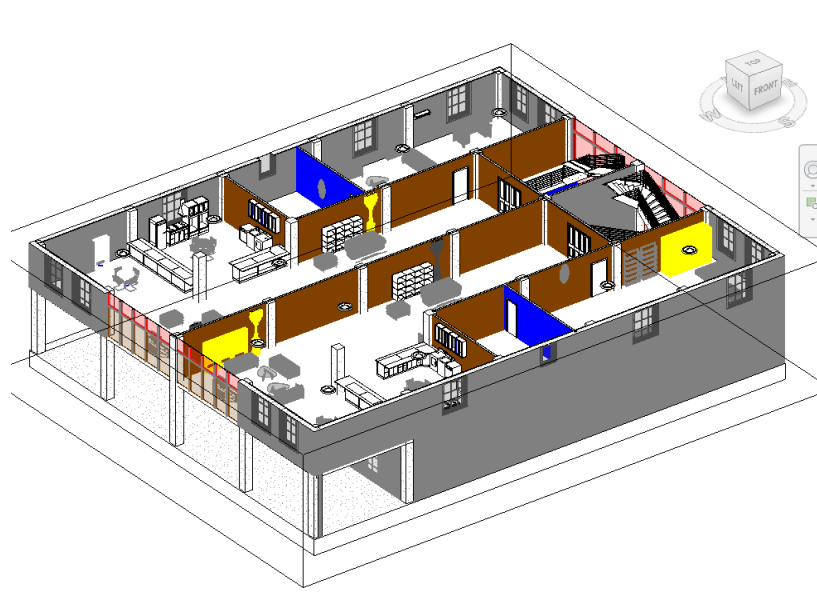
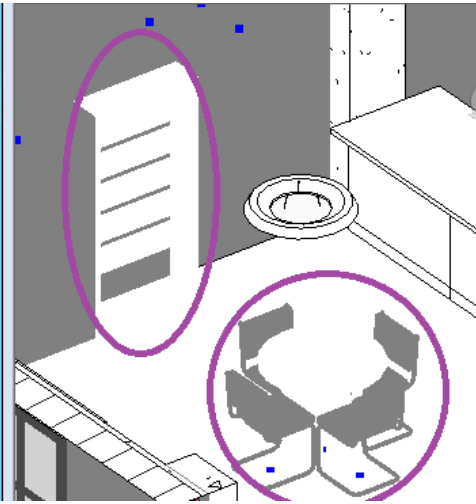


Figure 2-3: Color-coding of different ranges of seismic risk scores in the BIM model

The color-based representation of NSEs based on their seismic risk is an efficient way to visually identify the high-risk components and to study the effects of mitigation measures. For example, one parameter affected by the location of the NSEs can be the “LS RS”. If

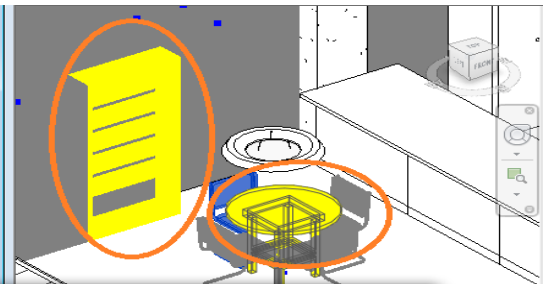
some NSEs, such as the shelving and dining room table as shown in Figure 2-4a are too close (e.g., less than the height of the shelving), according to the CSA-S832 standard the LS RS index is increased from one to five.

D	E	F	G
Family	Seismic Risk score	RS(Life safety)	Comments
Seating-Loung			null
Seating-Loung			null
M_Shelving	40.8576	5	Point(X = -12087.977, Y = 2050.403, Z = 4000.00
M_Shelving	40.8576	5	Point(X = -11172.977, Y = 2050.403, Z = 4000.00
M_Shelving	40.8576	5	Point(X = -10257.977, Y = 2050.403, Z = 4000.00
M_Entertainme	40.8576	5	Point(X = 14213.023, Y = 8860.403, Z = 4000.00
M_Entertainme	40.8576	5	Point(X = 14188.512, Y = -4136.397, Z = 4000.00
M_Table-Dining	8.17152	1	Point(X = -10354.659, Y = 11777.534, Z = 4000.0
M_Shelving	8.17152	1	Point(X = -12087.977, Y = 14110.403, Z = 4000.0
M_Shelving	8.17152	1	Point(X = -11172.977, Y = 14110.403, Z = 4000.0
M_Shelving	8.17152	1	Point(X = -10257.977, Y = 14110.403, Z = 4000.0
Shelving-Static	8.17152	1	Point(X = 11946.434, Y = 8642.003, Z = 4000.00
Shelving-Static	8.17152	1	Point(X = 10846.434, Y = 8642.003, Z = 4000.00
Shelving-Static	8.17152	1	Point(X = 11981.434, Y = -3749.997, Z = 4000.00
M_Shelving	8.17152	1	Point(X = 8872.023, Y = 14170.403, Z = 4000.00
M_Shelving	8.17152	1	Point(X = 14747.023, Y = 14170.403, Z = 4000.0



(a)

D	E	F	G
Family	Seismic Risk score	RS(Life safety)	Comments
Seating-Loung			null
Seating-Loung			null
M_Table-Dining	40.8576	5	Point(X = -9849.731, Y = 12562.194, Z = 4000.00
M_Shelving	40.8576	5	Point(X = -10257.977, Y = 14110.403, Z = 4000.0
M_Shelving	40.8576	5	Point(X = -12087.977, Y = 2050.403, Z = 4000.00
M_Shelving	40.8576	5	Point(X = -11172.977, Y = 2050.403, Z = 4000.00
M_Shelving	40.8576	5	Point(X = -10257.977, Y = 2050.403, Z = 4000.00
M_Entertainme	40.8576	5	Point(X = 14213.023, Y = 8860.403, Z = 4000.00
M_Entertainme	40.8576	5	Point(X = 14188.512, Y = -4136.397, Z = 4000.00
M_Shelving	8.17152	1	Point(X = -12087.977, Y = 14110.403, Z = 4000.0
M_Shelving	8.17152	1	Point(X = -11172.977, Y = 14110.403, Z = 4000.0



```

a // calculates difference between values
b dist = Math.Abs(a-b);
dist < 2000;
true
    
```

(b)

Figure 2-4: Automatic updating the seismic risk score and the color of elements based on their location

As shown in Figure 2-4a, the LS RS index of these two elements is one, and their seismic RS is 8.17. Therefore, they are represented in white. The distances of the shelving and dining table are 1.4 m and 1.18 m, respectively. In this case, the gap between the shelving and dining table is about 2.3 m. When the dining room table is moved closer to the shelving, the distance between them will be automatically updated in the BIM and so will the seismic score (Figure 2-4b). As shown in Figure 2-4b, when the dining room table was moved closer to the shelving, the LS RS was automatically updated to 5.0, the seismic RS was increased to 40.86, and consequently, the color changed from white to yellow. Automatic updating of the seismic RS of NSEs in the building model can be a useful tool for facilities managers to mitigate the seismic risk of the NSEs in buildings.

2.4. Conclusion

We proposed a method for BIM-based visualization using a 3D model of a building and its NSE with their corresponding seismic risk levels, location, and other related information. This paper's main contribution is the development of an easily understandable standardized framework for identifying and prioritizing the NSEs with high seismic risk by integrating the two relevant standards of CSA-S832 and FEMA-E-74 into a BIM. This method allows for an assessment of the seismic risk of an NSE in a building to be automatically updated based on the building's location and type. Integrating the seismic risk information of a building's NSEs into a visualization tool, allows for the interpretation of the data from a visual inspection after an earthquake to be easily integrated into the BIM model of a building and the assessment of different retrofit strategies. BIM models can be used as repositories to prioritize high-risk NSEs based on their likely damage, types,

and related retrofit actions. It improves the project participants' understanding of the vulnerability of NSEs in evaluating the seismic risk associated with NSEs in a building. The model can also capture the personnel involved and their responsibilities making management of retrofit actions efficient. The proposed method can potentially be applied to existing buildings to identify NSEs with high seismic risk potential such that suitable mitigation techniques can be adopted. It can also be used in the design stage for a new building. The paper demonstrated the BIM method utilizing a case study building and assessed the seismic risk of the OFCs or NSEs using the relevant Canadian and American standards. It should be noted that the proposed method is flexible regarding the standard or guidelines used for seismic risk assessment of NSEs, not restricted to those used for the demonstration.

References

- ASCE/SEI. (2010). "Minimum design loads for buildings and other structures." ASCE/SEI 7-10, American Society for Civil Engineers, Reston, VA.
- CSA-S832-14. (2014). "Seismic risk reduction of operational and functional components (OFCs) of buildings." Canadian Standard Association, CSA Group.
- Dynamo BIM. (2017), "Dynamo BIM – Community-driven Open-Source Graphical Programming for Design.". Retrieved from <http://dynamobim.org>.
- FEMA 74-FM. (sept 2005). "Earthquake Hazard Mitigation for Non-Structural Elements." Wiss, Janney, Elstner Associates, Inc.
- FEMA-E-74. (2011). "Reducing the Risks of Non-structural Earthquake Damage - A Practical Guide." U.S Department of Homeland Security, Federal Emergency Management Agency. Retrieved from <http://www.fema.gov/plan/prevent/earthquake/fema74/>.

Foo, S. and Cheung, M. (2004), “Seismic Risk Reduction of Operational and Functional Components of Buildings: Standard Development.” 13th World Conference on Earthquake Engineering, Vancouver, B. C., Canada, Page No.3432.

International Association for the Seismic Performance of Non-Structural Elements, SPONSE Association. (2015). “Special Issue on Seismic Performance of Non-Structural Elements in Buildings.”

International Risk Management Institute. (2017). “Earthquake Performance of Non-structural Components.” Retrieved from <https://www.irmi.com/articles/expert-commentary/earthquake-performance-of-nonstructural-components/>.

Wang, M. (2008). “Seismic Risk Assessment of Operational and Functional Components for New and Existing Buildings.”, the 14th World Conf. on Earthquake Engineering, Beijing, China.

Welch, D. P., Sullivan, T. J., and Filiatrault, A. (2014). “Potential of Building Information Modeling for Seismic Risk Mitigation in Buildings.” Bulletin of the New Zealand Society for Earthquake Engineering, 47(4): 253-263.

Updated Literature Review and Related Materials

This section focuses primarily on recent publications and related works not cited in the published paper above.

NSEs are more vulnerable against the vibration events such as earthquakes. The NSEs failure may lead to injury or loss of life. It might also lead to disruption of services during the operational phase or even during the transportation stage in modular construction projects, which is significant for public facilities such as hospitals, airports, and fire stations. The reports from

previous earthquakes have demonstrated extensive damages to NSEs, which led to the loss of their functionality (Miranda et al., 2012; Ricci et al., 2009; Filiatrault et al., 2001).

Developing a practical visual framework is critical to improving communication between engineers and owners to better understand most vulnerable NSEs. Despite the importance of better visualization and understanding of NSEs' vulnerability against vibration events, few studies have integrated it with an effective visualization tool such as BIM. Augulo et al. (2020) developed a methodology to use BIM for seismic performance assessment in a building. However, they only considered the structural elements, not NSEs, and utilized BIM only as an input into the FEM software for the structural analysis purpose. Perrone and Filiatrault (2017) developed a workflow for seismic design of NSEs using BIM. However, their study was not comprehensive (considered only a specific type of NSEs), and it did not benefit from the 3D visualization capability of BIM to highlight seismic vulnerability levels of NSEs, which might not be entirely understandable for non-experts.

As presented in this chapter, the developed method addressed these issues. Automatic seismic risk calculation and color-based representation of NSEs of a building in a BIM model is an efficient and fast method to identify high-risk components visually. As shown in Figure 2-3r (the updated version of Figure 2-3), NSEs are represented with different colors in the BIM model based on the pre-defined ranges of seismic risk as indicated in the figure legend.

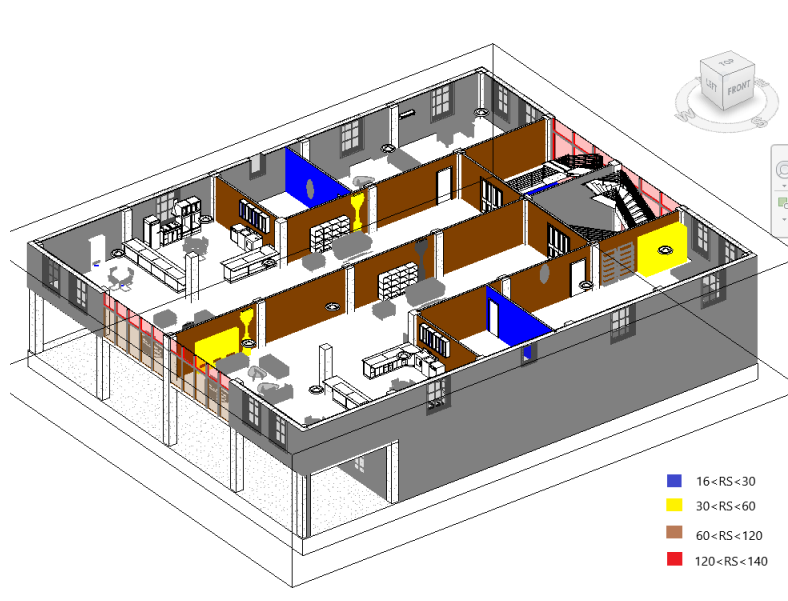


Figure 2-3r: Color-coding of different ranges of seismic risk scores in the BIM model

Chapter 3: Automated Damage Detection System for Prefabricated Building Modules during Transportation

General

This paper was submitted to the Journal of Automation in Construction in 2021*. The main objective of this paper is to develop a cost-effective sensor-based DAQ system and an efficient data analysis method to monitor and detect possible damage related to the structural condition of prefabricated modules during transportation.

Abstract

Transportation is a significant part of a prefabricated building module. The purpose of our research is to develop a novel data-driven structural health monitoring (SHM) system to monitor the structural condition of individual prefabricated building modules during transportation by detecting possible damages caused during their delivery. The developed system consists of two main components: a sensor-based data acquisition (DAQ) and storage module, (which measures and stores the acceleration response of the building module), and an automated data analysis module (which uses a data-driven approach to analyze the captured acceleration data and identify and classify damages). We explored the capability of the developed system via a real case study. We attached 8 vibration sensors to the walls and floors of a wooden prefabricated building module in the factory and monitored its structural behavior during road transport over 300 km. The accelerometer data were collected, cleaned, and preprocessed to extract damage-sensitive features

* Mojtaba Valinejadshoubi, Ashutosh Bagchi & Osama Moselhi (2021), Journal of Automation in Construction (under revision)

utilizing different data thresholds. The acceleration Root Mean Square (RMS) parameter, proved and used as an effective damage-sensitive feature in SHM projects, was used to derive a statistical pattern recognition algorithm for damage detection. We experimented with 4 common unsupervised clustering algorithms used in SHM studies to determine the best damage detection and classification process: k-means, mean shift, density-based spatial clustering of applications with noise (DBSCAN), and agglomerative clustering. After the initial analysis, we observed only one pattern of data, which meant that the building module was transported safely to the site. We established three different scenarios to simulate different levels of damage to the building modules. The performance of algorithms used in damage identification and classification was investigated by two parameters, *accuracy score* and *confusion matrix*. After detailed analysis based on different clustering algorithms, we found that the *DBSCAN* algorithm yielded the full accuracy score in the case of more than one level of damage compared with *k-means*, *mean shift*, and *agglomerative clustering* with accuracy scores of 0.81, 0.79, and 0.78 respectively. In the end, we developed a novel visualization-based method to identify the failed sensors. The system can allow for timely replacement of damaged parts of the prefabricated modules before installation, provide evidence to support manufacturers' insurance claims on repair and modification costs, and improve customer perceptions of the quality of prefab construction. However, the developed system should be tested further on more prefabricated building modules with a larger number of sensors.

Keywords: Modular construction; monitoring system; Structural Health Monitoring; Transportation phase; Clustering techniques, Damage sensitive feature.

3.1. Introduction

The construction industry is quite labor-intensive and is exposed to risks associated with markets, sites, and weather conditions (Boadu et al., 2020). Modular and offsite construction aims to address some of these issues. After the fabrication process, building modules are transported from the factory to the project site for installation. Transportation is a significant phase of modular construction that can affect the module delivery time and project completion (Sun et al., 2020). In North America, prefabricated modules are transported to the construction site (or to storage) on a flatbed tractor-trailer unit and are finally lifted and placed onto a pre-constructed foundation. The challenge during the transportation phase is that the building modules are subjected to additional stresses because of transportation-induced vibrational forces (Godbole et al., 2018). Vibrations imparted on the prefabricated modular building unit due to road unevenness have been experimentally quantified in (Innella et al., 2020). These additional stresses may damage individual modules, lead to rejection or rework at the building site, require additional resources and costs, and cause schedule delays because of mis-fitting and out-of-tolerance modules. Some manufacturers reported using up to 30% more reinforcing materials in modules to minimize damages arising from trucking (PATH Inventory, 2003). However, the amount and placement of the extra reinforcing materials are usually based on judgment rather than objective analysis. Inappropriate placement of reinforcing materials can lead to concentration of stresses at vulnerable locations, which may cause cracking in internal finishing materials.

The modules can be subjected to the road-induced vibrational forces caused by roughness originating from poorly finished roads, with design features such as construction joints, thermal expansion joints, and the presence of distress (such as cracks, bumps, potholes, corrugation, etc.). They may also be subjected to aggressive driving behavior such as lane changes, turns with or

without acceleration, sudden braking, rapid acceleration, and excess speed. Additionally, modules are also subjected to wind forces during transportation that can cause high-magnitude force for significant amounts of time (Gupta et al., 2008). The combination of transportation-induced vibrational forces and wind forces can produce more destructive effects, which can damage structural and non-structural components.

Even small amounts of transportation damage to building modules can disrupt the building envelope's continuity, causing substantial air leakage and moisture deposition, reducing its long-term durability, and causing mold problems and heat loss (Smith et al., 2007). From a structural perspective, transportation damages may impair the structural performance of the completed building. From a management perspective, transportation damages to building modules, if they are not detected and repaired right away, may lead to mis-alignment issues during the installation process, affecting the project's final delivery time and cost. Thus, shipping insurance is necessary so that the building modules are insured against all possible structural and non-structural damages to ensure compensation for the repair cost. Manufacturers usually buy shipping insurance to cover both all-risk and basic-risk conditions to ensure reimbursement for modules' repair costs if they are damaged. Basic-risk conditions cover collision, earthquake, cyclones, and other common losses, and all-risk coverage includes all possible risks (including partial and total loss) caused by physical loss or damage during door-to-door transit (Freight Insurance, 2003). In the case that damages are not detected on time before delivery, the repair cost might be very difficult to recoup from the insurance company because of the lack of timely evidence after delivery. Although transportation-induced damages to prefabricated building modules are possible, manufacturers rarely monitor prefabricated modules during transportation because of the monitoring costs and complexity. Therefore, utilizing a monitoring system is crucial for modular building manufacturers

to detect damaged modules after transportation and claim the insurance company's reimbursement for repair and modification costs.

3.2. Literature Review

Our literature review begins with the damage-related studies of prefabricated buildings and their limitations. It continues with a review of the classification methods and clustering algorithms studies that have been found to be more effective and practical in the cases of structural health monitoring (SHM) of prefabricated modules during transportation. Early damage detection is an initial and essential step in SHM that aims to evaluate a structure's overall condition and determine whether the damage is apparent throughout the structure.

Gupta et al. (2008) discussed preservice forces generated in a prefabricated wood light-frame building during handling and transportation based on field measurements and analyses. They investigated a single-story prefabricated mini home typical of those constructed throughout Canada and the USA as single-family dwellings. The only visible damages observed in this study were large cracks in the wall plasterboard radiating from corners of window and door openings and in the ceiling plasterboard. The cracks were detected based on visual inspections. The authors used finite element modeling (FEM) techniques to model the observed damages after transportation and validate their findings. Godbole et al. (2018) simulated the vertical motions experienced by the chassis of a truck trailer during transport. They concluded that a component mounting should be designed to withstand a vertical acceleration of the component. Bagchi et al. (2007) developed a FEM system for vibration-based damage identification in structures. Despite the impact of transportation-induced damages on the project cost and delivery time in modular construction projects (Lopez and Froese, 2016; Global Infrastructure Hub, 2020), very few studies, as discussed

above, have investigated the impact of transportation-induced forces on prefabricated buildings. Deformation is an essential parameter for localized damage detection. However, it was observed that deformations produced from FE models (a method for validating structural deformation data) were not consistent with those measured during the field test (Gupta et al., 2008) because of possible modeling errors and are not reliable for structural damage detection in the cases of transportation monitoring. For structural deformation monitoring, an excellent understanding of the structure is needed to design the instrumentation plan. If several similar types of members/connections exist (usually in prefabricated building modules), and if they are subjected to the same forces, identifying the most critical elements for monitoring may not be trivial, and planning to install one strain sensor (or more) on each element is not cost-effective. In such cases, global damage detection methods using vibration data could be more helpful and cost-effective as a smaller number of vibration sensors are required. Also, the previous studies and tests were on a prefabricated home, not on prefabricated individual modules. The FE method (physics-based approach) and deformation parameter might not be practical for monitoring the structural condition of individual prefabricated modules during transportation. The physics-based approach is costly, more computationally intensive, and can be complicated (Smarsly et al., 2016).

In modular building projects, individual modules are transported to the site. Using a physics-based approach is not practical because it would be very time-consuming and costly if numerical modeling is used and needs detailed data of each module in advance. Conversely, with the development of data acquisition (DAQ) and transmission technology, the SHM system's ability to collect data has increased over the years. Valinejadshoubi et al. (2018a) developed a building information model (BIM)-based data management system for SHM of modular buildings. In another study, researchers investigated the feasibility of using BIM in the SHM process

(Valinejadshoubi et al., 2017). They demonstrated the feasibility of creating and visualizing sensors data and information in the BIM model for SHM. Valinejadshoubi et al. (2018b) developed a preliminary scheme for utilizing BIM to manage SHM data for buildings. A significant amount of monitoring data is increasingly becoming available (Duan and Zhang, 2006). The management of the acceleration data captured during transportation, which may sometimes be hundreds of kilometers, can be a demanding task. Even with data compression and embedded systems to convert large quantities of data to more manageable amounts of information, there remains the need for procedures to manage the data (Brownjohn, 2005). Therefore, an appropriate approach such as a data-driven method is more valuable and practical for mitigating the above-mentioned issues.

Data-driven approaches are easier to implement, and generally less expensive, and are thus appealing for continuous monitoring (Catbas et al., 2011; Noman et al., 2012; Posenato et al., 2010). In a data-driven method, the difficulties lie in finding the physical meanings behind the model's outcomes and data visualization, given the high number of measurement points (Da Silva et al., 2007). The integrity of the sensor data needs to be preserved, specifically in a data-driven approach, to enhance the reliability and accuracy of the SHM system outputs (Smarsly et al., 2016). Because of the significant deviation or noise during measurement, it is essential to develop strategies for ensuring the reliability of the sensor data. For this reason, multiple sensors are usually employed rather than a single sensor to improve acquired information accuracy (Jafari, 2015). As a result, analyzing multi-channel sensors simultaneously increases the complexity of data analysis and reduces its speed. Another significant issue researchers have pointed out (Alamdari et al., 2017; Diez et al., 2016; Santos et al., 2015) is the non-availability of data from damaged states. SHM systems often only have data from the healthy conditions of structures. Thus, many contributors to the literature proposed damage detection methods based on unsupervised or one-class approaches.

Conventional classification methods include clustering algorithms (Amezquita-Sanchez and Adeli, 2015), that is, k-means, which is widely used in SHM. Pang et al. (2020) utilized the k-means algorithm as a classification technique to process the sensory data generated from full-scale seven-story reinforced concrete buildings to verify the classification performances. Agarwal and Reddy (2020) used different classifiers, including k-means clustering for the anomaly detection task. Diez et al. (2016) presented a clustering-based approach that incorporated K-Nearest Neighbors (K-NN) algorithm, k-means, and Fourier transform for vibration signal processing to detect damage and abnormal behavior in bridge joints. However, k-means is sensitive to the extracted data features and the initial choice of cluster centers (Bouzenad et al., 2019) that may lead to erroneous classifications (Amezquita-Sanchez and Adeli, 2015). Santos et al. (2016) presented an output-only technique based on mean shift clustering (MSC) to automatically discover an unknown number of clusters that correspond to the normal and stable-state conditions of a structure. However, the MSC performance suffers when the original distance metric fails to capture the underlying cluster structure (Anand et al., 2014). Silva et al. (2016) proposed an unsupervised cluster-based technique using agglomerative clustering to discern the structural response as a small number of structural states. Their proposed method revealed a better classification performance than the alternative one regarding false-positive and false-negative indications of damage, demonstrating its applicability for real SHM scenarios. Zhou et al. (2016) proposed a new approach for detecting structural damage using structural dynamic response and clustering techniques. They utilized agglomerative clustering to discriminate damaged patterns from undamaged ones. However, the hierarchical clustering algorithms, such as the agglomerative algorithm, have the disadvantage of low effectiveness and instability (Shi et al., 2020) and do not work with missing data, resulting in many arbitrary decisions. Entezari et al. (2018) presented a method based on the density-based spatial clustering of applications with noise (DBSCAN) clustering algorithm to

detect early damage using the vector of the sensitivity of modal strain energy as a damage-sensitive feature. Their results showed that the proposed sensitivity function is sensitive to damage and can be a reliable damage-sensitive feature in the applications of SHM. Entezami et al. (2020) introduced DBSCAN clustering to develop an innovative hybrid strategy for damage detection and localization. Li et al. (2020) utilized the DBSCAN algorithm in their proposed automatic modal parameter identification procedure and found robust enough to interpret the stabilization diagram.

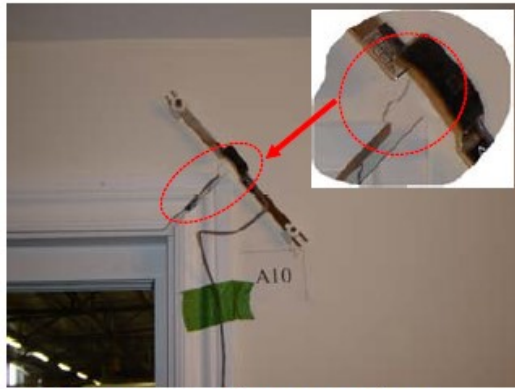
Although a significant amount of research has been done in studying the application of data-driven techniques in SHM of buildings and infrastructures, the development of statistical models (which are more practical than physical models), and the monitoring system to enhance the efficiency of the damage detection process in prefabricated building modules, especially during transportation, have received very little attention in the literature. Therefore, developing a data-driven-based framework for condition assessment of prefabricated modules during transportation can be helpful for the following reasons:

- a. To improve the damage detection process and allow for timely replacement of damaged parts of the prefabricated modules before installation.
- b. To provide evidence to support manufacturers' claims for repair and modification costs from insurance companies.
- c. To improve customers' perceptions of the quality of prefab construction.

3.3. Research Mission

Modular building design is more complicated than conventional design because of the different processes involved, such as manufacturing, transportation, and installation. Therefore, prefabricated modules are subjected to various loads in these processes in addition to

operational loads. Safe delivery of prefabricated building modules is critical for a successful modular building project. It improves customer perceptions of the quality of prefab construction and can prevent any adverse effects (caused by structural damages) during installation and operational phases. Damages can occur to sections or components of building modules during transportation. These damages can be costly to fix and may cause negative public perception of modular buildings. Based on Splittgerber (1978), damage due to vibration can occur for particle peak velocities (PPV) values ≥ 3 mm/s. Transportation monitoring of prefabricated mini home, conducted by Smith et al. (2007), revealed that the PPV values developed during transportation are much higher than for lifting processes. According to their study, based on PPV parameter values, in some locations of the instrumented prefabricated home, the ratio of the likelihood of transportation-related damage compared to damage during fabrication was more than 6, which indicates higher possibility of damage occurrence to prefabricated modules during transportation. Even small amounts of transportation damage to building modules can disrupt the building envelope's continuity, causing substantial air leakage and moisture deposition, thereby incurring long-term durability, mold, and heat loss problems (Smith et al., 2007). From a structural point of view, transportation damage may impair the structural performance of the completed building. From a management point of view, transportation damage to building modules, if not detected right away, can lead to misalignment issues during the installation process, affecting the project's delivery time and cost. Figure 3-1 shows some examples of damages that occurred on the prefabricated house in our example during transportation.



(a) corner of door opening



(b) ceiling opening (skylight)



(c) roof-to-ceiling junction

Figure 3-1: Damages observed in the prefabricated building after transportation (Smith et al., 2007)

Despite the importance of the transportation phase in modular building projects, studying the damage of modules during transportation has received the little attention. Moreover, researchers have not developed a cost-effective and rapid, automated SHM system to monitor prefabricated modules during transportation. Several factory-produced prefabricated modules may be transported daily to the construction site. Thus, using the popular FEM updating techniques (model-update methods) is costly (Smarsly et al., 2016) and impractical even sometimes not feasible. Therefore, a data-driven approach would be more helpful in these cases. There are some challenges in data-driven techniques, such as the need for many data points, the integrity of data,

the existence of noisy data in real SHM projects, the visualization of data (Da Silva et al., 2007), and the unavailability of data from the damaged structure (Alamdari et al., 2017; Diez et al., 2016; Santos et al., 2015). Developing a data-driven structural damage detection framework, which would address these challenges, is important to improve the damage detection process for the timely replacement of damaged module parts of before installation.

The main goal of our study is to develop a novel data-driven monitoring system to detect possible damages in prefabricated building modules after transportation. To achieve this goal, our objectives are as follows:

- a. To develop a sensor-based DAQ and storage module to be easily attached to the prefabricated modules to record and store acceleration data produced during transportation.
- b. To develop a novel and easily understandable visualization-based method to identify the failed sensors before starting the data analysis
- c. To test and evaluate the performance of different clustering algorithms to identify the algorithm with the highest damage identification and classification accuracy in the case of transportation monitoring via a real case study.

The system, we developed for this study, is intended to solve the issues that existed in previous studies (Gupta et al., 2008; Smith et al., 2007) such as the size of monitoring system (which is critical for monitoring individual prefabricated building modules during transportation), the cost and complexity of a model-based approach in the structural damage detection process, the inapplicability of a model-based approach (which is time consuming and requires detailed modeling data), and the possible uncertainties in loading data and temporary supports configurations (which might affect the outputs of a model-based approach in this case).

3.4. Research Methodology

The developed system was designed to monitor the structural health of individual building modules during transportation. It consists of two main components: a sensor-based DAQ system to acquire and store the captured vibrational data during transportation in the form of acceleration records, and a data-driven automated data analysis module to analyze the recorded acceleration data and identify damage accordingly. The DAQ system consists of ten components which the following section describes. The available sampling rate of the DAQ system to build the monitoring system was identified as 125 Hz. The data analysis module consists of six sub-modules: *data preprocessing*, *damage-sensitive feature extraction*, *noise elimination*, *dimensionality reduction*, *pattern recognition*, and *decision-making*. The Python programming language has been used here to code the submodules for the data analysis module. Figure 3-2 demonstrates the overall framework of the developed monitoring system.

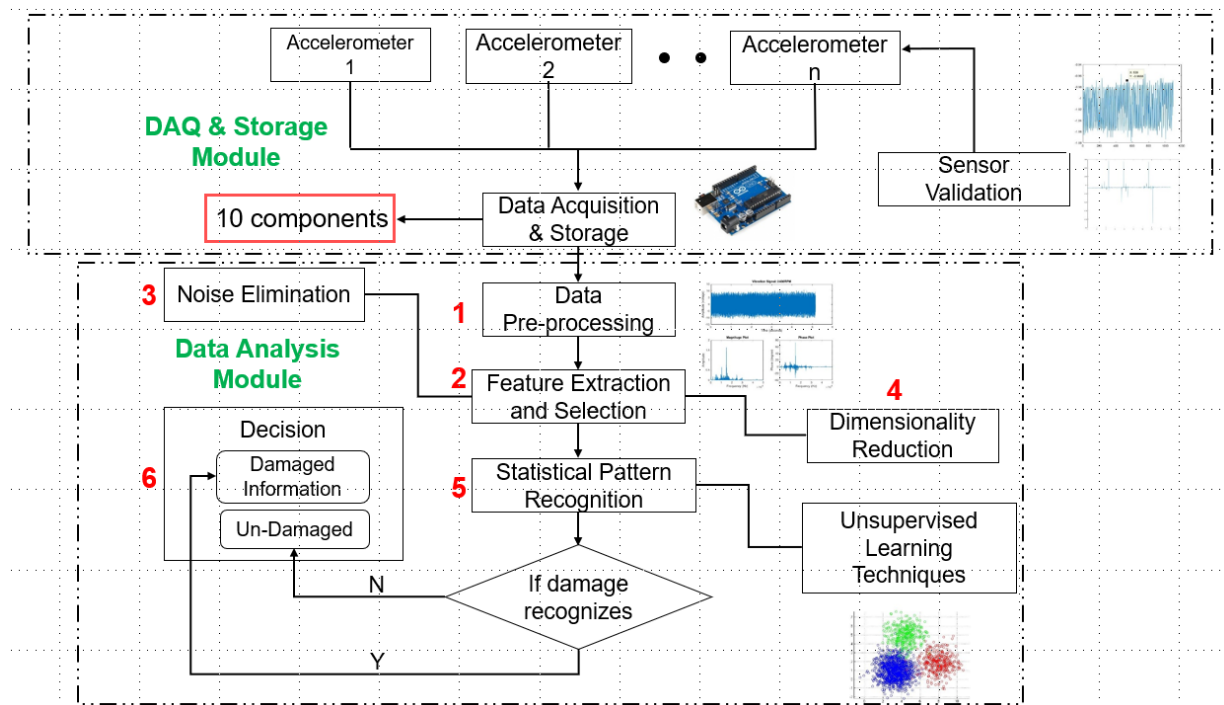


Figure 3-2: The overall architecture of the developed monitoring system framework

We attached the DAQ systems to the prefabricated modules at selected locations before transportation to collect and store transportation-induced vibrations in three directions using accelerometer sensors. When prefabricated modules were delivered to the site, we detached the sensors from them and analyzed the acceleration data recorded in the SD card. To amplify the reliability of readings, in each designated location, we used two sensors to increase the accuracy of acceleration data by averaging the two readings. Each of the six sub-modules are described below. Figure 3-3 shows the detailed architecture of the developed monitoring system framework.

1. Data preprocessing:

As shown in Figure 3-3, the sub-module contains defining and merging datasets, and data cleansing, a fundamental step for any machine learning technique. Datasets are defined, and missing values in each direction (X, Y, and Z) are replaced by the mean value, developing a robust model for our machine learning step.

2. Damage sensitive feature extraction:

The second step is to extract features sensitive to structural damages. Modal parameters, such as frequency and mode shape parameters, usually lead to the loss of information compared with the raw data, which can erase any small changes due to structural damages. Therefore, as a statistical parameter, we choose the root mean square (RMS) in our study as a damage-sensitive feature. RMS is directly associated with the vibration signal's energy level, which has been proved and used as a practical damage-sensitive feature in SHM studies (Avci et al., 2021). As indicated in Figure 3-3, acceleration data in three directions are classified based on the event size of 2500 data points, which means the prefabricated modules' structural characteristics over the truck during

the transportation was monitored and checked every 20s. Therefore, a new dataset of RMS data in XYZ directions is defined for the next step.

3. Noise Elimination:

The occurrences of noisy data in the data set can significantly affect the prediction of any meaningful information, leading to decreased classification accuracy and poor prediction results. As shown in Figure 3-3, in this sub-module, noise detection and removal are carried out using the quantile method (Han et al., 2012) to improve the quality of the dataset used in training and testing the machine learning algorithm used in this sub-module.

4. Data Dimensionality Reduction:

In this sub-module, principal component analysis (PCA) is used to decrease the dataset dimensionality from 3D to 2D for better visualization and decision making. PCA is an unsupervised linear transformation technique used to extract the critical information from the data and express it as a set of summary indices called principal components (Salem and Hussein, 2019; Jolliffe and Cadima, 2016).

5. Pattern Recognition:

Because there is no information about the damaged state of the building modules during transportation, unsupervised machine learning techniques are used. With an unsupervised training mode, detecting structural damages mainly depends on identifying abnormal data from the testing data. As shown in Figure 3-3, we use four clustering algorithms, *k-means*, *mean shift*, *DBSCAN*, and *agglomerative* in our study. The *elbow* method and *silhouette index (SI)* are used to optimize the number of clusters. For some clustering techniques, such as *mean shift* and *DBSCAN* clustering,

we search the optimum parameters' value by the trial-and-error method to discover which model's parameters' value resulted in the most skillful predictions.

6. Decision-Making:

When the clustering is implemented on the PCA dataset, the decision is made based on the number of detected clusters. If there are no separated, (i.e., compacted) clusters and we find only one pattern of data, then there is no damage found, indicating that the building module was transported safely to the site. Otherwise, some damages occurred to the building module. The damaged data clusters can be analyzed further to assess the size and location of damages.

Figure 3-3 shows the detailed architecture of the developed monitoring system framework.

3.5. The System Framework

3.5.1. Hardware configuration of the system

The developed DAQ system utilizes an accelerometer to monitor each module's dynamic characteristics during transportation to detect any possible damage before the delivery process.

The components of the system are as follows:

1. *Arduino Uno*: An Arduino Uno board is an open-source microcontroller board that works as the sensor's processing core.
2. *MPU6050*: An MPU6050 accelerometer consists of a 3-axis accelerometer with micro-electro-mechanical system (MEMs) technology. The sampling rate of the MP6050 in the developed system has been measured at 125 Hz.
3. *Data logger module*: A data logger module with 2GB micro-SD card is used for storing the vibration data for damage detection analysis.
4. *Battery*: A 9V battery is used to add a portability feature to monitoring system units.

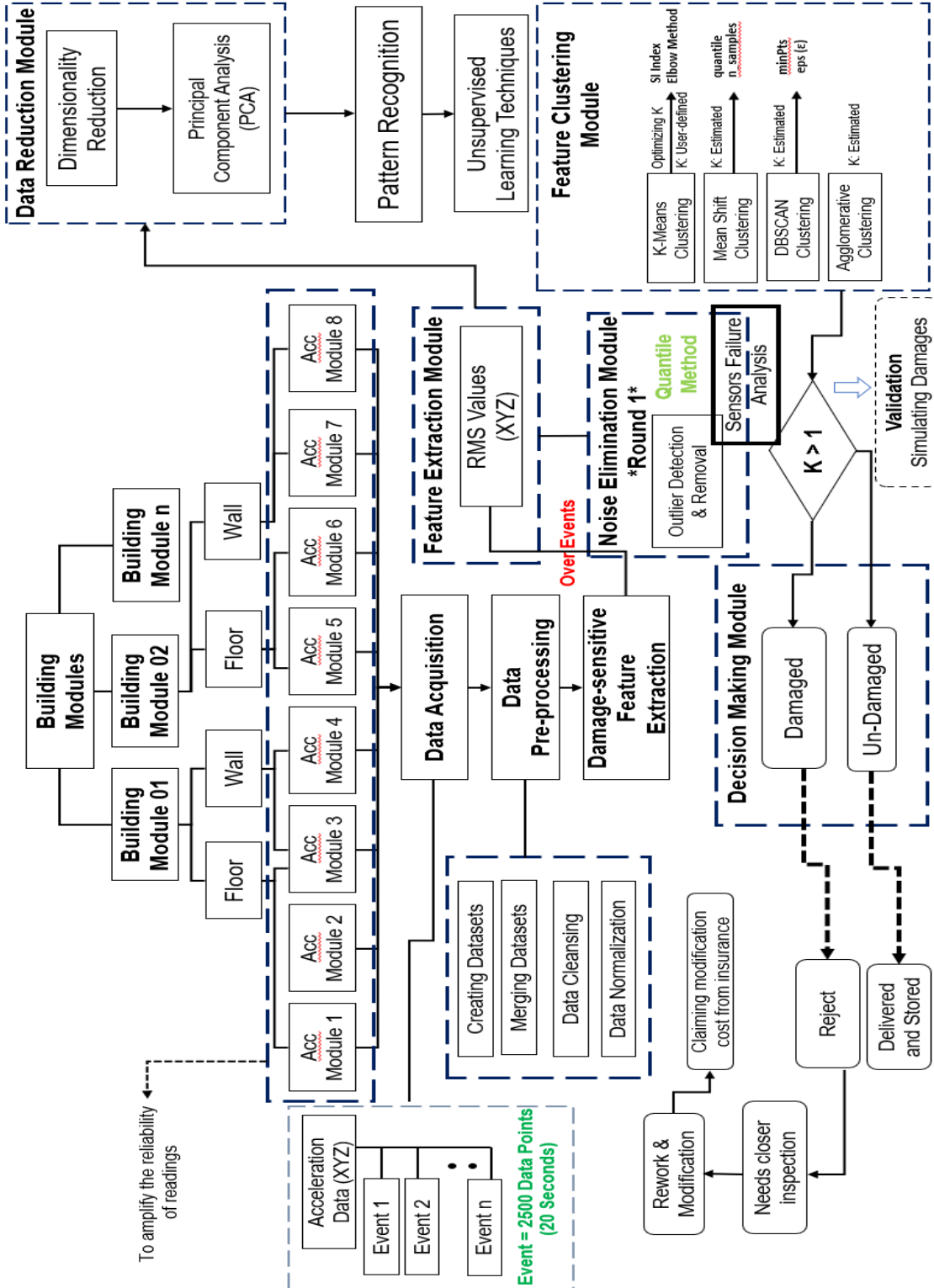


Figure 3-3: The detailed architecture of the developed monitoring system framework

5. *Switch*: An on-off switch is used to connect the battery to or disconnect it from the Arduino Uno board.
6. *Push buttons*: A push button is used to toggle between two operational states of the sensor.
7. *LED lights*: Red and green LED lights are used as indicators to show the system's operational state. When the switch turns on, the LED light turns red, indicating that the battery provides appropriate voltage for the Arduino board and peripherals. By pressing the push button, the LED light turns green, which shows the system is collecting the vibration data.
8. *Jumper wires*: Jumper wires connect the sensor and SD card module to the microcontroller and connect the microcontroller to the battery.
9. *Double-sided tape*: Double-sided tape is used to attach monitoring system units to the building modules.
10. *Protection box*: A protection box accommodates all the components and protects them against operational and environmental loads.

The hardware total cost is approximately \$100 CAD which is much more cost-effective than the alternative systems (shock and vibration sensors) used for monitoring shipments (EnDAQ, 2021; spotsee, 2021). Commercially available shock and vibration sensors (EnDAQ, 2021), produced to identify and respond to potential shipping hazards, use piezoelectric accelerometers that only allocate 32 kB of memory per "event," enough for 4,096 data points which are not suitable in the case of prefabricated building modules transportation where there are millions of data points available.

The switch supplies power for the Arduino Uno board in a fully assembled sensor with a functional battery. The Arduino Uno board's voltage regulator regulates and adjusts different

voltages to supply the main microcontroller and peripherals, including the SD card module and MPU6050 breakout board. A simple state machine controls the functionality of the components. Upon start, the red LED on the sensor box begins to blink, indicating the idle state of the sensor. It means the battery is providing appropriate voltage for the Arduino board and peripherals. The sensor should not remain in this state as the microcontroller and the peripherals are consuming power. After placing the protection box in the designated location, pressing the push button begins the sensor's sampling process. At this stage, the green LED on the board is "On" and the sensor goes through the following steps:

1. The microcontroller in the Arduino Uno board reads acceleration values for three directions (XYZ) through the I2C protocol and stores the acceleration values in its internal memory. Reading a sample from MPU6050 includes setting up some registers and reading the result from internal registers of MPU6050.
2. The microcontroller repeats step one 15 times.
3. After filling the internal memory, the microcontroller writes all the samples for 15 readings into the SD card.
4. The microcontroller returns to step one.

This process can be halted and restarted by the push button and the main switch. Switching off the device is considered a new reading in the memory, whereas the push button stops the sampling (push button stops cannot be seen in the log file). When the system starts working, the log file is created in the SD file, and X, Y, and Z data are separated by a tab (t) in each line.

3.5.2. Data Collection and Pre-processing

The data collection system stores acceleration data measured during transportation in an SD card. SD cards are removed from the system after transportation, and the acceleration data are

analyzed. The first step of data analysis is data preprocessing, where datasets are created, and missing values identified and filled by the mean value of acceleration readings in each direction.

3.5.3. Damage sensitive feature extraction

When the acceleration datasets are created and preprocessed, a damage-sensitive feature is extracted from the raw acceleration data in each direction. The structural behavior of the building modules is monitored and evaluated using $\bar{\mu}_{rms}$ per event during transportation. The $\bar{\mu}_{rms}$, as shown in the formula below, is the root-mean-square acceleration (or RMS acceleration) directly related to the energy level of the vibration signal. After calculating the RMS value for each event, new datasets are defined and merged to build a single comprehensive dataset.

$$\bar{\mu}_{rms} = \sqrt{\frac{1}{n} \sum_{i=1}^n y_i^2} \quad (1)$$

, where:

n is the number of data points in each event and

y is the acceleration data in XYZ directions.

3.5.4. Noise Elimination

The real-world data include meaningless data called *noise*, which can significantly affect various machine learning data analysis tasks such as classification and clustering. In this step, outliers are detected by the *quantile method* and removed from the datasets. Outliers are data

objects which their values are abnormally different (much higher or lower) from others (Han et al., 2021).

3.5.5. Data Dimensionality Reduction

The main idea of PCA is to reduce the dimensionality of a data set while retaining as much as possible of the variation the data set contains. This reduction is achieved by transforming data into a new set of variables, the *principal components (PCs)*, which are uncorrelated, and are ordered so that the first few retain most of the variation present in all the original variables (Salem and Hussein, 2019, Jolliffe and Cadima, 2016).

In this study, PCA is used to reduce the dimensionality of datasets from 3D to 2D for better visualization, and to remove the variance due to the environmental effect under the normal condition which can affect the damage detection process. Figure 3-4 shows the whole process of building a new sub-space based on principal components.

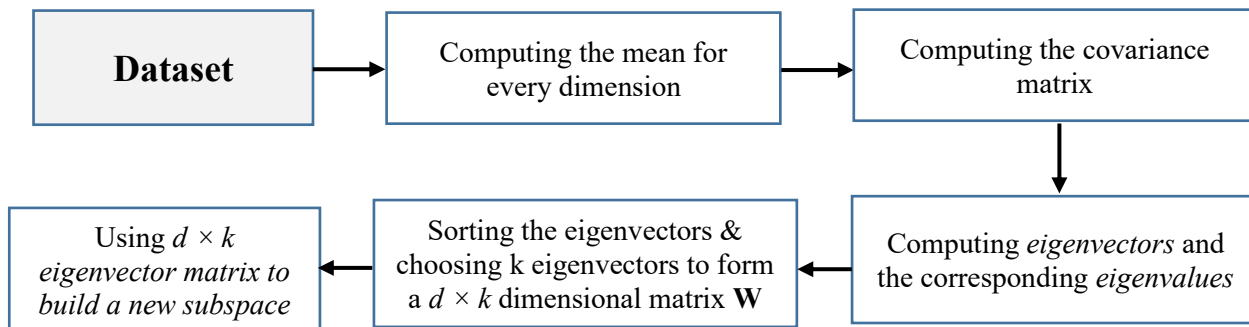


Figure 3-4: The PCA process

3.5.6. Pattern Recognition

As the most crucial unsupervised machine learning problem, the clustering technique is used to find a structure in a collection of unlabeled data. For pattern recognition, we use four clustering algorithms often found in the technical literature as popular for SHM projects, including *k-means*, *mean shift*, *DBSCAN*, and *agglomerative* clustering techniques. A cluster refers to a collection of data points aggregated together for certain similarities.

3.5.6.1. K-Means Clustering

The *k-means* algorithm is a partition-based clustering algorithm that searches for a pre-determined number of clusters within an unlabeled multidimensional dataset. It starts with the first group of randomly selected centroids used as the beginning points for every cluster and then optimizes the centroids' positions by performing iterative calculations. The *cluster center* is the arithmetic mean of all the points belonging to the cluster (Ali and Kadhum, 2017, Shukla and Naganna, 2014). Each point is closer to its cluster center than to other cluster centers. A critical part of the *k-means* clustering is choosing the number of clusters (K). The *elbow* and silhouette analysis methods optimize the number of clusters for the *k-means* clustering (Clayman et al., 2020; Horvat et al., 2021; Yuan and Yang, 2019; Syakur et al., 2018). The idea of the *elbow* method is to choose K at which the sum of squared error (*SSE*) or the sum of the squared distance between each member of the cluster and its centroid decreases abruptly.

$$SSE = \sum_{i=1}^n (y_i - f(x_i))^2 \quad (2)$$

Silhouette refers to a method that interprets consistency within data clusters. It represents how well each data point has been classified. The *SI*, which ranges from -1 to +1, is a measure of

how similar a data point is to its cluster than to other clusters. A higher SI value indicates that the data point is well matched to its cluster and poorly matched to neighboring clusters.

$$a(i) = \frac{1}{C_i - 1} \sum_{j \in C_i, i \neq j} d(i, j) \quad (3)$$

$$b(i) = \min_k \frac{1}{C_k} \sum_{j \in C_k} d(i, j) \quad (4)$$

where:

$a(i)$ is the mean distance between i and all other points in the same cluster.

$b(i)$ is the smallest mean distance of i to all points in any other cluster of which i is not a member (neighboring cluster (C_k), which has the smallest mean dissimilarity with the cluster i (C_i)).

$$s(i) = \frac{b(i) - a(i)}{\max(a(i), b(i))} \quad -1 \leq S(i) \leq 1 \quad (5)$$

where:

$s(i)$ is the *silhouette* value of data point i .

An $s(i)$ close to one means that the data is appropriately clustered. An $s(i)$ close to negative one means that the data is not appropriately clustered and belongs to its neighboring cluster.

3.5.6.2. Mean Shift Clustering

Mean shift clustering is a nonparametric, partition-based clustering technique that does not require prior knowledge of the number of clusters. The algorithm determines the number of clusters with respect to the data. It builds upon the concept of kernel density estimation (KDE), a

method to estimate the distribution in a dataset. It is also called a mode-seeking algorithm and is used to locate the maxima of a density function (Abdallah and Shimshoni, 2014). The strengths of mean shift clustering are that it does not assume any predefined shape on data clusters, and that it relies on choosing a single parameter: bandwidth.

3.5.6.3. DBSCAN Clustering

The density-based spatial clustering of applications with noise (*DBSCAN*) algorithm is a density-based, nonparametric clustering algorithm that groups data points close to one another based on two parameters: a distance measurement (*eps*) and a minimum number of points (*MinPoints*). If the distance between two points is lower or equal to the *eps* value, these points are considered neighbors. The *MinPoints* parameter is the number of points needed to form a dense region. Data points are classified as a core point (a point with at least *MinPoints* number of data points in its surrounding), a border point (a point which is reachable from a core point but with less than *MinPoints* number of data points in its surrounding), or an outlier (a point which is neither core point nor border point) based on *eps* and *MinPoints* parameters (Perafan-Lopez and Sierra-Perez, 2021; Deng, 2020).

Choosing good *eps* and *MinPoints* values is essential in the DBSCAN clustering algorithm. Selecting a minimal *eps* value prevents many data points from being clustered and makes them outliers and selecting a very high *eps* value leads to placing the majority of data points in the same cluster.

In general, small *eps* values are preferable. In contrast, larger *MinPoints* values are usually better, especially for the large dataset. One of the DBSCAN clustering algorithm's main strengths is that it is more efficient for arbitrary-shaped clusters. In contrast, partition-based and hierarchical clustering techniques are highly efficient with regular clusters.

3.5.6.4. Agglomerative Clustering

The *agglomerative* algorithm is a hierarchical clustering algorithm used to group objects in clusters based on their similarity. It works in a bottom-up manner, which means each data point is considered a single-element cluster initially. At each step, the two most similar clusters are combined into a new bigger cluster. The algorithm is iterated until all data points become a member of a single big cluster. The result is a tree-based representation of the data points called a dendrogram (Karthikeyan et al., 2020).

The *agglomerative* algorithm begins by measuring the distance between the data points via a clustering distance measurement such as *euclidean distance* using the following formula and grouping the data points close to one another.

$$d = \sqrt{\sum_{i=1}^n (x_i - y_i)^2} \quad (6)$$

3.6. Case Study

The significance of monitoring prefabricated modules during transportation is that the manufacturer had already experienced some damages on prefabricated modules during transportation caused by the vibrational forces. Figure 3-5 shows evidence of some prefabricated modules damaged during transportation, rejected by the client, and returned to the factory for the required modifications. However, some structural damages might be hidden. These damages need to be identified and investigated further.



Figure 3-5: Sample of actual damages (cracks) on prefabricated individual modules caused by the transportation-induced forces

We used two factory-finished wooden modular building units to demonstrate the use of the developed system. The modules were produced by *RCM Solutions Modulaires* Company located in Quebec, Canada, and transported about 300 km, by a tractor-trailer, as shown in Figure 3-6, from the factory to the installation site in Montreal, Canada. The size of the bigger module was 12.8 x 3.5m (42' x 11'-6.5 "). We attached four monitoring system units to each module. The number of sensors was selected in this study based on the budget and time of developing the monitoring systems. This is stated as one of the limitations of this work at the end of the Discussion section. To amplify the reliability of readings, two vibration sensors were attached to the floors and two monitoring system units to the walls. The location of sensors was selected close to the openings of each prefabricated module due to the concentration of stresses produced by the vibration force in these locations, as observed and recommended in the research conducted by Smith et al. (2007).

Figure 3-7 shows one of the modules' floor plans and the position of monitoring system units attached close to the window opening.

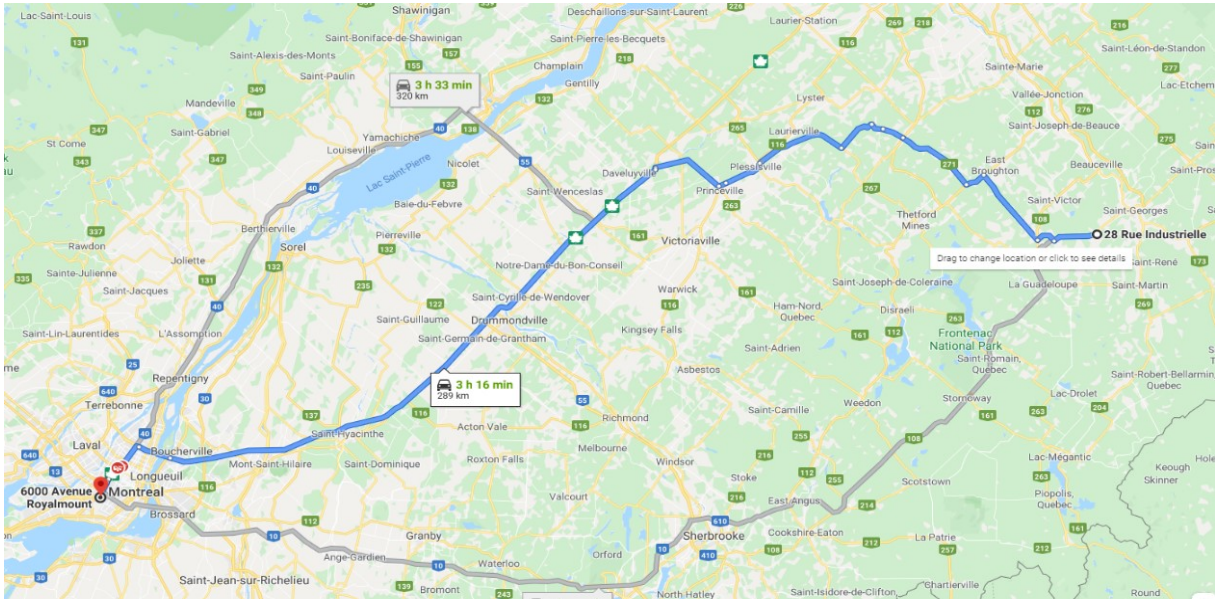


Figure 3-6: The transportation route of the instrumented prefabricated module

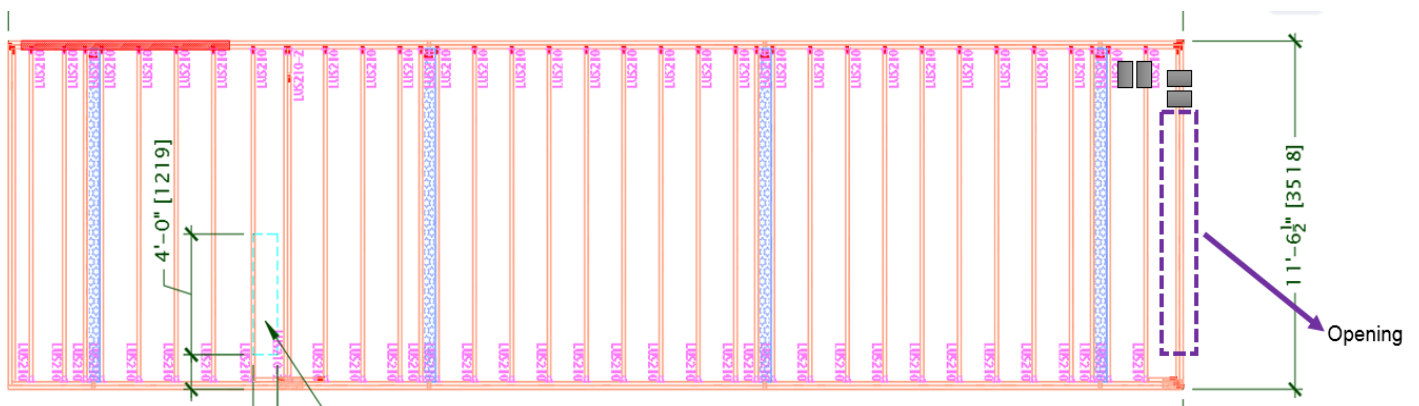


Figure 3-7: The instrumented prefabricated module's floor plan and the monitoring systems' position

The sensors and the associated monitoring systems were activated, and the transportation began after closing the temporary doors. Figure 3-8 shows some instrumented prefabricated modules in the factory and the installation site.

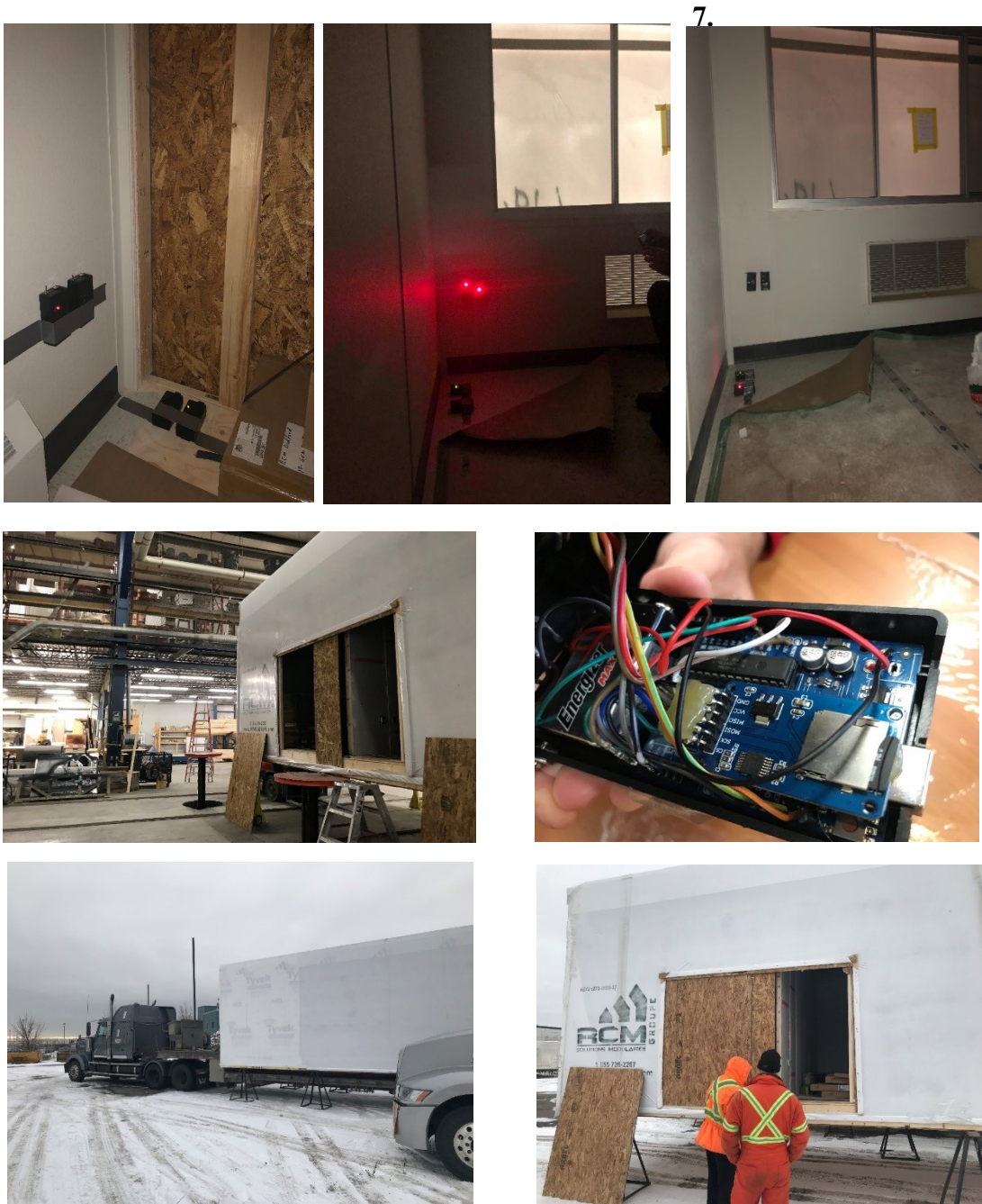
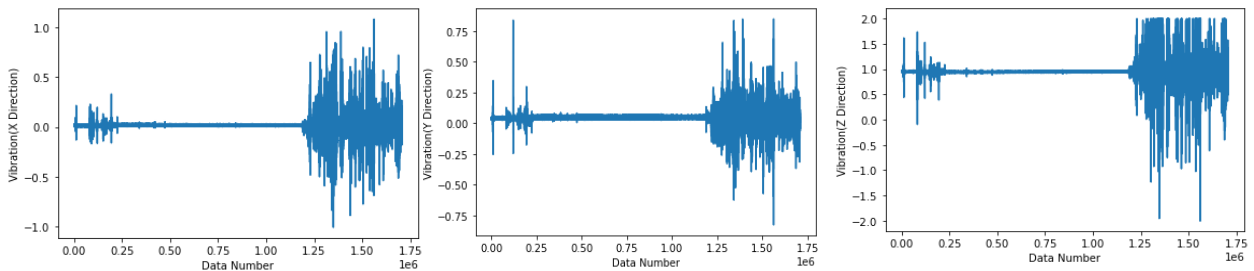


Figure 3-8: The pictures of the instrumented prefabricated modules in the factory and installation site

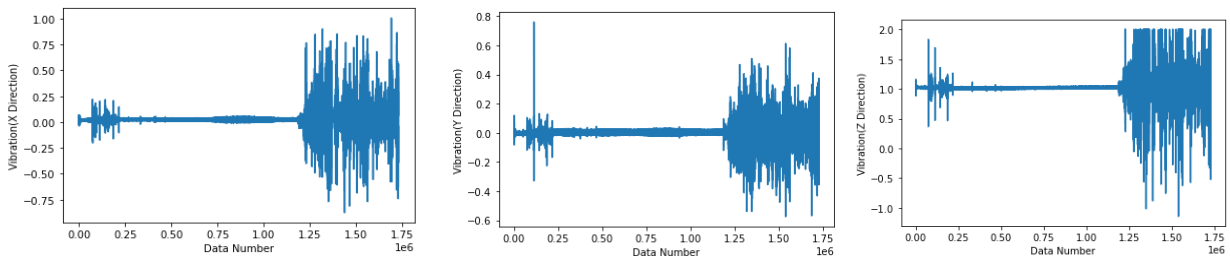
When the modules were delivered to the installation site, we detached the sensors for the data analysis.

3.7. System Implementation

We used the developed system to monitor and assess the structural behavior of two wooden prefabricated building modules during transportation. Eight sensors and their monitoring units were attached to the walls and floors of prefabricated modules to *measure* and *record* acceleration data for the duration of the monitoring period. In our study, only the data measured by two monitoring units with vibration sensors (*Module 1 & Module 7*) attached to one of the prefabricated module's floors were analyzed. More than 1.7 million raw acceleration data points were measured and stored in the system's SD card. Figure 3-9 shows the acceleration time history plot in XYZ directions for these monitoring system units. As shown in Figure 3-9, vibrational forces produced at the beginning and end of the transportation (on local and city roads) are much bigger than the vibrational forces produced during the middle of the transportation (on highways), indicating the poor road quality and conditions of local roads.



(a) Monitoring system unit number 1



(b) Monitoring system unit number 7

Figure 3-9: Acceleration data plot for two monitoring system units

After visualizing the acceleration data, the data analysis was carried out on the raw acceleration data.

a. Data Collection and Preprocessing Module

In the first step, a dataset was defined to accommodate the raw acceleration data in XYZ directions. When the dataset was created, the pre-processing module searched to detect if there were any missing values in the dataset. Then, the mean value of the available acceleration readings replaced the missing values in each direction (X, Y, and Z). It should be noted that missing values were replaced by the same mean value.

b. Damage Sensitive Feature Extraction

We grouped the created datasets based on a 2500 acceleration group size. We calculated the RMS value for use separately as a damage-sensitive feature of each group. Figure 3-10 shows the number of RMS values and RMS data points in XYZ directions. As shown in Figure 3-10, 691 RMS values were calculated and extracted from the raw acceleration dataset with 1,728,600 data points.

c. Noise Elimination Module

In this step, we identified and removed the noisy data from the dataset to improve the clustering accuracy. The *quantile* method was used to find the noise. Data were considered an outlier if their value was less than *low quantile* (1st percentile), the point where 1% of the data have values less than it, and greater than *high quantile* (99th percentile), the point where 99% of the data have values less than it and was tagged as *NaN* and then removed from the dataset. In this dataset, we identified and removed 36 outliers. Figures 3-11 and 3-12 show the outputs of the *Noise Elimination Module*. In Figure 3-12, outliers are marked with a circle (O).

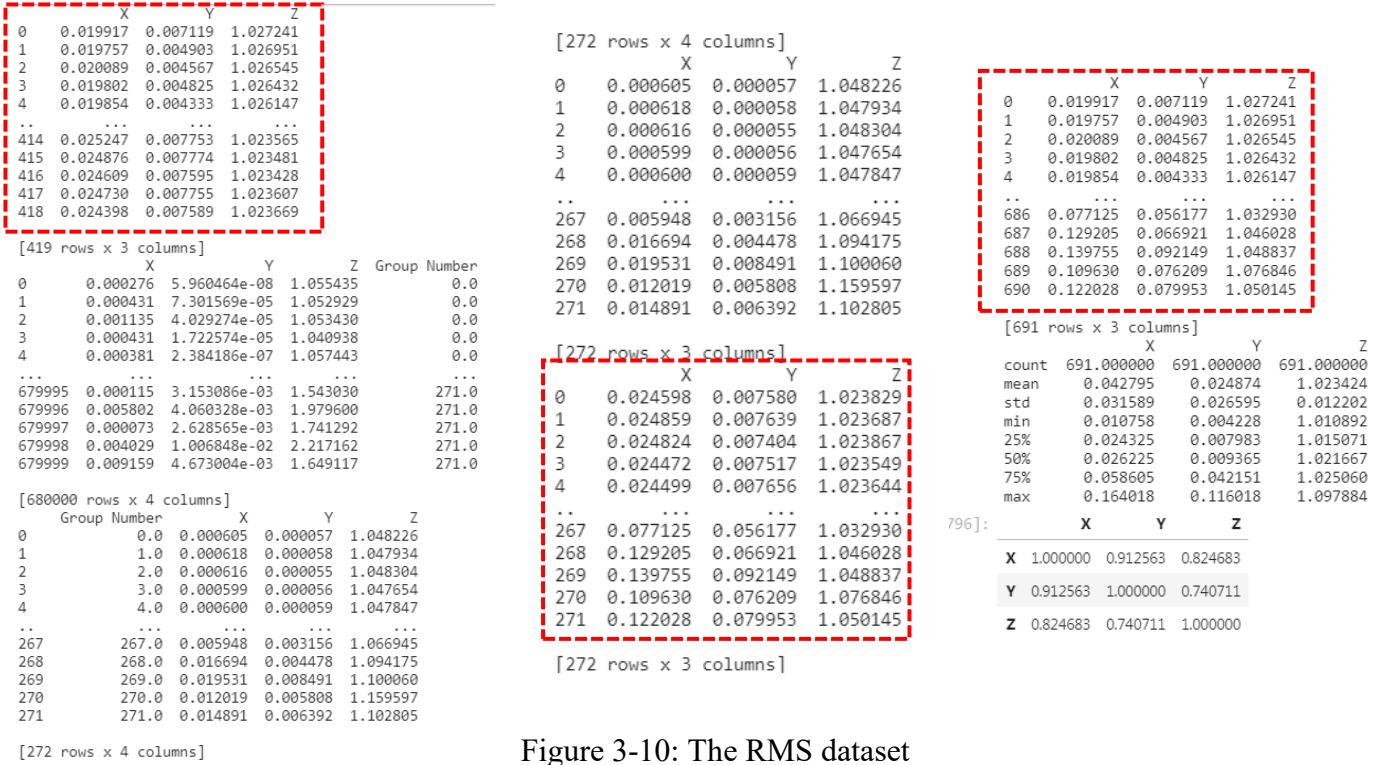


Figure 3-10: The RMS dataset

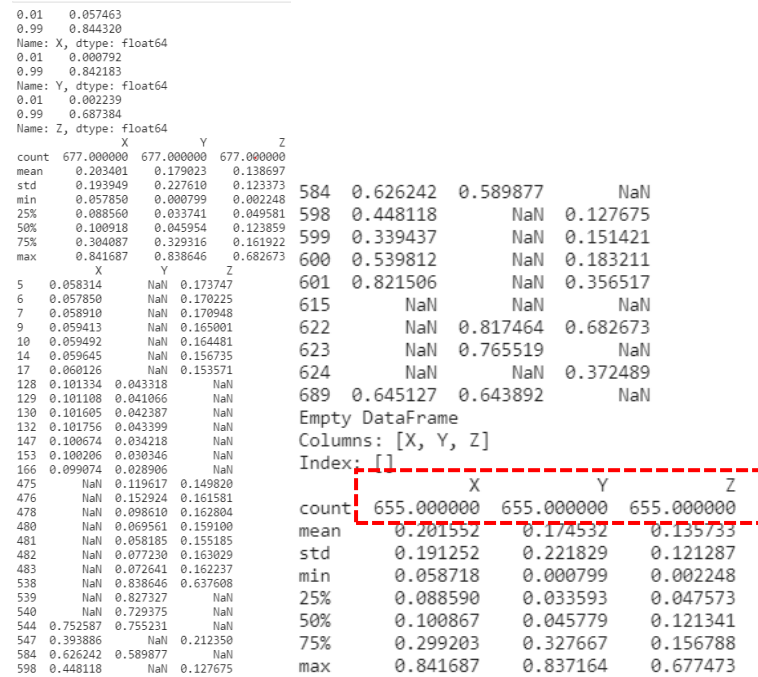
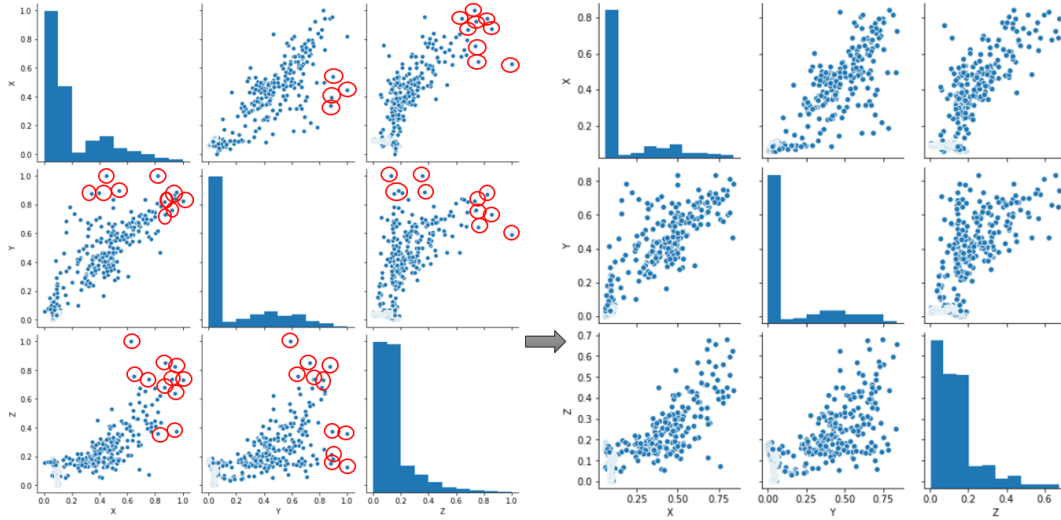


Figure 3-11: The number of RMS data points after noise elimination



(a) Before noise elimination

(b) After noise elimination

Figure 3-12: The pair plot of the RMS dataset before and after noise elimination step

d. Data Dimensionality Reduction Module

The *Data Dimensionality Reduction Module* uses the PCA algorithm to reduce the dataset's dimension from 3D to 2D. The PCA creates a low-dimensional representation of the samples from a data set, which is optimal because it retains as much variance in the original data set as possible. The first step of PCA is feature scaling. Standardization is a scaling technique where the values are centered on the mean with a unit standard deviation. The PCA calculates a new projection of the data set, and the new axis is based on the standard deviation of the variables. Therefore, a high standard deviation variable will have a higher weight for calculating the axis than a variable with a low standard deviation. If RMS data are standardized, all data points have the same standard deviation; thus, all features have the same weight, and the PCA calculates the relevant axis.

We used the *standard scaler* method to scale the RMS values in all directions. Equation (7) is the formula for standardization.

$$X' = \frac{(X-\mu)}{\sigma} \tag{7}$$

where:

μ is the mean of feature value,

and σ is the standard deviation of the feature values.

After standardizing the RMS dataset, we applied the PCA algorithm to decrease the dimension of the data set to 2D. Figure 3-13 shows both principal components (PCs) calculated for each feature (X, Y, and Z).

```

Index(['X', 'Y', 'Z'], dtype='object')
      X      Y      Z
0  0.019917  0.007119  1.027241
1  0.019757  0.004903  1.026951
2  0.020089  0.004567  1.026545
3  0.019802  0.004825  1.026432
4  0.019854  0.004333  1.026147
[[-0.72476746 -0.66808934  0.3129969 ]
 [-0.72983605 -0.75145998  0.28921561]
 [-0.7193196  -0.7641183  0.25595443]
 ...
 [ 3.07166606  2.53144536  2.08422431]
 [ 2.11731965  1.93162545  4.381315 ]
 [ 2.51007576  2.07252266  2.19150519]]
(691, 3)
(691, 2)
[[-0.64458033  0.77271922]
 [-0.7090543  0.8017254 ]
 [-0.72860988  0.78012096]
 ...
 [ 4.45623619 -0.37363664]
 [ 4.81824013  1.99575223]
 [ 3.91549884  0.08362928]]
[[ 0.59655232  0.57834625  0.55645391]
 [-0.20013904 -0.56423171  0.80099123]]
      0      1      2
0  0.596552  0.578346  0.556454
1 -0.200139 -0.564232  0.800991
<matplotlib.axes._subplots.AxesSubplot at 0xd9bd0a0>

```

Figure 3-13: The PCs of the RMS dataset for each direction

Therefore, the corresponding PCs multiplied by the RMS values in each direction calculate a new data point for the PC dataset. The first and second PCs are calculated based on the following formulas:

$$PC1 = (0.596552X) + (0.578346Y) + (0.556454Z) \quad (8)$$

$$PC2 = (-0.200139X) + (-0.564232Y) + (0.800991Z) \quad (9)$$

where:

X, Y, and Z are RMS values in X, Y, and Z directions, respectively.

The scatter plot, as shown in Figure 3-14, displays the results from PCA.

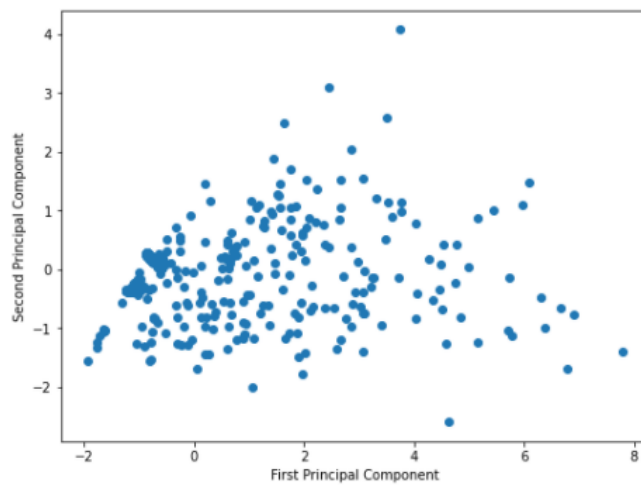


Figure 3-14: The scatter plot of PCA data

PCs are extracted to represent the patterns encoding the highest variance in the data set. However, in many high-dimensional real-world data sets, the most dominant patterns (i.e., those captured by the first principal components) separate the samples' subgroups from one another. Therefore, the PCA data can be used as a practical input into the clustering algorithms.

e. Pattern Recognition Module

The *Pattern Recognition Module* was applied to the PCA data to detect any dissimilarity between data. Figure 3-15 shows that only one data pattern was found by the *k-means* clustering

algorithm where the data are compacted, meaning that no structural damage occurred on the prefabricated module.

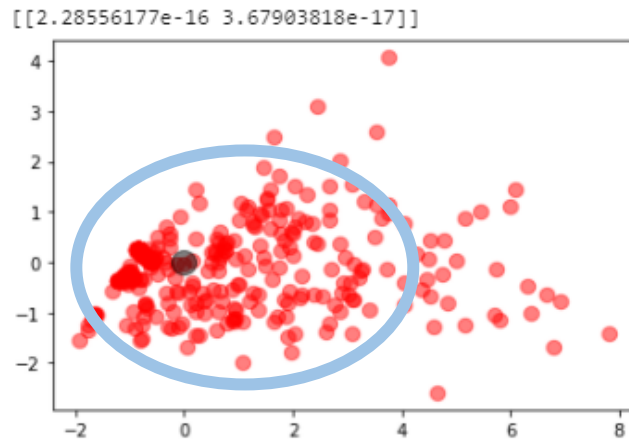


Figure 3-15: The cluster resulting from *k-means* clustering

3.8. Validation

3.8.1. Damage Simulation on the Test Data

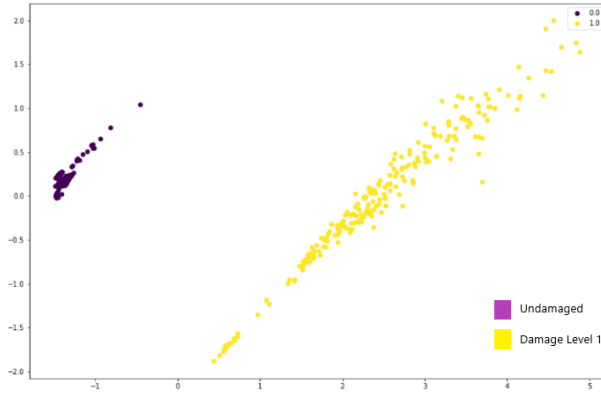
After analyzing the data measured by the monitoring system units, we determined that no damage occurred on the instrumented prefabricated building unit during transportation. As Table 3-1 shows, three scenarios were proposed to simulate different structural damage levels on the acceleration data to validate the developed system and workflow and select the best classification method. The damage simulation Scenarios, used in this study, were established based on the method used in the research conducted by Ding et al., (2014) for simulating the effects of structural damages on the RMS values of acceleration. Scenario 1 indicates two types of classification, intact and low damage data. Scenario 2 shows three types of classification, intact, low damage, and medium damage data. And finally, scenario 3 indicates four types of classification, intact, low, medium, and high damage data.

Table 3-1: The proposed scenarios description

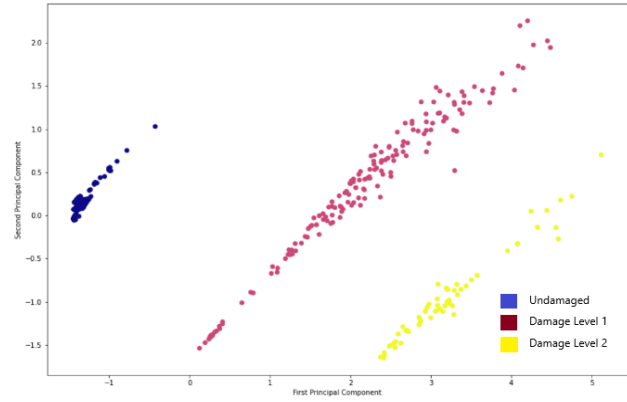
Scenario	Level of Damage	Damage Simulation Description
Scenario 1	One level of damage Damage Classification Number: Intact: 0 Damage Level 1: 1 (low)	<ul style="list-style-type: none"> Amplifying the last %35 of RMS data by a factor of 1.05
Scenario 2	Two levels of damages Damage Classification Number: Intact: 0 Damage Level 1: 1 (low) Damage Level 2: 2 (medium)	<ul style="list-style-type: none"> Amplifying the last %35 of RMS data by a factor of 1.05 & 1.10 <ul style="list-style-type: none"> %80 of data by 1.05 %20 of data by 1.10
Scenario 3	Three levels of damages Damage Classification Number: Intact: 0 Damage Level 1: 1 (low) Damage Level 2: 2 (medium) Damage Level 3: 3 (high)	<ul style="list-style-type: none"> Amplifying the last %35 of RMS data by a factor of 1.03, 1.06 & 1.08 <ul style="list-style-type: none"> %60 of data by 1.03 %25 of data by 1.06 %15 of data by 1.08

3.8.2. Evaluation of Clustering Methods Based on Proposed Scenarios

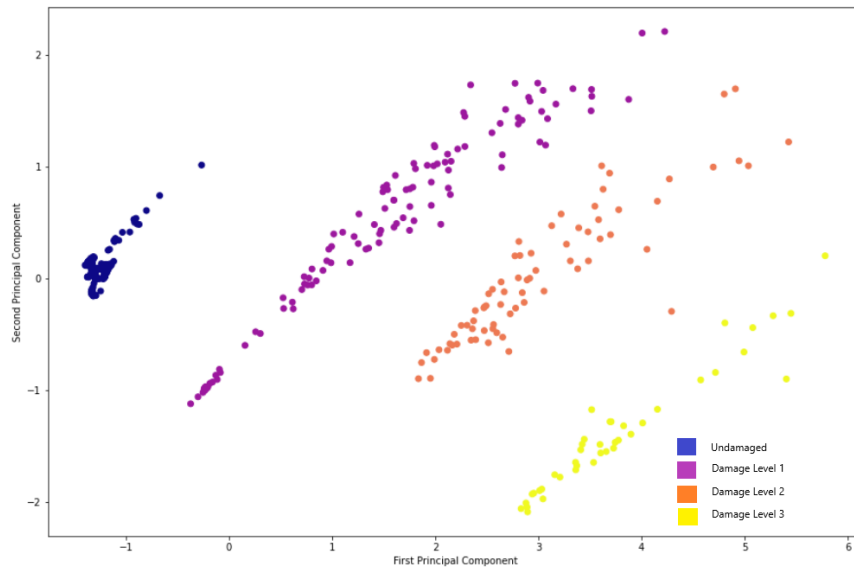
As Table 3-1 describes, in scenario 1, only one level of damage (low damage) was defined by amplifying the last 35% of RMS data points by a factor of 1.05. We standardized the modified RMS dataset, and applied PCA to it to use as the input to different clustering algorithms. We applied the PCA algorithm to the modified RMS dataset in all established scenarios. We classified the vibration data according to the damage classification numbers to evaluate the accuracy of different clustering algorithms used in this study and identify them visually. Figure 3-16 shows PCA plots based on different proposed damage simulation scenarios. A specific color shows each level of damages.



(a) Scenario 1



(b) Scenario 2



(c) Scenario 3

Figure 3-16: PCA plots based on different damage classifications

a. K-means clustering

The *k-means* algorithm was used to evaluate its effectiveness and accuracy in identifying and classifying damages in different proposed scenarios. Because the number of clusters must be predetermined in the *k-means* clustering, we used the *elbow* method and *silhouette* analyses to optimize the number of clusters. We applied both methods to the data of different scenarios' data

and determined their optimum number of clusters. We calculated the number of clusters for scenarios 1, 2, and 3 to be two, three, and four respectively, which was correct based on the damage simulation. Figure 3-17 shows the optimum number of clusters found by the *elbow* method for the first and third scenarios where Sum of Squared Errors (*SSE*) decreases abruptly. As shown, the number of clusters was identified as two and four correctly for the first and third scenarios, which means there are two and four damage classifications in scenarios number one and three, respectively.

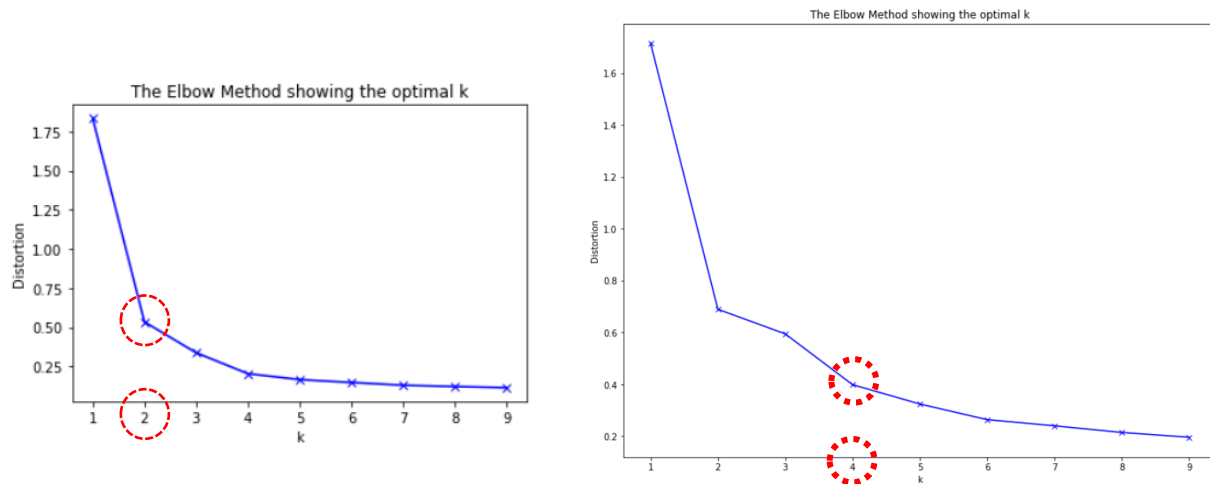


Figure 3-17: The optimum number of clusters for the first and third scenarios calculated by the Elbow method

We also applied *silhouette* analysis to the data of different scenarios to determine the optimum number of clusters and validate the *elbow* method results. The output (number of clusters) from the *silhouette* analysis was the same as the outputs determined by the *elbow* method, and for Scenarios 1, 2, and 3 we calculated two, three, and four, respectively. As shown in Figure 3-18, the *silhouette* score for $n_clusters = 4$ in scenario 3 has the highest value and is closer to one, which shows the optimum number of clusters.

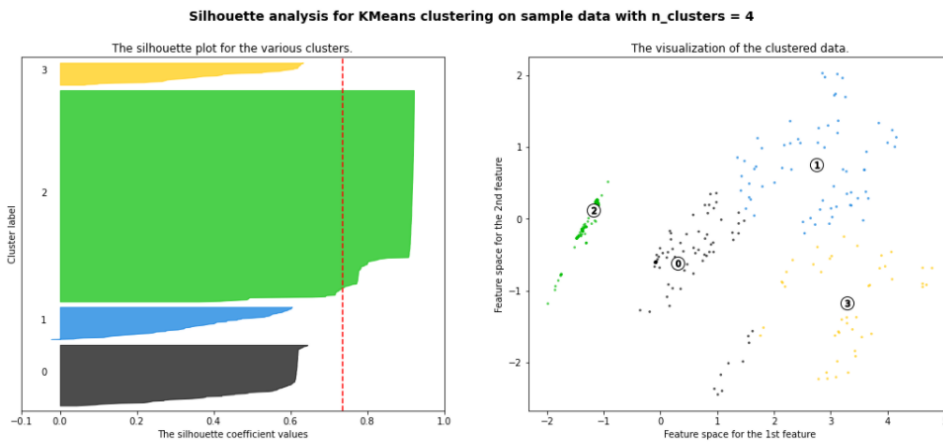
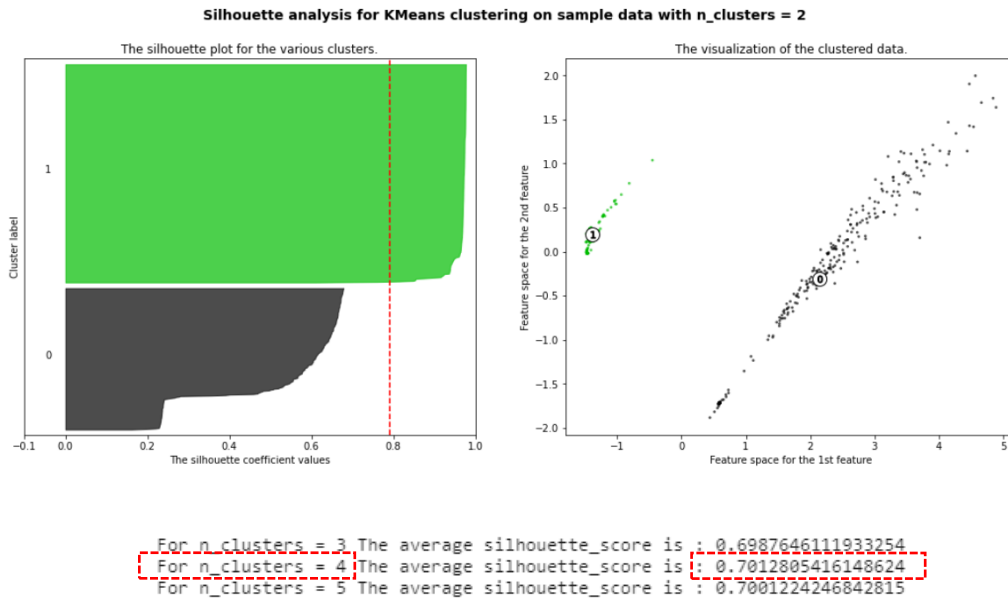


Figure 3-18: The optimum number of clusters for the first and third scenarios calculated by the *silhouette* analysis

After identifying the optimum number of clusters, we used the number of clusters as input for the *k-means* clustering. Figures 3-19 and 3-20 illustrate the classification results of scenarios 1, 2, and 3. As shown, although the algorithm accurately detected the number of clusters (damage classification), only the damaged and undamaged data in scenario one was grouped in suitable clusters, and the *k-means* algorithm could not classify all the damaged data accurately in scenarios 2 and 3.

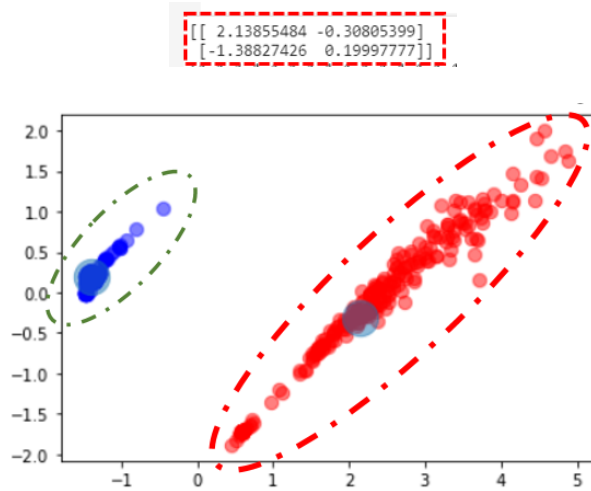


Figure 3-19: *K-means* clustering classification result on the scenario 1 data

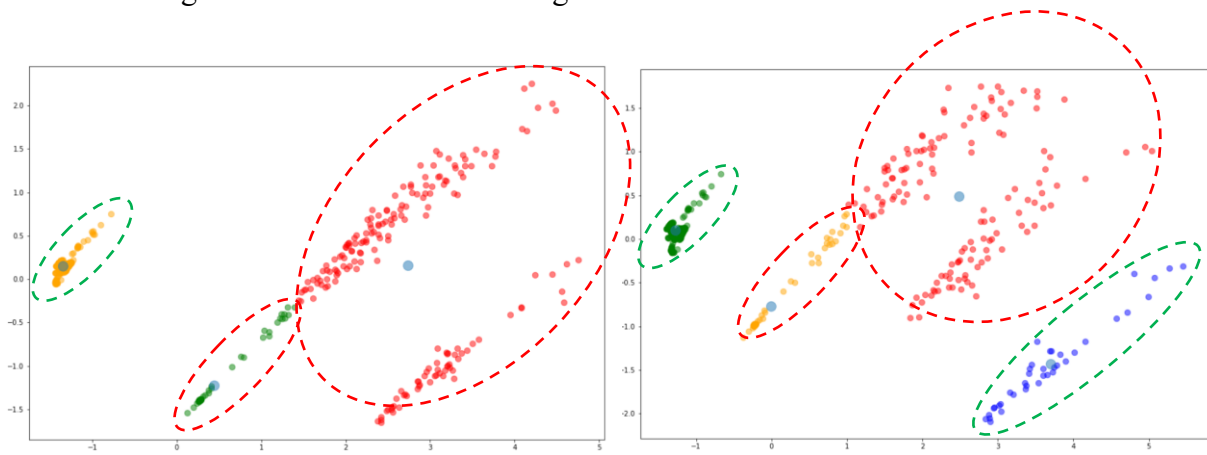


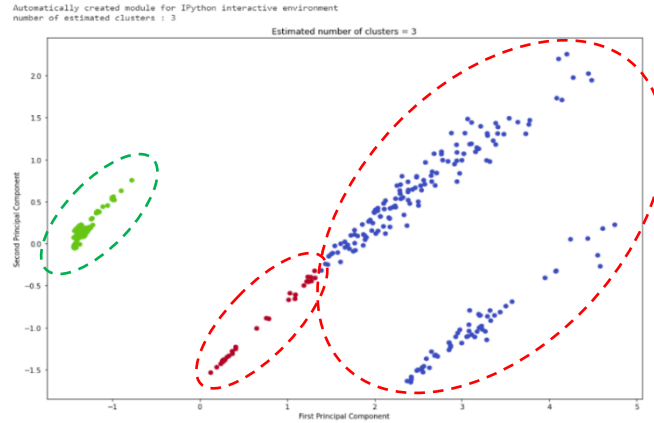
Figure 3-20: *K-means* clustering classification result on the scenario two and scenario three data

As shown in Figure 3-19, the *k-means* algorithm could successfully group all damaged and intact data into a separate cluster in scenario 1. However, in scenarios 2 and 3, as shown in Figure 3-20, *k-means* could only group intact and damage level 3 data correctly into a separate cluster. At the same time, it could not classify damage level 1 and damage level 2 accurately.

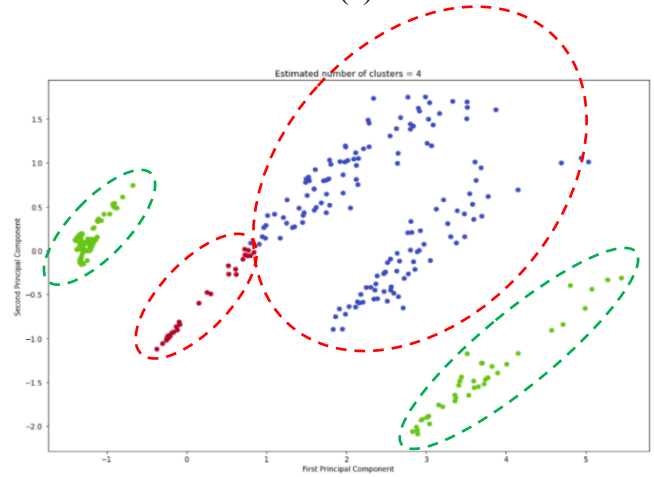
b. Mean shift clustering

Unlike the *k-means* algorithm, the number of clusters is estimated based on the *bandwidth* parameters such as *n_samples* and *quantile*. The bandwidth is the distance/size scale of the kernel function or *window* size across which the mean is calculated.

The *n_samples* parameter refers to the number of input points (in this case, the number of RMS data points). *Quantile* should be in the range of [0, 1]. The optimum value of “*quantile*” was identified as 0.5 for scenarios 1 and 2 and 0.3 for scenario 3, which also worked for scenarios 1 and 2, using the trial-and-error method to estimate the correct number of clusters for different scenarios. A quantile of 0.5 means that the median of all pairwise distances was used. Using the specified *quantile* parameter value, we estimated the number of clusters correctly (2, 3, and 4 for scenarios 1, 2, and 3, respectively). Like *K-means* clustering, the *mean shift* algorithm could successfully group all damaged and intact data into a separate cluster in scenario 1. Scenario two could only group intact and damage level 2 data correctly into a different cluster (Figure 3-21 [a]). In scenario three, the *mean shift* could only group intact and damage level 3 data correctly into a separate cluster (Figure 3-21 [b]). At the same time, it could not accurately classify damage level 1 and damage level 2 data into suitable clusters.



(a)



(b)

Figure 3-21: *Mean shift* clustering classification result on (a) scenario two and (b) scenario three data (b)

c. Agglomerative clustering

Agglomerative clustering uses the *euclidean distance* parameter to find similar data points and group them into the same cluster. Although the number of clusters cannot be estimated automatically by the algorithm, it can be identified by the algorithm dendrogram. As Figure 3-22 [a, b] shows, the number of clusters was identified correctly from the dendrogram. Like *k-means* and *mean shift* clustering, the *agglomerative* clustering could successfully group all damaged and

intact data into a separate cluster in scenario 1. However, in scenario 2, as shown in Figure 3-22 [c], it could only group the intact and damage level 2 data correctly into a separate cluster. Simultaneously, scenario 3 only grouped the intact and damage level 3 data correctly and could not accurately classify damage level 1 and damage level 2.

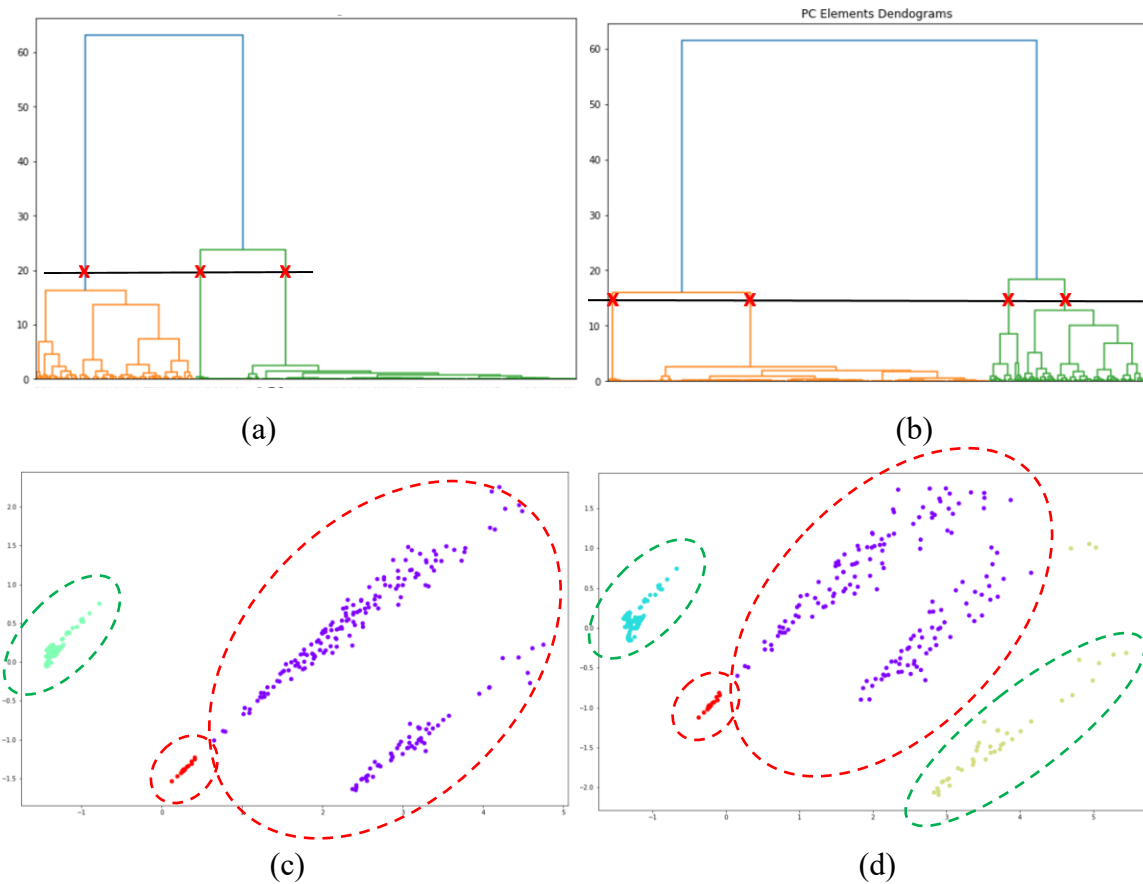


Figure 3-22: The *agglomerative* clustering classification result on the scenario two (a, c) and scenario three data (b, d)

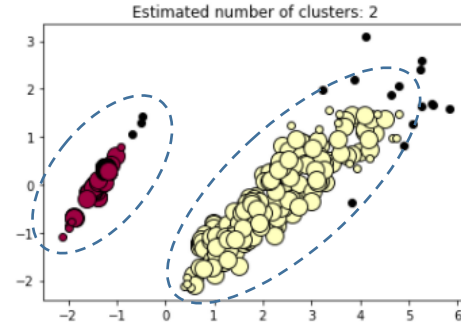
d. DBSCAN clustering

The *DBSCAN* algorithm is one of the most common clustering algorithms that separates high-density from low-density clusters. Some substantial advantages of the *DBSCAN* algorithm are estimating the number of clusters, sorting data into clusters of varying shapes, and being robust to

outliers. Because the simulated damaged data was already labeled based on different damage classifications, we considered different sets of values for the model's parameters, '*eps*' and '*MinPoints*', to achieve the correct number of clusters and classification. The optimum value of '*eps*' and '*MinPoints*' was identified as 0.6 and 15, respectively, using the trial-and-error method to estimate the correct number of clusters for different proposed scenarios. As Figure 3-23 shows, the number of clusters was estimated correctly using the specified *eps* and *MinPoints* parameter values (2, 3, and 4 for scenarios 1, 2, and 3, respectively). However, because in modular buildings, most of the individual modules have the same size and are transported to the site with the same temporary configuration of supports on the truck, the optimum values identified for the DBSCAN algorithm for the first individual modules and the same road profile can be used for other prefabricated modules.

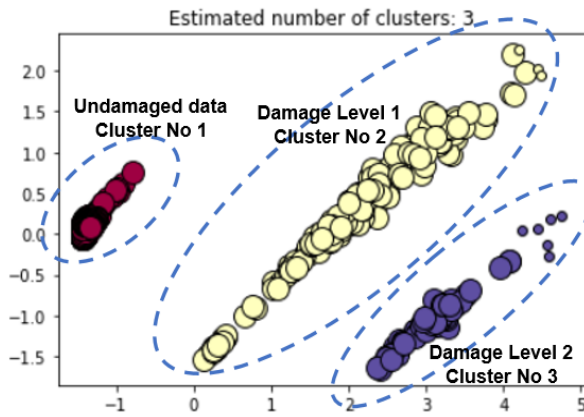
As Figure 3-23 shows, unlike other algorithms, the DBSCAN algorithm could classify all damage levels in all scenarios and group them correctly. It could group "densely grouped" data points into a single cluster, which plays a substantial role in correctly classifying different levels of damage. The most exciting feature of DBSCAN clustering is that it is robust to outliers. As shown in Figure 3-23, outliers were illustrated in black. In this case, because the dataset was already denoised, these outliers might be caused by the impact loads produced because of the weak road condition. Therefore, if required, outliers can automatically be added to their closest cluster for further analysis.

Automatically created module for IPython interactive environment
 Estimated number of clusters: 2
 Estimated number of noise points: 17



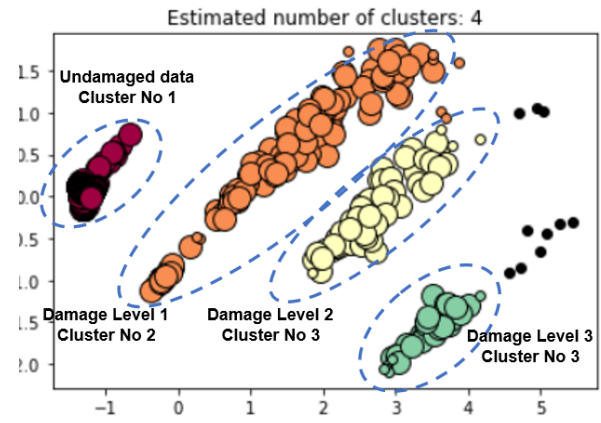
(a)

Automatically created module for IPython interactive environment
 ✓ Estimated number of clusters: 3
 ✓ Estimated number of noise points: 0



(b)

Automatically created module for IPython interactive environment
 Estimated number of clusters: 4
 Estimated number of noise points: 10



(c)

Figure 3-23: The *DBSCAN* clustering classification result on the scenario one, two and three (a, b, and c respectively)

3.9. Evaluating the Accuracy of Different Clustering Algorithms

We compared the classification accuracy of different clustering algorithms used in this study for different proposed scenarios (scenarios 1 and 2) and different sizes of event (625 [5s], 1250 [10s], and 2500 [20s]) to identify the most effective algorithm and optimum size of event for the developed framework. We investigated the accuracy of algorithms using two parameters: *accuracy score* and *confusion matrix*.

The *accuracy score* is the ratio of the number of correct predictions and the total number of predictions calculated by the algorithm. A *confusion matrix* is an N x N matrix used for evaluating the performance of a classification model, where N is the number of target classes. The matrix gives a holistic view of what kinds of errors it is making. Table 3-2 shows the structure of the *confusion matrix* for two types of classes (scenario one). In Table 3-2, the columns represent the actual values of the target variable, and the rows represent the predicted values of the target variable. In the *confusion matrix*, *TP* (true positive) and *TN* (true negative) show the number of data points correctly clustered by the algorithm, and *FP* (false positive) and *FN* (false negative) show the number of data points falsely predicted by the algorithm. Tables 3-3 and 3-4 show the accuracy of the clustering algorithms used in the developed framework for scenarios one and two for different events.

$$\text{Accuracy score} = \frac{\text{Number of correct predictions}}{\text{Total number of predictions}} \quad (10)$$

Table 3-2: The structure of *confusion matrix*

	Positive	Negative
Positive	TP	FP
Negative	FN	TN

As Table 3-3 shows, in scenario 1, in case of a single level of damage, for data windows of 10s and 20s, all algorithms could yield the complete accuracy score of 1. In the data window of 5s, the only algorithm that could not obtain a complete accuracy score was the *agglomerative* algorithm with two false negative (FN) predictions, which could be negligible.

Size of Event	625 (5s)					1250 (10s)					2500 (20s)					
	Kmeans	Mean Shift	DBSCAN	Agglomerative	Kmeans	Mean Shift	DBSCAN	Agglomerative	Kmeans	Mean Shift	DBSCAN	Agglomerative	Kmeans	Mean Shift	DBSCAN	Agglomerative
Accuracy Score	1.0	1.0	1.0	0.99	1.0	1.0	1.0	1.0	1.0	1.0	1.0	1.0	1.0	1.0	1.0	1.0
Confusion matrix	[1677, 0], [0, 1088]	[1677, 0], [0, 1088]	[1677, 0], [0, 1088]	[1675, 0], [2, 1088]	[838, 0], [0, 544]	[838, 0], [0, 544]	[838, 0], [0, 544]	[838, 0], [0, 544]	[419, 0], [0, 272]							

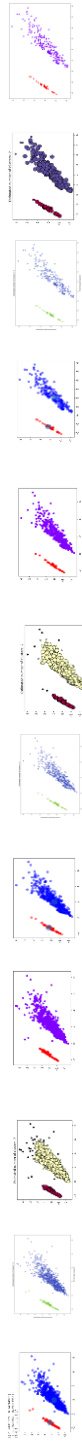


Table 3-3: The accuracy performance of different clustering algorithms for different sizes of the event in case of existing one level of damage

Size of Event	625 (5s)			1250 (10s)			2500 (20s)					
	Kmeans	Mean Shift	DBSCAN	Agglomerative	Kmeans	Mean Shift	DBSCAN	Agglomerative	Kmeans	Mean Shift	DBSCAN	Agglomerative
Accuracy Score	0.81	0.79	1	0.78	0.81	0.79	1	0.78	0.81	0.79	1	0.78
Confusion matrix	[1677, 0, 0], [0, 263, 485], [0, 27, 213]	[1677, 0, 0], [0, 505, 343], [0, 235, 5]	[1677, 0, 0], [0, 740, 0], [0, 0, 348]	[1677, 0, 0], [0, 240, 0], [0, 586, 262]	[838, 0, 0], [0, 173, 251], [0, 8, 112]	[838, 0, 0], [0, 254, 170], [0, 118, 2]	[838, 0, 0], [0, 423, 0], [0, 0, 121]	[838, 0, 0], [0, 120, 0], [0, 293, 131]	[419, 0, 0], [0, 83, 129], [0, 0, 60]	[419, 0, 0], [0, 60, 0], [0, 131, 81]	[419, 0, 0], [0, 212, 0], [0, 0, 60]	[419, 0, 0], [0, 40, 0], [0, 151, 81]

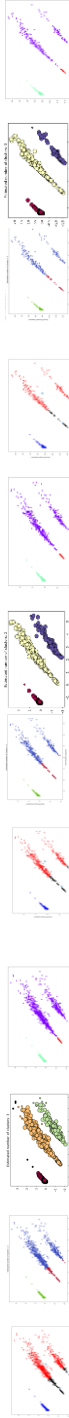


Table 3-4: The accuracy performance of different clustering algorithms for different sizes of the event in case of existing two levels of damage

As Table 3-4 shows, in the case of more than one damage level, most algorithms' *accuracy scores* were decreased. The only algorithm with the acceptable *accuracy score* of 1 in a case of existing different damage classifications in other data windows (5s, 10s, and 20s) was the *DBSCAN* algorithm which could classify all the data points in their associated clusters.

3.10. Sensor Failure Analysis Module

The developed sensor failure analysis module can be used to detect the sensor failure using a correlation matrix. We used RMS data, calculated in section 9.2, to evaluate the correlation between the variables on each axis of accelerometer sensors. As shown in Figure 3-24, a heat map plot was used to explain the correlation among the variables of each sensor. We evaluated the correlation of RMS acceleration data in X, Y, and Z directions, captured by the sensors placed on the same type of element. Therefore, the outputs of sensors attached to the walls and floors were compared to calculate their correlation. Correlation ranges from -1 to +1. Values closer to zero mean there is no linear trend between the two variables. The correlation coefficient close to 1 indicates that the data are more positively correlated. The diagonals are all yellow because those squares correlate each variable to itself (so it is a perfect correlation). The larger values are shown in lighter colors and indicate higher correlation between the two variables. The plot is also symmetrical about the diagonal because the same two variables are paired together in those squares.

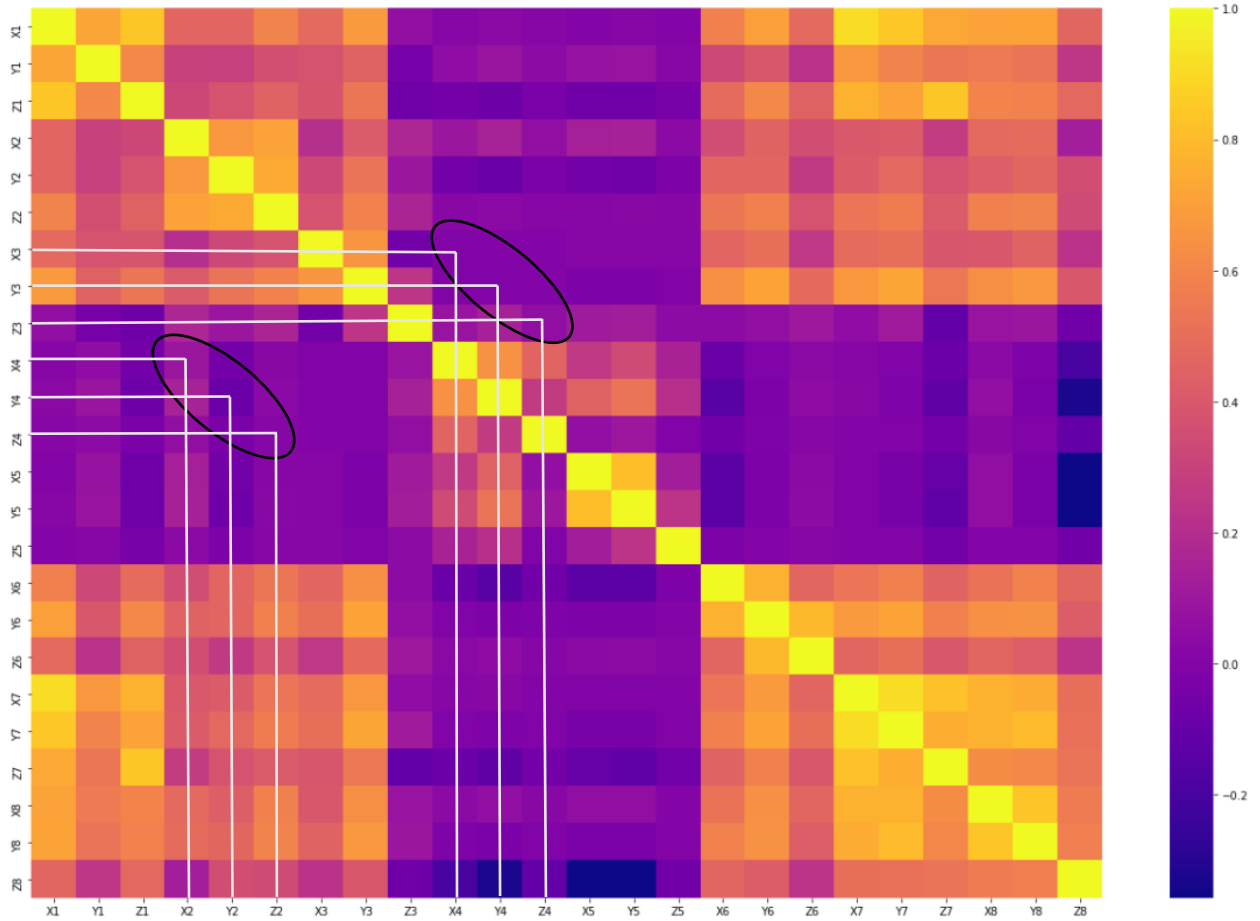


Figure 3-24: The heat map plot used to show the correlation between the sensors

The purple cells in the heat map plot (Figure 3-24) mean there is no correlation between the sensor data. For example, as Figure 3-24 shows, there is no correlation between sensor number 4 and sensors 2 and 3. Table 3-5 shows the correlation between pairs of associated sensors. According to Table 3-5, the checkmark means the sensors' data are correlated, and the cross mark means there is no correlation between them.

Table 3-5: The correlation between different sensors

Sensors Combination	RMS (X)	RMS (Y)	RMS (Z)
Sensor 1 _ Sensor 7	✓	✓	✓
Sensor 1 _ Sensor 5	✗	✗	✗
Sensor 1 _ Sensor 8	✓	✓	✓
Sensor 2 _ Sensor 6	✓	✓	✓
Sensor 2 _ Sensor 3	✓	✓	✗
Sensor 3 _ Sensor 4	✗	✗	✗
Sensor 2 _ Sensor 4	✗	✗	✗
Sensor 3 _ Sensor 6	✓	✓	✗
Sensor 4 _ Sensor 6	✗	✗	✗
Sensor 5 _ Sensor 8	✗	✗	✗
Sensor 5 _ Sensor 7	✗	✗	✗
Sensor 7 _ Sensor 8	✓	✓	✓

As Table 3-5 shows, there is no correlation between sensors 3-4, 2-4, and 6-4 (attached to the module's wall) and sensors 1-5, 8-5, and 7-5 (attached to the module's floor) in all directions, and there is no correlation between sensors 2-3, and 6-3 in the Z direction. Thus, we can conclude that sensors 4 and 5 failed in all directions (XYZ) and sensor number 3 failed only in the Z direction. The sensor failure analysis module can help SHM engineers find failed sensors quickly to exclude their data in the data analysis.

3.11. Discussion

Structural damages may occur because of transportation-induced vibration forces, which can lead to misalignment issues and continuity disruption in the building envelope, causing project delays and cost increase because of additional reworks, modifications, and substantial air leakage and moisture deposition, thereby creating long-term durability, mold problems, and heat loss respectively. This paper introduced a novel semi-automated data-driven monitoring system,

particularly for monitoring prefabricated building modules during their transportation, to ensure their structural integrity before their installation.

In terms of the size of the hardware system, the developed sensing system (set up in a protection box) can be attached to different parts of actual prefabricated building modules to track and monitor their structural behavior against the road and driver-induced vibrational forces during transportation to the site. The MPU6050 accelerometer was selected for the system, which is designed for low power, low cost, and high-performance requirements. The system can measure the modules' acceleration in XYZ directions and store the measurements in an embedded SD card during transportation. The SD card module was preferred over wireless-based, remote-sensing monitoring for two reasons. First, in case of structural damage occurring on prefabricated modules during transportation, the truck drivers cannot safely stop their vehicles on the road, and repairing the modules is impossible in transit. Second, it is much more cost-effective than wireless systems. Using an onboard card data storage module (in this case, using an SD card) is more practical and less costly. Therefore, the developed hardware system is efficient in monitoring prefabricated building modules in terms of size and power.

The developed system integrates the sensing system and machine learning technology to monitor the structural behavior of prefabricated building modules in a semi-automated manner. As we mentioned earlier, although structural damages (minor or major) might occur during transportation, few studies have examined this occurrence. In our current study, we selected the Python programming language to analyze data because of its simplicity, speed, and the availability of effective machine learning libraries and frameworks. After creating databases and preprocessing the acceleration data, we selected the RMS parameter as the damage-sensitive feature. The reason for choosing the RMS parameter over other common parameters such as acceleration frequency

was the sensitivity of RMS acceleration against minor structural damages usually hidden in the prefabricated modules. Modal parameters identification leads to a loss of information compared with the raw data and can erase any small changes caused by structural damage. We used the PCA algorithm to reduce dimensionality and remove the environmental effects for better visualization and damage classification and extract critical information from the data. As shown in Figure 3-25, PCA could make the damage detection and classification processes significantly easier. In scenario 3, where there were three levels of damage, as shown in Figure 3-25[a], damage identification and classification were not easily possible based on the initial RMS data point plot, whereas after the PCA process, different levels of damage could be visualized easily. Thus, RMS acceleration has been used as a practical damage-sensitive feature in transportation-induced vibration monitoring, and the PCA algorithm has been utilized in the data analysis module for an easier and more efficient damage detection and classification process.

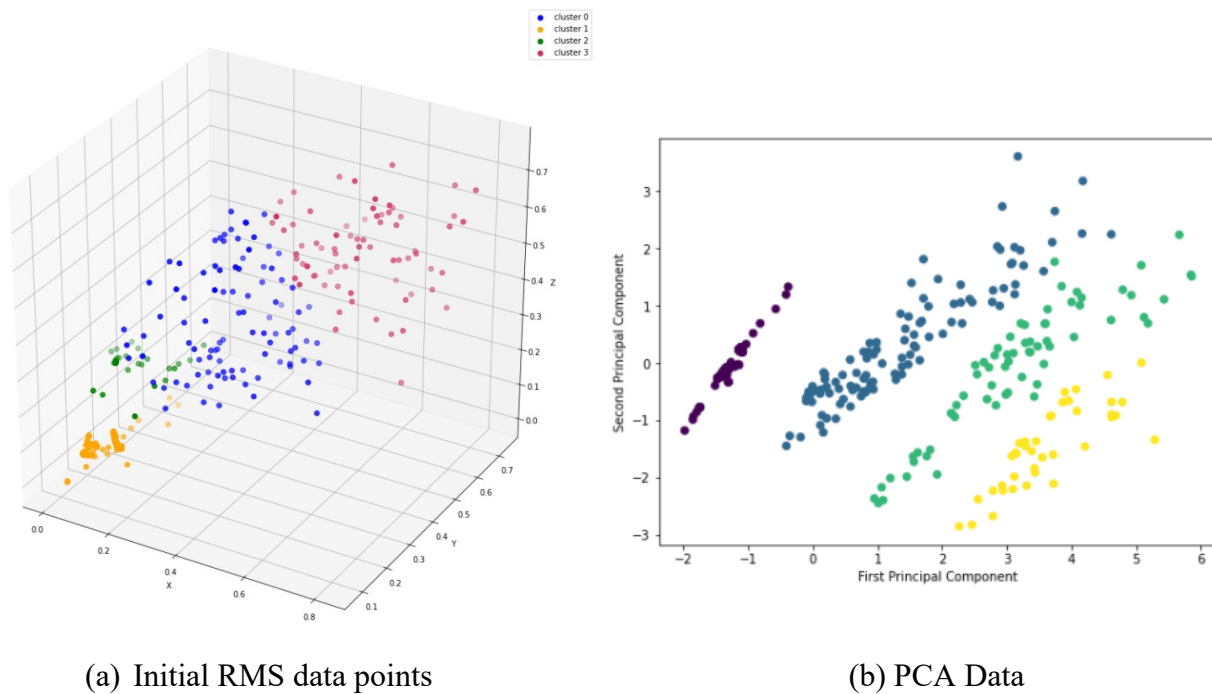


Figure 3-25: The data points plot before and after PCA

The output of PCA was used as input to the machine learning algorithms. The reason for using *k-means*, *mean shift*, *agglomerative*, and *DBSCAN* unsupervised clustering algorithms in this study was their application and popularity in SHM studies and projects (Bouzenad et al., 2019; Entezami et al., 2020; Agarwal and Reddy, 2020; Azimi et al, 2020, Andrade et al, 2020; Pang et al, 2020; Hamishebahar et al, 2020; Huang et al., 2019; Chen et al., 2018; Perera et al, 2019; Bull et al., 2018). After optimizing the clustering parameters, *k* (number of clusters) for the *k-means* and *agglomerative* algorithms using the *elbow* method and *Silhouette Index (SI)*, *quantile* for the *mean shift* algorithm, and *minPts* and *eps* for the *DBSCAN* algorithm by trial-and-error method, the algorithms' accuracy was evaluated based on intentional simulated damage labels. After analysis, it was found that density-based clustering such as the *DBSCAN* algorithm could classify different damage levels based on density levels. Because of random vibration production and unexpected road conditions, we found that the shape of clusters might be arbitrary, which can be distinguishable by density-based clustering, whereas partition-based and hierarchical clustering techniques are highly efficient with typical clusters. Figure 3-26 shows the high classification accuracy of the *DBSCAN* clustering algorithm. Figure 3-26 (a) shows the classification output of the *DBSCAN* algorithm on scenario 3 data, and Figure 3-26 (b) shows the classification based on the actual damage labels. As shown, *DBSCAN* could assign the data point in its correct cluster (cluster number 1), although it is further from other cluster members, which shows the high classification accuracy of the *DBSCAN* algorithm in this case. This result has been observed in the *accuracy score* and *confusion matrix* analysis in which the *DBSCAN* algorithm yields the full accuracy score in the case of more than one level of damage compared to other algorithms. Therefore, the *accuracy score* and *confusion matrix* have proven effective methods for comparing different types of clustering techniques to identify the algorithm with the highest classification accuracy.

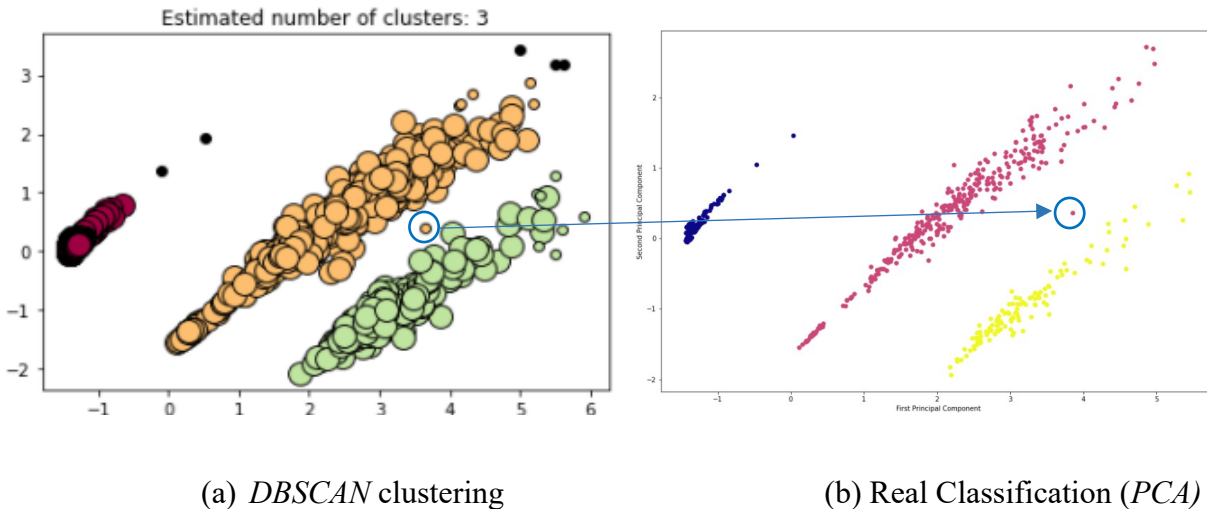


Figure 3-26: The high accuracy of *DBSCAN* clustering

According to Table 3-4, six monitoring modules (out of eight) could successfully measure and store acceleration data (with a sampling rate of 125 Hz) during transportation. When erroneous data produced by one kind of sensing unit out of a pair that result in serious consequences to the system operations and data analysis, identifying the faulty sensor plays an essential role in the correct functioning of the monitoring systems. On the other hand, identifying which sensor out of a pair is faulty can be challenging. Therefore, there is a critical need to detect such failures before starting the data interpretation. Most of the previous sensors' fault detection methods have been based on machine learning techniques, but researchers have found that, in this case, machine learning techniques are computationally intensive and need large training datasets (Weiss et al., 2016, Gaddam et al., 2020). The developed sensor failure identification module presented in our study effectively detects sensor's failure by using a correlation matrix between sensors. In this developed module, the correlation is considered among sensors placed in the same location and the sensors attached to the same components such as walls and floors. A sensor failure happens if there is no correlation between a pair of sensors installed in the same area. Because the elements of a prefabricated module experience almost the same vibrational force during transportation, the

developed module also investigates the correlation among sensors installed in different positions on a component (e.g., wall or floor) to compare the correlation between a sensor to all other sensors to identify the faulty one. Another benefit of this module is its integration with the developed framework, which works as a part of the system.

Our study introduced a multi-functional data-driven SHM system to monitor the structural behavior of individual building modules during transportation to detect any possible damages after the delivery. However, we note the following limitations to our study:

1. The system developed here was tested with a limited number of sensors (two sensors on a wall and two on each module's floor). The system can also be expanded to use different sensors for other purposes, such as strain sensors to monitor the deformation of structural elements. The developed system should be tested further on more prefabricated modules with a larger number and multiple types of sensors.
2. The developed monitoring system was tested on only two prefabricated individual modules transported by the same truck. Because the transportation-induced damages on prefabricated modules are inevitable, as observed in our visit to the factory site, more tests on prefabricated modules of different sizes should be conducted to validate the developed system on units with some actual structural damages.
3. The three damage scenarios used in our research were hypothetical to simulate different possible intensities of structural damage (low, medium, and high) on prefabricated building modules during transportation using amplification factors. However, more monitoring tests need to be conducted on prefabricated modules to find actual damaged data.

4. In our study, we searched for the optimum values of the following parameters for *mean shift* and *DBSCAN* clustering using the trial-and-error method to determine the most suitable predictions. An optimization technique is required to find the optimum clustering parameters' values automatically. However, because most of the building modules are prefabricated with the same size in modular building construction projects and transported to the site with the same configuration of temporary supports on the truck, the optimum values for the clustering algorithm for the same road profile can be used for other building modules.

3.12. Conclusion

Monitoring the structural integrity of prefabricated building modules during transportation is critical for manufacturers and owners to ensure that modules are delivered safely to the site. The main purpose of this research was to develop a data-driven monitoring system to monitor the structural condition of individual building modules during transportation to detect possible damages caused during their delivery. For this purpose, a system, which consists of two main components (DAQ and data analysis components), was developed. The system used acceleration data and unsupervised clustering techniques to detect and classify damaged and undamaged data. A user-friendly visualization-based method was also integrated into the system to identify sensors malfunction. The capability of the developed system was explored via a real case study.

Based on the study presented here, we made the following conclusions:

- The developed monitoring systems could successfully record the vibration of prefabricated building modules during the transportation to the site.

- ❑ Acceleration RMS was used as a practical and effective statistical damage-sensitive feature in the developed system.
- ❑ PCA was used as a solid and effective data reduction algorithm to remove environmental impacts during transportation and make the damage detection and classification process more efficient.
- ❑ Different clustering algorithms were applied to RMS data during the damage detection process, and *accuracy score* and *confusion matrix* parameters were used as effective parameters to evaluate the performance of these algorithms
- ❑ All algorithms could successfully estimate the correct number of clusters (two clusters) and appropriately assign data points to their corresponding clusters for one level of damage.
- ❑ After detailed analysis using different clustering algorithms, it was found that the *DBSCAN* algorithm yields the complete accuracy score of one in the case of more than one level of damage compared to *k-means*, *mean shift*, and *agglomerative* clustering with the accuracy score of 0.81, 0.79 and 0.78 respectively.
- ❑ Using the sensor failure identification module developed in this study, we identified two malfunctioning sensors (numbers 4 and 5), and their data were excluded from the analysis.

Timely modifications of damaged prefabricated modules can prevent problems of additional costs and time arising from misalignment issues during the installation phase and problems during the operational phase such as air leakage and moisture deposition which can negatively impact the performance of building envelope of the modules. The system we developed in our study aims to solve the issues that existed in previous studies, such as the size of the monitoring system (which is critical in the monitoring of individual prefabricated building modules during transportation), the cost and complexity of a model-based approach in the structural damage detection process, the

inapplicability of a model-based approach (which is time-consuming and requires detailed modeling data), and the possible uncertainties in loading data and temporary support configurations (which might affect the outputs of model-based approach in this case). The developed system can allow for timely replacement of damaged parts of the prefabricated modules before installation. It can also provide evidence to support manufacturers' insurance claims on repair and modification costs and improve customer perceptions of the quality of prefab construction. However, the developed system should be tested further on more numbers and types of prefabricated building modules with a larger number of sensors to be validated with some real damages rather than damages simulated in this study. Moreover, optimized parameters value of some clustering techniques, used in this study, should be found automatically by using some optimization technique which will be addressed in the feature research.

References

- Abdallah, L., and Shimshoni, I. (2014). "Mean Shift Clustering Algorithm for Data with Missing Values." International Conference on Data Warehousing and Knowledge Discovery, 8646, ISBN: 978-3-319-10159-0.
- Agarwal, S., Reddy, C. R. K. (2020). "A Comprehensive Study of Clustering Algorithms in Data Stream." International Journal of Engineering Research & Technology (IJERT), 9 (10).
- Alamdari, M. M., Rakotoarivelo, T., and Khoa, N. L. D. (2017). "A spectral-based clustering for structural health monitoring of the Sydney Harbour Bridge." Journal of Mechanical Systems and Signal Processing, 87, Part A: 384-400.
- Ali, H. H., and Kadhum, L. E. (2017). "K- Means Clustering Algorithm Applications in Data Mining and Pattern Recognition." International Journal of Science and Research (IJSR), 6(8): 1577 – 1584.
- Amezquita-Sanchez, J. P., Adeli, H. (2015). "Feature extraction and classification techniques for health monitoring of structures." *Sci. Iran.* 22:1931–1940.

- Anand, S., Mittal, S., Tuzel, O., and Meer, P. (2014), "Semi-Supervised Kernel Mean Shift Clustering." *IEEE Transactions on Pattern Analysis and Machine Intelligence*, 36(6): 1201 – 1215.
- Andrade, N. L., Finotti Amaral, R. P., Barbosa, F. D. S., and Cury, A. A. (2020). "A hybrid learning strategy for structural damage detection." *Structural Health Monitoring*, SAGE Journal.
- Avci, O., Abdeljaber, O., Kiranyaz, S., Hussein, M., Gabbouj, M., and Inman, D. (2021). "A review of vibration-based damage detection in civil structures: From traditional methods to Machine Learning and Deep Learning applications." *Journal of Mechanical Systems and Signal Processing*, 147.
- Azimi, M., Eslamlou, D. A., and Pekcan, G. (2020). "Data-Driven Structural Health Monitoring and Damage Detection through Deep Learning: State-of-the-Art Review." *Sensors*, 20, 2778.
- Bagchi, A., Humar, J. and Noman, A. (2007). "Development of a Finite Element System for Vibration Based Damage Identification in Structures." *Journal of Applied Sciences*, 7(17): 2404-2413.
- Boadu, E. F., Wang, C. C., and Sunindijo, R. Y. (2020), "Characteristics of the Construction Industry in Developing Countries and Its Implications for Health and Safety: An Exploratory Study in Ghana." *Int. J. Environ. Res. Public Health*, 17, 4110.
- Bouzenad, A. E., Mountassir, M., Yaacoubi, S., Dahmene, F., Koabaz, M., Buchheit. L., and Ke, W. (2019). "A Semi-Supervised Based K-Means Algorithm for Optimal Guided Waves Structural Health Monitoring: A Case Study." *Inventions*, 4, 17.
- Brownjohn, J. M. W., Omenzetter, P., and Moyov, P. (2005). "Data Mining and Visualisation for Anomaly Detection and Diagnosis in Civil Structures." 23rd International Modal Analysis Conference, At Orlando, USA.
- Bull, L., Worden, K., Manson, G., and Dervilis, N. (2018). "Active learning for semi-supervised structural health monitoring." *Journal of Sound and Vibration*, 437: 373-388.
- Catbas, F. N., Kijewski-Correa, T., and Aktan, A. E. (2011). "Structural Identification (ST-Id) of Constructed Facilities." American Society of Civil Engineers (ASCE) Structural Engineering Institute (SEI).

- Chen, W., Hu, X., Chen, W., Hong, Y., and Yang, M. (2018). "Airborne LiDAR Remote Sensing for Individual Tree Forest Inventory Using Trunk Detection-Aided Mean Shift Clustering Techniques." *Remote Sensing* 10(7):1078.
- Clayman, C., Srinivasan, S. M., and Sangwan, R. S. (2020), "K-means Clustering and Principal Component Analysis of Microarray Data of L1000 Landmark Genes." *Complex Adaptive Systems Conference with Theme: Leveraging AI and Machine Learning for Societal Challenges*, *Procedia Computer Science* 168: 97–104.
- Da Silva, S., Junior, M. D., and Junior, V. L. (2007). "Damage Detection in a Benchmark Structure Using AR-ARX Models and Statistical Pattern Recognition." *J. of the Braz. Soc. of Mech. Sci. & Eng*, XXIX(2): Pages:174-184.
- Deng, D. (2020). "DBSCAN Clustering Algorithm Based on Density." *2020 7th International Forum on Electrical Engineering and Automation (IFEEA)*: 949-953.
- Diez, A., Khoa, N. L. D., Alamdari, M. M., Wang, Y., Chen, F., and Runcie, P. (2016), "A clustering approach for structural health monitoring on bridges." *J Civil Struct Health Monit*, 6:429-445.
- Ding, Y., Sun, P., Wang, G., Song, Y., Wu, L., Yue, Q., and Li, A. (2014). "Early-Warning Method of Train Running Safety of a High-Speed Railway Bridge Based on Transverse Vibration Monitoring." *Hindawi Publishing Corporation, Shock and Vibration*, 2015.
- Duan, Z., and Zhang, K. (2006). "Data Mining Technology for Structural Health Monitoring." *Pacific Science Review*, 8: 27-36.
- EnDAQ, (2021), Retrieved from
<https://endaq.com/collections/endaq-shock-records-vibration-data-logger-sensors>.
- Entezami, A., Sarmadi, H., and Saeedi Rzavi, B. (2020). "An innovative hybrid strategy for structural health monitoring by modal flexibility and clustering methods.", *Journal of Civil Structural Health Monitoring*, 10: 845–859.

- Entezari, H. O., Ghalehnovi, M., and Entezami, A. (2018). "Early damage detection in structural health monitoring by a sensitivity method and DBSCAN clustering." 6th International Conference on Acoustics & Vibration (ISAV2016) At: K. N. Toosi University of Technology, Tehran, Iran.
- Freight Insurance Coverage Terms & Conditions. (2003). Retrieved 19, 2014, from pafins: <http://www.pafins.com/freightinsurancecoverage.htm>.
- Gaddam, A., Wilkin, T., Angelova, M., and Gaddam, J. (2020), "Detecting Sensor Faults, Anomalies and Outliers in the Internet of Things: A Survey on the Challenges and Solutions." *Electronics*, 9, 511.
- Global Infrastructure Hub. (Dec 2020). "Prefabrication of Building Parts and Modular Construction.", Retrieved from <https://www.gihub.org>.
- Godbole, S., Lam, N., Mafas, M., Fernando, S., Gad, E., and Hashemi, J. (2018). "Dynamic loading on a prefabricated modular unit of a building during road transportation." *Journal of Building Engineering*, 18: 260-269.
- Gupta, G., Asiz, A., and Smith, I. (2008). "Structural Performance of Prefabricated Wood Building during Handling and Transportation." *Proceeding of the 10th World Conference on Timber Engineering*, June 2-5, Miyazaki, Japan.
- Hamishebahar, Y., Li, H. Z., and Guan, H. (2020) "Application of Machine Learning Algorithms in Structural Health Monitoring Research." *EASEC*, 16: 219-228.
- Han, J., Kamber, M., and Pei, J. (2012). "Data Mining Concepts and Techniques." Third Edition, Morgan Kaufmann Publishers.
- Horvat, M., Jovic, A., and Burnik, K. (2021). "Assessing the Robustness of Cluster Solutions in Emotionally-Annotated Pictures Using Monte-Carlo Simulation Stabilized K-Means Algorithm." *Journal of Machine Learning and Knowledge Extraction*, 3: 435–452.
- Huang, F., Chen, Y., Li, L., Zhou, J., Tao, J., Tan, X., and Fan, G. (2019). "Implementation of the parallel mean shift-based image segmentation algorithm on a GPU cluster." *International Journal of Digital Earth*, 12(3).

- Innella, F., Bai, Y., and Xhu, Z. (2020). "Acceleration responses of building modules during road transportation." *Engineering Structures*, 210: 110398.
- Jafari, M. (2015). "Optimal redundant sensor configuration for accuracy increasing in space inertial navigation system." *Journal of Aerospace Science and Technology*. 47: 467-472.
- Jolliffe, I. T., and Cadima, J. (2016). "Principal component analysis: a review and recent developments." *Philos Trans A Math Phys Eng Sci*, 374(2065).
- Karthikeyan, G. B., Manikandan, G., and Thomas, T. (2020). "A comparative study on k-means clustering and agglomerative hierarchical clustering." *International Journal of Emerging Trends in Engineering Research*, 8(5): 1600–1604.
- Li, S., Pan, J., Luo, G., and Wang, J. (2020). "Automatic modal parameter identification of high arch dams: feasibility verification." *Earthquake Engineering and Engineering Vibration*, 19: 953–965.
- Lopez, D., and Froese, T. M. (2016). "Analysis of costs and benefits of panelized and modular prefabricated homes." *International Conference on Sustainable Design, Engineering and Construction, Procedia Engineering*, 145: 1291 – 1297.
- Noman, A.S., Deeba, F., and Bagchi, A. (2012). "Health Monitoring of Structures Using Statistical Pattern Recognition Techniques." *ASCE J of Performance of Constructed Facilities*, 27(5): 575-584, DOI: 10.1061/ (ASCE) CF.1943-5509.0000346.
- Pang, L., Liu, J., Harkin, J., Martin, G., McElholm, M., JavEd, A., and McDaid, L. (2020). "Case Study-Spiking Neural Network Hardware System for Structural Health Monitoring." *Sensors (Basel)*. 20(18): 5126.
- PATH Inventory. (2003). "Modular Multiple Dwellings, Partnership in Advanced Technology in Housing." Washington, DC, 2.
- Perafan-Lopez, J. C., and Sierra-Perez, J. (2021). "An unsupervised pattern recognition methodology based on factor analysis and a genetic-DBSCAN algorithm to infer operational conditions from strain measurements in structural applications." *Chinese Society of Aeronautics and Astronautics& Beihang University*, 34 (2): 165-181.

- Perera, R., Torres, L., Ruiz, A., Barris, C., and Baena, M. (2019). "An EMI-Based Clustering for Structural Health Monitoring of NSM FRP Strengthening Systems." *Sensors (Basel)*, 19(17): 3775.
- Posenato, D., Kripakaran, P., Inaudi, D., and Smith, I. F. C. (2010). "Methodologies for model free data interpretation of civil engineering structures." *Computers & Structures*, 88(7-8), 467–482.
- Salem, N., and Hussein, S. (2019). "Data dimensional reduction and principal components analysis." 16th International Learning & Technology Conference, *Procedia Computer Science*, 163: 292-299.
- Santos, A., Figueiredo, E., and Costa, J. (2015). "Clustering studies for damage detection in bridges: A comparison study." In *Proceeding of 10th International Workshop on Structural Health Monitoring: 1165–1172*, Stanford University, Stanford, CA-USA, Sep 2015
- Santos, A., Silva, M., Santos, R., Figueiredo, E., Sales, C., Joao, C. (2016). "Output-only structural health monitoring based on mean shift clustering for vibration-based damage detection." 8th European Workshop on Structural Health Monitoring (EWSHM 2016), Spain, Bilbao.
- Shi, P., Zhao, Z., Zhong, H., Shen, H., and Ding, L. (2020). "An improved agglomerative hierarchical clustering anomaly detection method for scientific data." *Concurrency and Computation: Practice and Experience*, 33(6).
- Shukla, S., and Naganna, S. (2014). "A Review on K-means Data Clustering Approach.", *International Journal of Information & Computation Technology*, 4 (17): 1847-1860.
- Silva, M., Santos, A., Santos, R., Figueiredo, E., Sales, C., Joa, C. (2016). "A structural damage detection technique based on agglomerative clustering applied to the Z-24 Bridge." 8th European Workshop on Structural Health Monitoring (EWSHM 2016), Spain, Bilbao.
- Smarsly, K., Dragos, K., and Wiggenbrock, J. (2016). "Machine learning techniques for structural health monitoring." 8th European Workshop on Structural Health Monitoring (EWSHM 2016), 5-8 July 2016, Spain, Bilbao.

- Smith, I., Asiz, A., and Gupta, G. (2007). "High Performance Modular Wood Construction Systems." Final Report, Value to Wood Program, Project UNB5, Natural Resources Canada, Ottawa, Canada, pp. 80.
- Spittgerber, H. (1978). "Effect of Vibration on Building and Occupants of Buildings." Conference on Instrumentation for Ground Vibration and Earthquakes, 147-152, Institution of Civil Engineers, London, UK.
- Sun, Y., Wang, J., Wu, J., Shi, W., Ji, D., Wang, X., and Zhao, X. (2020). "Constraints Hindering the Development of High-Rise Modular Buildings.", *Appl. Sci.* 2020, 10, 7159.
- Syakur, M. A., Khotimah, B. K., Rochman, E. M., and Satoto, B. D. (2018). "Integration K-Means Clustering Method and Elbow Method for Identification of The Best Customer Profile Cluster." *IOP Conference Series: Materials Science and Engineering*.
- Valinejadshoubi, M., Bagchi, A., and Moselhi, O., (2018a). "Development of a BIM-Based Data Management System for Structural Health Monitoring with Application to Modular Buildings: A Case Study." *ASCE J of Computing in Civil Engineering*, 33(3), 05019003.
- Valinejadshoubi, M., Bagchi, A., & Moselhi, O. (2017). "Managing structural health monitoring data using building information modelling." In *SMAR 2017, the Fourth international conference on smart monitoring, assessment and rehabilitation of civil structures*, (September 13-15, 2017).
- Valinejadshoubi, M., Bagchi, A., Moselhi, O., and Shakibaborough, A. (2018b). "Investigation on the potential of building information modeling in structural health monitoring of buildings." *CSCE annual conference*, June, Fredericton, NB (GC-136).
- Weiss, B., Helu, M., Vogl, G., Qiao, G. (2016). "Use Case Development to Advance Monitoring, Diagnostics, and Prognostics in Manufacturing Operations." *IFAC-PapersOnLine* 49(31), pp: 13-18.
- SpotSee. (2021). "Impact Sensors, Impact Monitors and Shock Sensors." Retrieved from www.spotsee.io.
- Yuan, C., and Yang, H. (2019). "Research on K-Value Selection Method of K-Means Clustering Algorithm.", *Multidisciplinary Scientific Journal*, 2(16): 226-235.

Zhou, Y., Maia, N. M. M., Sampaio, R. C., and Wahab, M. A. (2016). "Structural damage detection using transmissibility together with hierarchical clustering analysis and similarity measure." *Structural Health Monitoring* 21(6).

Chapter 4: Development of a BIM-Based Data Management System for Structural Health Monitoring with application to Modular Buildings: A Case Study

General

In this chapter, the published paper is presented as is, followed by an updated literature review section. This paper was accepted and published in the Journal of Computing in Civil Engineering in 2019*. The main objective of this paper is to develop an automatic workflow to integrate BIM into the SHM process to increase the speed and efficiency of structural condition assessment.

Abstract

Modular buildings or off-site construction of building units are increasingly gaining momentum. Although such construction practices have advantages in terms of cost competitiveness and delivery time, they have many issues related to structural integrity and secondary stresses from vibration during transit and misalignment during installation. Therefore, monitoring the vibration, strain, and deformation of the modules using structural health monitoring (SHM) techniques is important. The primary purpose of this study is to explore building information modeling (BIM) techniques to facilitate effective data management and the representation of sensory components of the SHM system in a building and to render or visualize the damage or distress in building components based on the interpretation of sensor data. The proposed framework consists of two main modules: (1) an automated sensor-based data acquisition and storage module, which extracts sensor data for a structure from a corresponding relational database; and (2) an automated data and

* Valinejadshoubi. M, Bagchi. A, and Moselhi. O, (2019), Journal of Computing in Civil Engineering, Vol. 33, Issue 3, Pages 1-16

damage visualization module, through which sensor data are interpreted to identify damage or anomalies in the structure and the affected building components are highlighted and tagged in the BIM of the building to facilitate visualization. The damaged or near-damaged elements of the modules are highlighted in the BIM model through color-coding based on predefined threshold strain values. Because detecting buckled or yielded steel members (local damages) in a building or a module is challenging given that these components are often hidden behind fireproof coating and drywall, the proposed SHM-based condition assessment system will contribute—especially in the preinstallation and operational phases—to providing efficient, near-real-time health monitoring of buildings and increasing the efficiency of the structural condition assessment process. These benefits could be particularly useful for modular buildings, for which the modules are constructed in a plant and transported to the site for installation. In these stages, a module may undergo hidden or visible damage, the installed sensors are expected to provide a mechanism to assess such damage, and the entire process can be managed through BIM. Importantly, note that although a similar concept was explored by other researchers to integrate SHM with BIM, the present study provides a more comprehensive methodology through the complete implementation of the system to demonstrate the concept through a case study.

Keywords: Structural Health Monitoring (SHM), building information modeling (BIM), Relational database, Damage visualization, Modular buildings

4.1. Introduction

The modular construction process represents the highest degree of industrialization of the building construction process, which is currently growing rapidly. Presently, in some construction projects, prefabrication/modular construction is approximately 85% (McGraw-Hill Construction, 2011). Clients' requirements for rapid construction, improved quality, and early investment returns are some of the motivating factors for modular construction.

Modular steel buildings are usually composed of prefabricated cold-formed steel assemblies or modules that are fabricated in a manufacturing plant and then shipped to the construction site to be installed to form a building. Compared with hot-rolled steel structures, cold-formed light steel structures are lighter but more susceptible to structural damage given normal and extreme loads (Yang and Bai, 2017). A sufficient understanding of the structural behavior of multistory modular buildings subjected to different load types is lacking (Ramaji and Memari, 2013). Different situations exist that could lead to the failure of a module, such as increased damage during erection or transportation. Geometric variability is inevitable and can cause problems in the assembly process. A module's component geometry can change from its original design because of problems arising from the manner in which it is handled in the plant, during transportation, and at installation (Rausch et al., 2017). The geometric change may lead exceed the tolerance of fit and generate secondary stresses at installation, causing further damage.

From the manufacturing to the operational phase, modules are subjected to different types of direct and indirect loads. The modules are required to be designed to withstand fabrication, transportation, and installation loads (Naqvi et al., 2014). Predicting the final and capacity of a modular building after being transported is difficult and lifting-induced stresses are not entirely predictable. Because the structural elements of a module of a building are usually hidden behind

the fireproof coatings or drywall, detecting the buckled or yielded steel members (local damages) in a module is challenging (Zhang and Bai, 2015). In this context, a useful monitoring tool such as SHM is needed for early structural condition assessment and damage detection in specific parts of the modules in each phase. SHM systems are ranked as one or a combination of the following SHM categories: sensor deployment studies (category 1), anomaly detection (category 2), model validation (category 3), threshold check (category 4), and damage detection (category 5), (Vardanega et al., 2016). Higher level categories (e.g., categories 4 and 5) have the potential to yield significant values to many stakeholders. According to Webb (2014) and Webb et al. (2014), most published SHM studies are devoted to categories 1 to 3 and the least to category 4.

In practice, monitoring the strain response contributes to an assessment of the structural condition (Park et al., 2013; Ni et al., 2010, 2008). Continuous monitoring of a real-time dynamic strain in a structure can provide valuable information for damage assessments, inspections, and decision making. Strain provides information about the local behavior of structural components and is one of the most used parameters in SHM. Strain is essential in condition monitoring of modular buildings, which can aid in the assessment of damage in structural members in building modules at different stages, and helps assess the reliability of structural components.

Fast and accurate assessment of the structural condition of modules and buildings (modular or other) is essential for timely maintenance and repair to avoid project delays, and is important for occupant safety and occupancy after extreme load events. The challenge, in general, is an effective visualization tool utilizing BIM to make the SHM information easily accessible, understood, and applicable (Zhang and Bai, 2015), which could increase the efficiency of the structural condition assessment process and facilities management. BIM can be used effectively to capture the real time building information that can be used for owners and facility managers to provide accurate and

upgraded details on the state of various parts of the building (Chen et al., 2014). BIM combined with real-time monitoring of structural health and damage assessment methods could provide a robust and intelligent system for managing modern buildings, including the modular building type (Seam et al., 2013). However, integrating SHM into the BIM environment has challenges. The study run by Rio et al. (2013) revealed that accomplishing a dynamic monitoring system for the structural behavior of a building to provide sensor data to BIM is not part of BIM functionality and is still a challenge. They concluded that BIM standards need to be extended to allow them to represent monitoring-related information. The study by Wang et al. (2017) found that applying BIM in SHM can improve the effectiveness of monitoring processes and decision making in construction informatics applications.

Despite its potential benefits, few attempts have been made to integrate BIM into SHM. Sternal and Dragos (2016) proposed BIM-based modeling of wireless SHM systems using the industry foundation class (IFC) standard. Although they believed that integrating monitoring-related information into BIM helps categorize, document, and update this information throughout the entire life cycle of the monitored structure, it was mentioned at the end that the current IFC standard does not provide sufficient entities to holistically model and digitally represent an overall wireless SHM system. Theiler et al. (2017) attempted to design a BIM-based prototype SHM and control system by using the extended IFC schema. Smarsly and Tauscher (2016) proposed a conceptual monitoring information modeling built on the IFC standard. Although the authors defined a semantic model to extend the existing IFC 4 standard for digital representation of monitoring-related information, the paper was conceptual and did not include implementation or validation. Del Grosso et al. (2017) attempted to explore the idea of integrating 6D digital models with SHM systems, but the study mainly focused on creating and modeling the sensor system in the BIM software application and did not provide the linkage to sensor data or facilitate

visualization. Although the authors of this study discussed the state of the art of the current and potential relationship between SHM and BIM, they believed that the topic is not explored well and needs further investigation. Additionally, it was noted that no preferred workflow exists to inform the BIM model with SHM and interpreted data regarding elements of the project. A preliminary scheme for utilizing BIM to manage SHM data for buildings was developed in Valinejadshoubi et al. (2018c, 2017). BIM was also effectively used in thermal comfort monitoring (Valinejadshoubi et al., 2018b) and the assessment of the seismic risk of non-structural components in buildings (Valinejadshoubi et al., 2018a).

Although BIM is desired as a dynamic workbench for managing all data related to a building project, connectivity between BIM and SHM is lacking. The full integration between virtual and physical sensors, connecting and inserting sensor data remotely into an external database through Internet of Thing (IoT) technology, and applying a three-dimensional (3D) visualization-based alarm system for SHM projects have not been adequately addressed in previous studies, and the BIM approach has not yet been fully applied and validated for SHM purposes. To address some of these issues, in the present study, a novel integrated system is developed for structural condition monitoring of building components. SHM data are stored in the database and automatically accessed by the BIM model, and the conditions of the relevant building elements are calculated and mapped on the BIM model to visualize the overall state of the structure. The main purpose of this study is to create a mechanism for a BIM model of a building or module to represent and access sensor data, run a data interpretation or damage assessment process, and map it on the corresponding building components. Doing so would facilitate an effective visualization capability for a rapid and efficient structural condition assessment based on the SHM data. The proposed framework can be applied by engineers and facility managers to interpret and assess the ongoing condition of modules during the transportation, installation, and operational phases, to identify

hidden damages, and to replace the damaged parts by providing and managing updated monitoring data in a rapid manner to promote timely repair.

4.2. BIM and its Role in the Modular Building Construction

Presently, the architectural, engineering, and construction (AEC) industries have been seeking an effective tool for reducing the cost and completion time of projects and increasing their productivity and quality (Azhar et al., 2008). BIM has significantly altered the way that building information is managed by the AEC industry. BIM incorporates digital modeling software to design and manage a project more efficiently (Nassar, 2010) and provides powerful new value to construction firms. BIM breaks down the barriers between disciplines by encouraging the sharing of knowledge throughout a project's lifecycle. BIM improves constructability and shortens a project's completion time. In a BIM project, multiple documents are not used in traditional ways; instead, they are digitized and added to a database in BIM software. All information is built into an intelligent BIM model instead of needing to look at separate drawings, schedules, and specifications for the information on a particular element.

BIM is an organized collection of building data. Regarding BIM, everything begins with a 3D building model. This model has more than just simple geometry added to it for visualization. A true BIM model consists of the virtual equivalent of actual building sections. These intelligent elements are the digital prototype of the physical elements, including walls, columns, windows, doors, specialty equipment, and others. The model allows us to simulate the building and understand its behavior before actual construction begins. Of course, the most basic BIM model is used to create realistic visualizations of the planned building. As previously mentioned, the data in a BIM model are not only used during the design and construction phases of the building project

but also throughout the building's life cycle. The building-related data can be easily archived in the BIM model for such things as future usage, analysis, retrieval, and maintenance.

Because modular construction has an additional manufacturing stage relative to conventional construction, utilizing BIM as a powerful information management tool is required. A current issue of offsite construction has been perceived as a process lacking flexibility in design. BIM can partially address this limitation by providing access to a vastly broader range of constituent parts in various levels of detail, from the micro level of an individual fastener to the macro level of a volumetric component (Patlakas et al., 2015). BIM can be used for proper information exchange between different disciplines, which is a fundamental need in multidisciplinary projects such as modular building projects. Data-rich models such as BIM can be used effectively by other members of the design team to coordinate the fabrication of a building's different systems (Nawari, 2012). BIM can be used in effective simulation and visualization of a building and its components in digital forms, which are useful for accurate planning of onsite module installations and can resolve any spatial constraints (Han et al., 2011). Due to the large number of elements in modular structures, an automated system is needed for visualizing and monitoring the structural condition of elements in modules in each phase of the project.

4.3. SHM in Modular Buildings

A modular building is erected by assembling individual modules. Every module is a primary rectangular frame made of steel or wood frames. The modular units are stacked on top of and or next to one another through a connector at every joint. Two types of connections—vertical (column to column) and horizontal—are used in modular building construction.

Potential failure modes in modular buildings include structural component failures within a modular frame and connection failures at the modular joints. Regarding component failures, corner posts buckling or load-bearing studs and bending of columns/beams may occur. Regarding connection failures at the joints, modular units become separated, which reduces their axial stiffness to zero, causing a critical situation concerning the overall integrity of the entire system. Local connection failure (LCF) occurs due to excessive concentrated force on the connection region, causing complications in the load transfer path. Different types of loads, such as manufacturing, transportation, installation, and operation, are applied to the modules. Any damage to the modules before installation may affect the operational performance of the same. Hence, the modules must be erected without any hidden damage. SHM can be applied for early and rapid structural condition assessment and damage identification of building modules during every phase to assist engineers in deciding on rehabilitation measures when the module's components experience unexpected changes in excessive deformation, deflection, and strain.

SHM system design is developed based on failure modes. It is advantageous for modules' components to be equipped with SHM systems as they are being manufactured. Particular care should be taken regarding the installed sensors on the elements from roughness-induced vibration forces during transportation. Different types of sensors can be applied in the SHM of the modules. For instance, linear variable displacement transducer (LVDT)/ultrasonic sensors are used to measure critical structural deformation (serviceability) and the module separation at the connection region (LCF). Moreover, strain gauges are used to measure the real-time strain on critical structural members in the modular system.

4.4. Determining the Locations of Strain Sensors

Modules can be made from light gauge/cold-formed steel or hot-rolled steel such as pipe chassis. However, compared with hot-rolled steel modules, cold-formed light steel modules are more susceptible to deformation and buckling due to applied loads.

The level of strain in structural elements serves as a significant indicator of the level of deformation and damage in the structural and non-structural elements. Considering this fact, SHM systems often employ strain gauges to measure strains in critical components. Modular construction projects are more complex than conventional ones given the additional manufacturing and transportation processes. Therefore, in addition to operational load, the building modules are subjected to manufacturing, transportation, and installation loads that make their structural elements more susceptible to damage or excessive deformations. For instance, transportation and handling of modules is an important part of the overall life of the modules when they experience high mechanical loads. To identify vulnerable and critical elements, a detailed and accurate structural analysis is needed for each phase for typical modules.

For example, the force from vibrations during the transportation of modules can be simulated in a finite element (FE) model of individual modules to identify their critical elements that could be damaged given road-induced vibration. For this purpose, random vibration data can be used to simulate field and transportation conditions. Random vibration is typically described by power spectral density (PSD) curves of average acceleration intensity in the frequency domain. Different transport vehicles can be related to different PSD shapes and amplitudes. In North America, modules are commonly transported by road (using tractor-trailers). The ASTM D4169 Truck Profile [ASTM D4169 (ASTM, 2016)] is among the most widely used road-induced vibration profiles for general simulation and random vibration tests in laboratory experiments. In

such cases, the vibration test on a truck is performed at a single intensity level (e.g., Assurance Level II) for the entire test duration. The recently updated version of the standard [ASTM D4169 (ASTM, 2016)] recommends the use of three different intensity levels: low, medium, and high, corresponding to the 90th, 95th, and 99th percentile intensities. Figure 4-1 shows the PSD levels for different frequencies according to the ASTM D4169 standard, which is typically used for performance testing of shipping containers and systems. The typical PSD units are acceleration $[G^2/Hz]$ versus frequency $[Hz]$. Note that the amplitude is actually $[GRMS^2/Hz]$, where RMS = root-mean square. The RMS notation is typically omitted for brevity. GRMS is used to define the overall energy or acceleration level of random vibrations. In Figure 4-1, profiles 1 to 3 correspond to low-, medium-, and high-level PSD levels, respectively.

As an example, the FE model of an industrial pipe chassis module (hot-rolled steel module) used by Shahtaheri et al. (2017) has been developed here using Autodesk’s Simulation Mechanical.

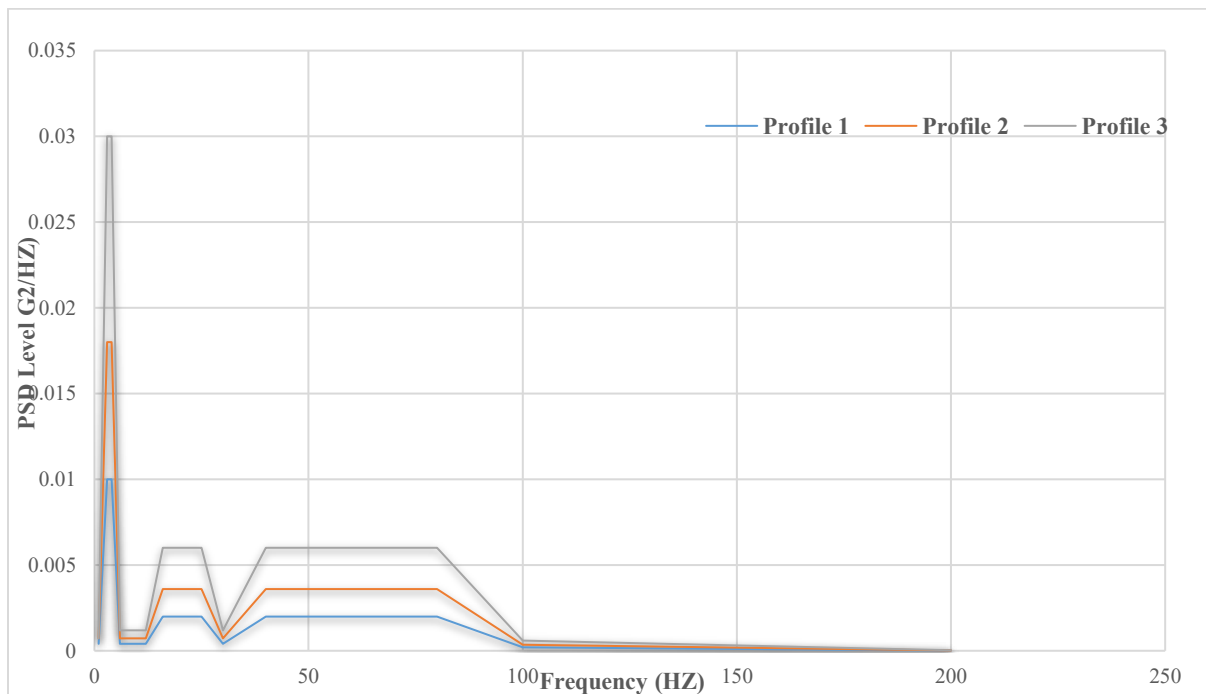
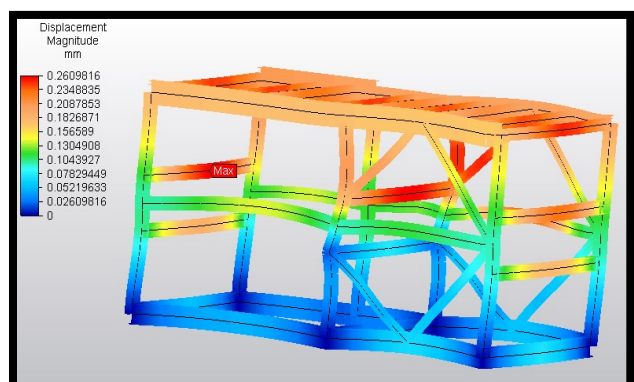
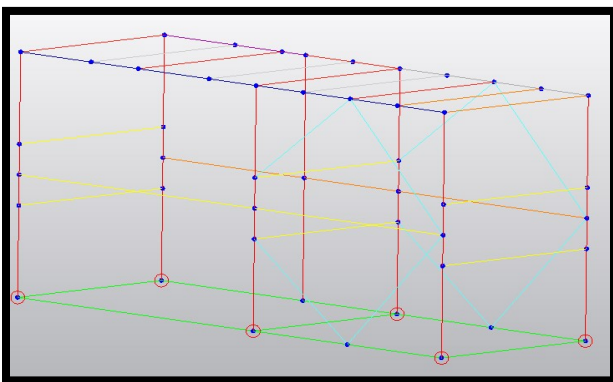


Figure 4-1: Random Vibration Profiles of Trucks (ASTM D4169 Truck Assurance Levels 1 to 3)

To simulate the transportation vibration forces, high PSD level, and its corresponding frequencies as given in Figure 4-1 were applied to the developed FE model. Figure 4-2 shows the FE model of a pipe chassis module. The arrangement of the temporary supports and module dimensions are assumed to be the same as that used in Shahtaheri et al. (2017). As shown in Figure 4-2, the most critical elements with the highest displacement should be monitored during the transportation phase. Although the maximum displacement obtained from the analysis is found to be very small (approximately 0.26 mm), in the case of a light gauge/cold formed steel module, it could be much larger. In contrast, uncertainties such as temporary support configuration, which is usually based on experiments rather than objective analysis, might even increase the magnitude of the maximum displacement in the structural elements of the module.



(a) The industrial pipe chassis module (Shahtaheri et al., 2017)



(b) The FE model

Figure 4-2: A sample of random vibration simulation of a pipe chassis module

Similarly, the structural behavior of modules could be analyzed against manufacturing, installation, and operational loads to determine their critical elements in each phase.

4.5. Data Management Challenges in SHM Process

One of the inherent challenges in SHM is high-volume data management. Management of all original raw data and all postprocessed data during the entire life cycle of the structure with possible size of hundreds of gigabytes can become a problem if all of the original data are to be kept for future processing (Rio et al., 2013). In periodic SHM installations, all data are stored onsite on a data acquisition (DAQ) unit. Additional computation and storage resources are required for continuous monitoring. In most cases, sensors are set at a frequency of 100 Hz and a 16- or 24-bit resolution per sample, yielding 26 megabytes of daily volume from a single sensor channel. Therefore, setting up network communications between an onsite DAQ system and a remote data server is necessary.

Efficient storage of SHM data facilitates easy examination and backup. The best approach for SHM data storage is storing them in a commercial database system or a database storage system from a third party such as MySQL or PostgreSQL. Taking the SHM data files saved in the DAQ system and loaded into the database is necessary (Karbhari and Ansari, 2009).

After collecting and analyzing the data from the DAQ system, SHM measurements need to be archived for their protection against data loss and to maintain a chronology record of the structures. Given the high volume of data in the SHM process, downsizing the data for better management is critical. Jeong et al. (2016) used NoSQL database technologies to propose a data management infrastructure framework for bridge monitoring applications.

Koo et al. (2011) presented an SHM data management system (SDMS) based on the MySQL database management system (DBMS) for efficient data storage, retrieval, and sharing of large measurement data sets acquired continuously from SHM systems. However, to solve SHM data management issues, a greater need exists for more efficient tools and integrated systems.

4.6. Research Methodology

The proposed framework consists of several modules and submodules. The objective of SHM-based condition assessment module is to assess the building modules' conditions through strain sensor data in an automated manner. Depending on the type of sensors, different methods can be applied. For example, in the case of strain sensors, the threshold value analysis (TVA) method is often employed to detect the exceedance of available threshold strain levels. In contrast, accelerometer data are often processed using different signal processing techniques in time or frequency domains to determine global parameters such as frequencies and mode shapes. By integrating SHM with the BIM model, the detected changes in the system properties or the local damage can be mapped on the BIM model and visualized dynamically. In the present study, only strain sensors are considered for demonstration purposes. Strain sensors can be used to rapidly identify and locate the spot wherein an element exceeds the pre-set strain threshold. The system is linked to the BIM model to highlight the damaged elements in an automated manner.

By linking SHM to BIM, the efficiency and speed of structural condition assessment processes can be increased, and the process can potentially help non-engineers interact with the building elements and gain an overall sense of the structural condition. Although this system is applicable for all types of structures and infrastructures, its uniqueness in modular construction is

in its ability to rapidly detect the buckled or yielded steel members (local damages) in a module, which are often hidden behind the fireproof coating and drywall at different phases (e.g., manufacturing, shipping and installation).

The developed framework consists of four subcomponents, including an Arduino Uno microcontroller (Arduino, Ivrea, Italy) equipped with a strain sensor, an amplifier and Wi-Fi shield (sensory system); Autodesk Revit 2017 (BIM software); Dynamo (visual programming environment); and SQL Server (database management system). In this framework, two links exist: the link between the sensory system and the SQL server and the link between the SQL server and the BIM model.

First, the BIM model is developed with all elements including the virtual sensor and its essential parameters, such as *StrainMaxPoint*, *DamageFlag*, *Sensor-ID*, and others. The BIM model is used as a central model to visualize and monitor the strain level remotely produced in critical elements. After developing the BIM model, a specific database is designed in a MySQL environment to house and update the captured sensors data. DAQ systems such as Arduino Uno are coded to remotely send the sensors' measurements in real time to an external database using the Arduino GSM Shield (Arduino, Ivrea, Italy). The Arduino GSM Shield connects the Arduino to the Internet using a GPRS wireless network. Before transferring the sensor data to MySQL server, a schema (database) table and essential parameters such as Record-ID and Sensor-Value are generated for the strain sensor in the database to accommodate the sensor information and the sampling data. In this study, only strain value is of concern. When strain sensor data are imported into the database, they need to be read by an external tool before processing. For this purpose, a visual programming and computational design tool called Dynamo is utilized for automation purposes (Dynamo BIM, 2017).

To link the MySQL database (physical sensors data) and the BIM model (virtual sensors), nine modules were developed and coded in Dynamo to automatically read the strain data stored in the database, sort the data, and update the BIM model with the latest real-time sensor data. These data were used to send notifications to engineers through their wireless devices, such as personal computers or smartphones, enabling them to then take the necessary actions if strain values exceed the predefined strain level. The individual steps of the workflow, developed in Dynamo, are subsequently described.

Once the strain data are read, a module is developed to automatically sort and interpret. For example, when strain sensors are used to measure the real-time strain on critical structural members in the modular system, the developed module sorts the strain data and obtains the maximum strain value in every time interval. Once the strain data are sorted, and the maximum strain value is extracted, an additional module then updates the corresponding virtual sensor parameter in the BIM model. One or more pre-set strain threshold values can be defined to automatically highlight the structural elements in the BIM model to rapidly identify and locate the elements for which pre-set threshold strain occurs. In this study, only one threshold is defined. The damaged elements for which the strain exceeds the threshold are highlighted in the BIM model to generate an alarm signal. The hierarchy of the processing modules is shown in Figure 4-3.

To illustrate the capabilities of the system developed, a set of strain values is utilized to mimic the data produced by a strain sensor.

4.7. The System Framework

4.7.1. The Conceptual Framework of Wireless Strain Monitoring System

The DAQ system recommended in this framework consists of strain gauges, a microcontroller and its software, an instrumentation amplifier module, a 9V battery, a Wi-Fi shield, jumper wires, and a computer with programmable software.

The system configuration is based on the Arduino Uno open-source microcontroller used for onboard data acquisition. The microcontroller is based on the ATmega328P, an Atmel AVR processor that can be programmed in a computer using the C language through a Universal Serial Bus (USB) port. The microcontroller can sense the environment by receiving input from a variety of sensors and can be powered by connecting to a computer with a USB cable, an AC-to-DC adapter, or a battery. In this study, a battery is used during monitoring. The Arduino board can operate on an external supply of 6 to 20 V. However, if supplied with less than 7V, it may be unstable. If using more than 12V, the voltage may overheat and damage the board. Therefore, the range should be between 7 and 12V. Hence, a 9V battery is recommended.

Strain gauges are variable resistors for which the resistance changes when they are stretched or compressed along their length. When bonded to a structural element, the resistance changes proportionally to the strain of the element depending on the force applied to deform it. Although directly reading the voltage change of the bridge of a strain gauge is possible, doing so is normally impractical without an amplifier. The maximum voltage change from the strain is too small for the digital to analog converter in an Arduino to register. The instrumentation amplifier boosts the signal to bring it to a readable range. For this purpose, an instrumentation amplifier, such as the INA125P amplifier, should be used when measuring the strain gauge data with the Arduino.

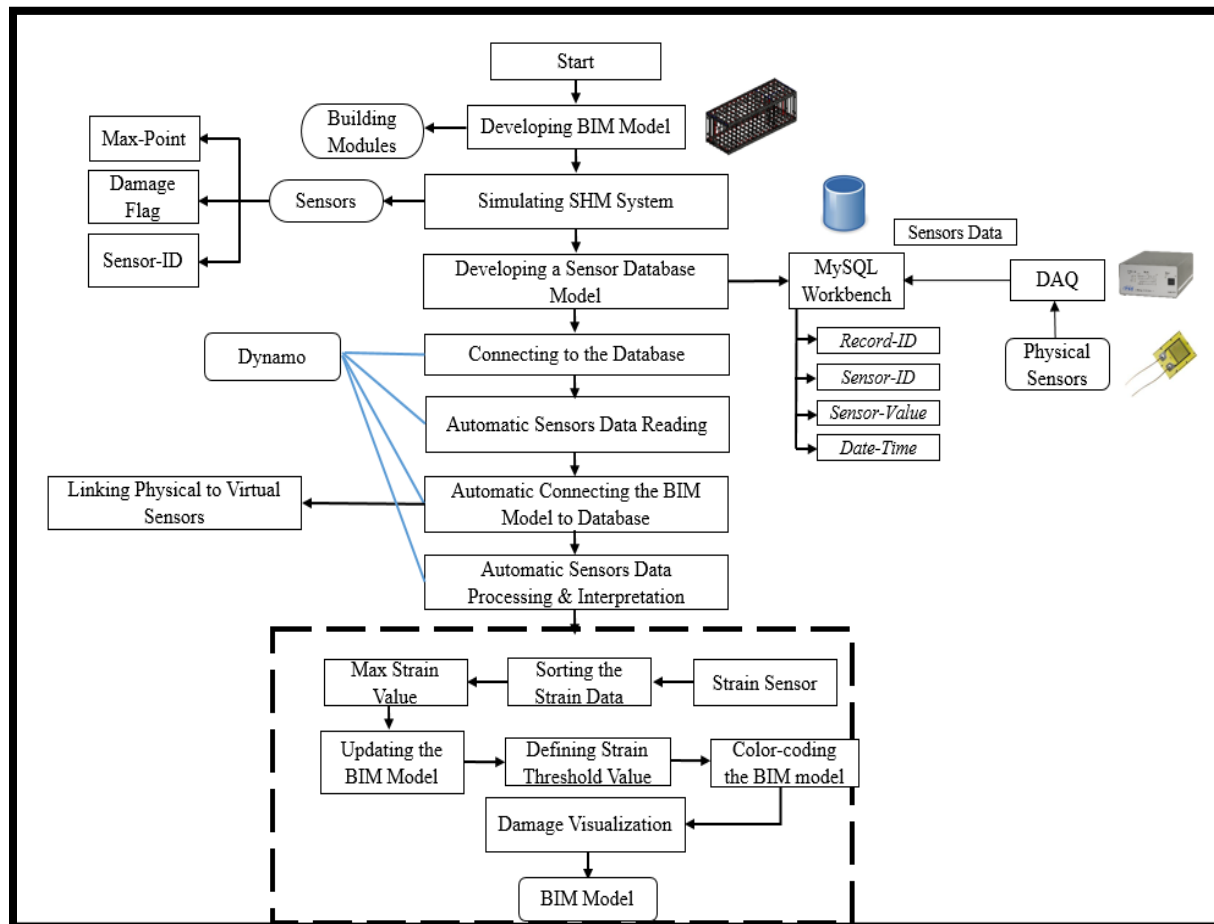


Figure 4-3: Hierarchy of the steps in this study

The open-source Arduino software (IDE) can program the Arduino Uno to process the raw data and extract the results of interest to be transmitted to a central station, thus reducing the data communication demand that is particularly suitable for wireless communication in SHM systems. Storing a sensor's data over a cloud-based database server such as an SQL database is also possible. Creating a website or another app to read the sensor values in the SQL database and track the events according to the threshold values will give considerable power to any SHM project. For this purpose, a Wi-Fi shield compatible with the Arduino Uno is recommended. An Arduino compatible shield, such as the ESP8266 WiFi Shield, equips the Arduino with the ability to connect

to the wireless networks that can be used for Internet of Things (IoT) or WiFi-related projects. Monitoring data such as strain values can be stored directly in a MySQL server using the MySQL Connector in the Arduino library. The MySQL Connector in the Arduino library can be used to connect the Arduino project directly to a MySQL server without using an intermediate computer or a web- or cloud-based service. When the strain values are measured and stored in a prebuilt MySQL database, they can be analyzed in remote wireless connected devices such as personal computers, tablets, or smartphones. An alarm system could be proposed in these devices for rapid detection of excessive deformation (plastic deformation) in structural elements for timely repair or replacement of the faulty elements. Figure 4-4 illustrates the architecture of a conceptual framework of a wireless strain monitoring system.

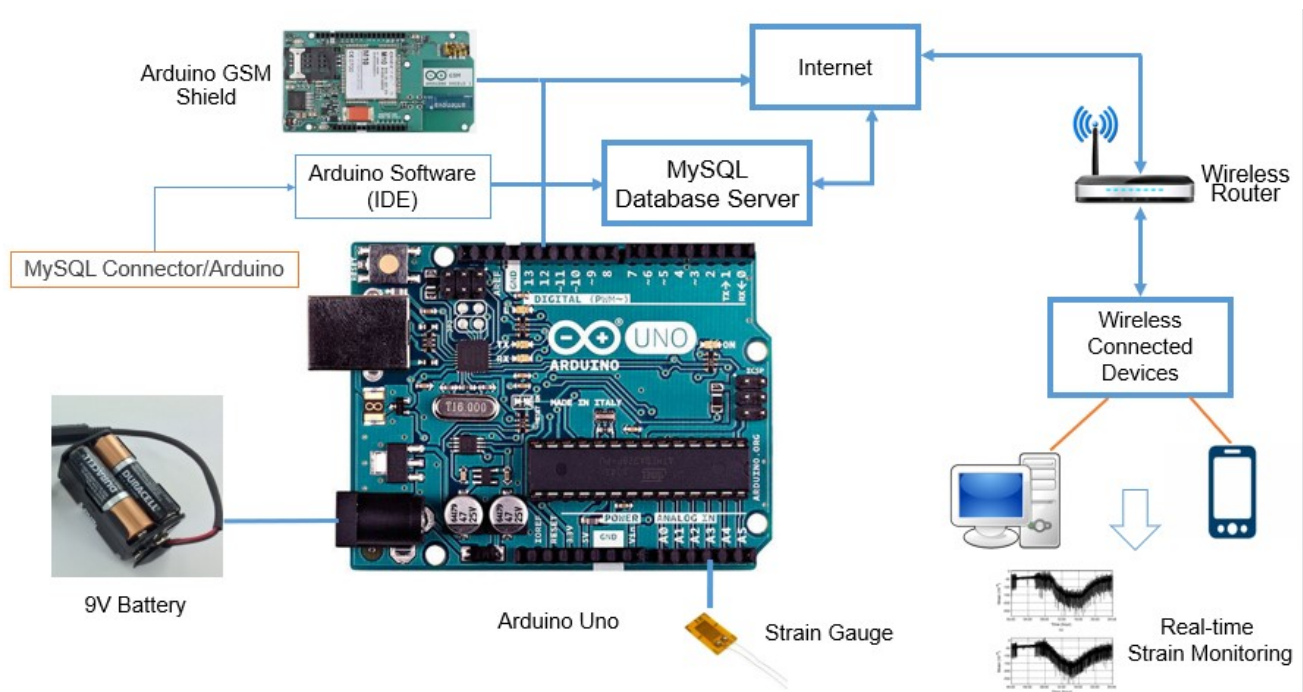


Figure 4-4: The conceptual framework of a wireless strain monitoring system

4.7.2. SHM System Modeling in the BIM Model

After developing the BIM model, SHM sensors need to be simulated in the model. A strain sensor is modeled and attached to its specified locations in the BIM model. Many different categories exist in the BIM objects, such as column, beam, floor, roof, door, window, and others. In BIM, each category has its own IFC class name, such as *IfcColumn* and *IfcRoof* to name a few, and in sensors—*IfcSensor* and *IfcSensorType* class names are categorized under the specific equipment category. Therefore, sensors in the BIM model must be developed subject to the specialty equipment category.

Different parameters are defined for the strain sensor during modeling: identity data (e.g., manufacturer, label, mark, model, cost), phasing, scope, station, and data (*StrainMaxPoint*, *DamageFlag*). Station parameter is defined to show the exact location of the sensors in the BIM model, and the mark parameter is set to link the physical sensors to virtual sensors in the BIM model. In fact, the physical sensors' specific identification (ID) must be assigned to each corresponding virtual sensor in the BIM model to link the physical and virtual sensor. *StrainMaxPoint* is the parameter created to accommodate the maximum strain value recorded by the strain sensor at each time interval, and *DamageFlag* is generated to show the structural elements condition rate. A building module and a strain sensor modeled in the BIM tool, along with some of its defined parameters, are illustrated in Figure 4-5.

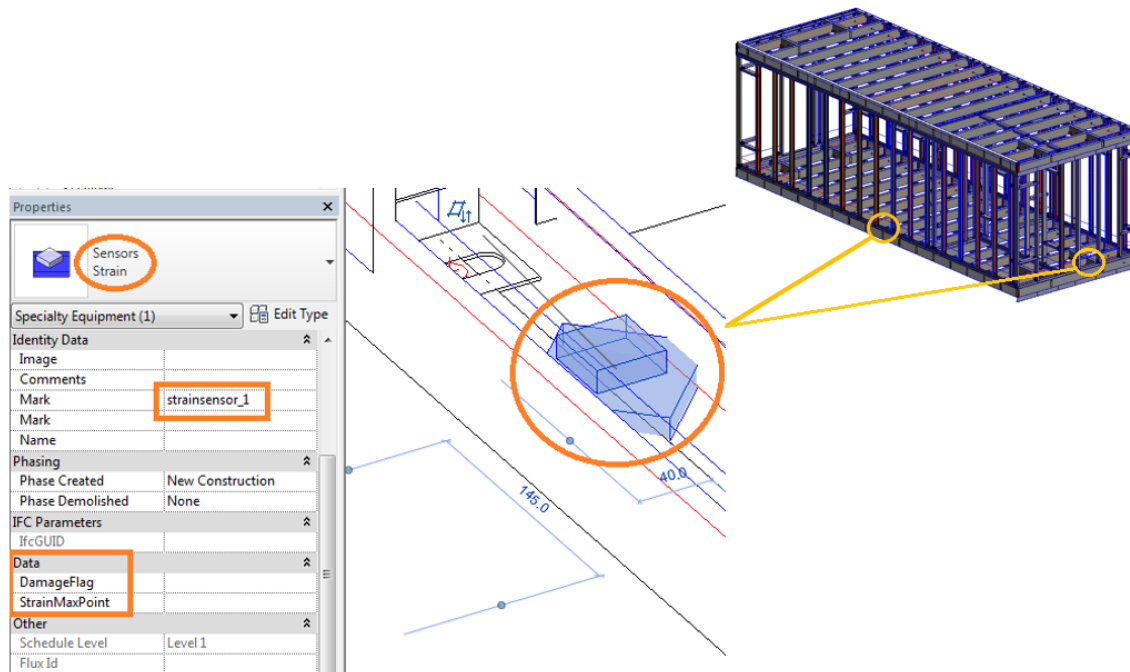


Figure 4-5: Developing the BIM model and the virtual strain sensor

4.7.3. Defining the Sensor Database Model

To insert the sensed data from a sensor into a database such as MySQL, a schema (database) and a table, along with all essential parameters, are to be defined. The table will embody the sensor data received from the DAQ system. To prevent users from manually generating the sensor database model, two modules are created in Dynamo to draw a schema, producing a table and columns in an automated manner. The schema—*shmsystem*—is defined along with a table called *strainsensor_1*. Three parameters are introduced for the *strainsensor_1* table: *Record_ID*, *Sensor_Value*, and *Sensor_Name*, where *Record_ID* constitutes the primary key. Appropriate nodes, code blocks, and connections are required to automate this process. The modules developed to generate the schema and table in the MySQL database in an automatic sense and to embody the strain sensor measurements are illustrated in Figure 4-6.

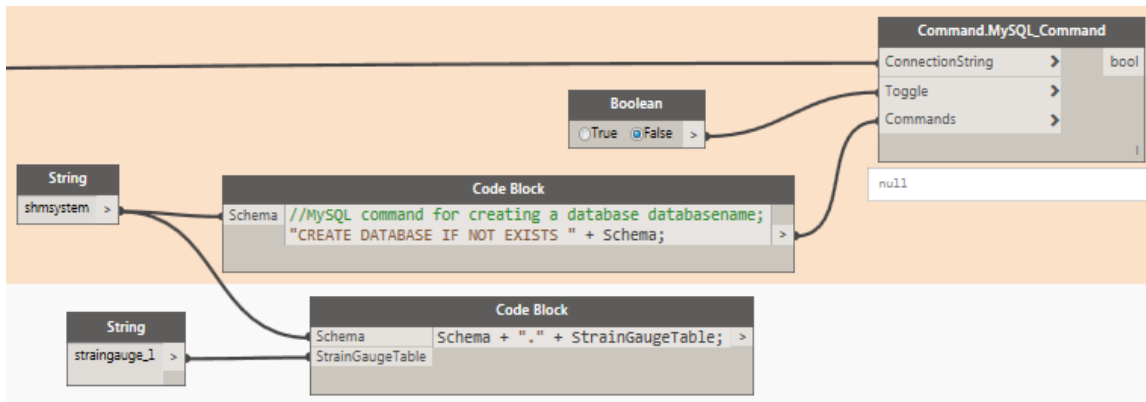
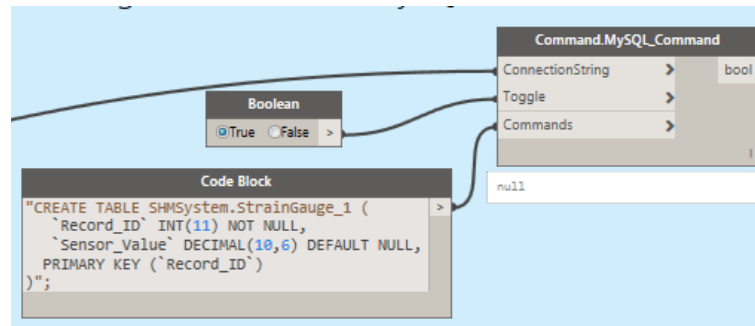


Figure 4-6: Automated generation of a schema and table for the strain gauge in database

Dynamo supports the use of code blocks, elements containing small scripts written in a textual programming language such as C++ and Python. These code blocks allow for the generation of short algorithms that introduce more complex functionalities that are not possible to be generated by other nodes. As shown in Figure 4-6, two code blocks are applied when generating a schema and its table, and one code block is employed to create the parameters of the table.

The database model can be expanded in the case of using strain sensors for multiple structural elements, and if a comprehensive database model for the entire sensory system, the information on the corresponding structural elements and their condition are required. Figure 4-7 shows the entity relationship diagram (ERD) of the proposed database model when using multiple strain sensors (e.g., four strain sensors) in the system.

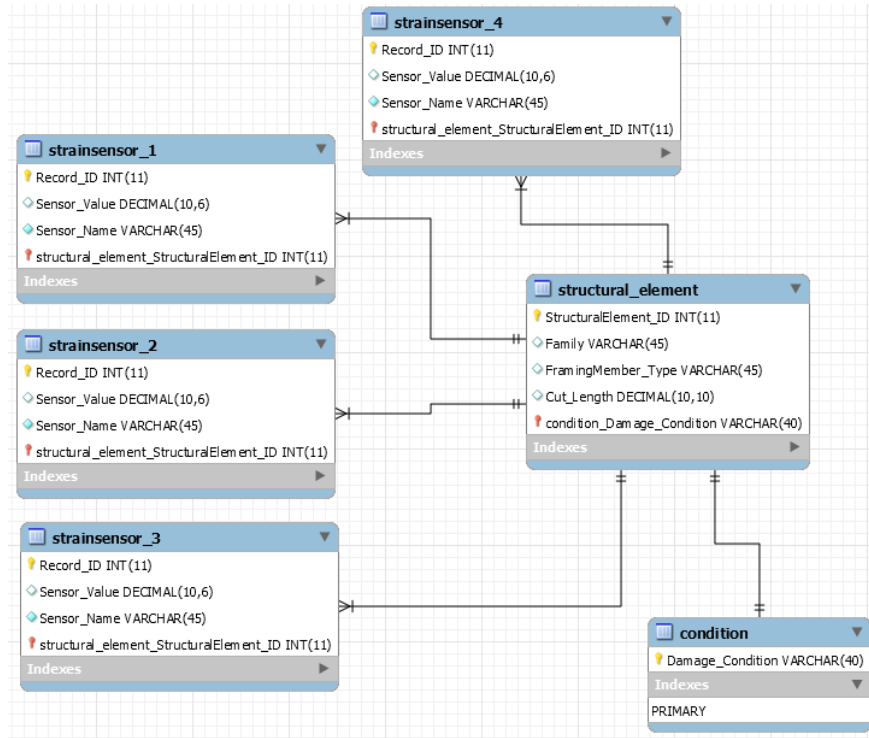


Figure 4-7: ERD of the SHM System Database

As shown in Figure 4-7, the ERD consists of six entities: *Strainsensor_1*, *Strainsensor_2*, *Strainsensor_3*, *Strainsensor_4*, *structural_element*, and *condition*. The relationship among the entities shows that a one-to-many relationship exists between *strainsensor* and *structural_element* entities, and a one-to-one relationship between *structural_element* and *condition* entities. Therefore, each strain sensor is installed on only one structural element, but a structural element may have multiple sensors. Each structural element may also have a condition: undamaged, partially damaged, or severely damaged.

4.7.4. Connecting to the Database

After generating modules for developing a sensor database model, the module(s) need to be connected to another module(s) to be integrated into the database. Consequently, a new module needs to be generated for connecting other modules to the MySQL database. In this module, several code blocks are involved in inserting server and port number, user id, and password. In fact, this module performs as a central module to which all other modules are to be connected.

4.7.5. Extracting Parameters from the BIM Model

Here, a module is generated to retrieve the virtual sensor parameters from the BIM model. The sensor parameters need to be obtained to check the latest values of these parameters in the BIM model.

In this module, first, the specialty equipment category is read from the list of categories in the BIM model because the virtual strain sensor object is modeled in this category. Next, all elements are selected in this category (virtual sensors in the BIM model). Then, the user-defined sensor parameters such as *StrainMaxPoint* and *DamageFlag*, the values of which are to be displayed, are extracted from the BIM model, and shown in one list.

4.7.6. BIM Model to the Database Linkage

After extracting the essential parameters from the BIM model, they need to be linked to the parameters in the database already generated for each sensor. This integration is required for any

future BIM model updating. A module is developed to connect the parameters extracted from the BIM model to the sensor parameters defined in the MySQL database.

Using this module, the *Sensor_Value* parameter generated in the MySQL database is linked to the *StrainMaxPoint* parameter generated in the BIM model. Inevitably, the module needs to be connected to the modules previously developed.

4.7.7. Automatic Reading of Sensor Values from MySQL Database Server

When a connection was established between the BIM model and the MySQL database server, the next step is to automatically read the sensed data from the MySQL database.

Different nodes are applied and connected to one another for this automatic sensor data reading. As previously mentioned, the *StrainMaxPoint* parameter is generated and assigned to the virtual sensor in the BIM model. Consequently, only the maximum strain value at every time interval is to be sent to the BIM model to update the *StrainMaxPoint* parameter of the virtual strain sensor. In this module, to find the maximum value of the strain at each time interval, the strain values are sorted because, for comparison purposes, only the maximum volume of the strain is required. If the maximum strain value is less than the predefined threshold strain value, then the structural element is not damaged and remains intact.

4.7.8. Updating the Virtual Sensor Parameter in the BIM Model

After retrieving and sorting the sensed values stored in the MySQL database, the associated virtual sensor parameters are updated in the BIM model using a module developed for that purpose.

In this module, the *SetParameterByName* node is used to update the *StrainMaxPoint* parameter of the strain sensor in the BIM model based on the maximum strain value recorded from the MySQL database. The maximum strain value is recorded at the end of each time interval, and the corresponding parameter in the BIM model is updated accordingly. A set of modules is developed for defining the threshold strain values and color-coding schemes for the damaged structural components to represent their status in the BIM model. Therefore, an alarm system can be generated and transmitted to the responsible personnel to attend to the structure.

4.7.9. Defining the Threshold Strain Value

Identifying an appropriate threshold value is essential for strain monitoring of critical structural elements. The allowable strain in the studs can be determined based on the yield strength (207.0 MPa) and Elastic Modulus (210,000 MPa) of the material, which is around 990 microstrain ($\mu\epsilon$) for the present case.

By applying this module, the condition of the *DamageFlag* parameter of the virtual strain sensor is classified into the following two cases: undamaged and damaged. If the maximum strain measurement does not exceed the predefined threshold strain value, the *DamageFlag* parameter is considered undamaged. Otherwise, it is flagged as damaged. To check these conditions, this module needs to be connected to the module previously developed for which the *StrainMaxPoint* parameter value is applied as one of the inputs that indicates the maximum strain value measured by the physical strain sensor.

4.7.10. Mapping a Virtual Sensor in the BIM Model to the intersecting Structural Framing Members

To visualize damaged elements in the BIM model, a parameter called condition needs to be updated based on the strain sensor's *DamageFlag* parameter. If the *DamageFlag* parameter is set, the structural element's condition parameter indicates the member as damaged. Before upgrading the condition parameter based on the *DamageFlag* parameter, the virtual sensor intersection by the correlating structural framing member in the BIM model must be assured.

In the module performing this function, first, the geometry related intersection between the virtual sensors (specialty equipment category) and structural members (structural framing category) is checked. If an intersection is found between these two members, then the module will update the condition parameter of the structural member based on the *DamageFlag* parameter of the correlating sensor in the BIM model. Accordingly, the damaged structural members are identified if their condition parameter identifies the member as damaged.

4.7.11. Color-Coding of Damage Structural BIM Element

After upgrading the 'Condition' parameter for structural framing members, the damaged elements are highlighted using a predefined color code. It works as an alarm system to highlight the elements where the strain produced by external forces exceed the pre-defined threshold value. For this purpose, a module is created, in which, the structural framing elements with damaged 'condition' parameter are filtered from the list of all structural framing members and highlighted in the BIM model.

4.8. Model Implementation

The initial step of integrating BIM into the SHM process is to link the physical sensors to virtual sensors and connect them to real data from the field. This integration is possible by attaching the physical sensor ID to the virtual sensor in the BIM model. To do so, first, a BIM model of an individual four-sided steel module is developed. Second, the process modules, as described in the previous section, are generated to introduce a workflow to link the virtual to the physical strain sensor, update the associated parameters, such as *StrainMaxPoint*, *DamageFlag*, and condition, and then highlight the damaged structural framing members in the BIM model.

The Arduino-based DAQ system can be coded to transfer the sensed data to an external database such as the MySQL database server. Before sending and accommodating the sensor data, the schema, tables, and relevant parameters need to be generated in the MySQL database. When sensors' data are sent to the database, they should be preprocessed before becoming exposed to further analysis. In this study, a list of one hundred strain data points is introduced to a MySQL database. The strain values and their record IDs are imported into the MySQL database, as shown in Figure 4-8.

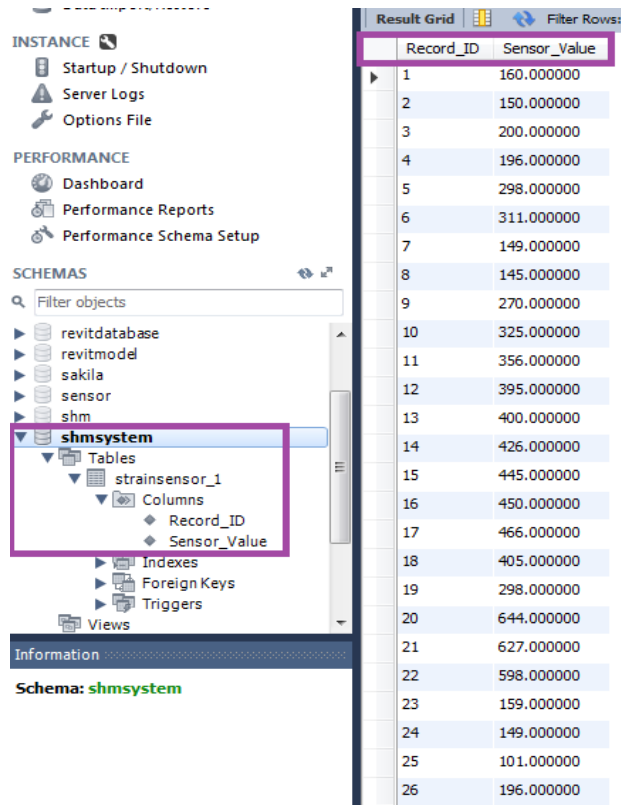


Figure 4-8: The physical strain sensor reading introduced to the database

As observed in Figure 4-8, the *shmsystem* schema and the *strainsensor_1* table with three parameters, including *Record_ID*, *Sensor_Value*, and *Sensor_Name*, are generated in the MySQL database before introducing the strain data. Once the strain data are added to the database, the values are read from the MySQL database server and sorted through the module previously developed in an automatic sense. All parameters are captured, read, and sorted. The maximum strain reading from the list of strain values is extracted after the values are sorted because, if the maximum strain value of an element in every time interval does not exceed the allowable strain (threshold) value, the element is regarded as undamaged. In contrast, if the maximum strain produced in a structural member exceeds the predefined allowable strain value, then the element is damaged and needs specific considerations and corrective action. How the strain sensor values are

read from the predefined schema and sorted to update the *StrainMaxPoint* parameter of the virtual strain sensor in the BIM model is illustrated in Figure 4-9.

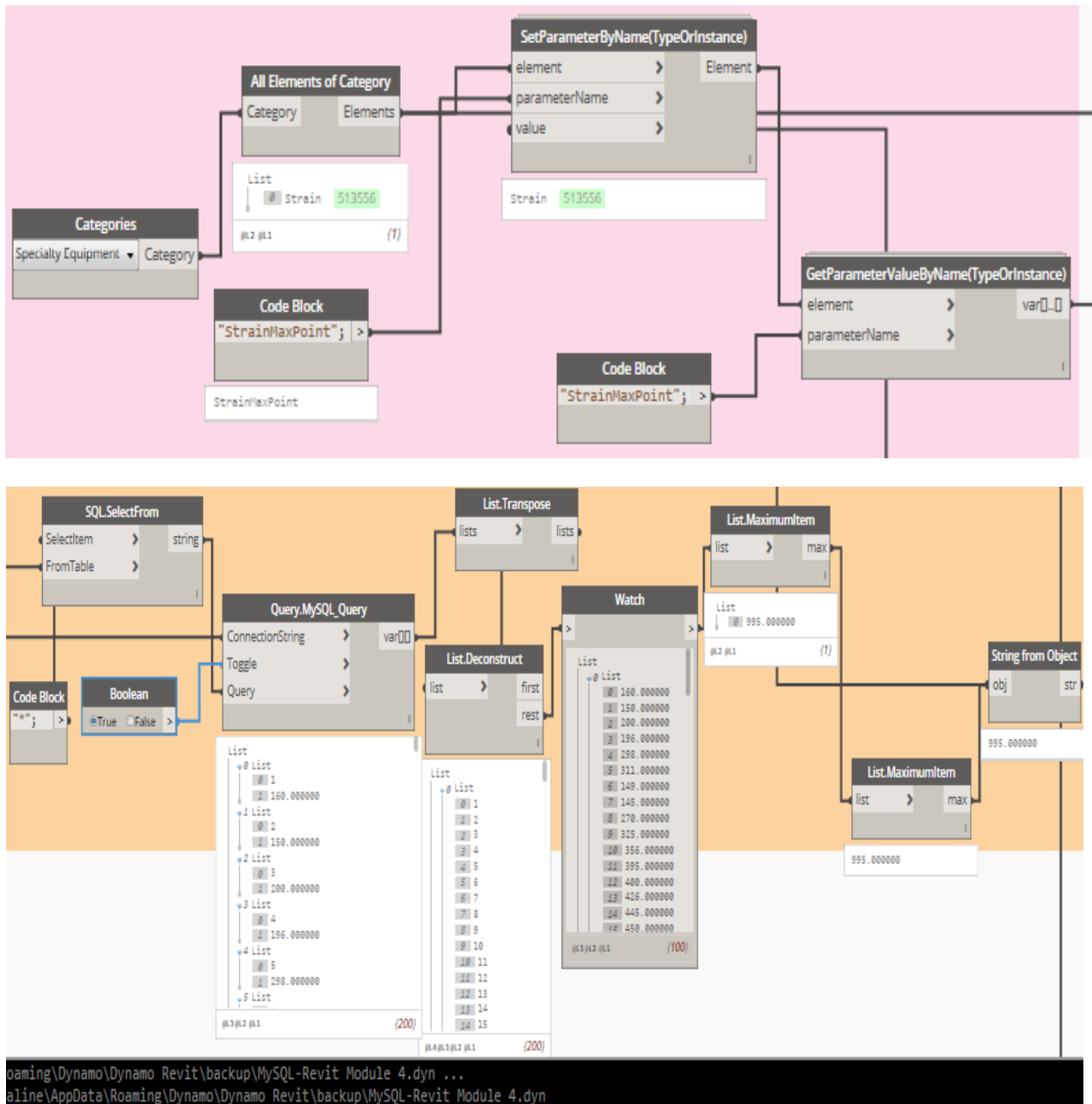


Figure 4-9: Automatic reading of strain sensor data and updating BIM model

As observed in Figure 4-9, only one strain sensor with ID number 513556 exists in the example BIM model. After reading the strain values from the database, the maximum strain value

is found to be $995 \mu\epsilon$, which is transferred to the next module to update the *StrainMaxPoint* parameter of the corresponding virtual sensor in the BIM model. The virtual strain sensor and its parameter updated in the BIM model are shown in Figure 4-10.

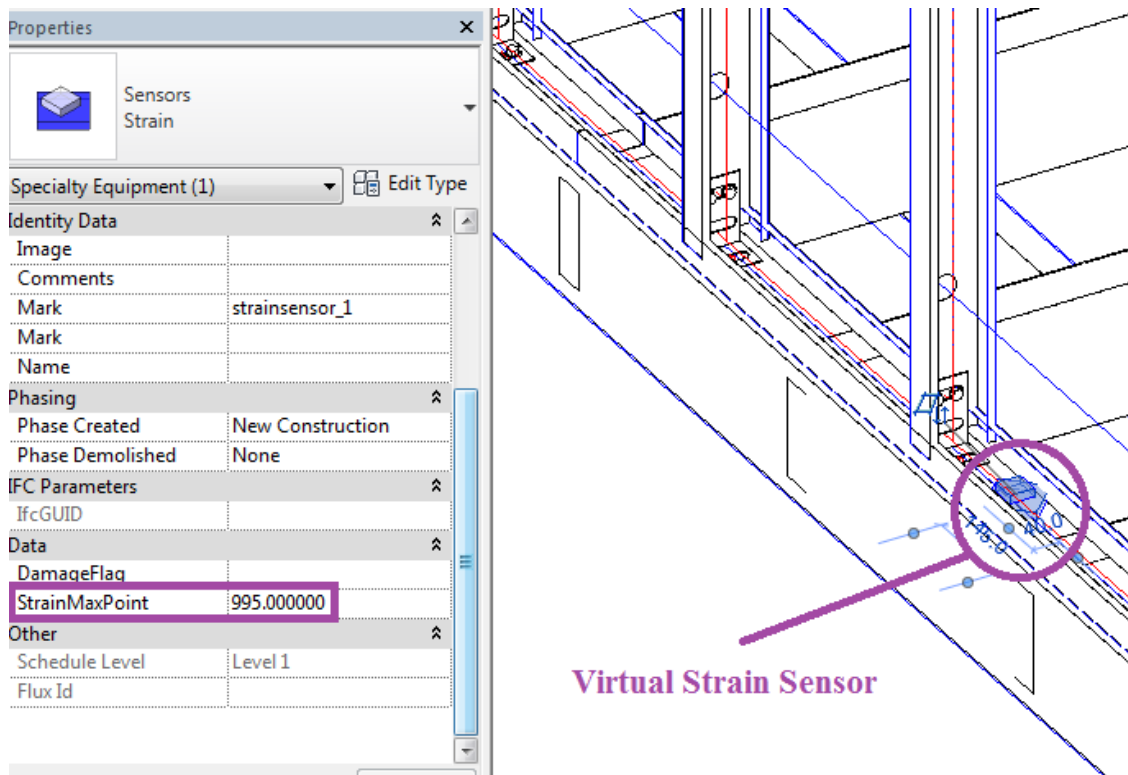


Figure 4-10: Updating BIM parameter based on maximum strain value in $\mu\epsilon$

As observed in Figure 4-10, after running the program, the *StrainMaxPoint* parameter is automatically updated. This step is an initial damage visualization process in the BIM model in a sense that the damage detection scenario begins from transferring the *DamageFlag* parameter information from a virtual strain sensor to the correlating structural framing member. By adopting the previously described module, the *DamageFlag* parameter becomes damaged because the extracted maximum strain value of $995 \mu\epsilon$ is more than the predefined threshold strain value of $990 \mu\epsilon$.

μ. To upgrade the condition parameter of the monitored structural member based on the *DamageFlag* parameter of the virtual strain sensor, the intersection between the virtual sensor and correlating structural framing member needs to be checked in the BIM model through the previously described module, as shown in Figure 4-11.

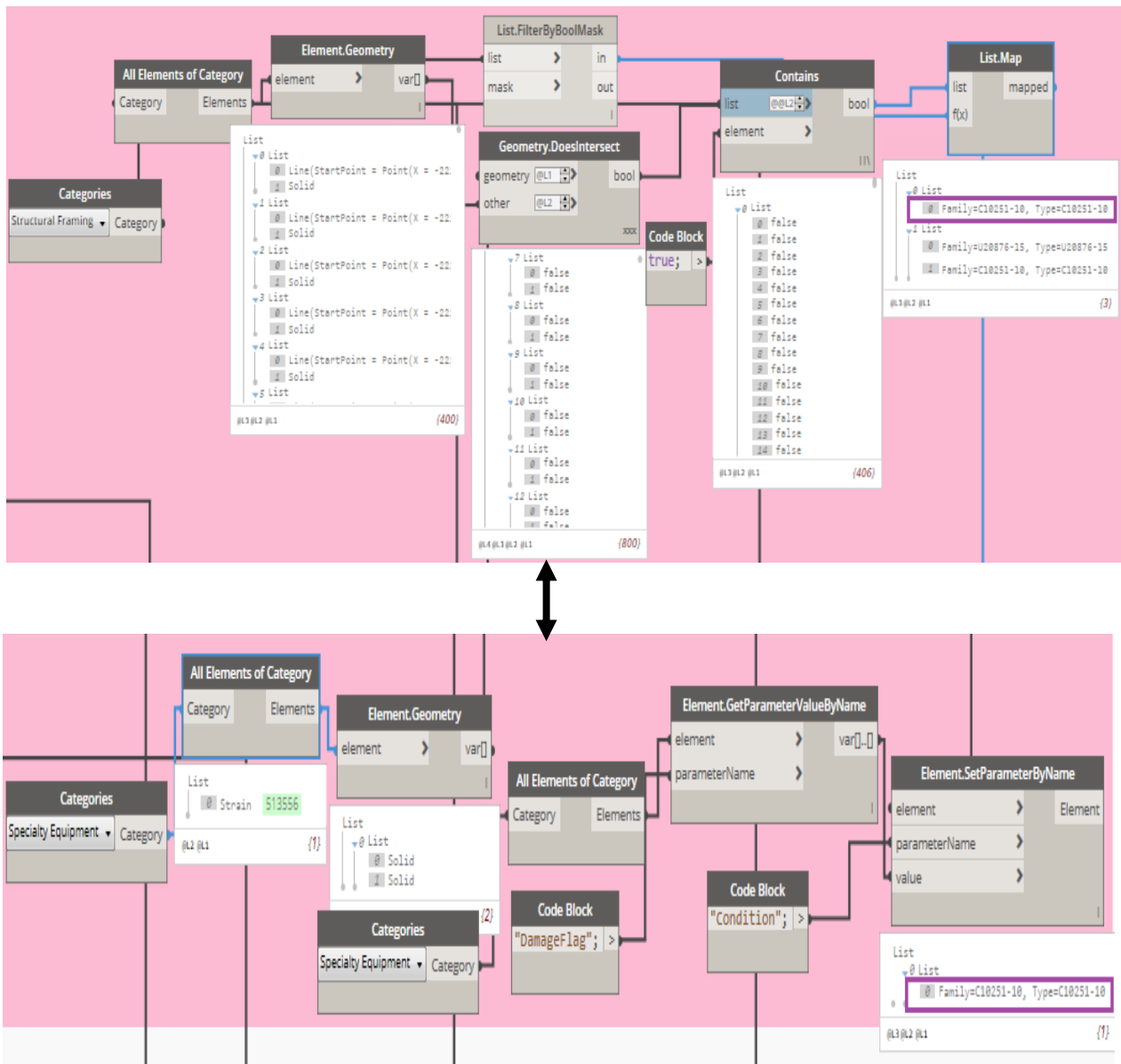


Figure 4-11: Checking the intersection between the virtual sensor and the BIM structural element

First, the geometry of all structural framing elements and virtual sensors are extracted from the BIM model. To identify the structural members to which the virtual sensors are attached, the structural members are filtered to separate the structural member to which the strain sensor is connected from other members. When the correlating structural member is separated from others, its condition parameter is updated based on the *DamageFlag* parameter of the corresponding virtual strain sensor. Consequently, because the *DamageFlag* parameter in the virtual strain sensor indicates the damage state, the condition parameter is updated to the damage state in the correlating structural member. When the condition parameter in a structural member indicates the damage state, the damaged element is highlighted in the BIM model through the module as described previously. As shown in Figure 4-12, the structural member to which the virtual strain sensor is attached is damaged and is highlighted in the BIM model shown in Figure 4-13.

One of the advantages directly attributed to BIM in the SHM integration process is that all of the information of the structure generated during its lifecycle is accessible, which can facilitate easier decision making for repair and maintenance plans. For instance, information on a damaged member such as material, type, cut length, type of connections, manufacturer address, phone number, date, time, minimum number of workers needed, and others, can all be easily extracted from the BIM model. The architecture of the developed system workflow and the correlation among its modules are shown in Figure 4-14. If the modules are not correctly connected to each other, the system might not work.

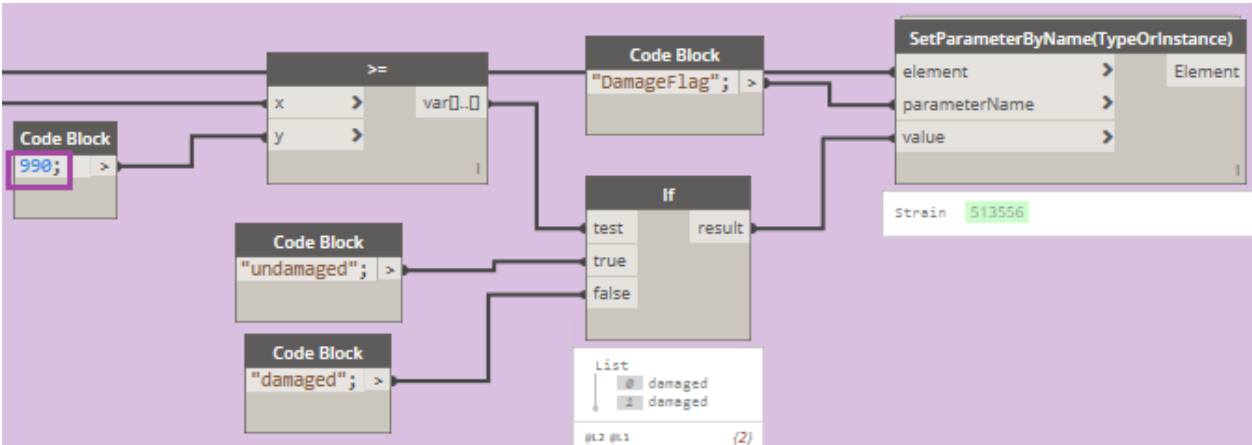
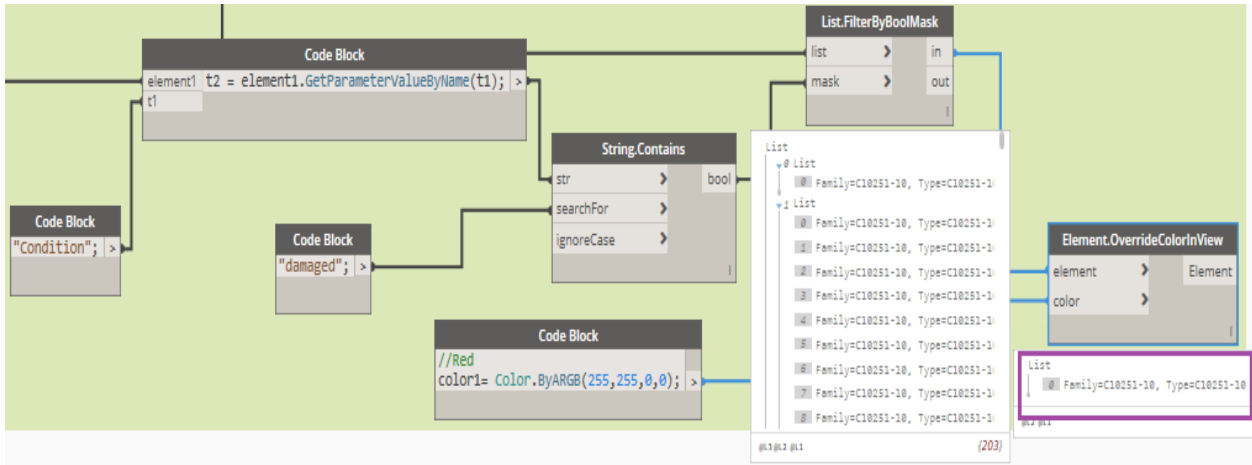


Figure 4-12: Threshold strain value definition and color-coding of damaged structural BIM elements

In Figure 4-14, the modules were numbered to better demonstrate their linkage. In Figure 4-14, the output of module number 1 that links the system to the MySQL server is connected to the following modules: number 2 (to connect the system to the monitoring database and table in the database), number 4 (to link the BIM model to the database containing sensor data), and module number 5 (to retrieve the sensor data from the database). The output of module number 3 (to extract strain sensor parameters from the BIM model) is connected to module number 4.

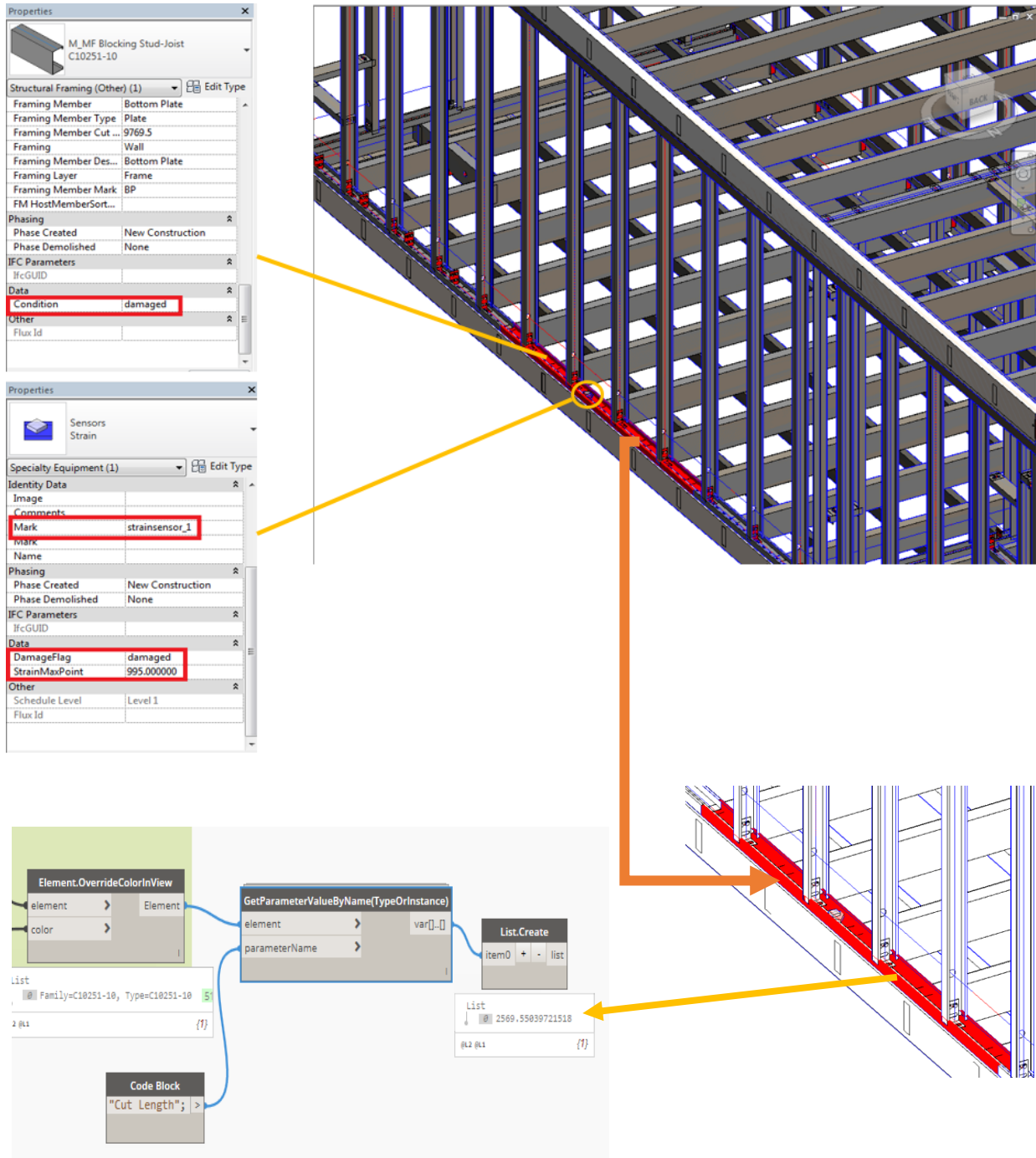


Figure 4-13: 3D damage visualization of damaged structural BIM element

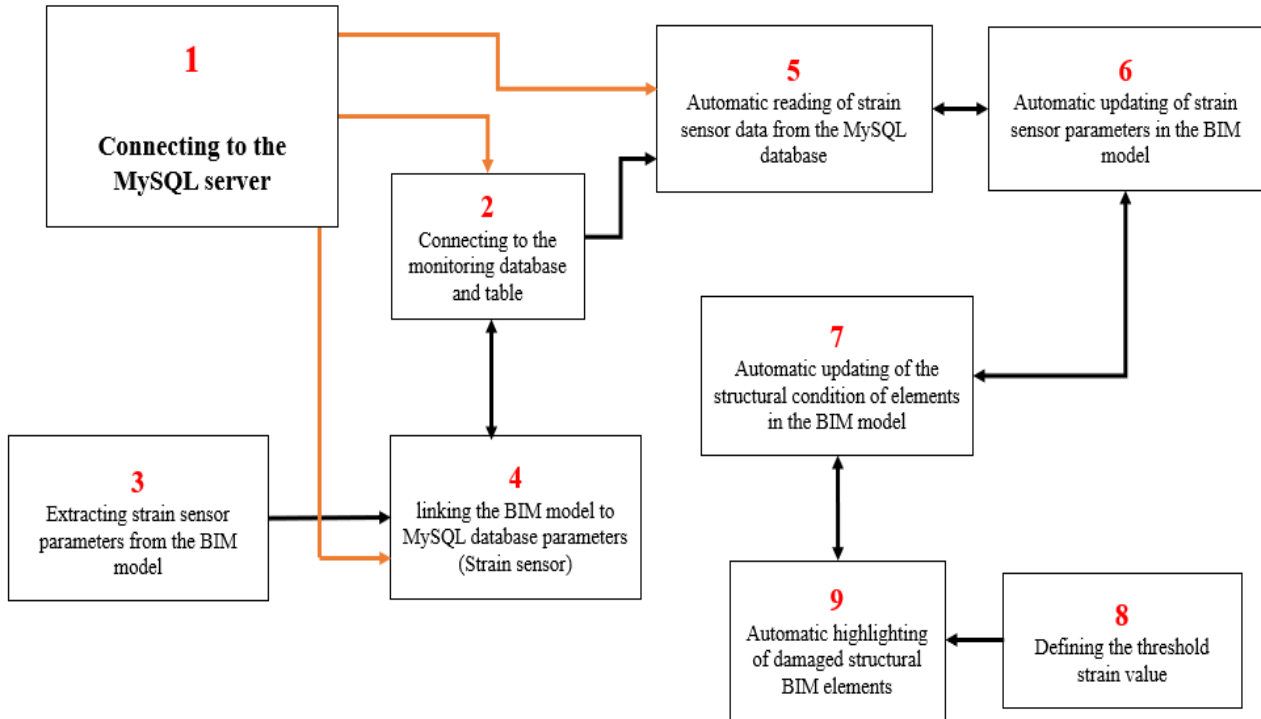


Figure 4-14: The workflow for integrating BIM into SHM process

As shown in Figure 4-14, a link exists between the following modules: numbers 2 and 4 to connect the maximum strain value in each event to the corresponding parameter in the BIM model. The output of module number 2 is connected to module number 5 (to automatically read and sort strain values stored in the database). The output of module number 5 is connected to module number 6 to update the sensor parameters in the BIM model. Finally, to automatically update and highlight the affected structural element in the BIM model based the threshold strain value defined in module number 8, module number 7 is connected to modules number 6 and 9 in the developed workflow.

4.9. Discussion

The main purpose of this paper was to investigate the potential of BIM in the damage visualization and rapid detection of damaged elements in structures such as building modules. This paper introduced a novel integrated strain-based monitoring system framework in BIM. The small size and low cost of the conceptual sensory system proposed in this study can be effective in modular structures that usually consist of small and narrow components. The system can also be utilized for rapid condition assessment of structural components. For this purpose, monitoring data were integrated into BIM through a novel workflow developed in a visual programming environment. The corresponding structural elements are automatically highlighted in the BIM model when strain measurements surpass the predefined threshold. Exceeding the strain threshold can be considered as damage or unacceptable deformations that can be further accentuated by repeated loading, especially during the operational phase.

To show the capabilities of the developed system, a set of strain values stored in a MySQL database was utilized to mimic the data produced by the proposed wireless strain gauge sensory system. Additionally, the BIM model of an individual light gauge steel module was used to demonstrate the capability of the developed framework in terms of damage visualization. The strain values studied in this paper were analyzed and compared with the threshold values detected by the developed system. For automatic recording, sorting and updating of strain values, and linking between the physical and virtual sensors (in the BIM model), a novel workflow consisting of nine modules as shown in Figure 4-13 was developed in a visual programming environment called Dynamo. The developed system was able to successfully transfer the sensor data stored in a central database server and map the strain sensors to the corresponding structural elements in the BIM model and update the related structural element parameters. The system was able to detect the

maximum strain values for each event as well as the values beyond the predefined threshold values. Through a color-coding scheme, the system was also able to automatically highlight the structural element in which case the strain values surpassed the threshold values. Incorporating BIM into the strain monitoring system provides engineers and facility managers the additional information required for deciding on repair and maintenance.

Although the approach is quite general and could be applied to any type of structure, such as buildings and bridges, this paper focuses on application to modular buildings as a case study. Additionally, modular construction has some challenges that differ from conventionally constructed buildings and bridges. In this case, the modules are subjected to different types of loads, such as manufacturing, transportation, handling, installation, and operational loads during their life cycle, and the main challenge is to detect buckled or yielded steel members (local damages) in a module, often hidden behind fireproof coating and drywall. For example, any possible damage that occurs in the building modules during transportation may cause misalignment issues during installation, affecting the structural performance and disrupting continuity in the envelope, which may significantly increase air leakage. Manufacturers usually buy shipping insurance that covers the all-risk and basic risk conditions to be reimbursed for repair costs of the modules if they are damaged during transportation. Therefore, the developed system can be used as an efficient, reliable, and rapid monitoring technique for timely detection of damages in modules after transportation and when claiming the repair and modification costs from the insurance company. The system is crucial to monitor the state of the critical elements of the modules in each phase to ensure their acceptable conditions before going to the next phase.

However, this work has some limitations, which are as follows.

1. The system developed here was tested using a limited number of sensors, and only strain sensors were used. The system should be tested further with a larger number and multiple types of sensors. Data from different types of sensors are interpreted in different ways. For example, strain data can be compared to a threshold value for a certain level of damage, whereas acceleration data can be used to determine the change in vibration modes and frequencies.
2. Deformation is a good parameter for localized damage detection, but a very good understanding of the structure is needed to design the instrumentation plan. If several similar types of members/connections are present and subjected to the same order of forces, identifying the most critical monitoring elements may not be trivial, and installing one or more sensor(s) on each element is not cost effective. Further study is required to automatically identify the critical locations and sensors.

4.10. Conclusions

Utilizing an effective data management system, such as BIM, for buildings can be extremely helpful for a rapid and efficient structural condition assessment and visualization. As a comprehensive, detailed, information-based strategy, BIM provides all of the information about the damaged elements, which is useful for effective repair/replacement of the damaged elements. Because the hidden structural damages (e.g., excessive deformation of structural elements in building modules) occurred during transportation or handling processes, they may lead to misalignment risks during installation. Rapid detection of such damages and repair or replacement

of the damaged components can help mitigate the misalignment risks and the possibility of further damage during installation.

An SHM framework in which a BIM was adopted for automated and graphical structural condition monitoring, particularly for modular structures, was proposed in this article. Building modules are more susceptible to damage during transportation and installation. In such cases, the structural elements are often hidden, and structural damage such as excessive deformation is difficult to detect. BIM can serve as an ideal four-dimensional graphical computing environment for SHM and repair and maintenance plans. The ability of BIM to visualize the SHM information of a structure will be beneficial for engineers and decision makers because it provides accurate and updated information on the current state of structural elements, structural reliability, and maintenance work to be scheduled. A BIM-based integrated structural health framework was developed for rapid and efficient monitoring of structural deformation.

Based on the findings, the following observations were made.

1. A virtual sensor's parameter in the BIM model can be updated based on the measured data from the corresponding physical sensor. This feature was applied to determine when a predefined threshold strain level is exceeded at the monitored location of a structure.
2. The capability of the developed framework was examined through a set of strain values stored in a specially designed MySQL database and a BIM model.
3. The state of a concerned structural framing member in the BIM model was updated and highlighted when the strain value exceeded the threshold value. Data from other sensors, such as an accelerometer, or temperature can be integrated in the same way.

Although the present study demonstrates the feasibility of remote strain sensing and decision making to monitor the state of a hidden structural element in a building module during its life

cycle, further studies are required to conduct a large-scale investigation that uses multiple types of sensors to monitor the critical elements with different types of materials in a module. Additionally, a need exists for experimental validation of the developed system using real-life applications.

References

- ASTM. (2016). "Standard practice for performance testing of shipping containers and systems." ASTM D4169. West Conshohocken, PA: ASTM.
- Azhar, S., Nadeem, A., Mok, A. Y. N., and Leung, B. H. Y. (2008). "Building information modeling (BIM): A new paradigm for visual interactive modeling and simulation for construction projects." In Proc., 1st Int. Conf. on Construction in Developing Countries. Karachi, Pakistan: Advancing and Integrating Construction Education, Research & Practice.
- Cantu, R. (2011). "Modular design: The advantages for contractors." Boston: Commonwealth Contractor.
- Chen, J., Bulbul, T., Taylor, J. E., and Olgun, G. (2014). "A case study of embedding real-time infrastructure sensor data to BIM." In Proc., Construction Research Congress, 296–278. Reston, VA: ASCE.
- Del Grosso, A. E., Basso, P., Ruffini, L., Figini, F., and Cademartori, M., (2017). "Infrastructure management integrating SHM and BIM procedures." In Proc., SMAR 2017-4th Conf. on Smart Monitoring Assessment and Rehabilitation of Civil Structures. Istanbul, Turkey: Istanbul Technical Univ.
- Dynamo BIM. (2017). "Dynamo BIM–Community-driven open-source graphical programming for design." Accessed February 10, 2017, Retrieved from <http://dynamobim.org>.

- Han, S. H., Olearczyk, J., Al-Hussein, M., Al-Jibouri, S., and Bouferguène, A. (2011). “3D visualization of modular building assembly: From a factory to construction site.” In Proc., 11th Int. Conf. on Construction Applications of Virtual Reality, Weimar, Germany: Bauhaus-Universität.
- Jeong, S., Zhang, Y., O’Connor, S., Lynch, J. P., Sohn, H., and Law., K. H. (2016). “A NoSQL data management infrastructure for bridge monitoring.” *Smart Struct. Syst.* 17 (4): 669–690. <https://doi.org/10.12989/sss.2016.17.4.669>.
- Karbhari, M., and Ansari, F. (2009). “Structural health monitoring of civil infrastructure systems.” Boca Raton, FL: CRC Press.
- Koo, K. Y., Battista, N. D., and Brownjohn, J. M. W. (2011). “SHM data management system using MySQL database with MATLAB and web interfaces.” In Proc., 5th Int. Conf. on Structural Health Monitoring of Intelligent Infrastructure, Mexico City: Instituto de Ingeniería, UNAM.
- McGraw-Hill. (2011). “Prefabrication and modularization: increasing productivity in the construction industry.”, *Smart Market Report*, New York: McGraw-Hill Construction.
- Naqvi, D., Wey, E., Morgan, J., Miller, M., and Nguyen, T. (2014) “Transportation consideration in module design.”. In Proc. Structures Congress, 1771–1782. Reston, VA: ASCE.
- Nassar, K. (2010). “The effect of building information modeling on the accuracy of estimates.” In Proc., 46th Annual Conf. Boston: Wentworth Institute of Technology.
- Nawari, N. O. (2012). “BIM standard in off-Site construction.” *J. Archit. Eng.* 18 (2): 107–113. [https://doi.org/10.1061/\(ASCE\)AE.1943-5568.0000056](https://doi.org/10.1061/(ASCE)AE.1943-5568.0000056).

- Ni, Y. Q., Hua, X. G., Chen, K. W., and Ko, J. M. (2008). "Condition assessment of bridge deck truss using in-service monitoring data of strain." In *World forum on smart materials and smart structures technology*, edited by B. F. Spencer, et al. London: Taylor & Francis.
- Ni, Y. Q., Xia, H. W., and Ko, J. M. (2010). "Estimation of probability density function of Long-term strain measurement for reliability assessment." In *Bridge maintenance, safety, management and life-cycle optimization*, edited by D. Frangopol, R. Sause, and C. Kusko. London: Taylor & Francis.
- Park, H. S., Lee, H. W., Choi, S. W., and Kim, Y. (2013). "A practical monitoring system for the structural safety of mega-trusses using wireless vibrating wire strain gauges." *Sensors* 13 (12): 17346–17361. <https://doi.org/10.3390/s131217346>.
- Patlakas, P., Livingstone, A., and Hairstans, R., (2015). "A BIM platform for offsite timber construction.", In Vol. 1 of *Proc., 33rd eCAADe Conf.*, 597–604, Vienna, Austria: Vienna Univ. of Technology.
- Ramaji, I., and Memari, A. M. (2013). "Identification of structural issues in design and construction of multi-story modular buildings." In *Proc., PHRC 1st Residential Building Design and Construction Conf*: 294–303, University Park, PA: Pennsylvania Housing Research Center.
- Rausch, C., Nahangi, M., Perreault, M., Haas, C. T., and West, J. (2017). "Optimum assembly planning for modular construction components." *J. Comput. Civ. Eng.* 31 (1): 04016039. [https://doi.org/10.1061/\(ASCE\)CP.1943-5487.0000605](https://doi.org/10.1061/(ASCE)CP.1943-5487.0000605).
- Rio, J., Ferreira, B., and Pocas-Martins. J. (2013). "Expansion of IFC model with structural sensors." *Informes de la Construccion* 65 (530): 219–228.

- Seam, A., Zheng, T., Lu, Y., Usmani, A., and Laurenson, D. (2013). "BIM integrated workflow management and monitoring system for modular buildings." *Int. J. 3-D Inf. Model.* 2 (1): 17–28.
- Shahtaheri, Y., Rausch, C., Wes, J., Haa, C., and Nahangi, M. (2017). "Managing risk in modular construction using dimensional and geometric tolerance strategies.", *Autom. Constr.* 83: 303–315. <https://doi.org/10.1016/j.autcon.2017.03.011>.
- Smarsly, K., and Tauscher, E. (2016). "Monitoring information modeling for semantic mapping of structural health monitoring systems." In *Proc., 16th Int. Conf. on Computing in Civil and Building Engineering*, Osaka, Japan: ICCCBE2016 Organizing Committee.
- Sternal, M., and Dragos, M. (2016). "BIM-Based modeling of structural health monitoring systems using the IFC standard." In *Proc., 28th Forum Bauinformatik*. Hanover, Germany: Leibniz Universität Hannover.
- Theiler, M., Dragos, K., and Smarsly, K. (2017). "BIM-based design of structural health monitoring systems." In *Proc., 11th Int. Workshop on Structural Health Monitoring 2017*, Stanford, CA: International Workshop on Structural Health Monitoring.
- Valinejadshoubi, M., Bagchi, A., and Moselhi, O. (2017). "Managing structural health monitoring data using building information modeling." In *Proc., 4th Int. Conf. on Smart Monitoring, Assessment and Rehabilitation of Civil Structures*. Istanbul, Turkey: Istanbul Technical Univ.
- Valinejadshoubi, M., Bagchi, A., and Moselhi, O. (2018a). "Identifying at risk non-structural elements in buildings using BIM: A case study application." *J. Earthquake Eng.* 1–12. Retrieved from <https://doi.org/10.1080/13632469.2018.1453407>.

- Valinejadshoubi, M., Bagchi, A., and Moselhi, O. (2018b). "Thermal comfort monitoring in buildings using a BIM-based automated system." In Proc., 1st Int. Conf. on New Horizons in Green Civil Engineering. Victoria, BC, Canada: BC Housing.
- Valinejadshoubi, M., Bagchi, A., Moselhi, O., and Shakibaborough, A. (2018c). "Investigation on the potential of building information modeling in structural health monitoring of buildings." In Proc., CSCE Annual Conf. Montreal: Canadian Society for Civil Engineering.
- Vardanega, P. J., Webb, G. T., Fidle, P. R. A., and Middleon, C. R. (2016). "Bridge monitoring." In Innovative bridge design handbook. Amsterdam, Netherlands: Elsevier.
- Wang, J., Fu, Y., and Yang, X. (2017). "An integrated system for building structural health monitoring and early warning based on an Internet of things approach." *Int. J. Distrib, Sensor Networks* 13 (1): 1–14.
- Webb, G. (2014). "Structural health monitoring of bridges." Ph.D. thesis, Centre for Construction Engineering and Technology, Univ. of Cambridge.
- Webb, G. T., Vardanega, P. J., and Middleton, C. R. (2014). "Categories of SHM deployments: technologies and capabilities." *J. Bridge Eng.* 20 (11): 04014118. Retrieved from [https://doi.org/10.1061/\(ASCE\)BE.1943-5592.0000735](https://doi.org/10.1061/(ASCE)BE.1943-5592.0000735).
- Yang, N., and Bai, F. (2017). "Damage analysis and evaluation of light steel structures exposed to wind hazards." *Appl. Sci.* 7 (3): 239, Retrieved from <https://doi.org/10.3390/app7030239>.
- Zhang, Y., and Bai, L. (2015). "Rapid structural condition assessment using radio frequency identification (RFID) based wireless strain sensor." *Autom. Constr.* 54: 1–11. Retrieved from <https://doi.org/10.1016/j.autcon.2015.02.013>.

Updated Literature Review and Related Materials

This section focuses primarily on recent publications and related works not cited in the published paper above.

The lack of enabling tools for understanding, visualizing, and documenting sensor outputs has encouraged researchers to use BIM-based systems. After reviewing 278 journal articles by Shafie Panah and Kioumars (2021), it was concluded that despite the introduced improvements, there are still some limitations, such as extending the IFC schema and interoperability issues, which affect the modeling and maintenance process.

O'Shea and Murphy (2020) explored the potential for implementing BIM on an existing structure for asset management and SHM. They developed a method for modeling and representing SHM sensors in the BIM model. However, the study only focuses on data visualization, and it does not consider damage and its related levels of intensities using visualization methods such as color-coding the BIM model based on the sensor data analysis. At the same time, the developed tool presented in this chapter is able to automatically highlight the structural element through a color-coding scheme, in which case the strain values surpassed specified threshold values. Also, their system does not work in real-time because for any update, the sensor data is converted to excel format, saved locally, and then read into the BIM model utilizing the Dynamo tool. The developed system presented in this chapter solves this problem by storing the SHM data in an external cloud-based database.

Angelosanti et al. (2021) developed a workflow between SHM sensors data and a BIM environment. Although they cited the manuscript presented in this chapter in their paper, there is still a lack of automation in their workflow by using a local database for transferring the sensor

data into the BIM environment. Moreover, their workflow is not able to be utilized as an alert system for facility managers, while the method developed in this chapter has the capability to solve the issues stated above.

Chapter 5: Development of an IoT and BIM-Based Automated Alert System for Thermal Comfort Monitoring in Buildings

General

In this chapter, the published paper is presented as is, followed by an updated literature review section. This paper was accepted and published in the Journal of Sustainable Cities and Society in 2021*. The main objective of this paper is to develop an automatic workflow to integrate IoT and BIM for monitoring thermal comfort in building spaces.

Abstract

A comfortable thermal indoor environment is crucial for occupants' well-being and productivity. Building Management System (BMS) is usually used to monitor the thermal condition of buildings. One of BMS's main challenges is in the data visualization stage, in which 2D vector graphics are used, which is not fully interactive and can only be manipulated by a trained operator. Building Information Modeling (BIM) has emerged as a useful tool in the construction industry, which can be applied in all stages of a project lifecycle. The use of BIM in facilities management is currently limited since BIM applications have primarily been implemented within the design and construction phases. The main objective of this study is to integrate a sensor-based alert system into BIM models for thermal comfort monitoring in buildings during the operational phase and visualize a building's thermal condition virtually. In order to improve the performance of environmental monitoring management of buildings in smart cities, this research presents a newly

* Valinejadshoubi. M, Moselhi. O, Bagchi. A, and Salem. A (2021), Journal of Sustainable Cities and Society, Vol 66

developed integrated solution based on a BIM platform and Internet of Things (IoT). The designed prototype explores the integration of commercial BIM platforms with sensor data to create a self-updating BIM model to provide real-time thermal condition monitoring based on the American Society of Heating, Refrigerating, and Air-Conditioning Engineers (ASHRAE) Standard within an office environment. The temperature and humidity values, measured by sensors, are sent to the MySQL database server. An integrated workflow was developed to compile, standardize, integrate, and visualize monitoring data in a BIM environment to facilitate interpretation, analysis, and monitoring data exchange. The developed system was able to detect the time and location of a case study office room experiencing the levels of thermal comfort/discomfort based on the targeted thresholds. In this case, thirteen levels of thermal discomfort cases, out of forty-nine data points during the test, were detected, and the developed system was also able to generate a trigger and transmit alarms to facility managers via their wireless devices in real-time. The results demonstrate that the proposed system is a visually effective monitoring system for environmental monitoring management. The fully automated developed system is expected to provide a robust and practical tool for reliable data collection, analysis, and visualization to facilitate intelligent monitoring of the thermal condition in buildings and help decision-makers make faster and better decisions, which may help in maintaining the level of occupants' thermal comfort to a satisfactory level.

Keywords: Building Information Modeling; Building Management System; Facilities management; IoT, Thermal comfort

5.1. Introduction

Approximately 90 % of an organization's operating costs are allocated to staff costs, including salaries and benefits (Health, Wellbeing & Productivity in Offices, 2014). Factors such as indoor environmental conditions may affect workers' comfort, consequently, their health and well-being, and their productivity (Sakellaris et al., 2016). When an office environment gets too warm, it makes employees feel tired, while if an office environment gets too cold, it causes the employees' attention to drift, making them restless and easily distracted. Charles, Reardon, and Magee (2005) argued that indoor air quality (IAQ) and thermal comfort are the most critical factors contributing to worker productivity, satisfaction, and well-being.

According to the Canadian Centre for Occupational Health and Safety (CCOHS), thermal comfort is met when a person wearing a reasonable amount of clothing feels neither too cold nor too warm. The study presented in Seppanen " and Fish (2006) showed that maximum productivity was observed at 21.6 °C, although adaptive comfort theory suggests optimum productivity can be attained over a broader range of indoor temperatures (De Dear & Brager, 1998). It is essential to ensure that different thermal comfort conditions are within acceptable limits. ASHRAE Standard 55 (ANSI/ASHRAE Standard-55, 2017) is an American National Standard published by ASHRAE that establishes the ranges of indoor environmental conditions to achieve acceptable thermal comfort for occupants of buildings. According to ASHRAE Standard 55, various factors influence the thermal comfort level, including air temperature, radiant temperature, air velocity, relative humidity, occupant's clothing insulation, and occupant's activity level. Due to low velocity, according to indoor climate studies (Kantor & Unger, 2011; Langner, Scherber, & Endlicher, 2013; Matzarakis & Amelung, 2008), air temperature is approximately equal to the radiant temperature in indoor environments.

According to the Health and Safety Executive (HSE, 2017) Standard, the most commonly used indicator of thermal comfort is air temperature. However, the temperature should be considered in relation to other environmental factors. Gupta (2006) suggested that comfort can be achieved only when the air temperature and humidity are within the specified range, often referred to as the 'comfort zone'. The Canadian Centre for Occupational Health and Safety (CCOHS) suggested that the humidity levels should be kept between 30% and 70%. Relative humidity levels below 30% can cause discomfort through drying of the eyes and skin, while relative humidity levels above 70% may make the area feel stuffy. Thermal comfort assessments are determined separately for the summer and winter seasons in accordance with relevant standards (Kalz and Pfafferott, 2014). Comfort ratings are analyzed in hours of exceedance during the time of occupancy. For either comfort model, the operative temperature should always be within the permissible ranges at all locations within the occupied zone of space (Kalz and Pfafferott, 2014). Comfort is a subjective issue and can vary widely from person to person. However, there is a generally agreed range of temperatures at which at least 80% of people will feel comfortable and will perform effectively and efficiently.

Despite high energy use in buildings, adequate thermal comfort levels may not be provided during hot and cold weather. This was observed in two case studies conducted by Quigley (2016) on light gauge steel modular buildings' energy and thermal performance that air leakage and overheating are the two main issues that led to reducing the thermal comfort. In another study conducted by Adekunle and Nikolopoulou (2016), it was revealed that lack of thermal mass and low U-values could risk increasing overheating in prefabricated timber buildings leading to thermal discomfort.

Gathering data and energy and environmental performance evaluation data are at the heart of energy efficiency strategies to reduce energy use in buildings. Environmental monitoring

technologies have a significant role to play in energy efficiency measures. There is also an increase in energy-related building legislations and regulations around the world. For example, the European Energy Performance of Buildings Directive (EPBD) (2014) encourages intelligent metering and active control systems in buildings through building regulations. In the USA, the Energy Policy Act of 2005 has metering requirements for federal buildings. Most US states, cities, and districts have adopted the International Energy Conservation Code (IECC) (2018), with enhanced metering and control requirements.

There are two methods to assess indoor climate and air quality in a controlled environment; surveys and questionnaires (Leo Samuel, Dharmasastha, Shiva Nagendra, & Prakash Maiya, 2017; Sakka, Wagner, & Santamouris, 2010; Seon, Jeong, & Yun, 2013; Singh, Mahapatra, & Teller, 2013; Yu, Li, Yao, Wang, & Li, 2017; Zinzi & Carnielo, 2017), and sensors. Building occupants may not be interested in answering accurately, long surveys frequently. Although thermal comfort data are commonly collected and stored in databases, they are not modeled and managed as a part of BIM models. The relationship between building spaces and their IAQ is more challenging to observe in tabular information than in the 3D model. It is important to note that the state of a building may change during its operational phase, and there is no robust standard to check if the building preserves its performance characteristics despite the changes in maintenance state, occupants' numbers, activities, and seasons.

As an effective visualization and management tool, BIM has recently become an essential tool in the construction industry. The use of BIM in facilities management is currently limited since BIM applications have primarily been implemented within the design and construction phases. It is advantageous to enable BIM models to provide real-time information through the monitoring process. Hence, this will allow the facility managers to interact with the built environment in real time and provide a better user interface than a traditional thermal condition monitoring system.

There is a limited volume of research available on BIM-based dynamic systems for real-time and near-real-time monitoring of thermal comfort in buildings. As discussed later, the literature shows some weaknesses in existing methods of thermal comfort monitoring, such as lack of automation and data retrieval (Rania and Isam, 2019; Wu & Liu, 2020), challenges in the continuous object tracking in IoTs in smart cities (Chauhdary, Hassan, Alqarni, Alamri, & Bashir, 2019), limited computer implementation (Cahill, Menzel, & Flynn, 2012; Del Grosso, Basso, Ruffini, Fagini, & Cademartori, 2017; Smarsly & Tauscher, 2016; Sternal & Dragos, 2016), and lack of integration of sensor-based alarm systems into BIM models for thermal comfort monitoring in buildings during the operational phase. The present work attempts to address some of these issues to narrow the research gap by integrating BIM and IoT technologies to automate thermal comfort monitoring. The conception of IoT had founded the smart cities, which support the city operations intelligently with minimal human interaction. A smart city emerged as a solution to address the challenges that arise with the exponential population (Silva, Khan, & Han, 2018).

The primary purpose of this integration is to benefit from the rich User Interface (UI) of BIM-based software and to supplement BIM models with real-time temperature and humidity sensor values. An integrated solution is proposed in this paper with the aim of real-time monitoring of thermal comfort in indoor environments to reduce health hazards inside buildings. The BIM-based software application is used to visualize building spaces, and the IoT-based system is used to monitor real-time temperature and humidity values. The proposed system sends alerts, notifications and all essential information such as room ID, room name, room location, occupancy, etc., using a cloud-based service to the building supervisors and facility manager to remotely acquire just the thermal condition status of monitored spaces to take necessary actions if the operating temperature exceeds the pre-defined thresholds. The proposed system can be an

alternative solution for smaller buildings that might not benefit from smart technology and are unmonitored. It could show the facility management engineers the climate's state in each room and occupants' wishes. Such a system could also be used by other specialists, such as building environment professionals, to locate places with potential IAQ issues, and get their most updated information required.

5.2. Literature Review

The architecture, engineering, and construction (AEC) industry uses BIM to reduce cost and completion time and improve productivity and quality of projects (Azhar, Nadeem, Mok, & Leung, 2008). BIM is a robust platform for managing complex building information and can be used to visualize a building virtually over its lifecycle. BIM incorporates digital modeling software to design and execute a project efficiently (Nassar, 2010). In a BIM project, multiple documents are used in non-traditional ways (Australian Construction Industry Forum, 2014): documents are digitized then added to a BIM software database. An accurate BIM model consists of the virtual equivalent of the actual building sections.

BIM models are useful in assessing buildings' energy efficiency in the design phase (Valinejadshoubi, Bagchi, & Shakibabarough, 2015) using different design parameters such as orientation and materials. Figure 5-1 shows the different levels of BIM. Although BIM up to level 2 is very well defined but BIM level 3 is still under development. BIM level 2 means that the model should be assessed for 3D (construction elements, quantities), 4D (time), and 5D (cost) representations of a building. The main requirement of BIM level 3 is integrated BIM (iBIM) and Lifecycle Management (Goodhew, 2016). Therefore, the integration of a monitoring system into BIM would help achieve this next level of BIM.

format compatible with different BIM tools that aid in standardizing projects (Grzybek, 2010). Katranuschkov, Weise, Windisch, Fuchs, and Scherer (2010) used IFC models to control the air conditioning system via temperature and humidity sensors in rooms with smart IT devices. Chen, Bulbul, Taylor, and Olgun (2014) tried to connect the data captured by real sensors embedded in a geothermal bridge deck system to the IFC-based BIM model. They concluded that the sensor data should be monitored in the BIM model for condition assessment under different climate conditions. Park, Kim, Chin, and Yun (2011) integrated online monitoring with BIM to efficiently deliver a vast amount of sensor data from the smart space to develop the manager's data accessibility and management convenience. Kim, Cheng, Sohn, and Chang (2014) presented a systematic and practical approach to assess the surface quality of precast concrete elements using BIM and a 3D laser scanning technique to prevent failure during construction. They held the manual inspection and surface quality assessment of prefabricated concrete components to be demanding and costly. Arslan, Riaz, Kiani, and Azhar (2014) offered a new methodology for integrating captured sensors' data from the hot and humid environment with BIM providing solutions for health and safety planning in buildings. Valinejadshoubi, Bagchi, and Moselhi (2017) investigated the feasibility of using BIM in the SHM process. They demonstrated the feasibility of creating and visualizing sensors data and information in the BIM model for the purpose of structural health monitoring. A preliminary scheme for utilizing BIM to manage SHM data for buildings was developed in Valinejadshoubi, Bagchi, Moselhi, and Shakibaborough (2018). Valinejadshoubi et al. (2019) developed a BIM-based integrated model for rapid structural damage detection using strain values. Some other BIM-Sensor based integrated solutions and their limitations are summarized in Table 5-1.

Although BIM is desired to be a dynamic workbench for managing all data related to a building project, there are still many challenges in the management of performance data using existing data specifications (e. g., IFC) such as the size of data sets, levels of detail, and interoperability with existing formats employed to store historical performance data (Gerrish, Ruikar, Cook, Johnson, & Phillip, 2015). The challenges of using existing standards like IFC in modeling monitoring systems for asset monitoring and management include lack of specific entities and attributes for modeling, lack of directives for data management and visualization, and lack of guidelines for connection with external sources of data and other standard data models (Davila Delgado, Butler, Brilakis, Elshafie, & Middleton, 2018). When transformed into IFC, the models lost some information included in the original proprietary format. As described in this section, most previous studies used the IFC standard in their framework, which has the challenges mentioned above.

It is apparent from Table 5-1 that the potential of using BIM in sensor-based monitoring has not been fully explored particularly when BIM is becoming a popular platform in the AEC industry. As shown, although some researchers tried to integrate BIM into IoT systems, most of them have been aimed at building conceptual frameworks, mapping the information coming from the sensors to the 3D model with limited attempts at computer implementation and development of an automated BIM-based integrated alarm system, especially for thermal comfort monitoring purpose.

Table 5-1: Previous studies on a BIM-based sensor-integrated solution

Authors	Type of Sensor Used	Purpose	Limitation
(Wu and Liu, 2020)	Temperature, Humidity, CO ₂	Integrating IoT into BIM	Storing Data into a local database, Lack of automation
(Natephra and Motamedi, 2019)	Temperature, Humidity, Light	Integration of environmental sensors and BIM	Lack of thermal data retrieval system
(Wehbe and Shahrour, 2019)	Temperature, Humidity, Light	Integrating IoT into BIM	Storing Data into a local database, Lack of automation
(Emad Al-Qattan et al. 2017)	Ribbon sensor	Generative modeling	Used only in the design stage
(Natephra et al., 2017)	Environmental sensor	Integrating BIM geometry data and environmental sensor data	The Lack of direct integration of sensor data and the BIM software. Humidity data have not been used to assess thermal comfort;
(Del Grosso et al, 2017)	SHM sensors	Integrating BIM into SHM system	Mostly focused on sensor simulation in BIM;
(Smarsly and Tauscher, 2016)	SHM sensors	Integrating BIM into SHM system	Only conceptual. No validation;
(Sternal and Dragos, 2016)	SHM sensors	BIM-based modeling of wireless SHM systems	No computer implementation. The inability of the IFC standard to provide sufficient entities to model overall wireless SHM;
(M. Rahmani Asl et al., 2015)	Daylight	Energy performance factor, daylighting performance factor	Not automated. Used only in the design stage
(K.M. Kensek, 2014)	Light, humidity, CO ₂	A link from the Revit model to a physical model	Used only in the design stage
(Cahill et al., 2012)	Temperature, humidity, light, CO ₂ , presence detection sensors	Optimization of building operations	No computer implementation. Only conceptual. No validation;

(Lee et al., 2012)	Load sensors	Crane navigation system for blind lifts	
(Woo et al., 2011)	Electricity consumption sensors	Building energy monitoring	No validation. Only focused on sensor data storage;
(Ryoo and Park, 2011)	Inclinometers and GPS sensors	Integration of BIM with sensors to improve the mobility of BIM models	Only conceptual. No validation;
(O'Flynn et al., 2010)	Temperature, humidity light sensors, motion and occupation sensors	IoT for building energy management application	Mostly focused on the hardware system. Conceptual in BIM part;
(Yin, 2010)	Temperature, CO2 and humidity	Use of BMS to monitor a building's operation and energy performance.	Only Conceptual. Lack of visualization;
(Katranchukov et al., 2010)	Temperature and humidity sensors	BIM based generation of multi-model views	No linkage between BIM and IoT.
(Keller et al., 2008)	Temperature and flow sensors	To identify, archive and manage building performance data and information	No computer implementation. Only conceptual;

Regarding the BIM-based thermal comfort monitoring, one of the few studies conducted could be the study conducted by Natephra, Motamedi, Yabuki, and Fukuda (2017) in which a BIM-based method was proposed for integrating BIM geometry data and environmental sensor data for assessing the indoor thermal comfort level per location. The findings show that there is no direct integration of sensor data and the BIM software (e.g., Autodesk Revit) in their method. The authors also mentioned that although relative humidity data were collected by the sensors, in their case study, such data have not been used to assess thermal comfort while evaluating the comfort level in an airconditioned building, relative humidity data should be integrated into the system.

Wu and Liu (2020) developed a BIM-based visual energy conservation system. They developed a system to integrate BIM into IoT for IAQ and thermal comfort monitoring. However,

they used PMV as an index for the thermal comfort analysis, which is not accurate in practical applications due to the parameters like clothing insulation and airspeeds. Their system was also not entirely automated due to using a local database like Excel, which needs manual updating.

Natephra and Motamedi (2019) proposed a method for an automated live sensor data visualization of building indoor environment conditions based on environmental sensors and BIM. They used Arduino microcontroller and Dynamo to record and transfer sensor data into the BIM model. Although the system works well in visualizing data, it does not have any data retrieval module to retrieve thermal condition data of building spaces if required.

In a study conducted by Wehbe and Shahrour (2019), the use of BIM to support decisions concerning comfort conditions in buildings was presented. Although they tried to link between IoT and BIM, they collected sensor data in a local database that prevents and minimizes the real-time updating of thermal comfort parameters in BIM and decreases collaboration works.

The full integration between virtual and physical sensors, the connection and insertion of sensor data remotely into an external database through the Internet of Thing (IoT) technology, and the application of a 3D visualization-based alarm system for thermal condition monitoring projects have not been adequately addressed in previous works. Also, the BIM approach has not yet been fully applied and validated for monitoring purposes. This paper designed a system to address some of these issues by developing a method for integrating the IoT system into BIM for thermal comfort monitoring in a building.

5.3. Thermal Comfort Assessment and Monitoring

There are relevant standards, such as ASHRAE Standard 55 and HSE standard pertinent to acceptable thermal comfort for occupants of buildings.

According to the Northeast Document Conservation Center (2012), to have an accurate record of existing environmental conditions throughout a building, temperature and relative humidity must be measured and recorded with instruments designed for that purpose. Table 5-2 shows the acceptable temperature ranges in hot and cold seasons based on more than 80 % occupants' satisfaction according to ASHRAE Standard 55-2017, which is widely used in North America.

Table 5-2: Acceptable operative temperature ranges (ASHRAE Standard 55, 2017)

Season	Relative Humidity (RH) (%)	Acceptable Operating Temperature (°C)	Reference
<i>Summer</i>	30=<RH<60	24.5 – 28	(ASHRAE Standard 55)
	RH=60	23 – 25.5	
Season	Relative Humidity (RH) (%)	Acceptable Operating Temperature (°C)	Reference
<i>Winter</i>	30=<RH<60	20.5 – 25.5	(ASHRAE Standard 55)
	RH=60	20 – 24	

Some thermal comfort indices, such as the Predictive Mean Vote (PMV) are used to predict thermal comfort. PMV index is used in the Standard ISO 7740. The PMV considers four physical variables (air temperature, air velocity, mean radiant temperature, and relative humidity) and two personal variables (clothing insulation and activity level of the occupant). The equation to calculate PMV is:

$$\begin{aligned}
 \text{PMV} = & [0.303 \cdot e^{(-0.036 \cdot M)} + 0.028] \cdot \{(M-W) - 3.05 \times 10^{-3} \cdot [5733 - 6.99(M-W) - p_a] \\
 & - 0.42 \cdot [(M-W) - 58.15] - 1.7 \times 10^{-5} \cdot M \cdot (5867 - p_a) - 0.0014 \cdot M \cdot (34 - t_a) \\
 & - 3.96 \times 10^{-8} \cdot f_{cl} \cdot [(t_{cl} + 273)^4 - (t_r + 273)^4] - f_{cl} \cdot h_c \cdot (t_{cl} - t_a)\} \quad (1)
 \end{aligned}$$

where:

tcl	Clothing surface temperature °C is related to the cloth that the person wears
M	Metabolic rate (W/m ²)
W	The mechanical power (W/m ²), zero for activities like writing
Ta	Indoor air temperature °C
tr	Radiant air temperature °C
var	Relative air velocity (m/s)
pa	Partial pressure of water vapor (Pa)

The factors which cause a discrepancy between the predicted and actual occupant thermal comfort level are inaccurate measurements of the person's characteristics (Clothing surface temperature (tcl) and Metabolic rate of the occupants (M)). Therefore, the PMV model's accuracy depends on accurately monitoring and controlling the airspeed and accurate measurement of clothing insulation, which could be challenging in practical applications.

Computerized BMS is usually used to monitor climate conditions and manage the HVAC system. BMS can also provide temperature and relative humidity data for analysis (Northeast Document Conservation Center, 2012). Analog and digital input signals tell the BMS what temperature, humidity, etc., are. BMS deployment usually involves installing sensors, software, a network, and cloud-based data storage mostly applied to decrease energy use and save money. However, BMS is complicated and requires specific installation, programming, and maintenance. BMS is a customized system applied to large buildings or groups of buildings. However, most buildings, particularly modular buildings, are categorized as low-rise or mid-rise building. For instance, high-rise buildings make up only 10 percent of the US commercial real estate stock and 90 percent of the total building stock in the US and might not benefit from a smart technology installed and are unmonitored or not managed at all for energy or operational savings

(Rawal, 2016). In a BMS, the data are first extracted from sensors using a Programmable Logic Controller (PLC). A Supervisory Control and Data Acquisition (SCADA) system is used to read data from PLC. The SCADA is hosted onto a database server to accommodate the transmitted data.

In the end, the Human-Machine Interface (HMI) collects the data from the SCADA and displays it to the facility manager to manage the operation of the infrastructure sustainably. One of the main challenges of BMS is in the data visualization stage, in which 2D vector graphics are used, which is not fully interactive and can only be manipulated by a trained operator (Reeser, Jankowski, & Kemper, 2015).

Therefore, integrating BIM with BMS data can be useful in order to help managers and users perform visual browsing of spatial data and to make building performance information more readily accessible to all building stakeholders, which can both boost energy management awareness and support decision-making during the operating stage.

5.4. Research Methodology

The indoor office building environment requires an efficient HVAC system to provide thermal comfort in compliance with the relevant standard like ASHRAE standard (2017), as shown in Table 5-2, and tolerable relative humidity ranges as recommended by CCOHS (2018). As shown in Table 5-2, for the relative humidity of 30–60, the temperature range for normal comfort level is 20.5–25.5. Although ASHRAE standard suggests the maximum humidity level as 60, CCOHS recommends the maximum humidity as 70, and above that level, the area may feel stuffy and uncomfortable. Accordingly, the following temperature and humidity ranges are used here, as shown in Table 5-3. Table 5-3 is based on winter temperature ranges. However, these

ranges of humidity and temperature values can be modified by the user of the proposed methodology, if different climatic conditions and standards are used.

Table 5-3: Acceptable operative temperature ranges in the wintertime used in this study

Relative Humidity (%)	Acceptable Operating Temperature (°C)
30= \leq RH<60	20.5 – 25.5
60= \leq RH<70	20 – 24

As shown in Figure 5-2, the proposed method is comprised of three main components: the IoT system, relational database, and BIM. Each is described in detail below.

The first component, the IoT system, is a smartboard associated with a microcontroller. Waspote microcontroller is used to communicate air temperature and humidity data in individual rooms. The smartboard is connected to temperature and humidity sensors for collecting the thermal comfort data in a specified time interval. The time interval of saving sensor data in a database can be increased or decreased by a user as required. In this study, the interval was set at 5 min in the field study, which is described further below. These time intervals, referred to later as delays, are specified within C++ language code via a programmable peripheral associated with the microcontroller. The microcontroller can also host a variety of wireless communication protocols (e.g., Bluetooth, ZigBee, and WiFi), allowing these technologies to send and receive data. ZigBee based sensor networks were experimented by researchers for some applications other than thermal comfort monitoring, such as materials tracking and supply chain management systems (Cho, Kwon, Shin, Chin, & Kim, 2011; Shin, Park, & Kwon, 2007). Such applications generally have more sensitivity to cyber-attacks. ZigBee has an advantage over Bluetooth as it has sensitivity, while WiFi is more sensitive but more expensive. Changing the data communication

shield allows the usage of any of the 3 communication protocols, but ZigBee has been chosen here for the reasons mentioned above.

The second component is a relational database developed in the MySQL environment to house and update the captured sensors data. The microcontroller can be coded to store and transfer sensors data to the database at predetermined time intervals. In this study, the microcontroller is coded to send the sensors' measurements and their measurement time to an online MySQL database via ZigBee every 5 min. Therefore, every 5 min, the MySQL tables are automatically updated based on the newly captured sensor data. The database developed for the proposed method consists of a schema, six tables, and corresponding parameters for the temperature and humidity sensors to accommodate the sensor-related sampling data.

The third component is the BIM-based model of a building. The BIM model is used as a central model to visualize and monitor the thermal comfort levels of rooms remotely and increase the monitoring process's speed. Every 5 min, when the MySQL tables are automatically updated based on the new sensor data, the BIM model is also updated. To link between MySQL database (physical sensors data) and the BIM model (virtual sensors), nine modules were developed and coded in *Dynamo* to automatically read temperature and humidity values stored in the database, sort the data, update the BIM model with latest real-time sensor data, and send data to the cloud using a cloud-based collaboration and data exchange services application like *Flux*, *Konstru* or *Speckle* to send notifications to building supervisors and the facility manager through their wireless devices, such as personal smartphones, so they can then take necessary actions if operating temperature data goes across the pre-defined thresholds. *Dynamo* is a visual programming and computational design tool applied for automation purposes (*Dynamo*

BIM, 2017). Space, referred to as room in the BIM model, is color-coded and automatically highlighted whenever a room’s operating temperature data violates a pre-defined threshold.

Therefore, the developed prototype comprises Waspnote microcontroller and smart sensing board equipped with humidity and temperature sensors (Sensory System); Autodesk Revit Architecture 2018 (BIM Software); Dynamo (Visual Programming Environment); SQL Server (Database Management System); and a cloud-based server (Flux).

The developed model has recently been applied in a real office unit located in Ville Saint Laurent, Quebec, Canada.

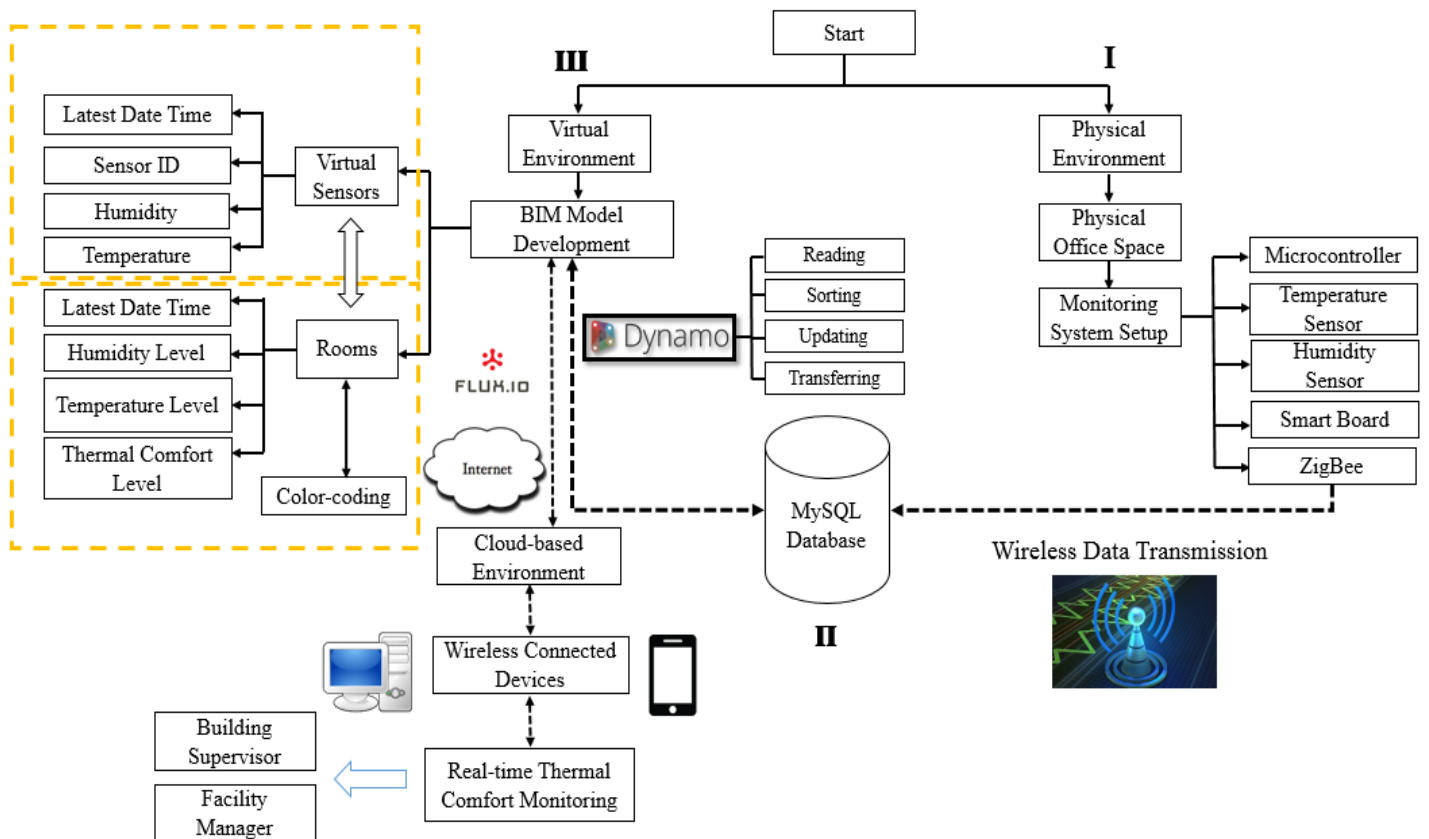


Figure 5-2: Hierarchy of the study

Figure 5-3 illustrates a schematic diagram that shows the data flow in the proposed method.

As shown, the temperature and humidity values, measured by the microcontroller, are sent to a

cloud-based database through a smart board and ZigBee module. The monitoring data is managed in a pre-designed database and are transferred to the BIM model and a cloud-based system through a specially designed workflow to let facility managers or building supervisors to monitor different spaces in a building remotely and identify the technical reasons for possible issues through their PC and wireless-connected devices.

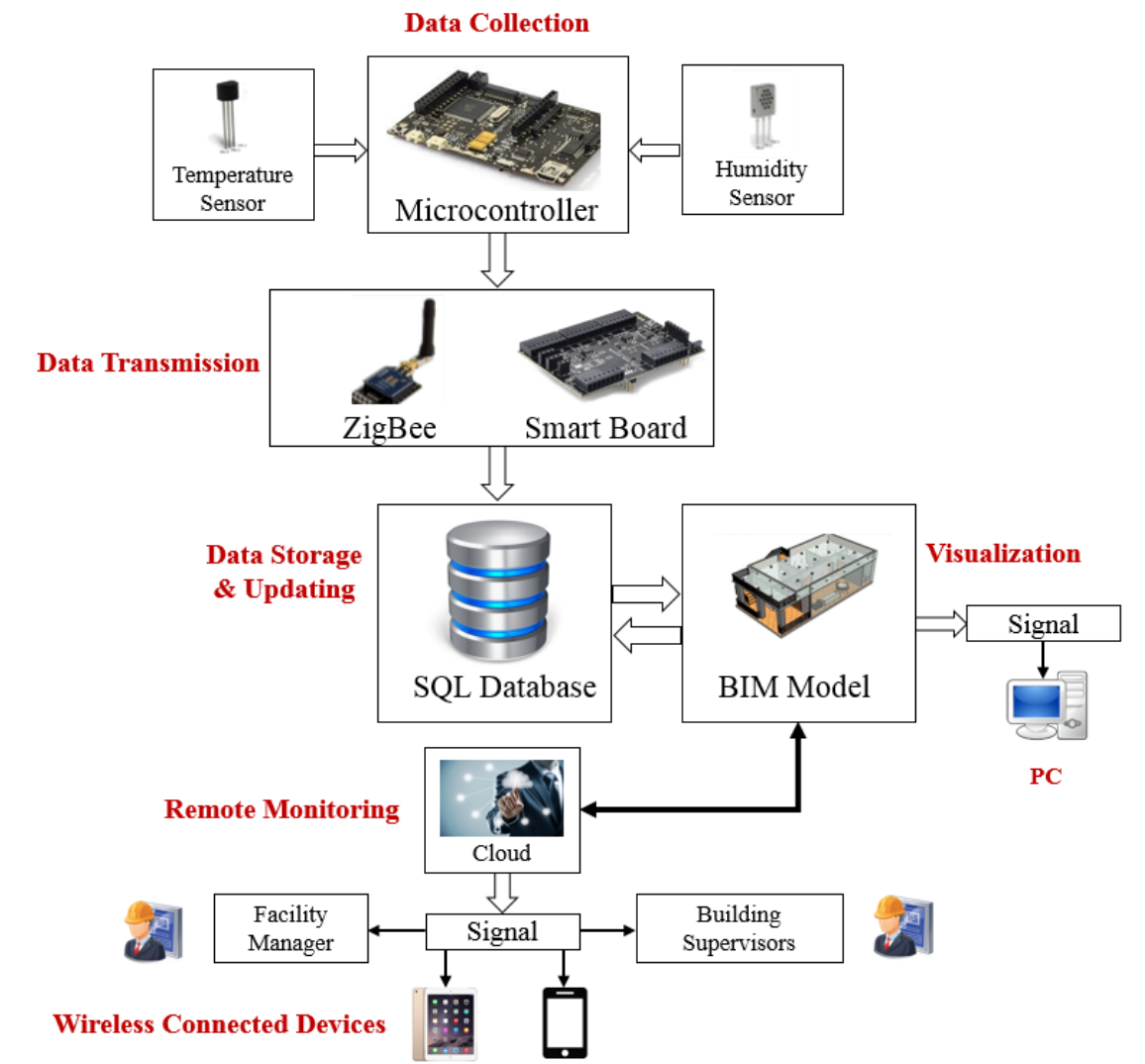


Figure 5-3: Developed dataflow schema

5.5. The System Framework

5.5.1. Hardware configuration of the system

Over recent decades, the automated data acquisition (DAQ) technology market has witnessed a remarkable advance in hardware and software. Most available technologies are expensive and in a black box format. Black box format users cannot access the relevant algorithms and modify them as they see fit. Also, the stored data are often difficult to obtain without using seller-specific software. Limited research was conducted to study and develop the customized design of automated DAQ systems to confront the above challenges and overcome the off-the shelf technologies-related limitations (open-source technologies allocate a minute portion in DAQ systems' marketplace).

There are two pioneers in the domain of cost-efficient open-source technologies, Arduino and Wasmote. Although Arduino is older than Wasmote, both platforms are using standard coding syntax. Arduino is considerably useful to learn how to use electronics and to do less costly, simple projects (e.g., home automation projects), while Wasmote is a device specially designed to create long lifetime IoT systems expected to be installed in a real scenario like a city, agriculture farm, or construction job site. However, although this case study has relatively the same incentives for using either technology, Wasmote was chosen as it alone has the radio certification for possible combinations of the communication modules (802.15.4, ZigBee, 3 G, ZigBee + 3 G).

The hardware consists of a microcontroller to perform specific tasks through programming. This microcontroller integrates with a board that can be attached to various peripherals, such as data transmitters. The acquisition system is used to collect the required thermal comfort data (temperature and humidity data) over a set of defined time intervals using temperature and humidity

sensors. The developed system is designed to acquire temperature and humidity data in uniform intervals (every 5 min. in this study), with ranges predefined in the microcontroller programming using C++ language. The received data are then transmitted to a MySQL database through the ZigBee data transmission module. Table 5-4 shows the specifications (such as Measurement Range, Sensitivity, accuracy, and operation temperature) of each type of sensor used in this study. Figure 5-4 shows the DAQ system hardware used in this study.

Table 5-4: Specifications of Sensors (Waspnote datasheets, 2012)

Type of Sensor	Measurement range	Sensitivity	Accuracy	Operation temperature
Temperature Sensor	-40°C ~ +125°C	10mV/°C	±2°C (range 0°C ~+70°C), ±4°C (range -40 ~+125°C)	-40 ~ +125°C
Humidity Sensor	0 ~ 100%RH	-	<±4%RH (range 30~ 80%), <±6%RH (range 0 ~ 100)	-40 ~ +85°C

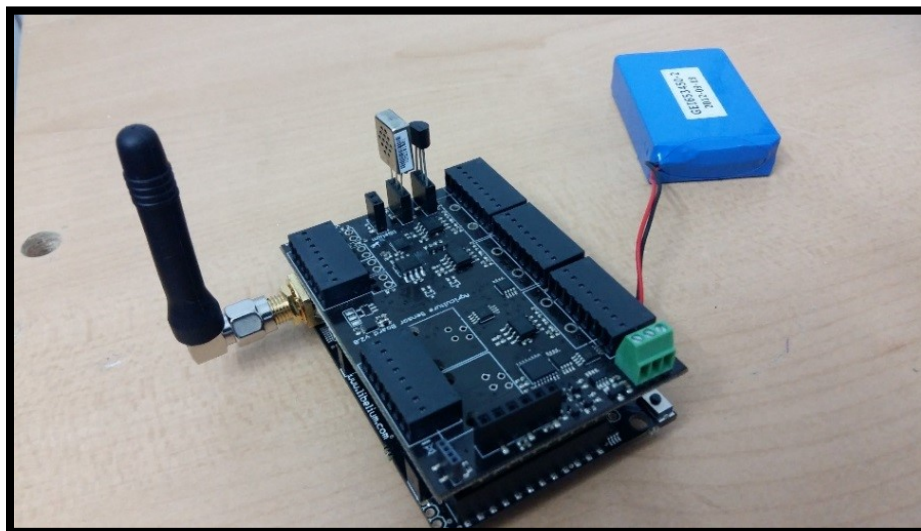


Figure 5-4: DAQ system hardware used in this research

5.5.2. Development of the BIM model

A small two-story office building located in Ville Saint Laurent, Quebec, Canada is modeled in Autodesk Revit Architecture 2018 in this case study. The building was chosen because the building includes office space above a restaurant and the old HVAC system in the office required upgrading.

The heat generated by the restaurant's kitchen is transferred to the above floors, reducing thermal comfort.

After developing the BIM model, virtual humidity and temperature sensors were embedded in the model. A set of parameters were introduced in the modeling process: '*LatestDateTime*', '*Sensor_ID*', '*Humidity*', and '*Temperature*' for the sensor objects; and '*Latest DateTime*', '*Humidity Level*', '*Temperature Level*', and '*Thermal Comfort Check*'. Two parameters, '*Humidity*' and '*Temperature*' were created to accommodate the maximum humidity and temperature values recorded by the humidity and temperature sensors at two-hour intervals. The '*LatestDateTime*' parameter was created to accommodate the maximum operative temperature measurement's date and time, and the '*Sensor_ID*' parameter was used to link the physical sensors to virtual sensors in the BIM model. The physical sensors' specific ID must be assigned to each corresponding virtual sensor in the BIM model to link the two types of sensors. '*Humidity Level*' and '*Temperature Level*' parameters were created for the '*Room*' object to accommodate the latest '*Humidity*' and '*Temperature*' parameters values of the correlating virtual sensors in the BIM model, and the '*Thermal Comfort Check*' parameter was used to monitor the working range condition of the instrumented room. Only the room located at the top of the restaurant's kitchen on level 1 above the ground floor, with an area of about 215 ft², was instrumented and used in this

study. Figure 5-5 shows how the virtual temperature and humidity sensors and their user-defined parameters are shown in the developed 3D BIM model.

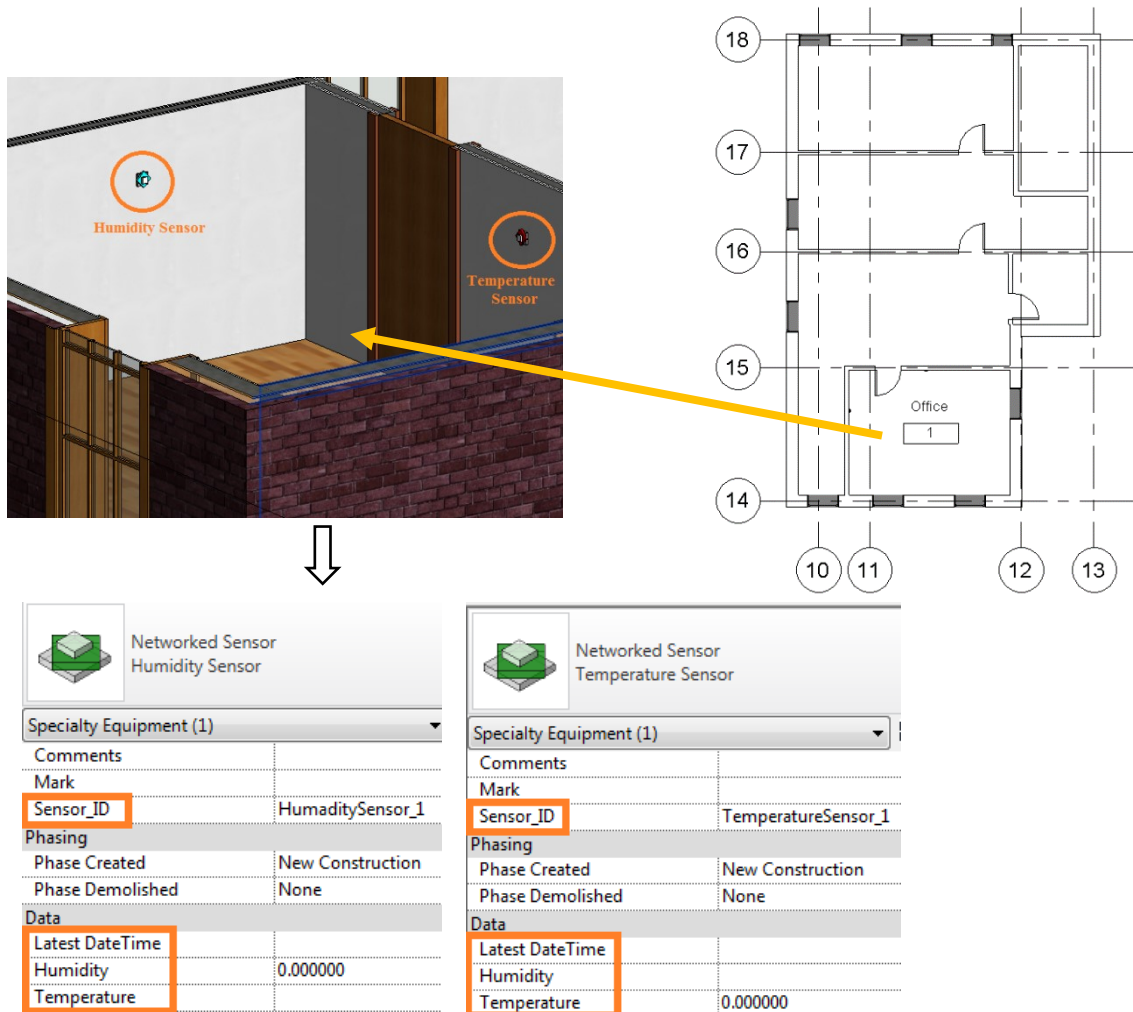


Figure 5-5: The instrumented office room, virtual sensors, and their parameters in the BIM model

5.5.3. MySQL database

To insert the sensed data into a database like MySQL, a schema (database), and tables and all essential parameters are to be defined. The tables house the sensor data received from the DAQ system.

The schema, named *'thermal_condition_monitoring'* is defined along with six tables named *'waspmote_humidity_sensor'*, *'waspmote_temperature_sensor'*, *'temperature_measurement_history'*, *'humidity_measurement_history'*, *'room'*, and *'room_info'*. The parameters defined for each table are shown in Table 5-5.

Table 5-5: MySQL database model specifications used in this study

Tables	Parameters
waspmote_temperature_sensor	'Record_ID', 'Sensor_ID', 'Sensor_Value', 'Recorded_AT'
waspmote_humidity_sensor	'Record_ID', 'Sensor_ID', 'Sensor_Value', 'Recorded_AT'
temperature_measurement_history	'Record_ID', 'Sensor_ID', 'Sensor_Value', 'Recorded_AT'
humidity_measurement_history	'Record_ID', 'Sensor_ID', 'Sensor_Value', 'Recorded_AT'
room	'Room_ID', 'Room_Name', 'Occupancy', 'Thermal_Condition', 'Latest_DateTime'
room_info	'Room_ID', 'Room_Name', 'Thermal_Condition', 'Latest_DateTime'

Four parameters were introduced for the sensor's tables: *'Record_ID'*, *'Sensor_ID'*, *'Sensor_Value'*, and *'Recorded_AT'* where *'Record_ID'* constitutes the primary key. Five parameters were introduced for *'room'* table: *'Room_ID'*, *'Room_Name'*, *'Occupancy'*, *'Thermal_Condition'*, and *'Latest_DateTime'* where *'Room_ID'* constitutes the primary key. Four parameters are also introduced for *'room_info'* table, including *'Room_ID'*, *'Room_Name'*, *'Thermal_Condition'*, and *'Latest_DateTime'*.

The temperature and humidity values are measured, stored in a DAQ system, and transferred to a MySQL database at a specified interval to be stored in their corresponding tables (*waspmote_temperature_sensor*, and *waspmote_humidity_sensor*). Here, an interval of 5 min is used as an example. Therefore, the *'Record_ID'*, *'Sensor_Value'*, and *'Recorded_AT'* parameters

in these tables are updated every 5 min. These tables are linked with the central BIM model which is also updated at the same interval (e.g., every 5 min, in this case). To have a history of the temperature and humidity values in the monitored space, the data at each time interval is transferred to the database and placed in the measurement history tables (*temperature_measurement_history*, and *humidity_measurement_history*). Once the BIM model is updated based on the sensor data, it updates the 'room' table in the MySQL database using the developed workflow. And finally, the 'room_info' table is populated based on the information updated in the 'room' table every 5 min if the room's thermal condition is not acceptable. Therefore, 'room_info' table is used as a history of the thermal condition of the room when the thermal condition is poor.

The database model can be expanded in case of using temperature and humidity sensors for multiple rooms. To construct a comprehensive database model for the whole sensory system, the information on the corresponding rooms and their conditions must be determined. Figure 5-6 shows the Entity-Relationship Diagram (ERD) of the proposed database model.

As shown in Figure 5-6, the ERD consists of six entities, *waspmote_temperature_sensor*, *waspmote_humidity_sensor*, *temperature_measurement_history*, *humidity_measurement_history*, *room*, and *room_info*. According to the relationship among the entities, it is observed that there is "One to Many" relationship between *temperature_measurement_history* and *waspmote_temperature_sensor*, *humidity_measurement_history* and *waspmote_humidity_sensor*, *room* and *waspmote_temperature_sensor*, *room* and *waspmote_humidity_sensor*, and *room_info* and *room* entities. It means that a given set of temperature and humidity sensors belongs to only one room, but a room element may have multiple sets of temperature and humidity sensors.

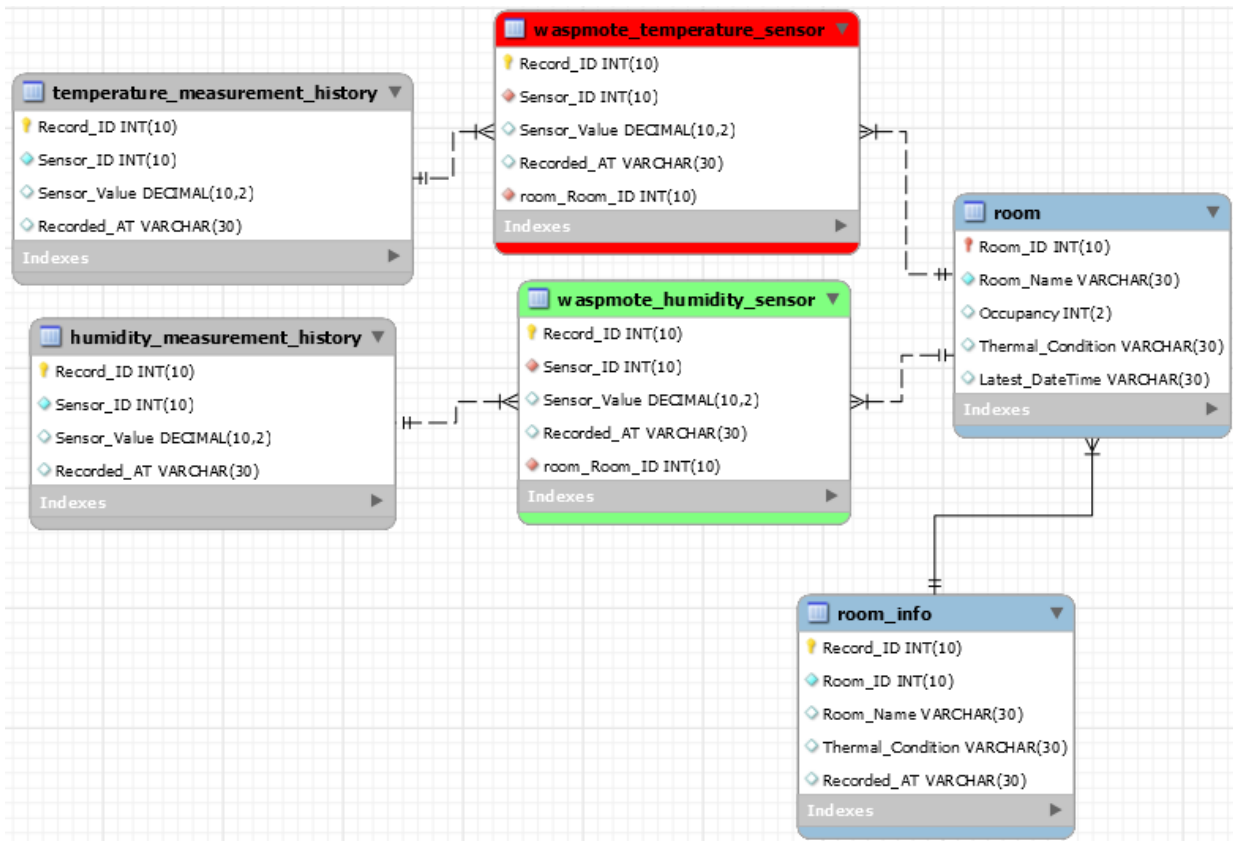


Figure 5-6: ERD of the Monitoring System Database

The following tables, `temperature_measurement_history` and `humidity_measurement_history`, may consist of one or more than one sensor that can be filtered by the `Sensor_ID` parameter. `Room_info` table may also have one or more monitored rooms containing the information about the room when the room's thermal condition is not perfect.

The database model was created to support the developed system utilizing nine specially designed modules in Dynamo, as depicted in Figure 5-7.

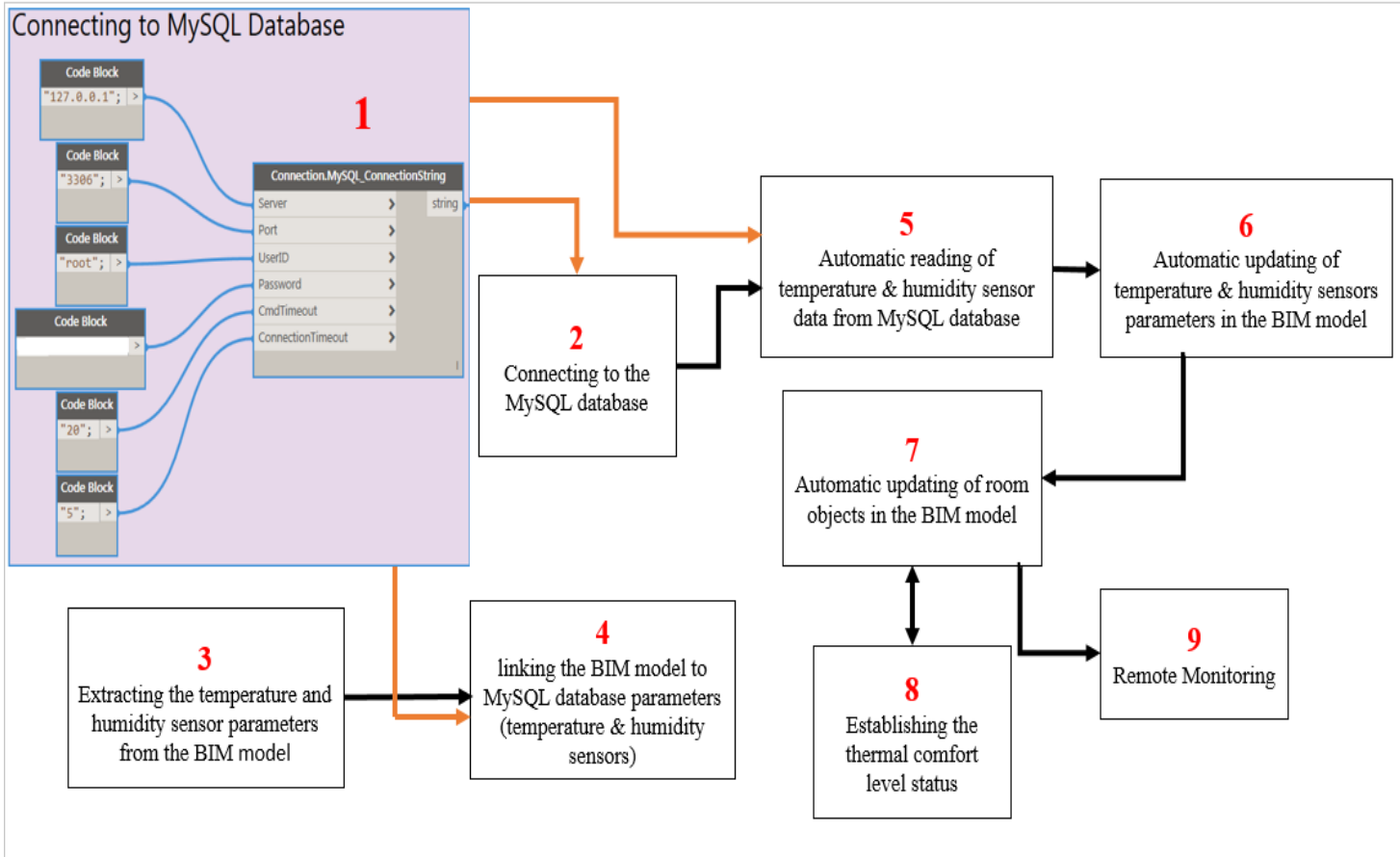


Figure 5-7: The overall workflow for integrating BIM into thermal comfort monitoring

In Figure 5-7, the modules were numbered to demonstrate their linkage better. In the figure, Module number 1 is used to connect the developed framework to the MySQL database server using server ID, port number, user ID, and password. The output of module number 1 is connected to modules number 2 (to connect the system to the created schema in MySQL database and its corresponding tables), number 4 (to link the virtual temperature and humidity sensors in the BIM model respectively to the database containing sensor data, and number 5 (to retrieve the temperature and humidity sensor data respectively from the database). Module number 2 is connected to module number 5. Module number 3 is connected to module number 4 (to extract the values of the relevant parameters of temperature and humidity sensors, respectively, from the

BIM model and link them to the corresponding parameters in the database). Module number 5 is connected to module number 6 (to update the temperature and humidity sensor parameters in the BIM model, respectively). Module number 7 is used to map the sensors to the corresponding rooms in the BIM model and update the related room parameters and is connected to modules number 8 and 9. Module number 8 is used to define the temperature ranges based on the humidity values and the room's corresponding thermal comfort level. And finally, module number 9 is used to transfer the related information to the cloud for remote monitoring using wireless devices, such as smartphones.

Only three modules, 5, 6, and 7, are presented here for space limitations. Module 5 was developed for automatic reading and sorting the sensed temperature values from the database. Module 6 was developed for the automatic updating of the temperature sensor parameter in the BIM model, and Module 7 was developed for the automatic updating of office room parameters in the BIM model. The modules shown in Figure 5-7 are described in the following sections.

5.5.4. Extracting parameters from the BIM model

Here, a module is developed to retrieve the virtual sensor parameters from the BIM model. The sensor parameters must be extracted to check the latest values of the parameters in the BIM model. The module consists of four parts. First, '*Networked Sensor: Temperature Sensor*' is read from the list of family types in the BIM model. Second, all elements are selected in this category. Third, the values for the user-defined sensor parameters, like *Sensor_ID*, *Temperature*, and *Latest DateTime*, are displayed, and fourth, extracted from the BIM model to be shown in one list. A similar structure is used for the virtual humidity sensor and its parameters from the BIM model.

5.5.5. Connecting the BIM model to the database

After extracting the essential parameters from the BIM model, they must be linked to the database's parameters already created for each sensor. This integration is required for any future BIM model updating. A similar workflow can also be used to link the virtual humidity sensor with the database. The 'Sensor_Value' parameter created in the MySQL database is linked to the 'Temperature' parameter of the virtual temperature sensor in the BIM model, 'Sensor_ID' parameter created in the database is linked to the 'Sensor_ID' parameter of the virtual temperature sensor in the BIM model, and 'Recorded_AT' parameter defined in the database is linked to the 'Latest DateTime' parameter in the BIM model. The relevant parameters are listed first and are then connected to the '*waspmote_temperature_sensor*' table and the values extracted from the BIM model.

5.5.6. Automatic reading of sensor values from MySQL database server

When a connection is established between the BIM model and the MySQL database server, the next step is to read the sensed data from the MySQL database in an automatic manner. Different nodes are applied and connected for this automatic sensor data reading. As mentioned earlier, the 'Humidity' and 'Temperature' parameters are created and assigned to the virtual sensors in the BIM model; consequently, the temperature and humidity values at every time interval (every 5 min) are to be sent to the BIM model to update the 'Humidity' and 'Temperature' parameters of the virtual humidity and temperature sensors. If the temperature value at each time interval is within the pre-defined acceptable operative temperature ranges, it means that the office room's thermal comfort is in excellent condition. A similar structure can be used for the humidity sensor.

5.5.7. Updating the virtual sensors parameters in the BIM model

After reading and sorting the sensed values stored in the MySQL database, the associated parameters of virtual sensors have to be updated in the BIM model at each time interval. For this purpose, a module is created to update the BIM model. The module first selects the temperature sensor and its elements in the BIM model. Then, the *Element.SetParameterByName* node is applied to update the *Sensor_ID*, *Temperature*, and *Latest DateTime* parameters of the temperature sensor in the BIM model based on the sensor information and maximum temperature value recorded from the MySQL database. In the first part of this module, the temperature or humidity value and its measurement time and the sensor ID are separated for use as the input in the second part of this module for updating the corresponding parameters in the BIM model. After every time interval, the temperature and humidity values are recorded, and the corresponding parameters in the BIM model are updated. A similar module was used to update humidity sensor parameters.

To design an alarm system in the BIM model, a conditional statement has to be defined, and the BIM model color-coded to highlight the Room object in the BIM model to which the sensors are attached subject to extreme temperature ranges. This alarm system works as a signal to the building supervisors or facility manager when the sensor readings exceed the pre-defined acceptable ranges.

5.5.8. Defining the conditional statements and updating room parameters

For thermal comfort visualization in the BIM model, a parameter named ‘Thermal Comfort Check’ was defined for the ‘Room’ object in the BIM model, which has to be updated based on the

'Humidity Level' and 'Temperature Level' values stored in room object. A module was created to cross the sensor value between the virtual temperature sensors and the correlating office room in the BIM model. A similar workflow was used for the humidity sensors. Then, a module was created to define the conditional statement, according to Table 5-3. By using the developed module, the sensors and the room where they are installed were identified. The instrumented office rooms were identified and separated from the un-instrumented ones in the BIM model. Then, when the instrumented office rooms were identified, 'Temperature Level' and 'Latest DateTime' parameters of the instrumented room were updated based on the 'Temperature' and 'Latest DateTime' parameters of the temperature sensor in the BIM model. A similar structure is used for the humidity sensor in this study.

The conditions shown in Table 5-3 are applied in this study. The status of the 'Thermal Comfort Check' parameter of the Room object in the BIM model was classified into four cases: 'Too Hot,' 'Too Cold,' 'Normal,' and 'Unacceptable Humidity Level.' If the temperature measurement does not meet the condition, the 'Thermal Comfort Check' parameter is considered 'too hot' or 'too cold'; otherwise, it is normal. However, if the humidity measurement was too high (more than 70 %) or too low (less than 30 %), then the 'Thermal Comfort Check' parameter showed an 'unacceptable humidity level'. When the office room's thermal comfort level was recognized, the 'Thermal Comfort Check' parameter of room objects was updated in the BIM model to inform the building supervisor and facility manager about the latest thermal comfort of the instrumented offices and their HVAC system performance. Through this module, some of the room's parameters such as *Room_ID*, *Room_Name*, *Occupancy*, *Thermal_Condition*, *Latest_DateTime* are extracted from the BIM model and transferred to the MySQL database to update the *room* table after each time interval. After each time interval, if the room's thermal condition is not normal, the *room*

table's information is transferred and saved in *room_info* table through a query used in MySQL server to have comprehensive information about the thermal condition of each room.

5.6. System Implementation

The modules described in the previous section were developed to introduce a workflow to link virtual and physical humidity and temperature sensor, update the associated parameters of '*Humidity Level*', '*Temperature Level*', '*Latest DateTime*', and '*Thermal Comfort Check*', and then highlight the corresponding office room in the BIM model based on its thermal comfort status at each time interval (e.g., every 5 min). The Waspnote-based DAQ system was coded to transfer the sensed temperature and humidity data to the MySQL database server at each time interval. A query was used in the MySQL server to update the predefined tables and parameters at each time interval.

The test was conducted on the 10th of November 2018. At each time interval, one temperature and one humidity data points were recorded. The system recorded Forty-nine data points during the test (four hours) to validate the proposed method. After each time interval, the BIM model and its corresponding user-defined parameters like *Sensor_ID*, *Temperature*, *Humidity* and *Latest DateTime* for the virtual temperature and humidity sensors, and *Thermal Comfort Check*, *Humidity Level*, *Temperature Level*, and *Latest DateTime* for room objects were updated. Once the BIM model was updated, the thermal condition-related information was transferred from the BIM model to the database to update the "*room*" table in the defined database. If the room's thermal condition was not perfect at each time interval, a query was used in MySQL to transfer room-related information from the "*room*" table and store them in the "*room_info*" table to have a thermal discomfort history of the room.

Figure 5-8 shows the temperature and humidity values and the room’s thermal condition measured in the 18th time interval, which were stored in their corresponding tables in MySQL server.

Record_ID	Sensor_ID	Sensor_Value	Recorded_AT
18	TemperatureSensor_1	26.00	11/10/2018 11:25
NULL	NULL	NULL	NULL

(a)

Record_ID	Sensor_ID	Sensor_Value	Recorded_AT
18	HumiditySensor_1	58.85	11/10/2018 11:25
NULL	NULL	NULL	NULL

(b)

Room_ID	Room_Name	Occupancy	Thermal_Condition	Latest_DateTime
344574	Office 1	4	Too Hot!	11/10/2018 11:25
NULL	NULL	NULL	NULL	NULL

(c)

Figure 5-8: Transferring sensors reading remotely to the database (18th-time interval)

As can be seen from Figure 5-8, temperature and humidity values, their measurement time, and the room information were successfully stored in their corresponding tables in the MySQL database. Once the sensors’ data was introduced to the database, the values were retrieved from the MySQL database and sorted automatically in the module described earlier. The ‘*Sensor_ID*’, ‘*Sensor_Value*’, and ‘*Recorded_AT*’ values were captured, read, and sorted for humidity and

temperature sensors installed in the office room. The humidity and temperature readings of sensor values were extracted after the values were sorted. Figure 5-9 shows the developed module described earlier to automatically read and sort temperature values from the database. As shown, the temperature value measured in the 18th time-interval was read from the proposed method successfully, and the temperature value and its measurement time were extracted from the list of measurements to be transferred to the corresponding parameters in the BIM model.

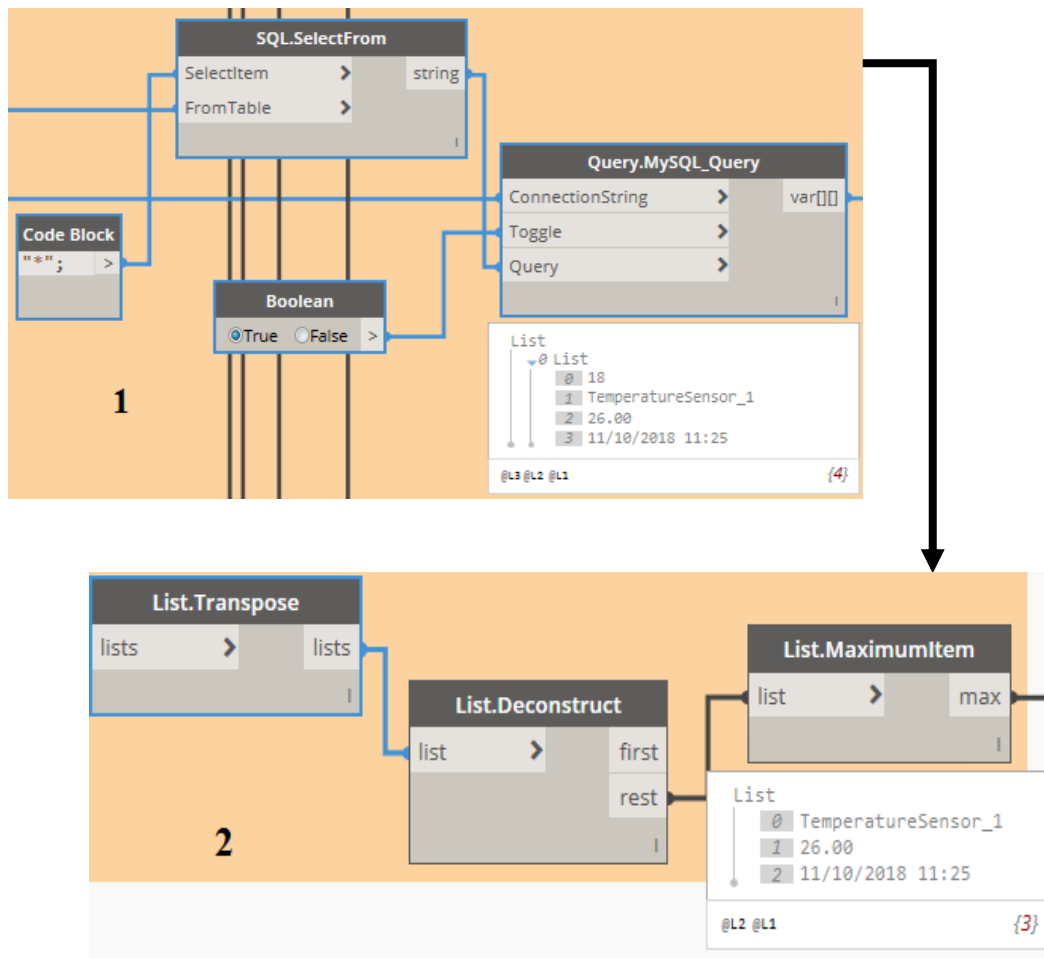


Figure 5-9: Reading and sorting the second time-interval temperature data from the database

In the developed workflow for integrating BIM into thermal comfort monitoring, *Periodic* mode was used with the time interval of 300,000 milliseconds (5 min.) to automatically read and

extract data from the MySQL database, update the BIM model and send the thermal condition info to the MySQL and cloud-based database every 5 min. As shown in Figure 5-10, the test started at 10:00 AM on Nov 10th, 2018, and the system was updated 49 times in the total test time (four hours).

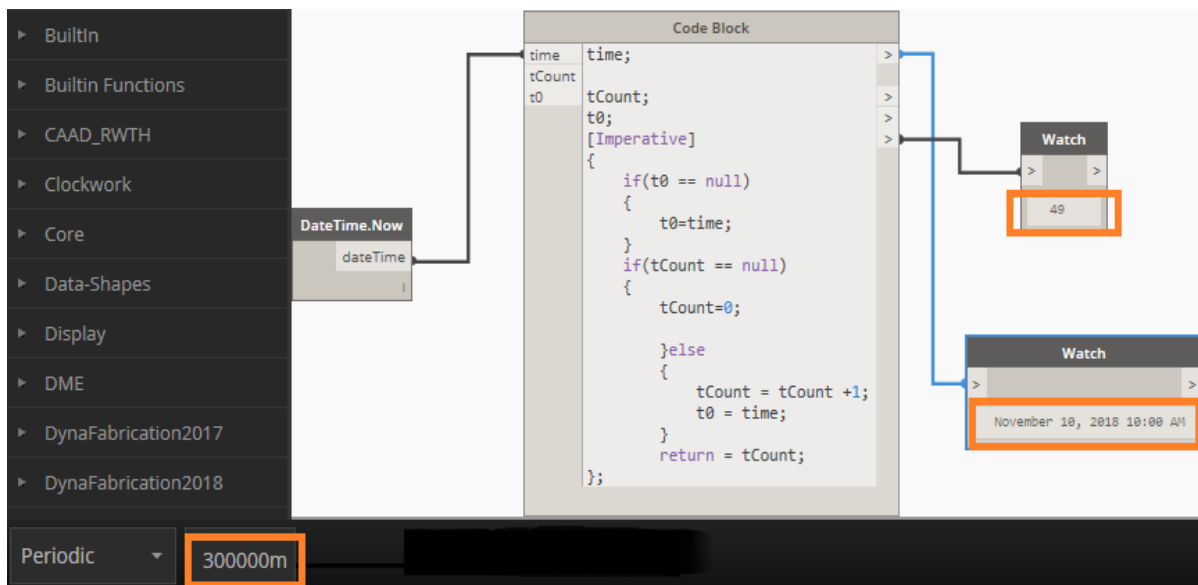


Figure 5-10: Setting the developed workflow to automatically update the system every 5 minutes

When the sensors' values were read and transferred, the BIM model's virtual sensors parameters were updated using the modules described earlier. The parameters defined for the office rooms in the BIM model (*'Humidity Level'*, *'Temperature Level'*, *'Thermal Comfort Check'*, and *Latest DateTime*) were updated using the modules described earlier.

Figure 5-11 shows the module developed to automatically update temperature parameters in the BIM model based on the captured sensor data. A similar module was used for the automatic updating of humidity parameters in the BIM model.

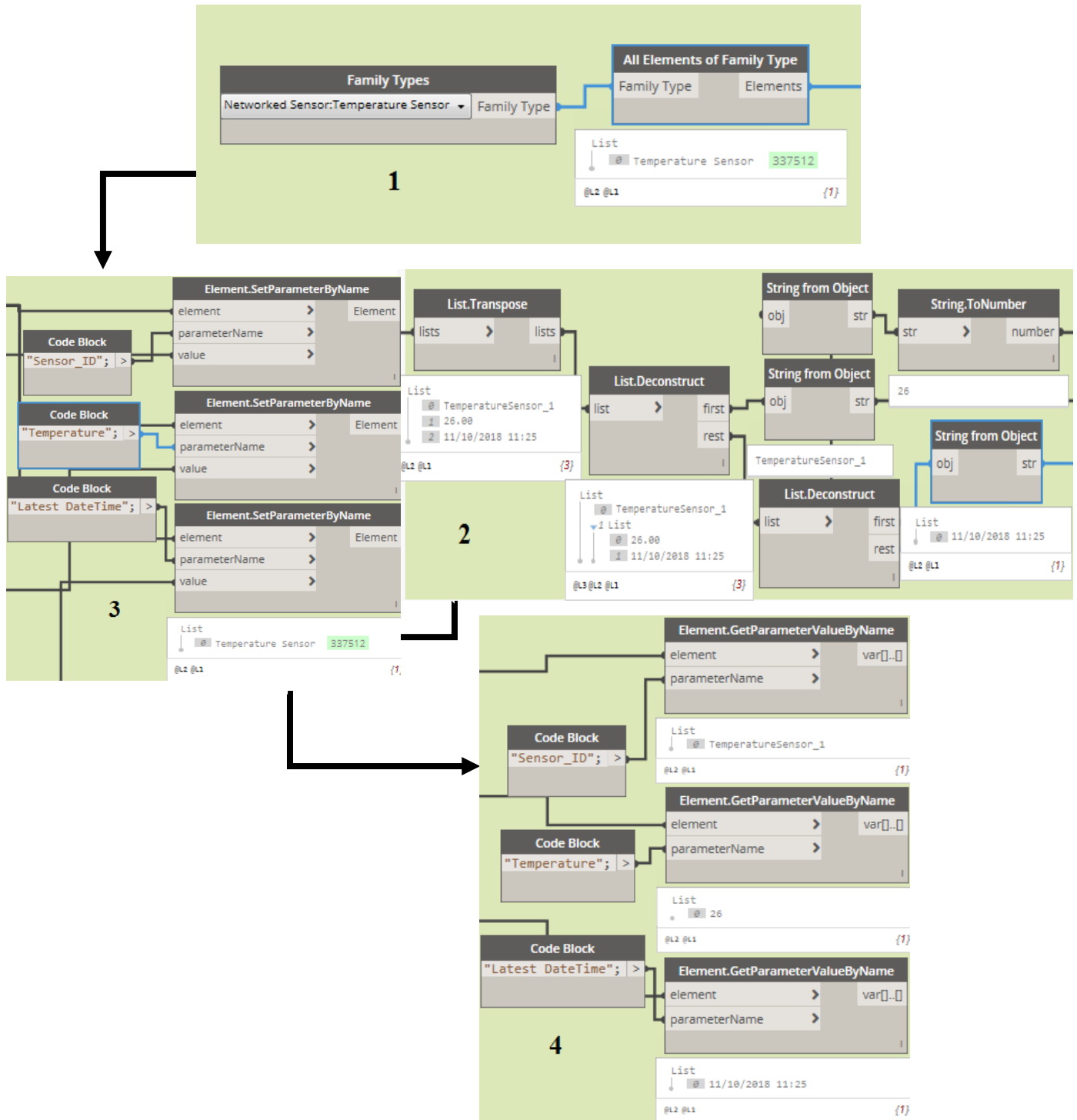


Figure 5-11: Automatic updating of temperature sensor parameters in the BIM model

When the room’s parameters were updated, the room was highlighted based on the colors defined in Table 5-6.

Table 5-6: Classification of office rooms based on their thermal comfort level and color

Thermal Comfort Check Parameter	Colour
Normal!	White
Too Hot!	Red
Too Cold!	Blue
Unacceptable Humidity Level	Purple

Figure 5-12 shows a picture of the developed BIM-IoT system in operation during the test when the room temperature level exceeded the acceptable threshold.

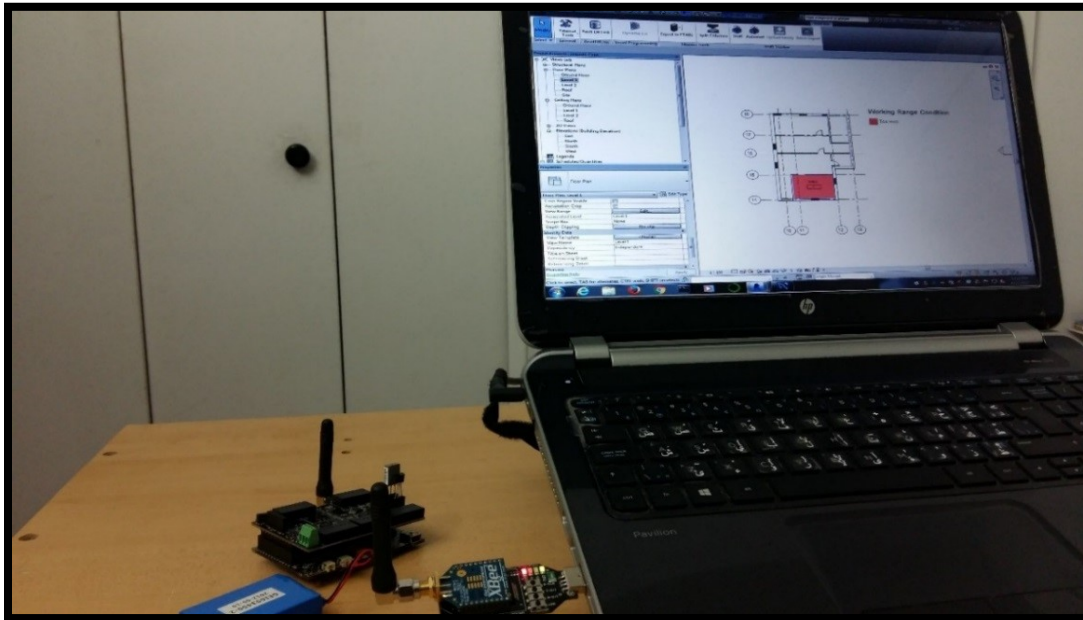
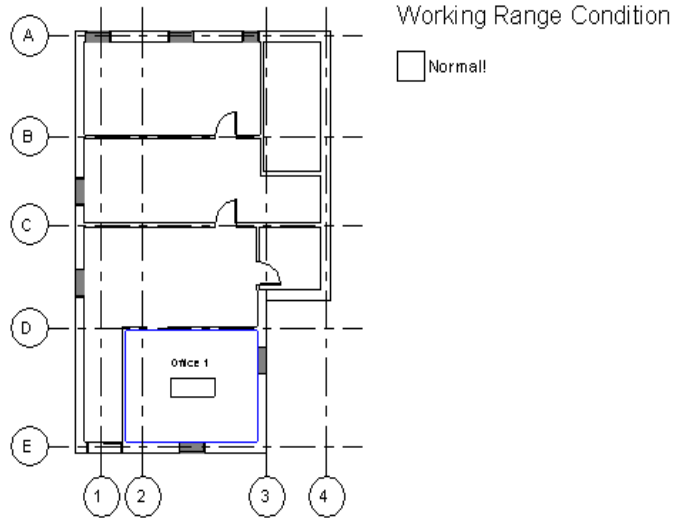


Figure 5-12: Picture of thermal comfort monitoring test setup in the second-time interval

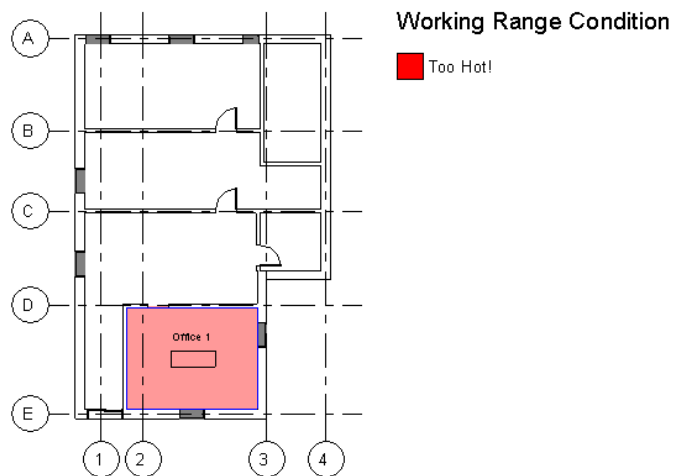
As shown in Figure 5-13, the instrumented office room's working range condition in the BIM model is 'Normal!' and 'Too Hot!', respectively, in the first- and eighteenth-time intervals. Therefore, the room was highlighted in red in the time interval eighteen. As observed, the maximum temperature value was measured at 26.0 °C at 11:25 AM.

Occupancy	4
Department	
Base Finish	
Ceiling Finish	
Wall Finish	
Floor Finish	
Occupant	
Phasing	
Phase	New Construction
Data	
Latest DateTime	11/10/2018 10:00
Thermal Comfort Check	Normal!
Humidity Level	47.790000
Temperature Level	22.500000



(a)

Occupancy	4
Department	
Base Finish	
Ceiling Finish	
Wall Finish	
Floor Finish	
Occupant	
Phasing	
Phase	New Construction
Data	
Latest DateTime	11/10/2018 11:25
Thermal Comfort Check	Too Hot!
Humidity Level	58.850000
Temperature Level	26.000000



(b)

Figure 5-13: Screenshots of BIM user interface: (a) first time interval (b) 18th time interval

As mentioned earlier, *waspmote_temperature_sensor* and *waspmote_humidity_sensor* tables only accommodate one row of data (data captured at each time interval). Therefore, to have a history of temperature and humidity measurements of each room, the data were transferred from *waspmote_temperature_sensor* and *waspmote_humidity_sensor* tables to

temperature_measurement_history and *humidity_measurement_history* tables in the MySQL database.

Figure 5-14 shows the layout of the *temperature_measurement_history* table in the “thermal_condition_monitoring” database, which accommodates all the temperature data recorded during the test. Figure 5-15 indicates the *room table* data, which shows where and when the thermal discomfort occurs.

The screenshot displays a MySQL database interface. On the left, the 'SCHEMAS' pane shows the 'thermal_condition_monitoring' database with tables 'humidity_measurement_history', 'room', 'room_info', and 'temperature_measurement_history'. The 'temperature_measurement_history' table is selected and highlighted with an orange box. Below the schema pane, the 'Information' section shows the table's columns: Record_ID (int(10) UN AI PK), Sensor_ID (varchar(30)), Sensor_Value (decimal(10,2)), and Recorded_AT (varchar(30)). On the right, the 'Result Grid' shows 18 rows of data for the selected table.

Record_ID	Sensor_ID	Sensor_Value	Recorded_AT
1	TemperatureSensor_1	22.50	11/10/2018 10:00
2	TemperatureSensor_1	22.50	11/10/2018 10:05
3	TemperatureSensor_1	22.00	11/10/2018 10:10
4	TemperatureSensor_1	22.50	11/10/2018 10:15
5	TemperatureSensor_1	23.00	11/10/2018 10:20
6	TemperatureSensor_1	23.50	11/10/2018 10:25
7	TemperatureSensor_1	23.50	11/10/2018 10:30
8	TemperatureSensor_1	23.00	11/10/2018 10:35
9	TemperatureSensor_1	23.50	11/10/2018 10:40
10	TemperatureSensor_1	24.00	11/10/2018 10:45
11	TemperatureSensor_1	24.30	11/10/2018 10:50
12	TemperatureSensor_1	24.50	11/10/2018 10:55
13	TemperatureSensor_1	24.50	11/10/2018 11:00
14	TemperatureSensor_1	25.00	11/10/2018 11:05
15	TemperatureSensor_1	25.20	11/10/2018 11:10
16	TemperatureSensor_1	25.50	11/10/2018 11:15
17	TemperatureSensor_1	25.50	11/10/2018 11:20
18	TemperatureSensor_1	26.00	11/10/2018 11:25

Figure 5-14: Temperature_measurement_history table data at the end of the test

Figure 5-16 illustrates the temperature variations in the instrumented office during the monitoring period. As shown, the temperature level exceeded the acceptable threshold thirteen times.

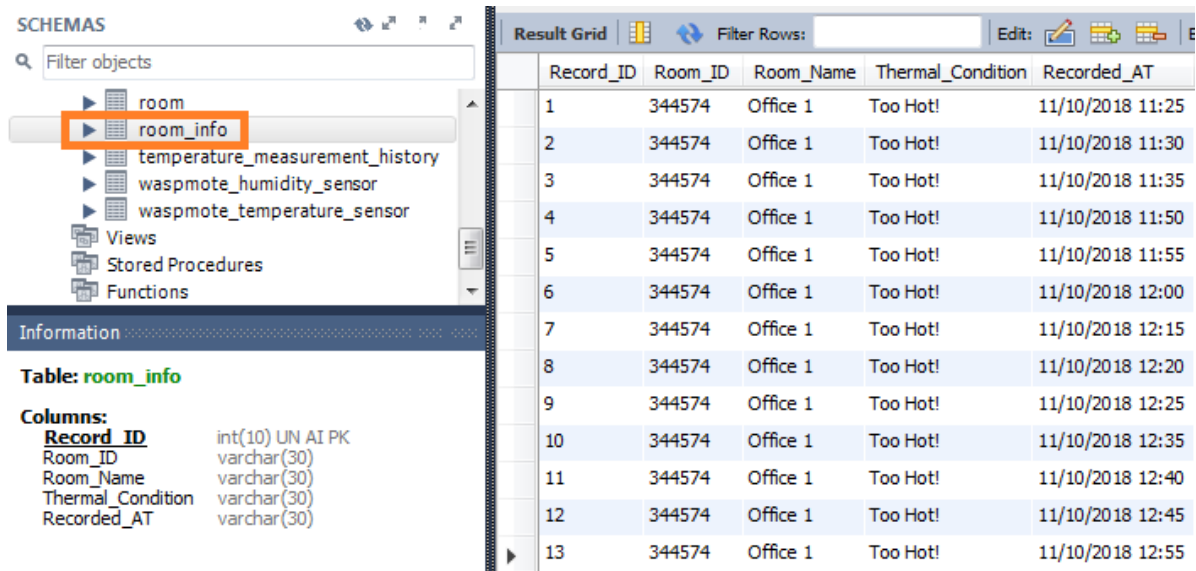


Figure 5-15: room table data at the end of the test

As shown in Figure 5-16, at thirteen data points (mostly at noon), the temperature level exceeded the acceptable threshold, and the thermal condition of the instrumented room was not ideal (*Too Hot*).

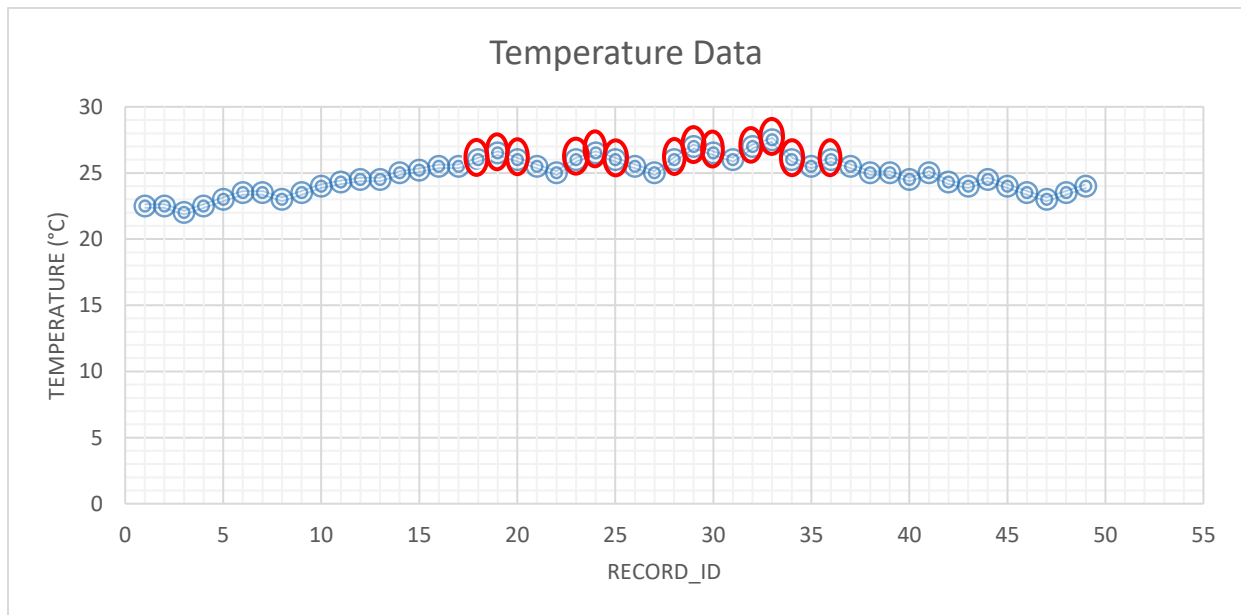


Figure 5-16: Temperature recording map in the instrumented office

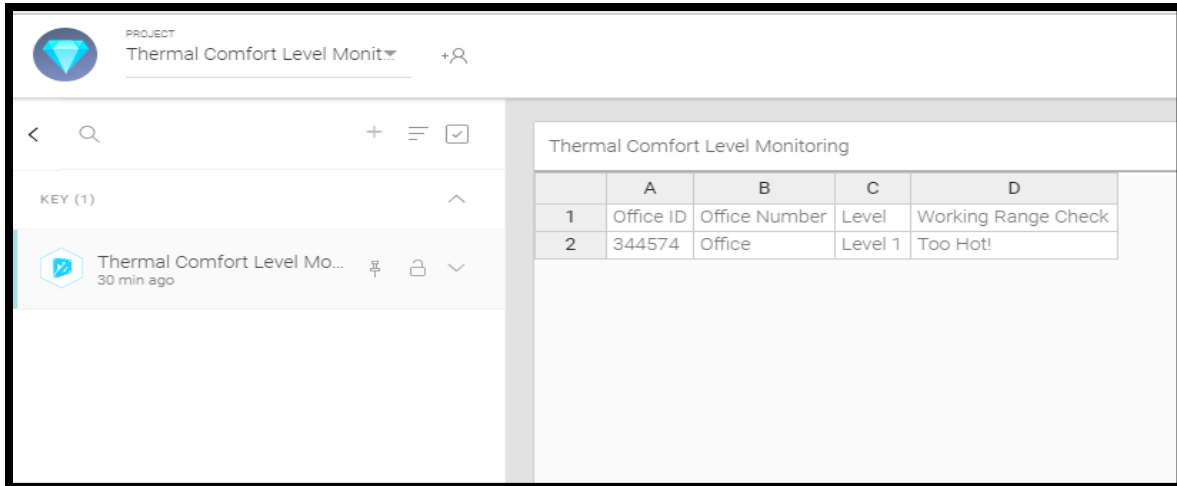
Sending real-time notifications to building supervisors and the facility manager through the wireless connected devices, such as smartphones or iPads, is critical for taking necessary actions if the operating temperature data does not fall within the predefined acceptable range. For this purpose, a module is also developed to send the room data from the BIM model to the cloud-based storage and collaboration service. As mentioned earlier, Flux is used in this study for this purpose.

Parameters of the instrumented room (i.e., '*Name*', '*Office ID*', '*Level*', and '*Thermal Comfort Check*'), are extracted from the BIM model and transferred to the cloud. To define an appropriate title for each data in the cloud, several parameters were defined: '*Office ID*' was defined for the '*Element.id*' parameter, '*Office Number*' was defined for the '*Name*' parameter, '*Level*' was defined for '*Level*' parameter, and '*Working Range Check*' was defined for '*Thermal Comfort Check*' parameter of the BIM model. Therefore, the building supervisors or the facility manager can access the room data and HVAC system performance remotely through their wireless devices, such as a smartphone (Figure 5-17(b)) besides their PC (Figure 5-17(a)), at any time and any location.

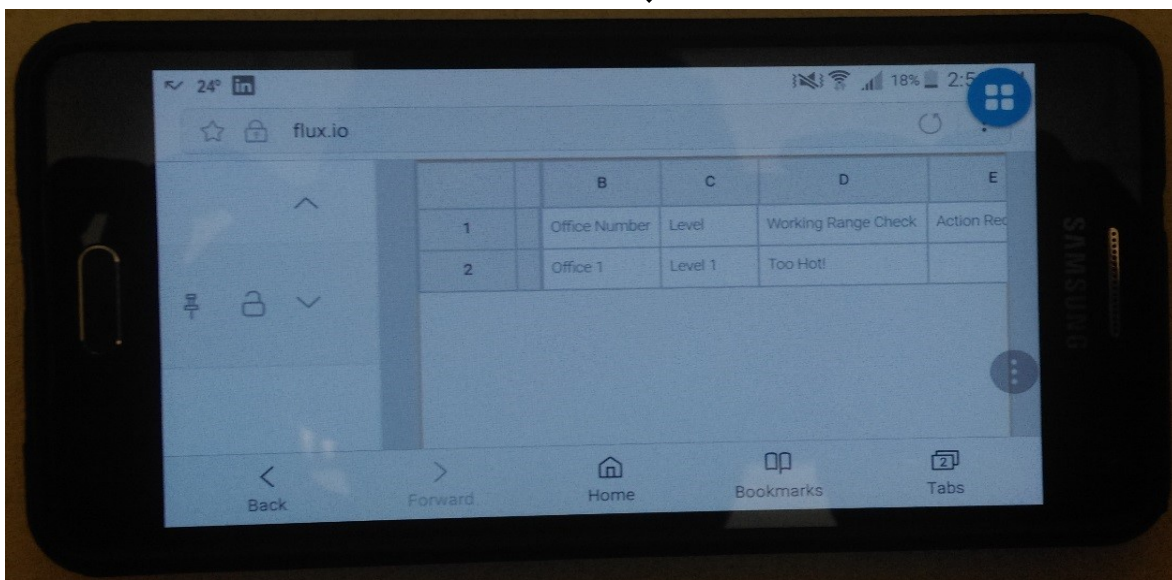
5.7. Policy implication

Policy-makers are not achieving the results expected from implementing energy-saving policies in buildings (Galvin, 2015). Currently, most Energy standards have been applied only to new buildings, and the challenge of high-energy consumption in existing buildings has not been adequately addressed. To make energy standards and policies more effective for existing buildings, one method is developing and using new and efficient technologies.

The system developed in this study can track the operation and improve the thermal performance of each room's utilities by monitoring the thermal condition in buildings, detecting any defects in HVAC systems, and avoiding energy waste.



(a) ↓



(b)

Figure 5-17: The data representation of the instrumented room in the cloud (a) with a smartphone

(b)

Residential or office buildings may have different energy policies for their rooms or offices depending on different factors such as the type and importance of rooms, the number of occupancies, etc.

Data extracted and analyzed by developed system can help managers create and even modify energy policies to control consumption and waste and maintain the thermal level in an acceptable range. The system can record the number of discomforts cases in each room and integrate it with the occupants' satisfaction level, analyzed by a daily computer-based questionnaire, to generate energy policies and alerts about the HVAC system performance or building envelop related issues leading to future savings on renovation projects.

Our system's central database can also be connected to a policy server of each department, office, or room. Such a system allows FMs to monitor any changes to their energy policies established to take timely action when the thermal condition exceeds the desirable levels.

Using information extracted from the developed system, policymakers can consider the risk of thermal discomfort on energy consumption and, consequently, on their policy outcome in the rooms with high thermal discomfort cases. Also, from the policy maker's perspective, outcomes of the developed system can indicate the need for better investigating the occupants' ventilation practices before taking any appropriate corrective action.

5.8. Discussion

Recent services such as Amazon CloudWatch and Google provide cloud services for data analytics, including platforms for data visualization. Although these kinds of services can collect data and create alarms and graphs, they are not flexible and cannot facilitate interaction between the building data model and sensor data.

This paper introduced a novel, fully automated integrated thermal comfort monitoring system, particularly for low-rise and mid-rise buildings that may not be equipped with BMS. The developed system integrated the IoT system and BIM technology to monitor the thermal comfort

level in office environments remotely in an automated manner. The system linked the virtual environment to the physical environment: IoT system was used to measure the humidity and temperature levels of the room, and the sensors data was transferred to a remote database via the internet, and BIM was used to visualize the monitored thermal comfort level of the room remotely through wireless-connected devices, as well as effective space and facility management. The temperature and humidity data collected from the case study were studied and analyzed. The values of these actual readings were compared with threshold values detected by the developed system. The system was able to detect values beyond the defined threshold values. The system could also trigger and transmit alarms to building supervisors and facility managers via their wireless devices in near real-time.

As mentioned earlier, BMS is usually used in huge buildings to manage the operation of their sustainability. BMS is not fully interactive and can only be manipulated by a trained operator (Reeser et al., 2015). In small- and medium-sized buildings where the BMS may not be used, or in buildings where the only purpose is to monitor the environmental quality factor (e.g., thermal comfort) of space not to control the electrical and mechanical components, the developed monitoring system, presented in this paper, can be an alternative one as a powerful data-driven asset management tool to provide a smart technology for energy savings and creating a healthy and productive workplace, especially in office buildings.

The data from sensors (humidity and temperature sensors) was extracted using a low-cost microcontroller and smartboard and transmitted to a SQL server in the developed system. The benefits of using the IoT system to transmit temperature and humidity data, as opposed to passing them over the wire, are increasing the flexibility and decreasing the installation complexity and cost. Using a wired monitoring system to transmit sensors data from different monitored rooms to

a central office using hundreds of meters of wire may not be feasible due to increased complexity and increased monitoring cost. A novel workflow including nine specially designed modules in the visual programming tool, Dynamo, was developed to read and sort data stored in the database, transfer them into the BIM model and update the BIM model automatically at every time interval. BIM was utilized to replace HMI in BMS, which currently uses 2D vector graphics for data visualization. The integration of BIM into thermal comfort monitoring would improve the building's maintenance plan by helping the facility managers inspect the monitored environments of the building inside the 3D model, while it is impossible to do this type of inspection within the conventional HMI interface.

Moreover, the HMI interface does not provide enough information about the building elements (e.g., wiring, ducts, pipes, envelopes, etc.), which are usually hidden. Therefore, for any reason that may cause thermal discomfort, whether HVAC failures or heat loss due to cracks in building envelopes, a rich BIM model information would help the facility managers seek a proper and fast possible solution providing an effective maintenance planning. Transferring the related information of building spaces such as the room location, the number of occupants, thermal condition, required actions, the type and location of HVAC systems, properties of building envelopes, etc., from the BIM model to the cloud would be beneficial to the facility managers to visualize the workspaces at any time in any place, observe their associated real-time environmental sensor data for timely and effective decision making without a physical inspection, and to support maintenance planning decisions, such as prioritizing maintenance works by considering different factors such as the importance of spaces and number of occupancies.

The present study attempts to fill the gaps found in the literature, as discussed in Table 5-1, such as the lack of automation (Asl, Zarrinmehr, Bergin, & Yan, 2015; Wehbe & Shahrour,

2019; Wu & Liu, 2020), lack of data retrieval system (Natephra & Motamedi, 2019), and the lack of computer implementation and validation (Del Grosso et al., 2017; Emad, Wei, & Philip, 2017; Natephra et al., 2017; Smarsly & Tauscher, 2016; Sternal & Dragos, 2016) in the thermal comfort monitoring. This study introduced a multi-functional BIM-based automated system for thermal comfort monitoring in buildings to have some of the features mentioned above (e.g., automation, data retrieval, computer implementation, etc.).

However, there are some limitations in this work, which are as follows:

1. While the present study demonstrates the feasibility of remote sensing and decision making to manage thermal comfort in buildings, the study is somewhat limited in terms of the space monitored. Further studies are required to conduct a large-scale investigation and review its integration with the facility managers and other stakeholders to test the system for its reliability, reproducibility, robustness, and ease of use.
2. The system developed here was tested with a limited number of sensors. The system can also be expanded to use different sensors for other purposes, such as indoor air quality sensors (e.g., an oxide gas sensor, a particle dust sensor, etc.) and facility management sensors (e.g., motion sensor, occupancy sensor, light sensor, etc.). The developed system should be tested further with a larger number and multiple types of sensors.

5.9. Conclusion

Monitoring of thermal comfort quality is a critical task for building supervisors and facility managers. In this paper, a developed BIM-based framework for automated monitoring of thermal comfort levels is described. Based on the study presented here, the following conclusions are made.

- BIM's ability to visualize the monitored information is expected to assist building supervisors and facility managers in locating spaces experiencing thermal comfort problems.
- The integration of BIM and IoT through a specially designed database and modules developed in a visual programming environment provides an effective visualization of office spaces associated with indoor air temperature and humidity levels.
- Storing related data in a cloud can provide concerned authorities appropriate and timely access to the thermal comfort condition data remotely through their wireless connected devices, leading to higher efficiency in monitoring building spaces.
- The system developed in this study was implemented, and its capabilities were illustrated through a case study. The system was able to detect the time and location of the office room, experiencing thermal discomfort based on targeted thresholds.
- The system could detect and record thirteen thermal discomfort cases that exceeded the thermal threshold value during the test.
- When sensor values crossed over the defined temperature level thresholds, the system highlighted the room in Red on the BIM model and generated text alarms.
- The temperature records showed that thermal discomfort mostly happened at noon in the instrumented room. It shows that the room's HVAC system did not work properly when the room was affected by the extra heat from the lower level.
- Using measurement history tables in the designed database, facility managers can retrieve and visualize the previously-stored sensor values from the central database, which can be used for future investigations, pattern analysis, and building controls optimization.

- By incorporating rooms' name into the database, in case of having HVAC problems according to the thermal condition data, facility managers can have access to relevant data, such as the amount of deviation from the thermal threshold from the database, and information like the number of occupancy, type, and location of the room to prioritize their maintenance tasks.
- The system can detect sensors' malfunction by sorting data based on each temperature and humidity sensors if more than one sensor of each type is installed in a room.
- The system presented in this study can motivate building owners to use it in low-rise and mid-rise buildings where BMS is not usually used.
- Although installing sensors on HVAC systems can monitor real-time temperature changes, the developed system can be used to make HVAC systems intelligent and manage them.
- The developed system can be used to detect defects in HVAC systems that avoid the high costs of the system's failure.
- The use of the developed system can help facility managers take timely actions related to occupants' thermal comfort and avoid property damage and hazardous situations.
- Such an approach (by taking real-time and accurate thermal data) can lead to better policymaking, which may help decision-makers or urban planners revise the existing guidelines, protocols, or building regulations.

References

- Adekunle, T. O., and Nikolopoulou, M, (2016). “Thermal comfort, summertime temperatures and overheating in prefabricated timber housing.” *Building and Environment* 103 (2016) 21-35.
- Arslan, M., Riaz, Z., Kiani, A. K., and Azhar. S. (2014). “Real-time environmental monitoring, visualization and notification system for construction H&S management.” *Journal of Information Technology in Construction*, 19: 72-91.
- ASHRAE. ANSI/ASHRAE Standard-55-2017. (2017). “Thermal environmental conditions for human occupancy.” American Society of Heating, Refrigerating and Air-Conditioning Engineers, Atlanta.
- Asl, M. R., Zarrinmehr, S., Bergin, M., Yan, W. (2015). “A framework for BIM-based performance optimization.” *Energy Build*, 108: 401–412.
- Australian Construction Industry Forum (ACIF). (2014). “A Framework for the Adoption of Project Team Integration and Building Information Modelling.” Retrieved from <http://www.acif.com.au/resources/strategic-forum-for-building-and-construction/a-framework-for-the-adoption-of-project-team-integration-and-building-information-modelling>.
- Azhar, S., Nadeem, A., Mok, A. Y. N., and Leung, B. H. Y. (2008). “Building Information Modeling (BIM): A New Paradigm for Visual Interactive Modeling and Simulation for Construction Projects.” First International Conference on Construction in Developing Countries (ICCIDC–I. Advancing and Integrating Construction Education, Research & Practice, Karachi, Pakistan.

BIM Task Group. (2011), “BIM: Management for value, cost and carbon improvement Strategy.) Paper for the government Construction Client Group from the BIM Industry Working Group _ March 2011, Retrieved from <http://www.bimtaskgroup.org>.

Cahill, B., Menzel, K., and Flynn, D. (2012). “BIM as a center piece for optimized building operation.” Taylor & Francis Group, London.

Canadian Centre for Occupational Health and Safety (CCOHS). (2018). Retrieved from http://www.ccohs.ca/oshanswers/phys_agents/thermal_comfort.html, (Document last updated on February 5, 2018), last accessed August 20, 2019.

Charles, R., Reardon, J. T., and Magee, R. J. (2005). “Indoor air quality and thermal comfort in open-Plan offices, Construction technology updates.” Institute for Research in Construction (IRC): National Research Council of Canada, 64: 1206–1220.

Chauhdary, S. H., Hassan, A., Alqarni, M. A., Alamri, A., and Bashir, A. K. (2019). “A twofold sink-based data collection in wireless sensor network for sustainable cities.”, *Sustainable cities and society*, 45:1-7

Chen, J., Bulbul, T., Taylor, J. E., and Olgun, G. (2014). “A Case Study of Embedding Real-time Infrastructure Sensor Data to BIM.” Construction Research Congress, ASCE, 296-278.

Cho, C. Y., Kwon, S., Shin, T.-H., Chin, S., and Kim, Y. S. (2011). “A development of next generation intelligent construction lift car toolkit for vertical material movement management.” *Automation in Construction*, 20(1), 14–27 Retrieved from <http://doi.org/http://dx.doi.org/10.1016/j.autcon.2010.07.008>.

Cooking Hacks. (2017). Retrieved from <https://www.cooking-hacks.com/shop/waspmote>.

- Davila Delgado, J. M., Butler, L. J., Brilakis, I., Elshafie, M. Z. E. B., and Middleton, C. R. (2018). "Structural Performance Monitoring Using a Dynamic Data-Driven BIM Environment." *J. Computing, Civ. Eng.* 32(3), 1-16.
- De Dear, J. R., and Brager, G. (1998). "Developing an Adaptive Model of Thermal Comfort and Preference." *ASHRAE Transactions*, 104 (1a), 145–167.
- Del Grosso, A. E., Basso, P., Ruffini, L., Fagini, F., and Cademartori, M. (2017). "Infrastructure management integrating SHM and BIM procedures." SMAR 2017 Fourth Conference on Smart Monitoring, Assessment and Rehabilitation of Civil Structures at: ETH Zurich 13-15 September 2017.
- Dynamo BIM. (2017). "Dynamo BIM – Community-driven Open Source Graphical Programming for Design." Retrieved from <http://dynamobim.org> (last accessed, Feb 10, 2017).
- Emad, A.-Q., Wei, Y., Philip, G. (2017). "Establishing parametric relationships for design objects through tangible interaction." In Proceedings of the 22nd International Conference of the Association for Computer-Aided Architectural Design Research in Asia (CAADRIA), Protocols, Flows and Glitches, Suzhou, China, 5–8 April 2017:147–157.
- European Commission, Energy Efficiency Directive. (2014). Retrieved from http://ec.europa.eu/energy/efficiency/eed/eed_en.htm (accessed 01.10.15).
- Gerrish, T., Ruikar, K., Cook, M. J., Johnson, M., and Phillip, M. (2015). "Attributing in-use building performance data to an as-built building information model for lifecycle building performance management." Proc., 32nd CIB W78 Conf., J. Beets, ed., International Council for Building Research Studies and Documentation: Information Technology for Construction, Rotterdam, Netherlands, 1-11.

- Grzybek, H. (2010). "Inclusion of Temporal Databases with Industry Foundation Classes-basis for adaptable intelligent buildings." ICISO 2010 Proceedings of the Twelfth International Conference on Informatics and Semiotics in Organizations, Reading, U. K. 24-31.
- Gupta, A. K. (2006). "Industrial and Safety Environment." Laxmi Publications (P) LTD.
- Goodhew, S. (2016). "Sustainable construction processes: A resource text." West Sussex: Wiley.
- Health, Wellbeing and Productivity in Offices. (2014). "World Green Building Council." Retrieved from www.worldgbc.org.
- Internal Code Council, International Energy Conservation Code. (2018). Google Scholar.
- IOT@INTEL. (2016). "Costs, Savings, and ROI for Smart Building Implementation." Retrieved from <https://blogs.intel.com>.
- Kalz, D., and Pfafferott, J. (2014). "Thermal Comfort and Energy-Efficient Cooling of Nonresidential Buildings." Cham, Heidelberg, New York, et. al.: Springer.
- Kantor, N., and Unger, J. (2011). "The most problematic variable in the course of human-biometeorological comfort assessment – the mean radiant temperature." Central European Journal of Geosciences, 3(1), 90-100.
- Katranuschkov, P., Weise, M., Windisch, R., Fuchs, S., Scherer, R. J. (2010). "BIM-based generation of multi-model views." Proceedings of the CIB W78, Cairo, Egypt, pp. 429–436.
- Keller, M., O'Donnell, J., Manzel, K., Keane, M., Gokce, U. (2008). "Integrating the Specification, Acquisition and Processing of Building Performance Information." Tsinghua Science and Technology, 13 (1): 1-6.

- Kensek, K. M. (2014). "Integration of Environmental Sensors with BIM: Case studies using Arduino, Dynamo, and the Revit API." *Informes Constr*, 66, 536.
- Kim, M., Cheng, J. C. P., Sohn, H., and Chang, C. C. (2014). "A framework for dimensional and surface quality assessment of precast concrete elements using BIM and 3D laser scanning." *Automation in Construction*, 49: 225-238.
- Langner, M., Scherber, K., and Endlicher, W. (2013). "Indoor heat stress: An assessment of human bioclimate using the UTCI in different buildings in Berlin." *Die Erde*, 144: 260-273.
- Lee, G., Cho, J., Ham, S., Lee, T., Lee, G., Yun, S. H., and Yang, H. J. (2012). "A BIM-and sensor-based tower crane navigation system for blind lifts." *Automation in construction*, 26, 1-1
- Leo Samuel, D. G., Dharmasastha, K., Shiva Nagendra, S. M., Prakash, M. M. (2017). "Thermal Comfort in Traditional Buildings Composed of Local and Modern Construction Materials." *International Journal of Sustainable Built Environment*, 6 (2): 463-475.
- Matzarakis, A., and Amelung, B. (2008). "Physiological Equivalent Temperature as Indicator for Impacts of Climate Change on Thermal Comfort of Humans." *Seasonal Forecasts, Climate Change and Human Health*, © Springer Science + Business Media: 161-172.
- Nassar, K. (2010). "The Effect of Building Information Modeling on the Accuracy of Estimates." *Proceedings of the 46th Annual Conference, Wentworth Institute of Technology - Boston, Massachusetts*.
- Natephra, W., Motamedi, A. (2019). "BIM-Based Live Sensor Data Visualization Using Virtual Reality for Monitoring Indoor Conditions." *Intelligent & Informed, Proceedings of the 24th International Conference of the Association for Computer-Aided Architectural Design Research in Asia (CAADRIA) 2019*, 2: 191-200.

- Natephra, W., Motamedi, A., Yabuki, N., and Fukuda, T. (2017). "Integrating 4D thermal information with BIM for building envelope thermal performance analysis and thermal comfort evaluation in naturally ventilated environments." *Building and Environment* 124: 194-208.
- Northeast Document Conservation Center. (2012). "Monitoring Temperature and Relative Humidity." Retrieved from <https://www.nedcc.org>.
- O'Flynn, B., Jafer, E., Spinar, R., Keane, M., Costa, A., Pesch, D., O'Mathuna, C. (2010). "Development of miniaturized Wireless Sensor Nodes suitable for building energy management and modelling." 8th European Conference on Product & Process Modelling. 14-16 Sep 2010, Cork, Ireland.
- Park, S., Kim, T. H., Chin, S., and Yun, H. S. (2011). "Smart space with a built-in ubiquitous sensor network (USN)-based online monitoring system at Sungkyunkwan University in Korea." *Proceedings of the CIB W78-W102: International Conference- Sophia Antipolis, France*.
- Quigley, E. S. (2016). "The energy and thermal performance of UK modular residential buildings." Loughborough University Institutional Repository, Doctoral Thesis.
- Rawal, G. (2016). "Costs, Savings, and ROI for Smart Building Implementation." *IOT@INTEL*, <http://blogs.intel.com/iot/2016/06/20/costs-savings-roi-smart-building-implementation/> (Accessed on 20 Jun 2016).
- Reeser, J., Jankowski, T., & Kemper, G. M. (2015). "Maintaining HMI and SCADA systems through computer virtualization." *IEEE Transactions on Industry Applications*, 51(3): 2558–2564.
- Rio, J., Ferreira, B., Pocas-Martins, J. (2012). "Expansion of IFC model with structural sensors." *Informes de la Construcción*, ISSN: 0020-0883, 65 (530): 219-228.

- Ryoo, B. Y., Park, H. K. (2011). "Enhanced platform for BIM to improve reality." Proceedings of the 28th ISARC, Seoul, Korea: 136–137.
- Sakellaris, A., Saraga, D. E., Mandin, C., Roda, C., Fossati, S., Kluizennar, Y. D., Carrer, P., Dimitroulopoulou, S., Mihucz, V. G., Szigeti, T., Hanninen, O., Fernandes, E. D. O., Bartzis, J. G., and Bluysen, P. M. (2016). "Perceived Indoor Environment and Occupants' Comfort in European "Modern" Office Buildings: The OFFICAIR Study." *Int J Environ Res Public Health*, 13(5).
- Sakka, A., Wagner, A., and Santamouris, M. (2010). "Thermal comfort and occupant satisfaction in residential buildings – Results of field study in residential buildings in Athens during the summer period." Proceedings of Conference: Adapting to Change: New Thinking on Comfort Cumberland Lodge, Windsor, UK. London: Network for Comfort and Energy Use in Buildings, Retrieved from <http://nceub.org.uk>.
- Seon, H. J., Jeong, T. K., and Yun, G. Y. (2013). "A Field Survey of Thermal Comfort in Office Building with a Unitary Heat-Pump and Energy Recovery Ventilator, Sustainability in Energy and Buildings." *SIST 22*, Springer-Verlag Berlin Heidelberg, DOI: 10.1007/978-3-642-36645-1_89: 1003–1010.
- Seppänen, O., and Fish, W. J. (2006). "Some Quantitative Relations between Indoor Environmental Quality and Work Performance or Health." *HVAC and Research*, 12(4): 957–973.
- Shin, S. Y., Park, H. S., & Kwon, W. H. (2007). "Mutual interference analysis of IEEE 802.15.4 and IEEE 802.11b. *Computer Networks.*", 51(12): 3338–3353. Retrieved from <http://doi.org/10.1016/j.comnet.2007.01.034>.

- Silva, N. B., Khan, M., Han, K. (2018). "Towards sustainable smart cities: A review of trends, architectures, components, and open challenges in smart cities.", *Sustainable Cities and Society*, 38: 797-713.
- Singh, M. K., Mahapatra, S., and Teller, J. (2013). "Study on Indoor Thermal Comfort in the Residential Buildings of Liege." Belgium, CISBAT 2013 – (September 4-6, 2013) - Lausanne, Switzerland: 481-486.
- Smarsly, K., and Tauscher, E. (2016). "Monitoring information modeling for semantic mapping of structural health monitoring systems." *The 16th International Conference on Computing in Civil and Building Engineering*, July 2016, At: Osaka, Japan.
- Sternal, M., and Dragos, K. (2016). "Bim-Based Modeling of Structural Health Monitoring Systems Using the Ifc Standard." 28. *Forum Bauinformatik 2016* 19.–21. September 2016, Leibniz Universität Hannover.
- Thermal Comfort in the workplace. (2017). "Health and Safety Executive (HSE)", Retrieved from http://www.lboro.ac.uk/media/wwwlboroacuk/content/healthandsafety/occupationalhealth/HS_G194_-_Thermal_Comfort.pdf (Accessed 22.08.2017).
- Valinejadshoubi, M., Bagchi, A., and Shakibabarough, A. (2015). "The Ability to Reduce the Operational Energy Consumption of the Building by Proper Use of Building Information Modeling Tools and Sustainability Approach." *Ain Shams Engineering Journal*, 6(1): 41-55.
- Valinejadshoubi, M., Bagchi, A., and Moselhi, O. (2017). "Managing Structural Health Monitoring Data Using Building Information Modelling." *SMAR 2017, the fourth International Conference on Smart Monitoring, Assessment and Rehabilitation of Civil Structures*, (September 13-15, 2017) - Zurich, Switzerland.

- Valinejadshoubi, M., Bagchi, A., Moselhi, O. and Shakibaborough, A. (2018a). "Investigation on the Potential of Building Information Modeling in Structural Health Monitoring of Buildings." CSCE Annual Conference, June, Fredericton, NB (GC-136).
- Valinejadshoubi, M., Bagchi, A., and Moselhi, O. (2018b). "Development of a BIM-Based Data Management System for Structural Health Monitoring with Application to Modular Buildings: A Case Study." *Journal of Computing in Civil Engineering*, 33 (3).
- Wang, J., Fu, Y., and Yang, X. (2017). "An integrated system for building structural health monitoring and early warning based on an Internet of things approach." *International Journal of Distributed Sensor Networks*, 13(1).
- Waspnote datasheets. v2.3 - 11/2012, Retrieved from <http://www.libelium.com/waspnote>.
- Woo, J. H., Diggelman, C., and Abushakra, B. (2011). "BIM-based energy monitoring with XML parsing engine." *Proceedings of the 28th ISARC, Seoul Korea*: 544-545.
- Wehbe, R., and Shahrour, I. (2019). "Use of BIM and Smart Monitoring for buildings' Indoor Comfort Control." *MATEC Web of Conferences* 295, 02010.
- Wu, I.C., Liu, C. C. (2020). "A Visual and Persuasive Energy Conservation System Based on BIM and IoT Technology." *Sensors (Basel)*, 20 (1): 139
- Yin, H. (2010). "Building Management System to support building renovation.", *The Boolean*: 172-177.
- Yu, W., Li, B., Yao, R., Wang, D., and Li, K. (2017). "A study of thermal comfort in residential buildings on the Tibetan Plateau, China." *Building and Environment*, 119: 71-86.
- Zinzi, M., and Carnielo, E. (2017). "Impact of urban temperatures on energy performance and thermal comfort in residential buildings." *The case of Rome, Italy, Energy and Buildings*, 157: 20-29.

Updated Literature Review and Related Materials

This section focuses primarily on recent publications and related works not cited in the published paper above.

Building Management System (BMS) usually monitors the thermal condition of building spaces, utilizing sensor-captured temperature and humidity data. However, due to the high cost of BMS deployment it is usually applied to large or groups of buildings which make up only 10 percent of commercial real estate stock in the US (Rawal, 2016). Moreover, while existing BMS systems provide some access to sensor information, the way such information is presented often lacks the context of 3D building information.

Desogus et al. (2021) developed a workflow to obtain a dynamic and automated data exchange between the environmental sensors and the BIM model using the Dynamo visual programming platform and Application Programming Interface (API). However, their study does not include the capability to rapidly identify problematic areas in built facilities. The developed tool presented in this chapter utilizes a color scheme to highlight building areas where comfort conditions are not met.

Recently, Autodesk has been working on developing a tool called Autodesk Project Dasher to increase building performance. Project Dasher (2021) is an ongoing Autodesk research project that uses a BIM-based platform as a visual analytics tool to help improve the performance monitoring of buildings. In that project a BIM model is combined with sensors from a BMS to give rich, in-context visualization of building operations.

The main differences between Project Dasher and the developed tool in this paper are:

- Autodesk Project Dasher is still in development state and is not commercial software yet. But the development process of the tool, presented in this chapter, has been finalized, and its validation effort has been completed.
- The primary capability of the Autodesk Project Dasher tool is visualizing the thermal range of building spaces using temperature values, while the tool developed in this study has been established based on the combination of different temperature and relative humidity ranges for different thermal comfort conditions according to relevant standards such as ASHRAE standard which is widely used in North America.
- The thermal comfort ranges might need to be modified based on different weather conditions and seasons. The developed tool in this study is flexible to be used in different seasons and weather conditions in which the thermal comfort ranges can be adjustable. But Autodesk Project Dasher is in a black box format, where users cannot modify it and extend to address related applications. The developed tool can work as an alert system by sending real-time notifications to facility managers and their staff through their wireless connected devices to take necessary actions if required. At the same time, Autodesk Project Dasher does not have that capability.
- The developed tool integrates with an external database to record and store all daily thermal discomfort cases of building spaces in a specific entity which allows facility managers to track any changes to the established building or department energy policies, while Autodesk Project Dasher does not have this capability.

Chapter 6: Integrating BIM into Sensor-based Facilities Management Operations

General

This paper was published in the Journal of Facilities Management in 2021*. The main objective of this paper is to develop an automated workflow to generate alerts in the events of malfunctioning sensors used in Facility Management (FM).

Abstract

Purpose – To mitigate the problems in sensor-based facility management (FM) such as lack of detailed visual information about a built facility and the maintenance of large-scale sensor deployments, an integrated data source for the facility's life cycle should be used. Building information modeling (BIM) provides a useful visual model and database that can be used as a repository for all data captured or made during the facility's life cycle. It can be used for modeling the sensing-based system for data collection, serving as a source of all information for smart objects such as the sensors used for that purpose. Although few studies have been conducted in integrating BIM with sensor-based monitoring system, providing an integrated platform using BIM for improving the communication between FMs and Internet of Things (IoT) companies in cases encountered failed sensors has received the least attention in the technical literature. Therefore, the purpose of this paper is to conceptualize and develop a BIM-based system architecture for fault detection and alert generation for malfunctioning FM sensors in smart IoT environments during the operational phase of a building to ensure minimal disruption to monitoring services.

*Valinejadshoubi, M., Moselhi, O. and Bagchi, A. (2021), "Integrating BIM into sensor-based facilities management operations", Journal of Facilities Management, ISSN: 1472-5967.

Keywords: Building information modeling, Operational phase, Sensor-based facility management, Fault detection, Smart IoT environments, Sensor management

Design/methodology/approach – This paper describes an attempt to examine the applicability of BIM for an efficient sensor failure management system in smart IoT environments during the operational phase of a building. For this purpose, a seven-story office building with four typical types of FM-related sensors with all associated parameters was modeled in a commercial BIM platform. An integrated workflow was developed in Dynamo, a visual programming tool, to integrate the associated sensors maintenance-related information to a cloud-based tool to provide a fast and efficient communication platform between the building facility manager and IoT companies for intelligent sensor management.

Findings – The information within BIM allows better and more effective decision-making for building facility managers. Integrating building and sensors information within BIM to a cloud-based system can facilitate better communication between the building facility manager and IoT company for an effective IoT system maintenance. Using a developed integrated workflow (including three specifically designed modules) in Dynamo, a visual programming tool, the system was able to automatically extract and send all essential information such as the type of failed sensors as well as their model and location to IoT companies in the event of sensor failure using a cloud database that is effective for the timely maintenance and replacement of sensors. The system developed in this study was implemented, and its capabilities were illustrated through a case study. The use of the developed system can help facility managers in taking timely actions in the event of any sensor failure and/or malfunction to ensure minimal disruption to monitoring services.

Research limitations/implications – However, there are some limitations in this work which are as follows: while the present study demonstrates the feasibility of using BIM in the maintenance

planning of monitoring systems in the building, the developed workflow can be expanded by integrating some type of sensors like an occupancy sensor to the developed workflow to automatically record and identify the number of occupants (visitors) to prioritize the maintenance work; and the developed workflow can be integrated with the sensors' data and some machine learning techniques to automatically identify the sensors' malfunction and update the BIM model accordingly.

Practical implications – Transferring the related information such as the room location, occupancy status, number of occupants, type and model of the sensor, sensor ID and required action from the BIM model to the cloud would be extremely helpful to the IoT companies to actually visualize workspaces in advance, and to plan for timely and effective decision-making without any physical inspection, and to support maintenance planning decisions, such as prioritizing maintenance works by considering different factors such as the importance of spaces and number of occupancies. The developed framework is also beneficial for preventive maintenance works. The system can be set up according to the maintenance and time-based expiration schedules, automatically sharing alerts with FMs and IoT maintenance contractors in advance about the IoT parts replacement. For effective predictive maintenance planning, machine learning techniques can be integrated into the developed workflow to efficiently predict the future condition of individual IoT components such as data loggers and sensors, etc. as well as MEP components.

Originality/value – Lack of detailed visual information about a built facility can be a reason behind the inefficient management of a facility. Detecting and repairing failed sensors at the earliest possible time is critical to ensure the functional continuity of the monitoring systems. On the other hand, the maintenance of large-scale sensor deployments becomes a significant challenge. Despite its importance, few studies have been conducted in integrating BIM with a sensor-based monitoring

system, providing an integrated platform using BIM for improving the communication between facility managers and IoT companies in cases encountered failed sensors. In this paper, a cloud-based BIM platform was developed for the maintenance and timely replacement of sensors which are critical to ensure minimal disruption to monitoring services in sensor-based FM.

6.1. Introduction

Facility management (FM) is focused on the efficient operation and maintenance of commercial and industrial properties. According to the International Facilities Management Association (IFMA, 2009), FM is defined as a multidisciplinary task to provide a satisfactory built environment by coordinating people, places, processes, technology and the environment.

The use of different types of intelligent technologies in the workplace necessitates the connectivity of these technologies through enabling digital platforms. The Internet of Things (IoT) is an enabler of such connectivity that facilitates efficient maintenance decisions. The data collected by the IoT allow FM teams to be more effective in preventing maintenance issues and reducing the time spent on repairs and regular maintenance tasks. Sensors play a significant role in data collection on an IoT platform.

A study from The National Institute of Standards and Technology's (NIST), (2020) showed that most efficiency-related losses in US capital facilities come from insufficient interoperability among the software systems of computer-aided design, engineering and FM communication, while interoperability issues and a lack of well-integrated information management systems and documentation techniques can make FM an expensive task. The most significant FM cost portion is allocated to data verification and validation, data transfer, interoperability and information delays

(Gallaher et al., 2004). One of the main challenges in sensor-based FM is in the data visualization stage in which 2D vector graphics are used because these are not sufficiently interactive and can only be manipulated by a trained operator (Reeser et al., 2015). Lack of detailed visual information about a built facility can be a reason for that facility's inefficient management. Given the importance of health monitoring applications, it is critical to monitor and maintain the functionality of the IoT deployment continuously. Hence, detecting and repairing failed sensors simultaneously is critical to ensure the monitoring systems' functional continuity. On the other hand, the maintenance of large-scale sensor deployments has become a significant challenge.

To mitigate these problems, an integrated data source for the facility's life cycle should be used. Building information modeling (BIM) provides a useful visual model and database used as a repository for all data captured or created during the facility's life cycle. Currently, BIM is increasingly applied to FM in the operations and maintenance stage. Simultaneously, IoT technology can be used to acquire operational data on building facilities to support FM. BIM can be used for modeling the sensor-based system for data collection, serving as a source of all information for smart objects such as the sensors used for that purpose. Although few researchers have investigated the integration of BIM with sensor-based monitoring systems (Suprabhas, 2016; Kazado et al., 2019; Chang et al., 2018; Kensek, 2020), most of them have focused exclusively on the automatic transmission of sensor information to BIM models. Providing an integrated platform using BIM to improve communication between FM and IoT companies in the event of sensor failure has received the least attention in the technical literature. The main objective of this paper is to conceptualize and develop a BIM-based system architecture for fault detection and alert generation for malfunctioning FM sensors in smart IoT environments during the operational phase of a building for the maintenance and timely replacement of sensors.

6.2. Building Information Modeling

The architecture, engineering and construction (AEC) industry has been seeking a useful tool for reducing projects' cost and time to completion and for increasing productivity and quality (Azhar et al., 2008). Typically, there are hundreds to thousands of documents for each project, and human interpretations are required to tie them together. Effective coordination between design disciplines and the communication of design information to the field is a constant challenge. BIM has significantly altered the way building information is managed by the AEC industry. It incorporates digital modeling software to design and manage a project more efficiently (Nassar, 2010). BIM breaks down the barriers between disciplines by encouraging knowledge sharing throughout the project's life cycle. BIM improves constructability and can shorten the project's completion time. In a BIM project, multiple documents are not used in traditional ways (Australian Construction Industry Forum [ACIF], 2014); instead, they are digitized and added to a BIM software database. All information is built into an intelligent BIM model so that users need not look at separate drawings, schedules and specifications for the information on a particular element or a component in the project.

BIM is an organized collection of building data in a 3D building model (Graphisoft, a Nemwtschek Company, 2015). The model is a virtual equivalent of the actual building and its elements (Graphisoft, a Nemwtschek Company, 2015). These intelligent elements are the digital prototype of the physical elements, including walls, columns, windows, doors and stairs. The model allows us to simulate the building and understand its behavior before the commencement of construction. The building-related data can be easily archived in the BIM model for future use, analysis, retrieval and maintenance.

6.3. Utilizing Building Information Modeling in Sensor-Based Facilities Management

BIM models can be valuable tools in FM because they are essentially 3D model interfaces with links to information on the building components and the equipment that needs to be maintained. For instance, information about installation, operation and maintenance manuals; spare part lists; and construction materials can be stored in a BIM model. The applications of BIM for operation and FM can include record modeling, preventive maintenance scheduling, building system analysis, asset management, space management, tracking and disaster planning.

For managing older buildings, BIM integrated within the clouds generated by a 3D scanning of the building can be used to overcome the absence of data. This process can serve several purposes, including spatial analysis, renovation and retrofitting. Using Web services and cloud-based hosting, the project's participants (e.g., owners, facility managers, engineers and contractors) can secure access to the shared data. FM companies have recently added value and have increased profit margins by using IoT solutions to reduce costs and increase value to end users.

A significant number of studies have been conducted to integrate BIM into the monitoring system, but it remains challenging. Wang et al. (2013) found that applying BIM in monitoring systems can improve the effectiveness of monitoring processes. Valinejadshoubi et al. (2017, 2018a) investigated the feasibility of using BIM in the structural health-monitoring process. They demonstrated the feasibility of creating, visualizing and managing sensor data and information in a BIM model for structural health monitoring. Valinejadshoubi et al. (2018b) developed a BIM-based integrated model to rapidly detect structural damage using strain values. Suprabhas and Nicholas Dib (2017) developed an application that integrates sensor data collected using a wireless sensor network; the application reports the data via a virtual model of the building to aid FM personnel in the early detection of defects. Cahill et al. (2012) examined the implementations of

BIM to potentially support a static data value from a sensor data source to assist stakeholders in making appropriate decisions regarding a building's life cycle. Zhang et al. (2015) developed an FM tool to support energy management in buildings.

The benefits to the FM discipline of using sensors are numerous, and the failure of these sensors can increase operational costs and lead to undesirable consequences. A sensor takes measurements at regular intervals and helps facility managers make decisions based on a combination of captured sensor data. If a sensor suddenly fails or malfunctions, the building facility manager should inform the IoT companies at the earliest possible juncture to fix the problem because such a failure can negatively affect or even interrupt the monitoring system, and accordingly, any decision based on the data. Therefore, timely maintenance of failed sensors is critical in such deployments to ensure minimal monitoring service disruption. Despite the importance of timely detection of a failed sensor in IoT monitoring, it has received the least attention in the literature. To mitigate this issue, an integrated BIM-based workflow was developed to integrate the associated sensor maintenance-related information to a cloud-based tool to provide a fast and efficient communication platform between the building facility manager and IoT companies for intelligent sensor management.

6.4. Research Methodology

In this case-based research study, the authors developed a sensor-based FM integrated with a cloud-based service tool, which can be used for real-time communication between different disciplines. A seven-story office building, shown in Figure 6-1, was simulated in Autodesk Revit software. Sensors typically used in FM, such as *occupancy detection sensors*, *temperature sensors*,

humidity sensors, and *CO2 sensors*, were modeled and placed in their designated locations in the building's BIM model. Parameters such as *Sensor Name*, *Model*, *Mark*, *Website* and *Comment* were used for the sensors' identification, and parameters such as *Level* and *Station* were used to identify the sensors' location. Rooms were assigned to each specified space on all floors to work as the sensors' stations (locations) in the BIM model. Information such as sensors' models and sensors' marks (physical IDs) were given to the building facility manager by the IoT company to accommodate them into their central BIM model upon installing the sensory system in the building.

For effective and fast communication between the facility manager and IoT company in case of a sensor failure, a real-time BIM-based communication platform was developed in this study. To create this platform, a workflow was designed in Dynamo to automatically extract and send all information such as the sensor's type, model and exact location from the detailed BIM model to the IoT company whenever a sensor failure was reported to the facility manager. In case of a diagnosis of multiple sensor failures, sensor replacement can be prioritized by considering the average number of daily occupants in each room based on the occupancy sensor data.

Cloud-based collaboration and data exchange service applications such as Flux, Konstru or Speckle can be used to send notifications to the IoT company through their wireless devices, such as personal smartphones and to receive sensor failure notifications and all essential information from the BIM model. Figure 6-2 illustrates the dataflow schema used in this study.

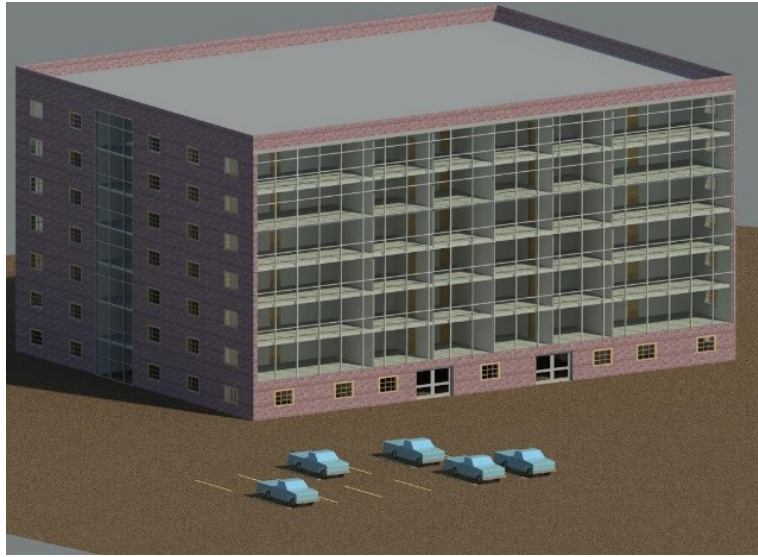


Figure 6-1: 3D view of the case-study building

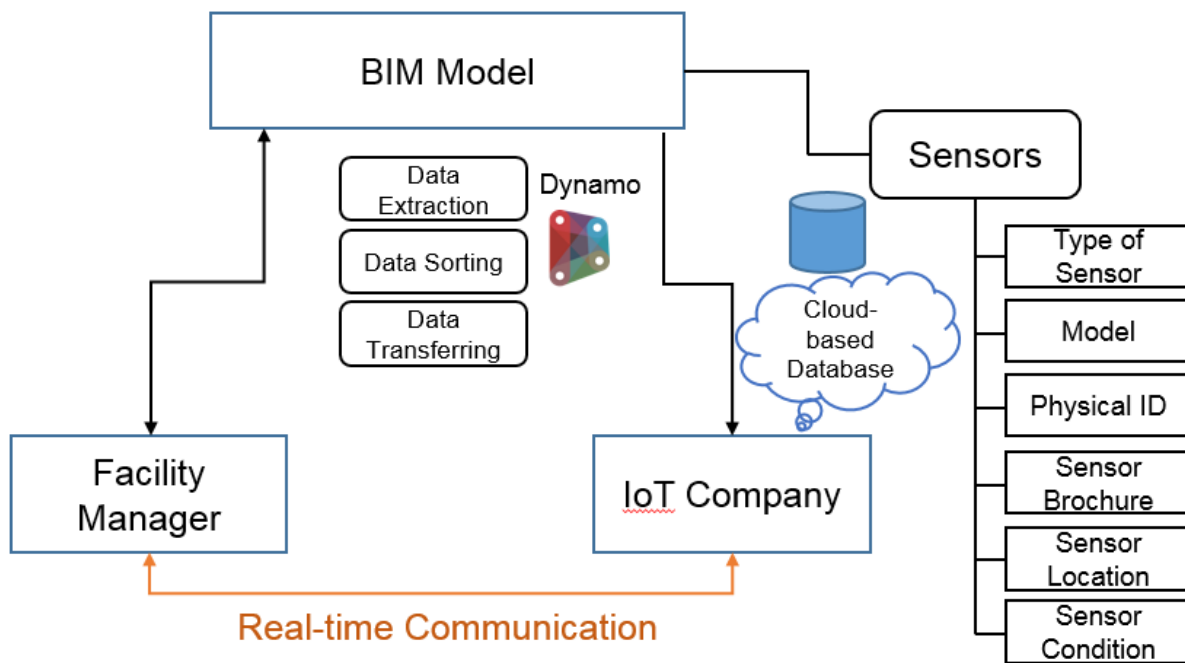


Figure 6-2: Developed dataflow schema

6.5. Integrating Sensor-Based Facilities Management with Building Information Modeling

6.5.1. Placing sensors in the Building Information Modeling model

Categories in Revit include column, beam, floor, roof, door, and window. There is also a category pertinent to specialty equipment, enabling the inclusion of sensor classes such as *IfcSensor* and *IfcSensorType*. In Revit, each category has its own industry foundation class (IFC) name; for example, a column is *IfcColumn*, and a roof is *IfcRoof*.

Four sensors – occupancy, temperature, humidity and CO₂ – are used in this study. These are shown in Table 6-1 along with their respective purposes. Each sensor was modeled and placed in its appropriate location in the building's BIM model. Two sets of parameters were defined for each sensor. The first includes *IfcExportType* and *IfcExportAs*, and the second includes Name, Station, Level, Model, Mark and Sensed Data. The Station parameter was defined to show where sensors were installed. The Mark parameter was determined to map virtual sensors in the BIM model onto their real-world sensors. This was designed to link the collected data from each physical sensor stored in the data acquisition system with virtual sensors in the BIM model through Web-based methods such as the internet protocol address and programming methods such as the application programming interface. After defining the four aforementioned sensors, these sensors were placed in their locations in the BIM model.

Figure 6-3 shows the location of sensors in each room of Level 1 in 2D and 3D views. As shown in Figure 6-3, the temperature sensor, CO₂ sensor, humidity sensor, and occupancy sensor are displayed by the colors red, violet, blue, and green, respectively.

Table 6-1: Types of sensors used in this study

Type	Location	Application	Benefits
Occupancy sensor	On the wall/ceiling	To detect the presence or absence of people in a space to activate and deactivate the lights	Lighting energy savings Increased comfort level
Temperature sensor	On the wall (should not be near outside doors/windows)	HVAC environmental control	Heating energy savings Increased comfort level
Humidity sensor	On the ground/wall	Monitoring the humidity levels in any room of a building	Preventing unsafe or undesirable moisture levels in the room
CO ₂ sensor	On the same wall as the temperature sensor (48 in, or 122 cm, is standard)	Monitoring the room's CO ₂ level	Increased indoor air quality

6.5.2. Creating a schedule of sensors used in the BIM model

After placing all sensors in their locations, their information can be sorted and managed. The BIM software can provide the schedule table for each type of 3D element. As many parameters as are needed can be considered in the table. As illustrated in Figure 6-4, parameters such as Name, Station, Level, Model, Mark and Sensed Data were considered in the sensor schedule table. As mentioned earlier, the physical sensors' specific IDs must be provided and assigned manually to each sensor in the model using the Mark parameter. The ID numbers shown in the Mark column in the schedule table were hypothetical in this study. The Station parameter was used to indicate the location of each sensor in the model. In the BIM model, each element had a specific ID. By using the elements' ID, the exact position of each sensor was marked in the model. In the Station column, sensors' locations were identified by the room ID where they were installed. Figure 6-4

shows the sensors' schedule table in the BIM model for offices 1 to 5 and the sensors' locations in each office.

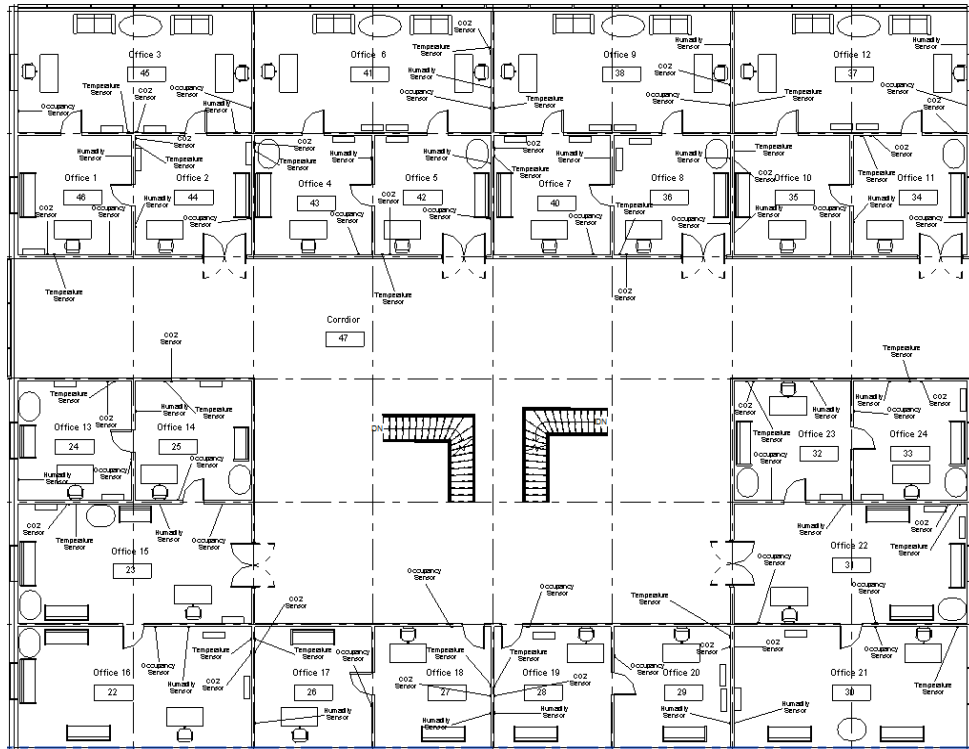


Figure 6-3: Visualization of sensors in 2D and 3D views in the BIM model

<Sensor Schedule (Level 1)>					
A	B	C	D	E	F
Name	Station	Level	Model	Mark	Sensed Data
Office 5 (Room ID: 394483)					
Occupancy Sensor	Office 5 (Room ID: 394483)	Level 1	Peco S200	ID no: 31256	
Temperature Sensor	Office 5 (Room ID: 394483)	Level 1	TS33C-M with LCD	ID no: 45268	
CO2 Sensor	Office 5 (Room ID: 394483)	Level 1	AZ-0004	ID no: 75557	
Humidity Sensor	Office 5 (Room ID: 394483)	Level 1	AcuRite 00613A1	ID no: 80256	
Office 4 (Room ID: 394486)					
Occupancy Sensor	Office 4 (Room ID: 394486)	Level 1	Peco S200	ID no: 31255	
Temperature Sensor	Office 4 (Room ID: 394486)	Level 1	TS33C-M with LCD	ID no: 45267	
CO2 Sensor	Office 4 (Room ID: 394486)	Level 1	AZ-0004	D no: 75556	
Humidity Sensor	Office 4 (Room ID: 394486)	Level 1	AcuRite 00613A1	ID no: 80255	
Office 3 (Room ID: 394492)					
Occupancy Sensor	Office 3 (Room ID: 394492)	Level 1	Peco S200	ID no: 31254	
Occupancy Sensor	Office 3 (Room ID: 394492)	Level 1	Peco S200	ID no: 31253	
Temperature Sensor	Office 3 (Room ID: 394492)	Level 1	TS33C-M with LCD	ID no: 45266	
CO2 Sensor	Office 3 (Room ID: 394492)	Level 1	AZ-0004	D no: 75555	
Humidity Sensor	Office 3 (Room ID: 394492)	Level 1	AcuRite 00613A1	D no: 80254	
Office 2(Room ID: 394489)					
Occupancy Sensor	Office 2(Room ID: 394489)	Level 1	Peco S200	ID no: 31252	
Temperature Sensor	Office 2(Room ID: 394489)	Level 1	TS33C-M with LCD	ID no: 45265	
CO2 Sensor	Office 2(Room ID: 394489)	Level 1	AZ-0004	D no: 75554	
Humidity Sensor	Office 2(Room ID: 394489)	Level 1	AcuRite 00613A1	ID no: 80253	
Office 1 (Room ID: 394495)					
Occupancy Sensor	Office 1 (Room ID: 394495)	Level 1	Peco S200	ID no: 31251	
Temperature Sensor	Office 1 (Room ID: 394495)	Level 1	TS33C-M with LCD	ID no: 45264	
CO2 Sensor	Office 1 (Room ID: 394495)	Level 1	AZ-0004	D no: 75553	
Humidity Sensor	Office 1 (Room ID: 394495)	Level 1	AcuRite 00613A1	ID no: 80252	

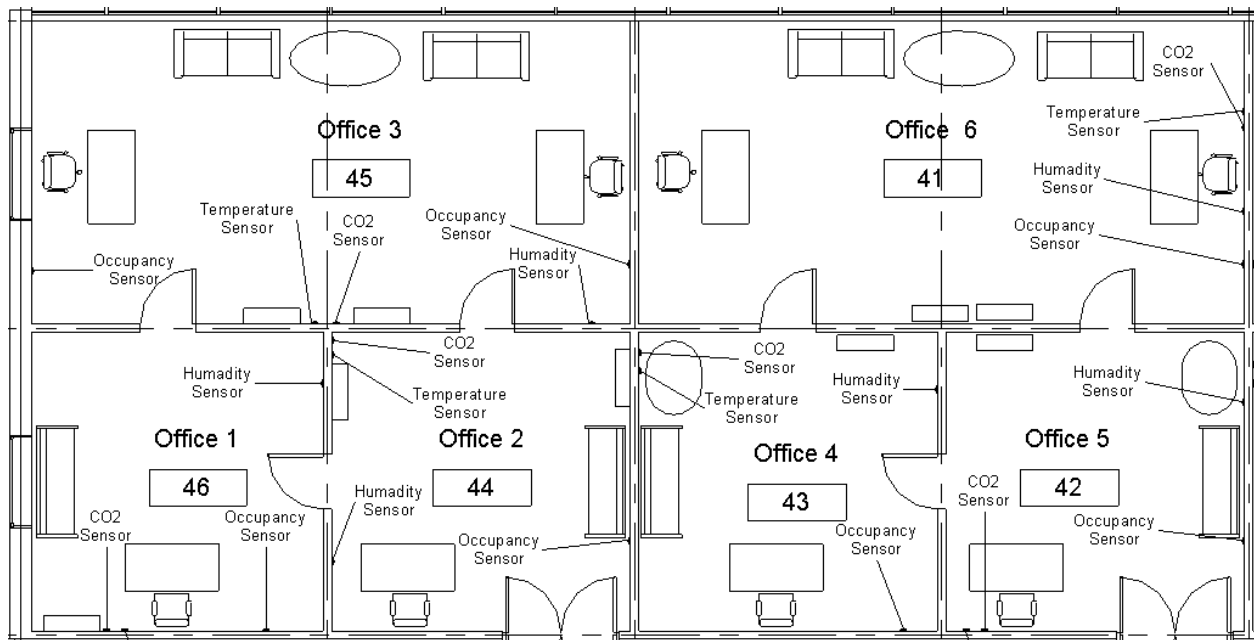


Figure 6-4: Sensor schedule table created in the BIM model and location of sensors in 2D view

6.6. Results

Cloud-based applications can improve mobility and accessibility. Cloud-based application tools can take data from different sources and combine them into one online navigation 3D model. The model provides access to all building data and associated operation manuals, manufacturer specs, equipment catalogs and images. It can help facility managers be involved in a real-time collaborative environment. Facility managers will have access to the building data from anywhere with an internet connection at any time, which can help when making significant decisions. It can improve the real-time collaboration between team members, such as engineers and facility managers.

The emerging cloud-BIM technology is considered to be an enabling tool that can deal with the standalone nature of traditional BIM. It can lead to higher levels of cooperation and collaboration and can provide an effective real-time communication platform for project team members (Wong et al., 2014). For example, if the building facility manager notices that some sensors in the building are not working, then he or she, through a cloud-based application, can inform the service personnel from the IoT company and ask them to replace the sensors and provide the sensors' locations, ID numbers and model and specifications. Simultaneously, he or she can inform the building manager to ensure that the specified room is unoccupied at specific times. In this study, Dynamo was used to integrate the BIM model with a Web-based service. Dynamo is a visual programming and computational design tool that extends BIM with the data and logic environment of a graphical algorithm editor, and it is ultimately linked with the BIM environment. Building data from the model are extracted, sorted, updated and shared with a third party in the cloud-based environment.

Room-related parameters such as Name, Level, Room ID, Occupancy and Number of Occupants as well as sensor-related parameters such as *Sensor Name*, *Sensor Station*, *Mark*, *Comments* and *Website* were extracted from the BIM model and sent to a cloud-based collaboration and data exchange service application such as Flux, Konstru or Speckle to share them between the IoT company and the building manager and inform them about any updated information.

Figures 6-5 and 6-7 show the modules developed in Dynamo to extract, combine and sort Rooms and Sensors information from the BIM model and automatically update them in the cloud-based platform. As shown, an appropriate relationship between the nodes is essential for automating this process. The building facility manager provides information such as the names and occupancy status of the rooms. The number of occupants can be provided either by the facility manager or as detected by occupancy sensors. The rooms' location is derived from the BIM model. The IoT company provides the sensors' names, physical IDs and websites. The sensors' location is provided from the BIM model, and the facility manager supplies information about the status of the sensors. As shown in Figure 6-8, it is assumed that occupancy sensors in office number four and office number five are not working correctly. Therefore, the building facility manager can request the IoT company to replace the failed sensors and ask the building supervisor to ensure the associated rooms are unoccupied according to the maintenance schedule. Consequently, parameters in the cloud are automatically updated through Dynamo, and the IoT company, as well as the building manager, will both be informed simultaneously about these requests through their desktop computer or smartphone, email and/or iPad (Figure 6-9). Therefore, the IoT company's service personnel will be informed of the failed sensors' location, ID number and specifications. Some other parameters, such as the preferred replacement date and time and sensors image, can also be added to this list.

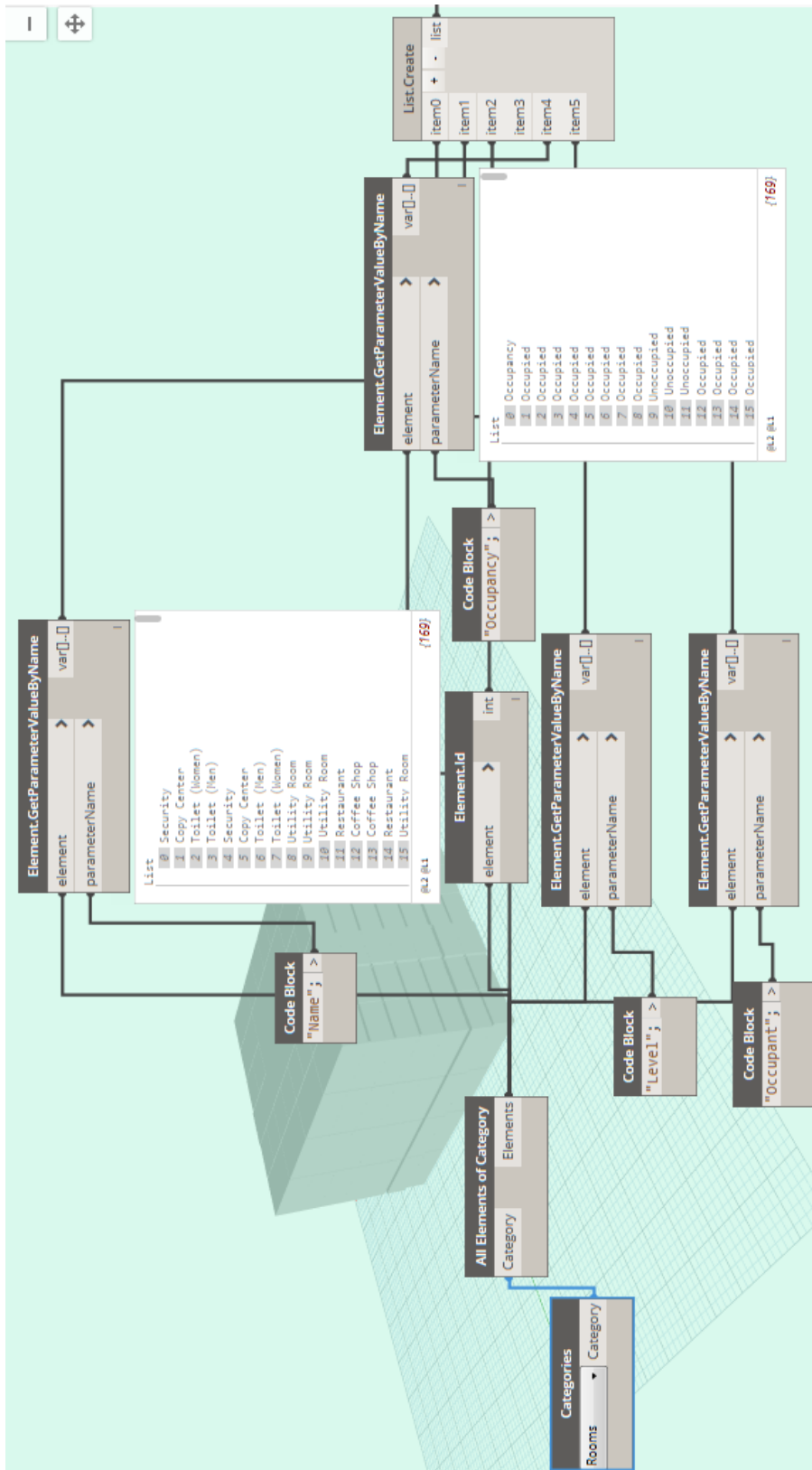


Figure 6-5: Extracting, combining, and sorting room information from the BIM model

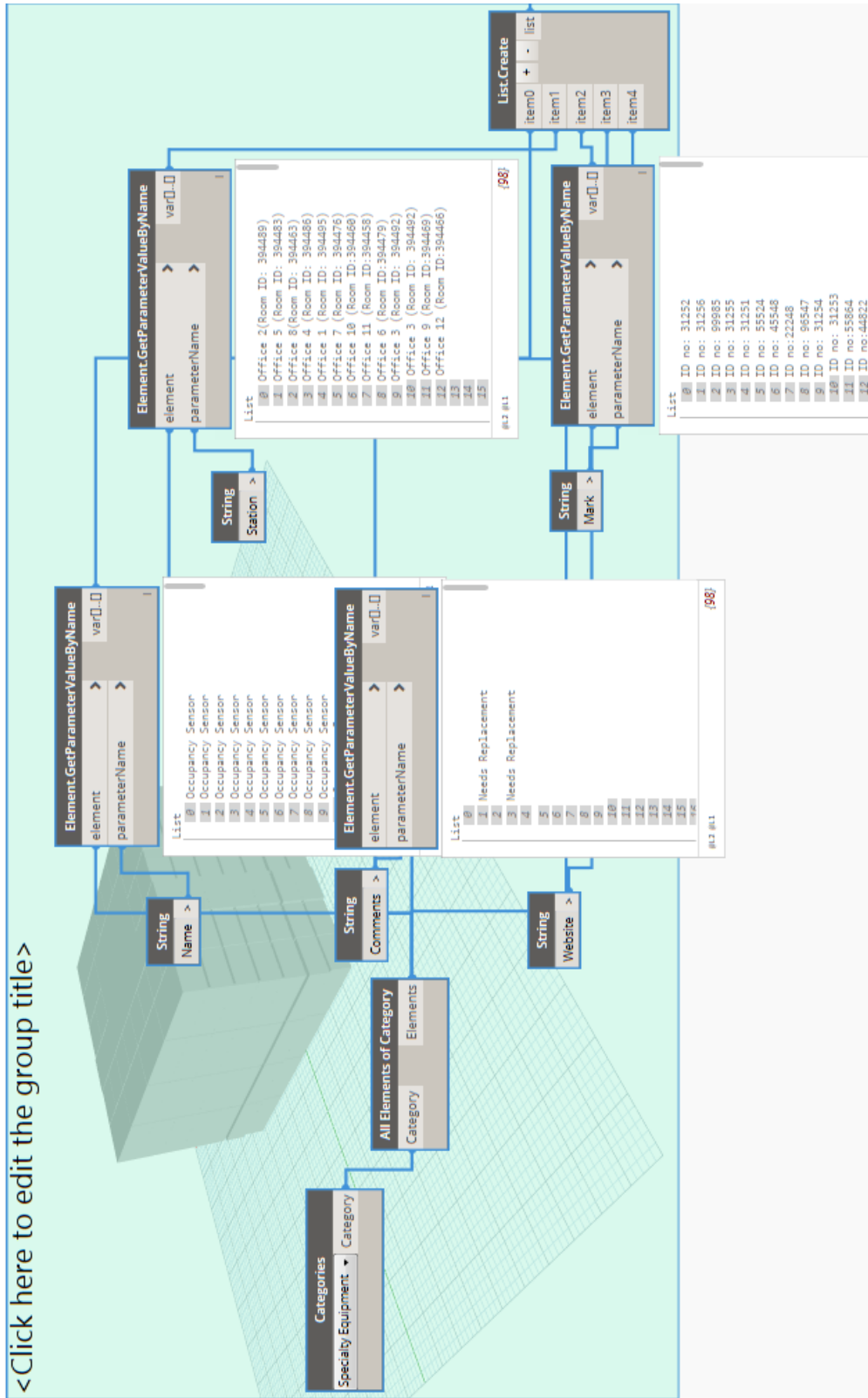


Figure 6-6: Extracting, combining, and sorting sensor information from the BIM model

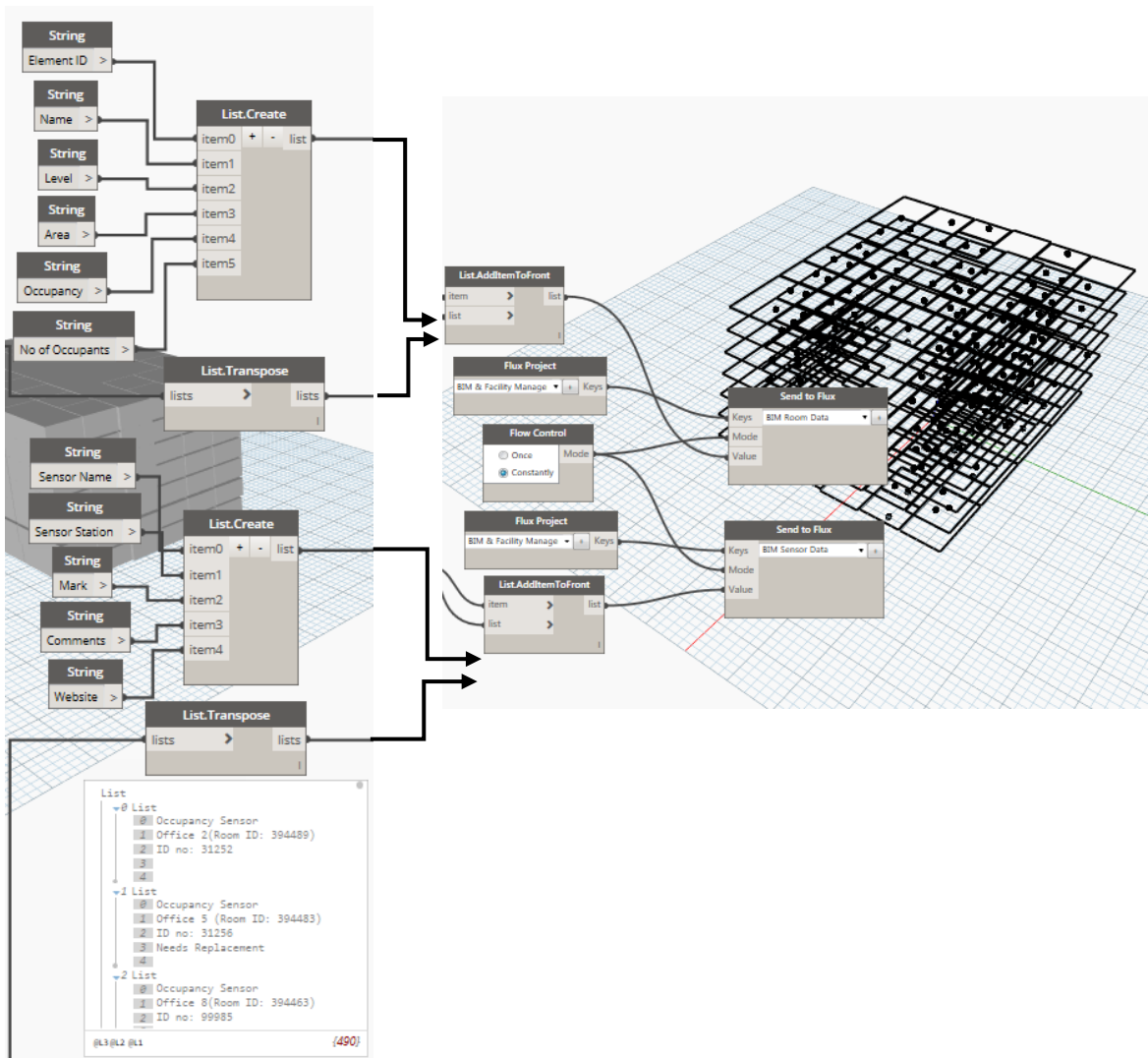


Figure 6-7: Integrating BIM model into a cloud-based database

As explained in this section, the parameters of the virtual sensors in the BIM model can be successfully updated by building facility managers and transferred to the cloud-based database to generate an alert for malfunctioning FM sensors in smart IoT environments to be used by the IoT company.

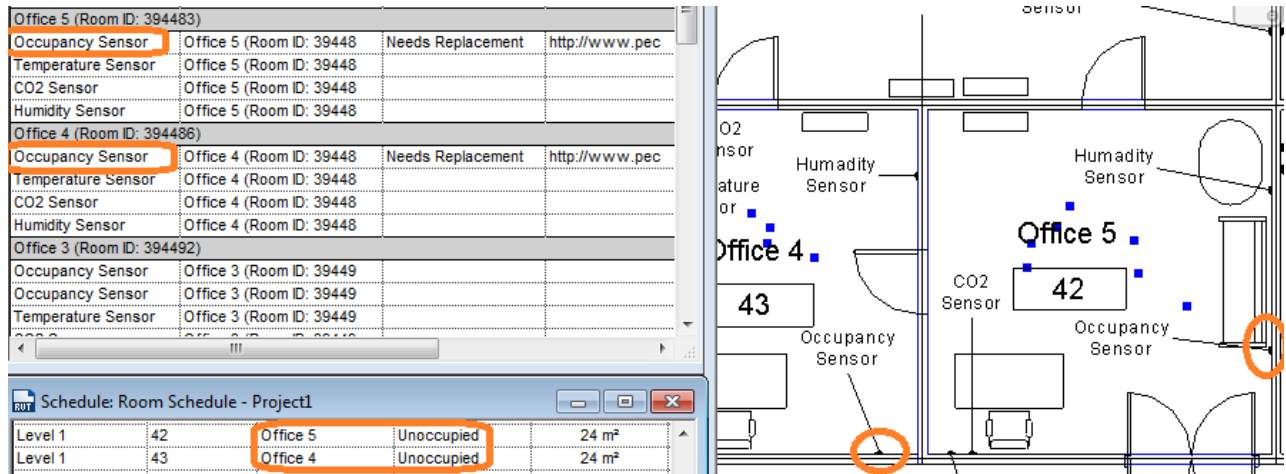


Figure 6-8: Updating some of the parameters of sensor and room elements in the BIM model

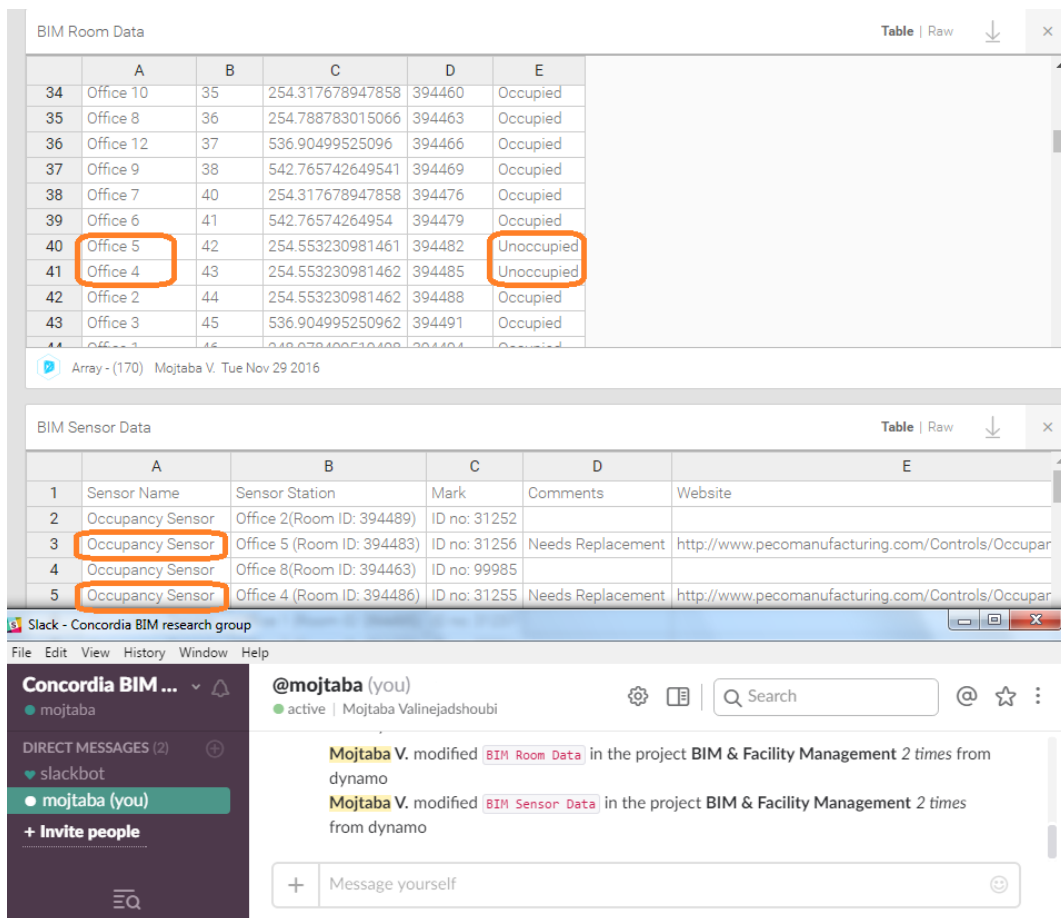


Figure 6-9: Real-time notification and updating of rooms and sensors status in a cloud database

6.6.1. Discussion

Building maintenance is a complex process that requires a significant flow of information and a quick call to action. Despite this, many facility managers do not have access to a unique platform with centralized information, where they can check the status of all operations, including any failure reports. The solution may involve centralizing all daily work and using mobile devices to register every failure and to manage and monitor the next steps in real time. To address this issue, this study introduced an automated, integrated workflow to use BIM information to provide a fast and efficient communication platform between the building facility manager and the IoT companies for sensor replacement management in case any sensor failure or sensor malfunction occurs in the building.

In this study, the BIM model was developed to accommodate all essential parameters. Two types of parameters were used to identify the type and location of each virtual sensor in the BIM model. To develop a real-time BIM-based communication platform, an integrated workflow (including three specifically designed modules) was developed in Dynamo to automatically extract and send all essential information such as the sensor's type, model and location to the IoT company in the event of sensor failure. The integration of the monitoring system into the BIM would improve the sensors' operation and maintenance plan during the building operational phase by helping the facility managers inspect the monitoring system and the sensors' performance and by sending the relevant information to the model in the event of any sensor failure and/or malfunction. It would then transfer all essential information to the IoT company for timely sensor replacement to ensure minimal disruption to monitoring services.

The developed framework also benefits preventive maintenance work. The system can be set up according to the maintenance and expiration schedules, automatically sharing alerts with

FMs and IoT maintenance contractors in advance about the IoT parts replacement. For effective predictive maintenance planning, machine learning techniques can be integrated into the developed workflow to efficiently predict the future condition of individual IoT components like data loggers and sensors as well as MEP components. For instance, when temperature sensors are used to monitor the thermal condition of different rooms in a building, a threshold can be defined, according to a specific standard or energy policy, to send an automatic thermal comfort alert to the cloud to inform the building FMs whenever the operating temperature exceeds the predefined thresholds. When FMs receive thermal discomfort alerts, they can initiate a root cause analysis to identify and locate the problem. For sensor fault detection, machine learning techniques can also be used in the developed system to establish, for example, the initial thermal pattern of each room using temperature sensors to find malfunctioning sensors when the sensor records a different thermal pattern than another sensor in the same room.

Transferring related information such as the room location, occupancy status, number of occupants, type and model of the sensor, sensor ID and required action from the BIM model to the cloud would help the IoT companies to visualize the workspaces in advance and to plan for timely and effective decision-making without any physical inspection, thereby reducing the inspection cost. It would also help support maintenance planning decisions, such as prioritizing maintenance works, by considering different factors such as the importance of spaces and number of occupancies.

However, there are some limitations in this work, which are as follows:

1. Although the present study demonstrates the feasibility of using BIM in the maintenance planning of monitoring systems in the building, the developed workflow can be expanded by integrating some types of sensors like occupancy sensors into the developed workflow to

automatically record and identify the number of occupants and visitors to prioritize the maintenance work.

2. The developed workflow can be integrated with the sensors' data and machine learning techniques to automatically identify the sensors' malfunctions and update the BIM model accordingly.

6.7. Conclusion

IoT technology dramatically reduces operation and maintenance costs. Using IoT sensors, the building equipment maintenance can be automatically scheduled. One of the most significant inefficiencies in building operations is the general lack of access to credible building and sensor information. This study's author investigated BIM's capability in sensor information management using cloud services in smart IoT environments during a building's operational phase. The research has highlighted the applicability of BIM in an efficient and rapid sensor failure management system. Based on the study presented here, the following conclusions are made:

- The information within BIM allows better and more effective decision-making for building facility managers.
- Integrating building and sensor information from BIM into a cloud-based system can facilitate better communication between the building facility manager and the IoT company for effective IoT system maintenance.
- The system developed in this study was implemented, and its capabilities were illustrated through a case study. The developed system (including three specifically designed modules)

was able to automatically extract, read and transfer all essential information to a cloud database to be used by an IoT company for timely sensor replacement.

- The use of the developed system can help facility managers take timely actions in the event of any sensor failure and/or malfunction to ensure minimal disruption to monitoring services.

References

Australian Construction Industry Forum (ACIF). (2014). “A framework for the adoption of project team integration and building information modelling.” Retrieved from www.acif.com.au/resources/strategic-forum-for-building-and-construction/aframework-for-the-adoption-of-project-team-integrationand-building-information-modelling.

Azhar, S., Nadeem, A., Mok, A.Y. N., and Leung, B.H.Y. (2008). “Building information modeling (BIM): a new paradigm for visual interactive modeling and simulation for construction projects.” First International Conference on Construction in Developing Countries (ICCIDC–I. Advancing and Integrating Construction Education, Research and Practice, Karachi.

Cahill, B., Menzel, K. and Flynn, D. (2012). “BIM as a Centre piece for optimised building operation.”, *eWork and eBusiness in Architecture, Engineering and Construction*, Gudnason and Scherer (Eds) © 2012, Taylor and Francis Group, London: 549-555.

Chang, K. M., Dzung, R.J. and Wu, Y.J. (2018). “An automated IoT visualization BIM platform for decision support in facilities management.” *Applied Sciences*, 8 (7): 1086.

Gallaher, M. P., O’Connor, A.C., Dettbarn, J. L., and Gilday, L.T. (2004). “Cost analysis of inadequate interoperability in the US. Capital facilities industry.”, NIST GCR 04-867.194.

Graphisoft, a Nemetschek Company. (2015). Retrieved from: www.graphisoft.com/archicad/open_bim/about_bim/.

IFMA (2009). “Facts about the international facility management association.”, Retrieved from: www.ifma.org.

- Kazado, D., Eskicioglu, R., and Kavagic, M. (2019). "Integrating building information modeling (BIM) and sensor technology for facility management." *Electronic Journal of Information Technology in Construction*, 24: 440-458.
- Kensek, K. (2020). "A BIM-based visualization tool for facilities management: Fault detection through integrating Real-Time sensor data into BIM." *Journal of Architectural Engineering Technology Research*, 9: 228.
- Nassar, K. (2010). "The effect of building information modeling on the accuracy of estimates." *Proceedings of the 46th Annual Conference*, Wentworth Institute of Technology, Boston, MA.
- Reeser, J., Jankowski, T. and Kemper, G. M. (2015). "Maintaining HMI and SCADA systems Through computer virtualization." *IEEE Transactions on Industry Applications*, 51 (3): 2558-2564.
- Suprabhas, K., and Nicholas Dib, H. (2017). "Integration of BIM and utility sensor data for facilities management.", *Computing in Civil Engineering, Computing in Civil Engineering: Information Modeling and Data Analytics*. Selected papers from sessions of the ASCE International Workshop on Computing in Civil Engineering 2017, held in Seattle, Washington, DC, June 25–27, 2017.
- Suprabhas, K. (2016). "Integration of BIM and utility sensor data for facilities management." *Theses and Dissertations*, Purdue University.
- The National Institute of Standards and Technology's (NIST). (2020). Retrieved from: www.nist.gov/
- Valinejadshoubi, M., Bagchi, A. and Moselhi, O. (2018b). "Development of a BIM-Based data management system for structural health monitoring with application to modular buildings: a case study.", *Journal of Computing in Civil Engineering*, 33(3).
- Valinejadshoubi, M., Bagchi, A., and Moselhi, O. (2017). "Managing structural health monitoring data using building information modelling.", *SMAR 2017, the fourth International Conference on Smart Monitoring, Assessment and Rehabilitation of Civil Structures*, (September 13-15, 2017) - Zurich, Switzerland.

- Valinejadshoubi, M., Bagchi, A., Moselhi, O. and Shakibabarough, A. (2018a). “Investigation on the potential of building information modeling in structural health monitoring of buildings.” Building Tomorrow’s Society, CSCE 2018 Fredericton Annual Conference, Jun 13, 2018 – Jun 16, 2018, Fredericton, NB, Canada.
- Wang, Y., Wang, X., Wang, J., Yung, P., and Jun, G. (2013), “Engagement of facilities management in design stage through BIM: framework and a case study.” *Advances in Civil Engineering*, Article ID 189105, p. 8.
- Wong, J., Wang, X., Li, H., Chan, G., and Li, H. (2014). “A review of cloud-based BIM technology in the construction sector.”, *Journal of Information Technology in Construction*, 19: 281-291.
- Zhang, J., Seet, B. H., and Lie, T.T. (2015). “Building information modelling for smart built environments.”, *Buildings*, 5 (1): 100-115.

Chapter 7: Summary and Conclusions

7.1. Summary

In this thesis, a set of automated management solutions were developed for building management, focusing on structural safety and monitoring and managing occupants' thermal comfort to assist facility managers in tracking the status of deployed sensors.

The main contributions of this thesis are:

- Developing a method for an automated BIM-based system for identifying and prioritizing the NSEs with high seismic risk.
- Developing a methodology for updating some seismic risk score parameters using the elements' geometry and location in the BIM model.
- Developing the small size and low-cost DAQ system for vibration monitoring for modules in transit.
- Developing a solution for Data storage cost reduction by integrating onboard memory into the hardware system.
- Developing a damage detection method using different clustering techniques for vibration monitoring during transportation.
- Developing a technique for detecting sensor failure.
- Developing a method to integrate BIM and SHM for increasing the speed and efficiency of structural condition monitoring.
- Integrating multiple cost-effective sensing technologies and external databases to improve the data storage and retrieval process for thermal comfort monitoring.

- Developing an automated workflow to link between the virtual and physical sensors.
- Developing a workflow for improving the maintenance plan for sensors as a part of a building's operation.
- Developing an automated data-driven SHM system to provide a cost-effective solution for modular building manufacturers and building owners to verify safe delivery of prefabricated modules. This multi-functional system can be used for different purposes, such as structural damage detection and sensor failure analysis.
- Developing an integrated strain-based monitoring system framework for better damage visualization and rapid detection of damaged structural elements using an effective visualization technique such as BIM. The small size and low cost of the sensory system proposed here can be effective in modular structures, usually consisting of small-sized and narrow components.
- Developing an integrated BIM-based monitoring system to work as a 3D visualization-based monitoring and alarm system for indoor thermal condition monitoring. The Building Management System (BMS) is not fully interactive and can only be manipulated by a trained operator. Moreover, while existing BMS systems provide some access to sensor information, the way they present often lacks the context of 3D building information. The developed system can solve this problem.
- Development of the framework presented in Chapter 6 could be beneficial for facility managers who may not have access to a specialized platform with centralized information to register every failure and manage and monitor the next

steps in real-time, especially for smaller buildings. The application of the framework is expected to reduce inspection costs by helping the IoT companies to visualize the workspaces in advance and plan for timely and effective decisions without any physical inspection.

BIM is a process of creating and managing information in construction projects used in the AEC industry to improve efficiency and reduce the costs of projects. How BIM was used in this thesis is listed below:

Chapter 2:

- Modeling 3D structural and non-structural elements of the building, including MEP elements.
- Creating user-defined parameters for the indices required for the seismic risk score calculation
- Calculating and prioritizing the seismic risk of each NSEs and highlighting them utilizing a color scheme.
- Updating the seismic risk score of NSEs based on their geometry information and position in the building.

Chapter 4:

- Modeling all the elements of the structure.
- Modeling the virtual sensors and defining all the parameters required for the monitoring purpose.
- Updating the value and status of monitoring parameters using the workflow developed in the visual programming tool, Dynamo.

- Highlighting the damaged structural element based on the SHM sensor data and the pre-defined threshold value using the developed workflow.
- Providing information such as the cut length for the repair and replacement of damaged elements.

Chapter 5

- Building the architectural 3D model of the building, including all the monitored spaces.
- Modeling the virtual temperature and humidity sensors and defining all the parameters required for the monitoring purpose.
- Updating the value and status of monitoring parameters using the developed workflow.
- Highlighting building spaces automatically using the developed workflow where comfort conditions are not met.
- Generating automatic text alarms using the developed workflow to notify building facility managers shows when thermal discomfort situation occurs.

Chapter 6:

- Building the 3D model of the building, including all the architectural elements and virtual sensors, and defining their maintenance-related parameters.
- Updating parameters such as “sensor condition” and “room occupancy”.
- Transferring information to the cloud database to generate an alert for sensors malfunction using the developed workflow.

7.2. Conclusions

Based on the studies presented in this thesis, the following conclusions are made:

- The automated tools developed in this study can support digital transformation over the project life cycle in the AEC industry.
- The developed BIM-based tool for visualizing the NSEs seismic score (presented in chapter 2) can be used during the operational phase to identify the most vulnerable NSEs and their position to assess different retrofit strategies. The developed method could also be extended to building modules during transportation to construction sites.
- The developed data-driven SHM system (presented in chapter 3) could be used as a quick and effective solution to verify the safety of prefabricated building modules during their transportation.
- The developed BIM-based SHM tool (presented in chapter 4) could be adopted for automated and graphical structural condition monitoring, which is useful for engineers and decision-makers to visualize updated information about the current state of structural elements in 3D models.
- The developed IoT-BIM-based thermal comfort monitoring tool (presented in chapter 5) can be used as an alert and database tool to store indoor thermal data of rooms and notify FMs if the rooms' temperature exceeds defined thresholds.
- The integrated BIM-based tool (presented in Chapter 6) can be used to notify the IoT companies in cases of sensor failure events and provide them with required info via a cloud-based database. This tool can facilitate communication between FMs and the IoT companies and can lead to a more efficient IoT system maintenance environment.

7.3. Limitations and future research

While the present research provides a proof of concept for the developed framework and its feasibility, it is essential to test it more rigorously to ascertain its generality. The following can be considered in future work:

1. Increasing the number of monitoring tests on different types (steel and wooden) and sizes of prefabricated modules to compare and assess their structural behavior and identify damages to further test and validate the developed system and its robustness.
2. Although the optimum values for parameters of the machine learning algorithms used in the developed transportation monitoring system were searched using a trial-and-error, an optimization technique such as Genetic Algorithm can be applied to find the optimum values automatically.
3. The integrated BIM-based monitoring system was tested using only one virtual sensor. It should be tested further with a larger number of virtual sensors to investigate and test their impact on the performance of the system.
4. While the developed BIM-based thermal comfort monitoring and alarm system demonstrate the feasibility of remote sensing and decision-making to manage thermal comfort in buildings, the study is somewhat limited in terms of the space monitored. Further studies are required to conduct a large-scale investigation and review its integration with the facility managers and other stakeholders to test the system for its reliability, reproducibility, robustness, and ease of use.
5. While the developed integrated BIM-based sensor failure management workflow demonstrates the feasibility of using BIM in tracking the performance of the configured sensors-based plan for monitoring the status of the sensors used in buildings, the developed

workflow can be expanded to integrate other types of sensors such as occupancy sensors to automatically record and identify the number of occupants in the monitored facility to prioritize the sensor maintenance works.

References

Angelosanti, M., Dabetwar, S., Curra, E., and Sabato, A. (2021). “3D-DIC analysis for BIM-oriented SHM of a lab-scale aluminium frame structure.” *Journal of Physics: Conference Series* 2041 012009.

Angulo, C., Diaz, K., Gutiérrez, J. M., Prado, A., Casadey, R., Pannillo, G., Rivera, F. M., Herrera, R. F., and Vielma, J. C. (2020). “Using BIM for the Assessment of the Seismic Performance of Educational Buildings.” *International Journal of Safety and Security Engineering* Vol. 10(1): 77-82.

Autodesk. (2021). “Autodesk Project Dasher.”. <http://dasher360.com>

Agarwal, R., Chandrasekaran, S., and Sridhar, M. (2016). “The Digital Future of Construction.” Retrieved from <https://www.globalinfrastructureinitiative.com/sites/default/files/pdf/The-digital-future-of-construction-Oct-2016.pdf>.

Autodesk. (2020). “Digital Transformation: The Future of Connected Construction.” Retrieved from http://constructioncloud.autodesk.com/rs/572-JSV-775/images/Autodesk-IDC-Digital%20Transformation_The-Future-of-Connected-Construction.pdf.

BIMplus. (2020), Retrieved from <https://www.bimplus.co.uk/analysis/poor-digital-skills-hold-back-bim-adoption/>.

- Desogus, G., Quaquero, E., Rubiu, G., Gatto, G., and Perra, C. (2021). “BIM and IoT Sensors Integration: A Framework for Consumption and Indoor Conditions Data Monitoring of Existing Buildings.” *Sustainability*, 13, 4496.
- Filiatrault, A., Christopoulos, C., and Stearns, C. (2001). “Guidelines, Specifications, and Seismic Performance Characterization of Nonstructural Building Components and Equipment.” PEER Report, Pacific Earthquake Engineering Research Center College of Engineering University of California, Berkeley.
- McKinsey Global Institute. (2017). “Reinventing Construction: A Route to Higher Productivity.”, Retrieved from <https://www.mckinsey.com/industries/capital-projects-and-infrastructure/our-insights/reinventing-construction-through-a-productivity-revolution>.
- Miranda, E., Mosqueda, G., Retamales, R., and Pekcan, G. (2012). “Performance of Nonstructural Components during the 27 February 2010 Chile Earthquake.” *Earthquake Spectra* 28(S1): 453-471.
- Morgan, B. (2019). “Organizing for Digitalization through Mutual Constitution: The Case of a Design Firm.” *Construction Manag. Econ.* 37 (7): 400–417.
- Murray, S. (2018). “Five Keys to Unlocking Digital Transformation in Engineering and Construction.” Boston Consulting Group: A Global Industry Council Report.
- O’Shea, M., and Murphy, J. (2020). “Design of a BIM Integrated Structural Health Monitoring System for a Historic Offshore Lighthouse.” *Buildings*, 10, 131.
- Pan, M., Linner, T., Pan, W., Cheng, H., and Bock, T. (2020). “Structuring the Context for Construction Robot Development through Integrated Scenario Approach.” *Automation in construction*, 114, 103174.

Perrone, D., and Filiatrault, A. (2017). “Automated seismic design of non-structural elements with building information modelling.” *Automation in Construction*, 84: 166-175.

Ricci, P., Luca. F, D., and Verderame, G. M. (2011). “6th April 2009 L'Aquila earthquake, Italy: Reinforced concrete building performance.” *Bulletin of Earthquake Engineering*, 9(1): 285-305.

Shafie Panah, R., and Kioumars, M. (2021). “Application of Building Information Modelling (BIM) in the Health Monitoring and Maintenance Process: A Systematic Review.” *Sensors*, 21, 837.